Acta Universitatis Agriculturae Sueciae

Doctoral Thesis No. 2025:87
Faculty of Natural Resources and Agricultural Sciences

Syngas Biomethanation in Trickle-Bed Reactors

Impact of Nutrient Media Supply and Syngas Composition

Florian Gabler

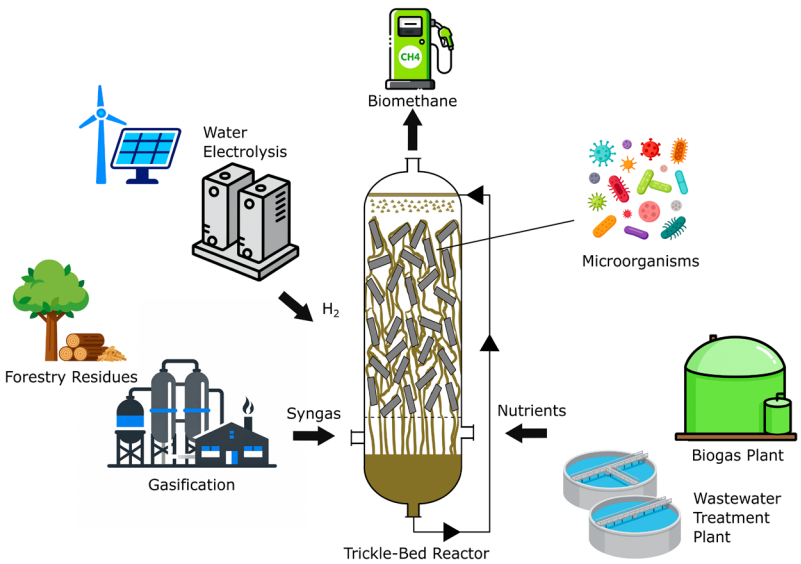

Syngas Biomethanation in Trickle-Bed Reactors

Impact of Nutrient Media Supply and Syngas Composition

Florian Gabler
Faculty of Natural Resources and Agricultural Sciences
Department of Energy and Technology
Uppsala

SLU
SWEDISH UNIVERSITY OF AGRICULTURAL SCIENCES

DOCTORAL THESIS
Uppsala 2025

Acta Universitatis Agriculturae Sueciae
2025:87

Cover: TBR Syngas Biomethanation pathway (Florian Gabler, 2025)

ISSN 1652-6880
ISBN (print version) 978-91-8124-071-9
ISBN (electronic version) 978-91-8124-117-4
https://doi.org/10.54612/a.3m2t1b64np

Swedish University of Agricultural Sciences, Department of Energy and Technology, Uppsala, Sweden

Print: SLU Grafisk service, Uppsala 2025

“Tired of lying in the sunshine, staying home to watch the rain.
You are young and life is long, and there is time to kill today.
And then, one day, you find ten years have got behind you.
No one told you when to run; you missed the starting gun.”
Pink Floyd, “Time” (1973)

Syngas Biomethanation in Trickle-Bed Reactors

Abstract

Biomethanation of syngas in trickle-bed reactors (TBRs) presents a promising route for producing renewable methane (CH_4), coupled with the gasification of recalcitrant biomass, such as forestry residues. The overall objective of this thesis was to achieve efficient and stable syngas biomethanation in TBRs using liquid organic waste streams as nutrient media by varying process and operational conditions, based on the assessment of CH_4 productivity and conversion rates of H_2 and CO.

This work presents long-term lab-scale studies (a total of 1,600 days of operation) where mainly digestate and reject water were used as nutrient media to evaluate potential macronutrient limitations, nutrient supply rates, liquid recirculation regimes, and microbial community development. Additionally, the effect of increasing H_2 content in syngas to enhance CH_4 concentration in the product gas was investigated.

Methane evolution rates up to 4.5 $L/(L_{pbv} \cdot d)$ were achieved under thermophilic conditions with H_2 and CO conversions consistently above 90 %. Adequate phosphorus and sulfur supply, proper nutrient addition, and efficient liquid recirculation were crucial for sustaining high performance, while nutrient limitations or short gas retention times reduced stability and productivity. With an experimental upper limit of 71 % H_2 in the syngas, the maximum CH_4 concentration reached 65 %. High H_2 partial pressures promoted hydrogenotrophic methanogenesis but limited CO conversion.

Despite performance variations, microbial communities remained stable, dominated by *Methanothermobacter* and supported by syntrophic acetate-oxidizing bacteria, while performance shifts were linked mainly to activity changes rather than community restructuring.

The results highlight the potential of TBRs as a reactor concept for integrating syngas biomethanation into renewable energy systems, while identifying nutrient management, gas–liquid mass transfer optimization, and syngas composition control as key priorities for future development.

Keywords: Biosyngas, Hydrogen, Carbon Monoxide, Reject Water, Digestate, Microbial Community, Biotrickling Filters, E-Methane

Biometanisering av syntesgas i droppbäddsreaktorer

Sammanfattning

Biometanisering av syntesgas i droppbäddsreaktorer (TBR) utgör en lovande möjlighet för förnybar metanproduktion i kombination med förgasning av biologiskt svåromsättbar biomassa som skogsavfall. Det övergripande målet med denna avhandling var att uppnå effektiv och stabil biometanisering av syntesgas i TBR med hjälp av näring från organiska reströmmar, genom att utvärdera CH_4-produktivitet och omsättningseffektivitet av H_2 och CO under varierande process- och driftsförhållanden.

Avhandlingen presenterar långvariga studier i laboratorieskala (totalt 1.600 dagars drift) där huvudsakligen biogas-rötrest och rejektvatten från reningsverk användes som näringsmedier för att utvärdera potentiella makronäringsbegränsningar, näringstillförselhastigheter, vätskecirkulationsstrategier och utveckling av mikrobiell sammansättning. Dessutom undersöktes effekten av att öka H_2-halten i syntesgas för att höja CH_4-koncentrationen i produktgasen.

Metanproduktionshastigheter på upp till 4,5 $L/(L_{pbv} \cdot d)$ erhölls under termofila förhållanden med H_2 -och CO-omsättning konsekvent över 90 %. Tillräcklig fosfor- och svavelförsörjning, korrekt näringstillförselhastighet och effektiv vätskecirkulation var avgörande för att upprätthålla hög prestanda, medan näringsbegränsningar eller korta gasuppehållstider minskade stabiliteten och produktiviteten. Med en övre gräns på 71 % H_2 i syntesgasen nåddes maximalt 65 % CH_4-koncentration. Höga H_2-partialtryck främjade hydrogenotrofisk metanogenes, men begränsade CO-omvandlingen. Den mikrobiella sammansättningen förblev dock stabil, dominerad av *Methanothermobacter* och syntrofiska acetat-oxiderande bakterier, varför prestandaförändringar främst var kopplade till aktivitetsförändring snarare än förändringar av den mikrobiella sammansättningen.

Resultaten belyser potentialen hos TBR som reaktorkoncept för biometanisering av syntesgas i förnybara energisystem, samtidigt som hantering av näringsämnen, optimering av gas-vätskeöverföring och sammansättning av syngas identifieras som viktiga prioriteringar för framtida forskning och utveckling.

Nyckelord: Biosyntesgas, väte, kolmonoxid, rejektvatten, rötrest, mikrobiell sammansättning, biotricklingfilter, e-metan

Biomethanisierung von Synthesegas in Rieselbettreaktoren

Zusammenfassung

Die Biomethanisierung von Synthesegas in Rieselbettreaktoren (TBR) stellt einen vielversprechenden Ansatz zur Erzeugung von erneuerbarem Methan (CH_4) aus der Vergasung schwer abbaubarer Biomasse, wie forstwirtschaftlichen Reststoffen, dar. Das Ziel dieser Arbeit war es, eine effiziente und stabile Biomethanisierung von Synthesegas in TBR unter Verwendung nicht definierter Nährmedien zu erreichen. Hierzu wurden verschiedene Prozessbedingungen auf Grundlage der CH_4-Produktivität sowie der H_2- und CO-Umwandlungsraten angepasst.

Diese Arbeit präsentiert Langzeitversuche im Labormaßstab (insgesamt 1.600 Betriebstage), bei denen hauptsächlich flüssige organische Abfallströme als Nährmedien dienten. Bewertet wurden potenzielle Makronährstoffbeschränkungen, Nährstoffzufuhrraten, Flüssigkeitsrezirkulation sowie die Entwicklung mikrobieller Gemeinschaften. Zudem wurde der Einfluss erhöhter H_2-Gehalte im Synthesegas auf die CH_4-Konzentration im Produktgas untersucht.

Unter thermophilen Bedingungen wurden Methanbildungsraten von bis zu 4,5 $L/(L_{pbv} \cdot d)$ erreicht, wobei die H_2- und CO-Umwandlung konstant über 90 % lag. Eine ausreichende Phosphor- und Schwefelversorgung, eine angemessene Nährstoffzugabe und eine effiziente Flüssigkeitsrezirkulation waren entscheidend für die Aufrechterhaltung hoher Leistungen, während Nährstoffbeschränkungen oder kurze Gasverweilzeiten die Stabilität und Produktivität beeinträchtigten. Bei einer experimentellen Obergrenze von 71 % H_2 im Synthesegas betrug die maximale CH_4-Konzentration 65 %. Hohe H_2-Partialdrücke förderten die hydrogenotrophe Methanogenese, schränkten jedoch die CO-Umwandlung ein.

Trotz Leistungsschwankungen blieben die mikrobiellen Gemeinschaften stabil, dominiert von *Methanothermobacter* und unterstützt durch syntrophen acetatoxidierende Bakterien. Die Ergebnisse unterstreichen das Potenzial von TBR als skalierbare, erneuerbare Energietechnologie und heben Nährstoffmanagement, Stofftransportoptimierung und Synthesegaszusammensetzung als zentrale Entwicklungsfelder hervor.

Schlüsselwörter: Bio-Synthesegas, Wasserstoff, Kohlenmonoxid, Klärschlamm-Zentrat, Gärrest, mikrobielle Gemeinschaft, Tropfkörper

Dedication

To my girls, Doreen, Svea, and Ida.
Thank you for your love. ♥

Contents

List of Publications

This thesis is based on the work contained in the following papers, referred to by Roman numerals in the text:

I. Cheng, G., Gabler, F., Pizzul, L., Olsson, H., Nordberg, Å., Schnürer, A. (2022). Microbial community development during syngas methanation in a trickle bed reactor with various nutrient sources. Applied Microbiology and Biotechnology, 106 (13), 5317-5333. https://doi.org/10.1007/s00253-022-12035-5

II. Gabler, F., Cheng, G., Pizzul, L., Schnürer, A., Nordberg, Å. (2025). Comparative evaluation of digestate and reject water as nutrient media for syngas biomethanation in thermophilic trickle-bed reactors. Bioresource Technology, 435, 132893, https://doi.org/10.1016/j.biortech.2025.132893

III. Gabler, F., Cheng, G., Pizzul, L., Schnürer, A. Nordberg, Å. (2025) Influence of Nutrient Media Supply Rate and Liquid Recirculation Regime on Syngas Biomethanation in Thermophilic Trickle-Bed Reactor. Bioresource Technology Reports. 32, 102353, https://doi.org/10.1016/j.biteb.2025.102353

IV. Gabler, F., Cheng, G., Pizzul, L., Schnürer, A., Nordberg, Å. Limit of Hydrogen Addition for Enhanced Methane Concentration and Production During Syngas Biomethanation in Thermophilic Trickle-Bed Reactors (manuscript)

The contribution of Florian Gabler to the papers included in this thesis was as follows:

I. Participated in parts of the subsequent laboratory work. Performed data analysis of the TBR operation parameters and variables. Co-author of the paper.

II. Participated in the planning of the experimental setup. Main conductor of the experimental work. Performed operational control of the TBRs together with data analysis and its interpretation, and conducted the chemical analysis of the liquid phases. Main writer of the manuscript.

III. Partly responsible for planning the study design. Main conductor of the experimental work. Performed operational control of the TBRs in combination with data analysis and its interpretation, and conducted the chemical analysis of the liquid phases. Main writer of the manuscript.

IV. Main responsibility for study design. Main conductor of the experimental work. Performed operational control of the TBRs together with data analysis and its interpretation, and conducted the chemical analysis of the liquid phases. Main writer of the manuscript.

During the doctoral project, Florian Gabler contributed to the following papers, which are not included in this thesis.

I. Gabler, F., Cheng, G., Pizzul, L., Janke, L., Schnürer, A., Nordberg, Å. (2025). Impact of Nutrient Media and Temperature Shift on Methane Productivity and Carbon Monoxide Conversion in Syngas Biomethanation. Waste and Biomass Valorization, doi.org/10.1007/s12649-025-03257-5

II. Cheng, G., Gabler, F., Bongcam-Rudloff, E., Schnürer, A. Unveiling species involved in acetate metabolism within syngas biomethanation systems (manuscript)

List of Tables

List of Figures

Abbreviations

AD	Anaerobic Digestion
AF	Anaerobic Filter
CSTR	Continuous Stirred Tank Reactor
GRT	Gas Retention Time
HRT	Hydraulic Retention Time
LHV	Lower Heating Value
MBR	Membrane Bioreactor
MER	Methane Evolution Rate
MFR	Mass Flow Regulator
NMSR	Nutrient Medium Supply Rate
PBV	Packed Bed Volume
PCR	Polymerase Chain Reaction
RFNBO	Renewable Fuels of Non-Biological Origin
SAO	Syntrophic Acetate Oxidation
SAOB	Syntrophic Acetate-Oxidizing Bacteria
SQI	Syngas Quality Index
TBR	Trickle-Bed Reactor
VFA	Volatile Fatty Acids
WWTP	Wastewater Treatment Plant

1. Introduction

The growing urgency to mitigate climate change and promote sustainable resource management has driven global efforts to transition toward renewable energy systems. Enhancing energy security and reducing dependency on imported fossil fuels due to geopolitical instability are additional driving forces. Biomass, as a renewable and carbon-neutral feedstock, plays a central role in this transition. The production of biogas — comprising methane and carbon dioxide — via anaerobic digestion (AD) is an established large-scale technology mediated by microorganisms that utilize various substrates such as manure, sewage sludge, food waste, or energy crops (EBA, 2024b). Biogas can be combusted to generate heat and power, but may also be upgraded to biomethane by removing carbon dioxide, thereby increasing methane concentration and enabling injection into gas grids or use as a vehicle fuel (Angelidaki et al., 2018).

In 2024, Swedish biogas production was 2.4 TWh/y, insufficient to meet the demand of 4.1 TWh/y (Energigas Sverige, 2025). Major Swedish companies project a growing demand of up to 10 TWh/y by 2030 (Industrins Biogaskommission, 2025). This raises the question of whether currently used biogas substrates alone can satisfy future biogas demand (Lönnqvist et al., 2015; SOU, 2019:63).

Additional biogas potential lies in several substrates that are not biodegradable — or require intensive pretreatment — within traditional AD systems, such as forestry residues, which have an energetic potential of 4–12 TWh/y (Hjort, 2019). When using such recalcitrant materials for biomethane production, gasification is particularly attractive because it can convert a wide range of lignocellulosic residues and organic wastes into a versatile synthesis gas (syngas) (Joshua Abioye et al., 2025). This syngas, primarily composed of hydrogen (H_2), carbon monoxide (CO), carbon dioxide (CO_2), along with minor fractions of nitrogen (N_2) or methane (CH_4), can serve as an intermediate energy carrier or chemical precursor for the production of heat, power, fuels, and other valuable compounds (Neto et al., 2025).

Syngas can be converted to CH_4 through either chemo-catalytic or biological methanation, producing a renewable substitute for fossil natural gas that can be injected into the existing gas grid or used as biofuel in compressed or liquefied form (Ren et al., 2020). While catalytic syngas

methanation has been extensively studied and applied at demonstration industrial scale (20 MW output) (Thunman et al., 2019), its technical limitations — such as high temperature and pressure requirements, catalyst deactivation, and sensitivity to impurities such as tar and hydrogen sulfide (H_2S) — reduce operational flexibility (Ren et al., 2020).

In contrast, biological syngas methanation, performed by members of the domains Bacteria and Archaea, offers several compelling advantages: operation under mild temperature and pressure conditions, greater tolerance to gas impurities, and the use of microbial consortia capable of adapting to varying syngas compositions and loads (Grimalt-Alemany et al., 2017). These traits make biological conversion particularly attractive for integration with variable biomass gasifiers, which often produce syngas with fluctuating $H_2/CO/CO_2$ ratios and minor contaminants (Molino et al., 2016). Archaea convert syngas components into CH_4 and also facilitate the transformation of acetate and other intermediates derived from bacterial activity, resulting in numerous syntrophic relationships between the two domains (Thauer et al., 2008). However, the presence of CO in syngas can inhibit microbial activity and thus impair CH_4 formation (Sancho Navarro et al., 2016; Grimalt-Alemany et al., 2017; Neto et al., 2025). Additionally, limited gas–liquid mass transfer of syngas components represents one major bottleneck (Grimalt-Alemany et al., 2017; Asimakopoulos et al., 2018).

To overcome this limitation, trickle-bed reactors (TBRs) offer a reactor design particularly well-suited for gas conversion processes involving biofilms. TBRs are gastight columns filled with carrier material for biofilm immobilization, which provide a high gas–liquid contact area, passive mixing, low energy input, and high biomass retention. These features make them promising for robust and continuous CH_4 production from syngas. Thus far, only a few research groups have assessed TBR syngas biomethanation — mostly at bench scale — and no long-term studies (>200 days) have been reported (Asimakopoulos et al., 2019; Aryal et al., 2021; Andreides et al., 2022; Ali et al., 2024; Goonesekera et al., 2024; Bilgiç et al., 2025).

Accordingly, the application of TBRs for syngas biomethanation — especially under long-term continuous operation — remains poorly understood. Several challenges must be addressed before this technology can be scaled up or implemented in practice. Sustaining microbial activity and growth requires an adequate nutrient supply. Evaluating liquid organic waste streams such as manure, digestate, or reject water as alternative nutrient

media, rather than relying on artificial stock solutions is economically important due to the large volumes required. Along with the choice of a suitable non-defined nutrient medium, operational parameters such as the applied nutrient medium supply rate (NMSR) and liquid recirculation regime (trickling) are critical to ensure adequate macronutrient supply. These parameters also influence gas–liquid mass transfer, which is a major bottleneck for efficient TBR syngas biomethanation. Furthermore, syngas composition directly affects the product gas composition, as increasing the H_2 fraction raises the CH_4 concentration and broadens the potential utilization options of the product gas. The challenges mentioned above are addressed in this thesis.

2. Objectives and Structure

2.1 Objectives

The overall objective of this thesis was to achieve efficient syngas biomethanation in operationally stable trickle-bed reactors using non-defined nutrient media during long-term operation. This was accomplished by varying process and operational parameters based on the assessment of CH_4 productivity and H_2 and CO conversion rates.

Specific objectives were:

- to examine the influence of different defined and non-defined nutrient media on CH_4 productivity and conversion rates of H_2 and CO, and to identify potential macronutrient limitations under mesophilic (Paper I) and thermophilic conditions (Paper II);
- to assess the influence of nutrient medium supply rate (NMSR) and liquid recirculation regime on syngas biomethanation (Paper III);
- to investigate the effect of an increasing H_2 share in the syngas composition to increase the CH_4 concentration in the product gas, aiming at biomethane quality (Paper IV);
- to study microbial community development (Papers I–IV).

2.2 Structure of the Thesis

This thesis is based on four studies conducted with two different TBR setups over more than 1,600 days of operation (Fig. 1).

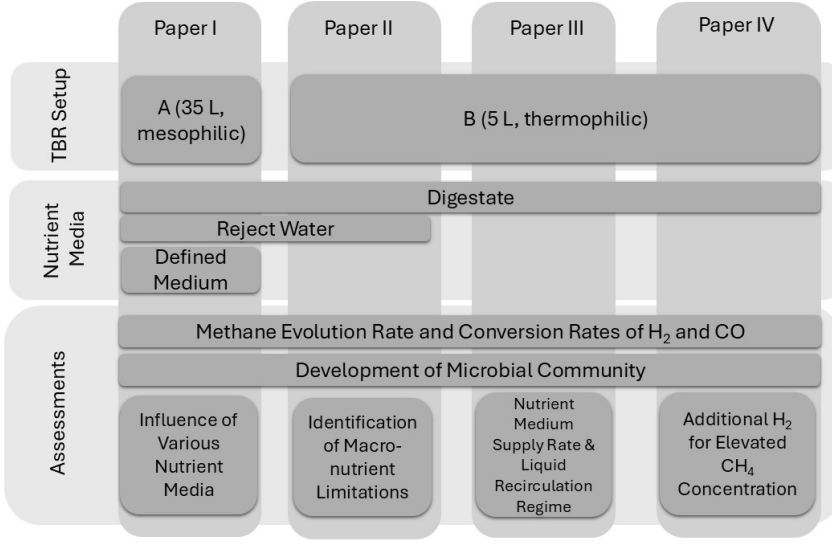

Figure 1. Thesis structure

Paper I evaluated various defined and non-defined nutrient media in a consecutive manner using a 35 L mesophilic trickle-bed reactor (TBR). Paper II compared the biomethanation performance of two non-defined media in two identical 5 L TBRs under thermophilic conditions. Paper III examined the influence of key operational parameters — namely the nutrient medium supply rate (NMSR) and the liquid recirculation regime — on process performance. Paper IV investigated the effect of an increasing H_2 share in the syngas on syngas biomethanation. The studies presented in Papers II–IV were conducted using the same thermophilic TBR setup.

3. Background

3.1 Energy Supply and Climate Impact

The global energy landscape is undergoing a critical transformation as nations struggle with the dual challenge of meeting the growing energy demand and mitigating climate change. Reliance on fossil fuels remains the dominant driver of greenhouse gas emissions, driving global warming and its associated environmental and socio-economic impacts (IPCC, 2014). As the effects of climate change become increasingly evident — through rising temperatures, extreme weather events, and ecosystem disruptions — the transition to sustainable energy systems has become a central policy and research priority.

In this context, renewable energy sources and circular bio-based systems are gaining attention as viable alternatives to fossil fuels. Sweden, with approximately 68 % of its land covered by forests (SCB, 2023), has a strong foundation for bio-based energy production. In 2023, biofuels accounted for nearly 30 % of the country's total energy supply (Energimyndigheten, 2025). Moreover, Sweden generates substantial amounts of forestry residues — such as branches, tops, and sawmill by-products — that are currently underutilized for energy production (Börjesson et al., 2016; Hjort, 2019). Lignocellulosic biomass, although poorly suited for AD due to its high lignin content and low biodegradability (Xu et al., 2019), has been identified as a promising substrate for thermal gasification (Ren et al., 2020). Forestry residues represent a significant renewable CH_4 energy potential — estimated at up to 12 TWh/y — that could help to meet the growing biomethane demand, reduce fossil fuel dependency, and support both national and international climate goals. Given the growing concern about the "food vs. fuel" debate, using non-food biomass, such as lignocellulosic residues, is preferable to dedicating farmland to energy production.

3.2 Thermal Gasification and Syngas Composition

Thermal gasification is a thermochemical process that converts carbon-based feedstocks into syngas, a gas mixture primarily composed of H_2, CO, and CO_2, with minor amounts of other gases (e.g., N_2, CH_4) (Garcia-Casado et al., 2025).

The composition of syngas generated by gasification depends on several factors: biomass type, gasifier configuration (e.g., moving bed, fluidized bed), operating conditions (e.g., temperature and pressure), and the choice of gasification agent (EBA, 2024a). Common gasification agents include air, oxygen-enriched air, pure oxygen, and steam. The use of air results in syngas with a high nitrogen content, whereas steam gasification yields higher H_2 and CO concentrations (Molino et al., 2016). However, the resulting syngas composition determines its suitability for different downstream applications, such as direct use as a fuel or for biological conversion to CH_4, ethanol, or other products (Garcia-Casado et al., 2025).

Traditionally, gasification feedstocks have included fossil fuels such as coal (Minchener, 2005), but attention is increasingly shifting toward more sustainable alternatives (Taqvi et al., 2024). Promising options include lignocellulosic biomass residues from forestry and agriculture, byproducts from the production of first-generation biofuels (biodiesel and bioethanol) (Molino et al., 2016), and residual materials from conventional AD plants, which typically account for 50–70 % of the organic feedstock input (Luo et al., 2013). Other potential feedstocks include algal biomass (Milledge et al., 2014) and municipal solid waste, which is expected to increase steadily due to global population growth (Kumar et al., 2025). Considering that landfilling of organic waste — a practice that poses significant environmental risks — remains common even within the EU, gasification represents a more sustainable alternative for waste management and energy recovery.

Thermal gasification of forest biomass has already been demonstrated at industrial scale (Rauch et al., 2004; Larsson et al., 2019), e.g., in projects such as GoBiGas (Gothenburg, Sweden) or BioSNG (Güssing, Austria), as well as by companies such as Cortus Energy AB (Höganäs, Sweden).

3.3 Conversion of Syngas

Syngas serves as a versatile intermediate for a broad product portfolio and can be processed either chemo-catalytically, using metal-based catalysts, or biologically, via anaerobic microorganisms (Khosravani et al., 2023; Khalid et al., 2024).

The most well-known chemo-catalytic processes include the Fischer–Tropsch (FT) synthesis, which converts syngas into liquid hydrocarbons and

synthetic fuels; the Sabatier reaction, which transforms H_2 and CO_2 into CH_4; and methanol synthesis (Fig. 2). In addition, processes such as syngas-to-olefins and syngas-to-aromatics, using bifunctional catalysts, further expand the syngas-derived product spectrum. Key products of chemo-catalytic syngas conversion are shown in Figure 2: methanol (a platform chemical for fuels and plastics), dimethyl ether (DME; an alternative to LPG and diesel), light olefins such as ethylene and propylene (precursors for plastics), FT-fuels (e.g., gasoline, diesel, and jet fuel), synthetic natural gas (via methanation), and ammonia (via syngas-derived H_2 and N_2 in the Haber–Bosch process) (Khosravani et al., 2023; Khalid et al., 2024).

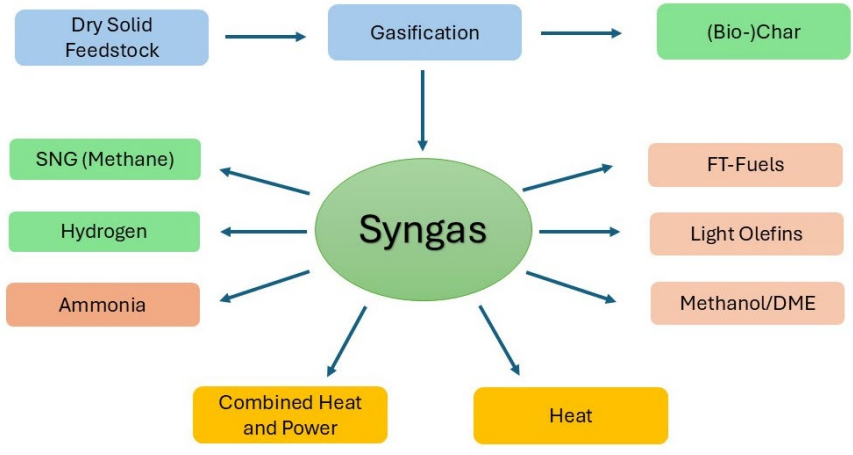

Figure 2. Catalytic syngas products and applications (adapted from IEA Bioenergy (2022)).

Chemo-catalytic methods typically require temperatures up to 550 °C and pressures of up to 350 bar (Khosravani et al., 2023). The catalysts used are sensitive to impurities and demand stable process conditions (Molino et al., 2016). Consequently, chemical syngas conversion is only economically viable at large industrial scales, where economies of scale significantly improve cost-effectiveness (Blumberg et al., 2017).

In contrast, biological syngas conversion is mediated by microorganisms (biocatalysts) capable of creating a wide range of products. The biological production of ethanol (as a biofuel and chemical precursor) and acetate (as a solvent and building block for plastics) is already implemented at industrial scale (Garcia-Casado et al., 2025), whereas other products such as methanol,

n-butanol (biofuel and industrial solvent), biopolymers (PHA), and biomethane have been successfully demonstrated at the laboratory scale (Grimalt-Alemany et al., 2017; Wainaina et al., 2018; Dhakal & Acharya, 2021; Khalid et al., 2024). Another promising biological product is H_2, which holds significant potential as a renewable and clean energy carrier. Moreover, certain fermenting bacteria can utilize intermediates such as syngas-derived acetate to produce CH_4.

Biological processes offer several advantages over chemo-catalytic methods. The involved microorganisms exhibit high tolerance to inhibitory impurities (e.g., H_2S or tar), which typically deactivate chemical catalysts (Ren et al., 2020). Furthermore, they can adapt to varying syngas compositions, unlike metal catalysts, whose activity is highly dependent on fixed gas ratios (Grimalt-Alemany et al., 2017). In addition, biological conversions are odorless, non-hazardous, and environmentally friendly, aligning well with the principles of sustainable production.

3.4 Conversion Routes for Biomethanation

Biological methanation is mediated in an anaerobic environment by microorganisms of the domains Archaea and Bacteria, typically at temperatures between 30 °C and 70 °C (Feickert Fenske et al., 2023c). This process can be divided into two closely related but distinct subdisciplines: biomethanation of H_2/CO_2 and biomethanation of syngas.

H_2/CO_2 biomethanation, also known as biological hydrogen methanation, is commonly applied for biogas upgrading with external H_2 addition. In this process, CO_2 in the biogas — typically accounting for 30–50 % in conventional AD systems (Angelidaki et al., 2018) — is converted into CH_4 by methanogenic archaea through the addition of exogenous H_2. This increases the CH_4 concentration in the product gas, enabling compliance with biomethane standards for gas grid injection or vehicle fuel production (Asimakopoulos et al., 2021a).

In contrast, syngas biomethanation is characterized by the presence of CO, which can inhibit microbial activity under certain conditions and increase the number of different involved species (Sancho Navarro et al., 2016; Grimalt-Alemany et al., 2017). Both processes face similar challenges, primarily the limited gas–liquid mass transfer due to the low solubility of H_2 and (in the case of syngas) CO in aqueous media, as well as low microbial

cell density in reactors. These factors reduce productivity compared to chemo-catalytic methanation (Grimalt-Alemany et al., 2017; Asimakopoulos et al., 2018). Thus, while both biomethanation processes share mechanistic similarities and allow for knowledge transfer, their comparability remains limited due to the presence of CO in syngas.

Despite these limitations and differences in substrate composition, both biomethanation processes ultimately rely on the conversion of H_2, CO_2, and (in the case of syngas) CO into CH_4 through distinct microbial pathways (Fig. 3).

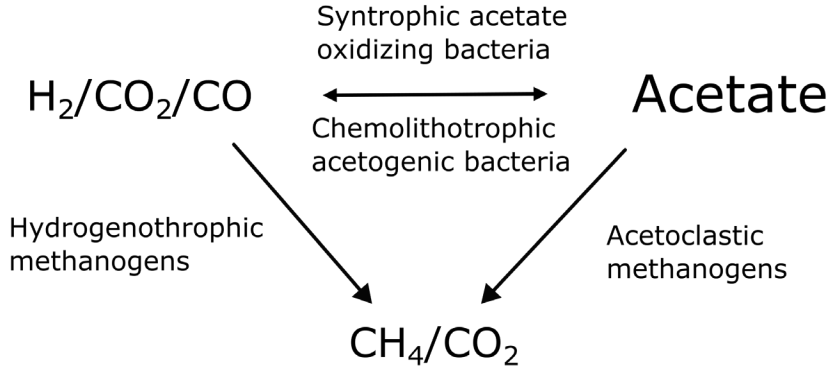

Figure 3. Microbial groups involved in biomethanation.

H_2, CO_2, and CO are converted into CH_4 either directly by hydrogenotrophic methanogenic archaea or indirectly via acetate as an intermediate, which is initially produced by acetogens via the Wood–Ljungdahl pathway and subsequently consumed by acetoclastic methanogens (Fig. 3). Under thermodynamically favorable conditions, acetate can be oxidized into H_2 and CO_2 by syntrophic acetate-oxidizing bacteria, in collaboration with hydrogenotrophic methanogens (Grimalt-Alemany et al., 2017). Biomethanation is further influenced by environmental factors such as temperature, pH, CO and H_2 partial pressures, and competition with other H_2-consuming microorganisms, including sulfate-reducing bacteria (Grimalt-Alemany et al., 2017; Feickert Fenske et al., 2023c).

Table 1 presents an overview of key microbial groups, their corresponding biochemical reactions, and their Gibbs free energy changes ($\Delta G°$).

Table 1. Biochemical reactions within syngas biomethanation mediated by different microbial groups and their corresponding Gibbs free energy change ΔG°; Adapted from Sancho Navarro et al. (2016).

Microbial group	Biochemical reaction	ΔG° [kJ/mol]
Hydrogenotrophic methanogens	$CO_2 + 4H_2 \rightarrow CH_4 + 2H_2O$	-131
Homoacetogens	$2CO_2 + 4H_2 \rightarrow CH_3COOH + 2H_2O$	-104
Acetoclastic methanogens	$CH_3COOH \rightarrow CH_4 + CO_2$	-31
Syntrophic acetate-oxidizing bacteria (SAOB)	$CH_3COOH + 2H_2O \rightarrow 4H_2 + 2CO_2$	+95
Carboxydotrophic methanogens	$4CO + 2H_2O \rightarrow CH_4 + 3CO_2$	-212
Carboxydotrophic acetogens	$4CO + 2H_2O \rightarrow CH_3COOH + 2CO_2$	-176
Carboxydotrophic hydrogenogens	$CO + H_2O \rightarrow CO_2 + H_2$	-20

3.4.1 Homoacetogenesis and Carboxydotrophic Acetogenesis

Acetogenic bacteria can produce acetate through chemolithoautotrophic pathways, utilizing inorganic compounds as both energy and carbon sources (Poehlein et al., 2025). However, acetogens are also metabolically versatile and can generate acetate from various organic substrates when such compounds are available in the nutrient medium. Depending on the available electron donor, acetate can be synthesized either from 4 mol of CO and 2 mol of H_2O (carboxydotrophic acetogenesis; Tab. 1) or from 4 mol of H_2 and 2 mol of CO_2 (homoacetogenesis). The central precursor in acetate formation is acetyl coenzyme A, which is synthesized via the Wood–Ljungdahl pathway, in which carbon monoxide dehydrogenase (CODH) acts as a key enzyme.

3.4.2 Carboxydotrophic Hydrogenogenesis (Water–Gas Shift)

Carboxydotrophic hydrogenogenesis, also known as the biological water–gas shift reaction, represents one of the most straightforward mechanisms of biological energy conservation. In this process, CO is oxidized and coupled with proton reduction to yield H_2 and CO_2 (Tab. 1). This reaction is catalyzed by three key enzymes: CODH, which facilitates CO oxidation; an electron transfer protein associated with CODH; and an energy-converting, membrane-bound hydrogenase (Diender et al., 2015).

3.4.3 Hydrogenotrophic Methanogenesis

Hydrogenotrophic methanogenic archaea, belonging to the phylum *Euryarchaeota*, conserve energy by converting CO_2 and H_2 into CH_4. Genera such as *Methanothermobacter*, *Methanobacterium*, and *Methanoculleus* are frequently detected in biomethanation systems and represent the primary archaeal groups responsible for CH_4 formation, particularly in combination with syntrophic acetate oxidation (Tab. 1) (Grimalt-Alemany et al., 2017; Feickert Fenske et al., 2023c). From a thermodynamic perspective, this pathway yields slightly more free energy (ca. 131 kJ/mol) than acetoclastic methanogenesis (Tab. 1), allowing hydrogenotrophic methanogens to persist even in relatively energy-limited environments.

3.4.4 Acetoclastic Methanogenesis

Only two known genera, *Methanosarcina* and *Methanothrix*, are capable of conserving metabolic energy by converting acetate into CH_4 (Stams et al., 2019). However, these organisms differ in substrate affinity and growth kinetics. *Methanothrix* has a high affinity for acetate and typically dominates in environments with low acetate concentrations. In contrast, *Methanosarcina* thrives under conditions with higher acetate levels due to its faster growth rate and greater metabolic versatility.

3.4.5 Carboxydotrophic Methanogenesis

The biological conversion of CO to CH_4 was first discovered in 1931. However, it has received relatively little research attention since then (Diender et al., 2015). To date, only a limited number of species have been reported to perform this direct conversion. Several studies suggest that it is not the preferred metabolic route during syngas biomethanation, as CO acts as a potent inhibitor of many enzymes (Sipma et al., 2003; Arantes et al., 2018; Grimalt-Alemany et al., 2019). Consequently, only a few microorganisms can tolerate and metabolize CO. According to Diender et al. (2016), the metabolic pathway responsible for CO-to-CH_4 conversion is thought to function similarly to hydrogenotrophic methanogenesis.

3.4.6 Syntrophic Acetate Oxidation

Syntrophic acetate oxidation (SAO) represents the reverse of homoacetogenesis, in which 1 mol of acetate is converted into 4 mol of H_2

and 2 mol of CO_2. This reaction is highly endergonic under standard conditions, with a Gibbs free energy change of +95 kJ/mol. Consequently, the reaction can only proceed if the partial pressure of H_2 is maintained extremely low (typically below 10^{-4} at 35 °C), thereby shifting the Gibbs free energy into the negative range (Lee & Zinder, 1988). This is achieved through collaboration with hydrogenotrophic methanogens, which efficiently consume H_2, rendering the SAO pathway thermodynamically feasible (Sancho Navarro et al., 2016). At higher (thermophilic) temperatures, the SAO reaction becomes less thermodynamically constrained, allowing it to tolerate higher H_2 levels while still proceeding favorably (Dolfing, 2014).

3.5 Influence of Process Parameters on Biomethanation

Establishing optimal growth conditions for both syngas and H_2/CO_2 biomethanation using mixed microbial consortia is challenging, as each microbial species within the community has its own preferred conditions, including pH, temperature range, and partial pressures of H_2 and CO (Grimalt-Alemany et al., 2017). Although complex, it is crucial to understand how these operational parameters affect the metabolic activities of archaea and bacteria within the mixed microbial consortium. Indeed, such knowledge provides key insights into the most favorable conditions for maximizing CH_4 productivity under stable conditions.

In addition to the continuous supply of H_2, CO, and CO_2, the microbial community requires essential nutrients for growth and efficient CH_4 production. These include macronutrients such as nitrogen (N) and sulfur (S), as well as micronutrients — particularly trace elements such as iron (Fe), nickel (Ni), and cobalt (Co) — which are critical for sustaining microbial metabolism and driving methanogenic activity. These compounds play vital roles in enzyme function, electron transport, and buffering capacity (Feickert Fenske et al., 2023c). Without adequate supply, process stability and syngas conversion rates decline, potentially resulting in process failure.

The following sections present selected parameters reported to have a significant influence on biomethanation.

3.5.1 Temperature

Temperature is well understood to play a critical role in the microbial community structure and activity within reactors inoculated with a non-defined mixed consortium (Grimalt-Alemany et al., 2019). Moreover, higher temperatures reduce the solubility of H_2, CO, and CO_2 in the liquid phase according to Henry's law (Sander, 2023).

As such, temperature becomes one of the most effective parameters of microbial selection once the feedstock is defined. Under mesophilic conditions, acetate acts as the key intermediate in the conversion of CO to CH_4. In contrast, under thermophilic conditions, CO is typically converted to H_2 and CO_2 via the biological water–gas shift reaction (hydrogenogenesis), followed by hydrogenotrophic methanogenesis (Grimalt-Alemany et al., 2017) (Tab. 1).

When syngas serves as the sole source of carbon and electrons, different microbial populations dominate at different temperatures. Under mesophilic conditions of around 37 °C, acetogenic bacteria such as *Sporomusa* and *Acetobacterium* (Arantes et al., 2018; Grimalt-Alemany et al., 2019), along with methanogenic archaea from the genera *Methanobacterium* and *Methanosaeta* (Arantes et al., 2018; Grimalt-Alemany et al., 2019), are typically prevalent. In contrast, thermophilic conditions between 50–65 °C favor the growth of carboxydotrophic hydrogenogens such as *Carboxydothermus hydrogenoformans*, and *Thermincola carboxydiphila* (Zhao et al., 2013; Grimalt-Alemany et al., 2019) as well as thermophilic methanogens such as *Methanothermobacter* (Bu et al., 2018; Grimalt-Alemany et al., 2019). SAO is also thermodynamically favorable at higher temperatures (Li et al., 2020).

Beyond determining the microbial community structure and metabolic pathways, temperature also significantly affects the kinetics of syngas biomethanation. For example, one study observed that CH_4 production under thermophilic conditions was twice that under mesophilic conditions when mixed microbial consortia were cultivated in biofilm-based sachets at 37 °C and 55 °C, respectively (Youngsukkasem et al., 2015). Additionally, hydrogenotrophic methanogenic activity increased 5.3-fold from 37 °C to 60 °C and 2.8-fold from 55 °C to 65 °C, reflecting that homoacetogens become less competitive with hydrogenotrophic methanogens as temperature rises (Grimalt-Alemany et al., 2019).

3.5.2 pH

Maintaining a stable pH is essential for the efficient and stable operation of syngas biomethanation. Hydrogenotrophic methanogens typically function within a narrow pH range of 6 to 8, with optimal activity occurring near neutral pH (Paniagua et al., 2022). In contrast, acetogens exhibit remarkable pH tolerance, with some strains capable of growing optimally across a broad pH range (5.4–9.8) when using syngas as the substrate (Bengelsdorf et al., 2018a).

For effective methanogenesis, maintaining a near-neutral pH is critical to prevent microbial inhibition and to sustain high CH_4 productivity.

3.5.3 Pressure and Syngas Composition

Reactor pressure and syngas composition, often expressed as the partial pressures of H_2, CO, and CO_2, are key factors that influence gas–liquid mass transfer, microbial kinetics, and the thermodynamics of syngas biomethanation (Grimalt-Alemany et al., 2017). In general, increasing the total pressure increases the solubility of gaseous substrates, thereby improving mass transfer and potentially increasing methane evolution rates (MERs). Significantly, the effects of pressure and composition are modulated by the microbial community's capacity and substrate toxicity.

Studies have shown that these theoretical improvements translate into practical gains. For example, Figueras et al. (2023) reported MERs of up to 23 $L/(L_{pbv} \cdot d)$ with >80 % conversion of H_2 and CO when operating a thermophilic 10 L continuous stirred tank reactor (CSTR) at 4 bar and a syngas containing 40 % H_2, 40 % CO, and 20 % CO_2. However, an earlier study using the same reactor configuration and syngas composition reported inhibition of CO conversion via carboxydotrophic hydrogenogenesis (biological water–gas shift) at a total pressure of 2 bar (Figueras et al., 2021). Thus, the benefits of elevated pressure may be limited by CO inhibition. Similar trends were observed in H_2/CO_2 biomethanation. Ullrich et al. (2018) demonstrated improved CH_4 productivity at 5 bar. However, further increases to 9 bar led to a decline in microbial activity, underscoring the existence of an optimal pressure window for these processes.

Aside from total reactor pressure, the partial pressures of individual syngas components play a decisive role in microbial activity. They not only determine the stoichiometric gas composition but also the maximum achievable CH_4 concentration in the product gas. A stoichiometric excess of

carbon-based gases, such as CO_2, leads to the accumulation of unconverted gases, whereas a surplus of electron donors (i.e., H_2) results in elevated residual levels in the product gas (Asimakopoulos et al., 2021a). Moreover, CO is toxic to numerous microorganisms, and elevated CO partial pressures can suppress microbial kinetics or even cause cell death (Hurst & Lewis, 2010). Sancho Navarro et al. (2016) investigated syngas biomethanation by anaerobic granular sludge, using CO as the sole substrate at partial pressures ranging from 0.1 to 1.5 atm. They observed the highest methanogenic activity at 0.1 atm, whereas methanogenesis was inhibited entirely at 1 atm. Maximum acetate accumulation occurred at 0.5 atm, indicating a shift toward acetate-mediated pathways, while acetoclastic methanogens were inhibited at partial pressures as low as 0.2 atm.

In contrast, no direct inhibitory effects of H_2 on microbial metabolism have been reported in syngas biomethanation (Andreides et al., 2021). However, H_2 partial pressure influences both pH and the thermodynamic feasibility of key microbial reactions such as carboxydotrophic hydrogenogenesis and SAO (Grimalt-Alemany et al., 2017). Furthermore, acetogens become more competitive at high H_2 partial pressures (Li et al., 2021). For instance, shifts in hydrogenotrophic methanogenesis rates can drive transitions between homoacetogenesis and SAO. When dissolved H_2 and CO_2 concentrations are low but sufficient to sustain hydrogenotrophic methanogenesis, a threshold acetate concentration exists below which homoacetogenesis is favorable, and above which SAO predominates (Grimalt-Alemany et al., 2019).

3.6 Reactor Setups for Biomethanation

The most commonly used reactor configurations for biomethanation of $H_2/CO/CO_2$ include the CSTR, the (hollow fiber) membrane bioreactor (MBR), and the TBR, each of which is presented in Figure 4 (Paniagua et al., 2022; Chatzis et al., 2024).

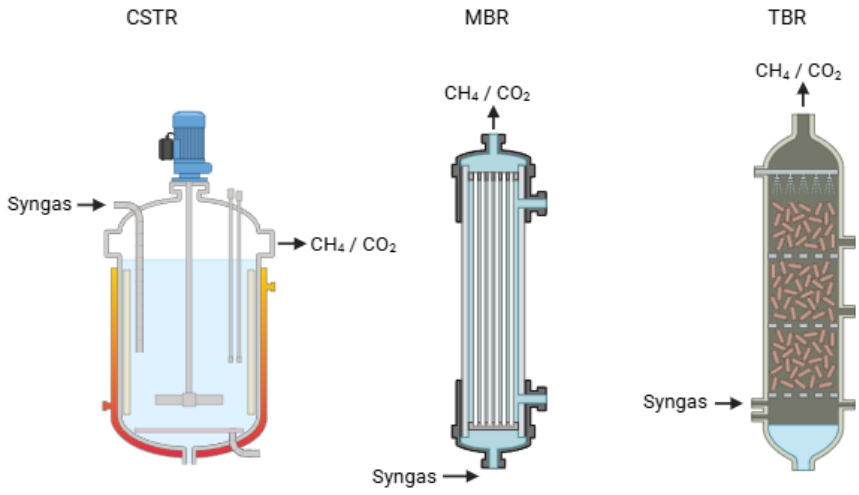

Figure 4. Common biomethanation reactor concepts, including CSTR (continuous stirred tank reactor), MBR (membrane bioreactor), and TBR (trickle-bed reactor) (created with BioRender.com).

Initial studies and scale-up efforts have primarily focused on CSTR. In this setup, microorganisms are suspended in the liquid phase, and the feed gas is bubbled through the medium. Mechanical stirring is used to reduce bubble size and promote homogeneous gas distribution, thereby enhancing contact between the microbes and the gas substrates (Asimakopoulos et al., 2018). As stirring speed increases, gas–liquid mass transfer increases, boosting the conversion rates of the feed gas (Yasin et al., 2015). However, this comes at the cost of significant energy consumption, which becomes even more critical during scale-up (Götz et al., 2016).

In contrast, TBRs and MBRs are based on biofilm processes and generally require less energy to operate. Membrane reactors represent a newer approach to biomethanation. These systems feature membranes submerged within a liquid phase, with microorganisms immobilized as a biofilm on the membrane surface. As feed gases diffuse through the membranes, the microbes convert them without bubble formation, resulting in more efficient substrate utilization (Asimakopoulos et al., 2018).

Due to their improved gas–liquid mass transfer characteristics, TBRs have garnered considerable research interest in recent years. While early research focused on CSTRs, the trend has now shifted toward TBRs (Asimakopoulos et al., 2018; Thema et al., 2019; Andreides et al., 2022; Ali

et al., 2024; Goonesekera et al., 2024). The concept of TBRs for syngas biomethanation dates back to the 1990s, with Kimmel et al. (1991); however, interest in the TBR technology surged following the publication by Burkhardt and Busch (2013), which led to a proliferation of studies on the topic, including those focused on the biomethanation of H_2/CO_2.

TBRs are vertically oriented, gas-filled columns packed with bio-carrier material. The process liquid is stored in a reservoir at the base and recirculated (trickled) over the packing material to supply nutrients to microorganisms immobilized on the packing surface. A packing medium with a high surface-to-volume ratio is preferred, as it provides ample space for microbial colonization and facilitates gas-substrate contact. Since the gas does not need to be sparged into the liquid, there is a reduced need for energy-intensive mixing and pressurized gas systems. TBRs are characterized by applied gas loads often together with the applied gas retention time (GRT), which defines the average duration of the gas remaining in the reactor´s packed bed (assuming no conversion). The high height-to-diameter ratio of TBRs enables near plug-flow operation, which can further improve CH_4 production by increasing the local partial pressure of the feed gas at the inlet (Feickert Fenske et al., 2023b).

Beyond the technical feasibility of TBRs, it is equally important to recognize the general operational thresholds for syngas biomethanation, particularly for TBRs, as these currently limit their reliability and scalability. The supply of syngas introduces a threshold, as elevated CO partial pressures pose toxicity risks that may impair microbial kinetics and compromise long-term reactor stability. Furthermore, hydraulic loading rates of nutrient medium and liquid recirculation strategies likewise impose operational limits: inadequate liquid recirculation (trickling) decreases nutrient delivery and biofilm hydration, whereas excessive rates promote biomass washout and hinder retention. Additionally, for the techno-economic viability of TBRs at an industrial scale, non-defined nutrient media, such as digestates, offer a cheap and widely available alternative, providing satisfactory nutrient concentrations for sustainable TBR biomethanation.

3.7 Nutrient Management in Biomethanation

The microorganisms situated on the biocarriers in the TBR require essential nutrients, which are supplied by recirculating the liquid phase and trickling

through the packed bed. To sustain microbial activity and ensure stable performance, an external addition of nutrient medium is necessary to maintain adequate nutrient concentrations in the liquid phase. Table 2 presents examples of studies on TBR biomethanation of H_2/CO_2 and syngas, categorized by the nutrient media used.

Table 2. H_2/CO_2 and syngas biomethanation TBR studies, along with the corresponding nutrient medium.

Gaseous Substrate	Nutrient Medium	References
H_2/CO_2	Defined nutrient medium (artificial stock solution)	(Rachbauer et al., 2016; Dupnock & Deshusses, 2017; Strübing et al., 2017; Strübing et al., 2018; Burkhardt et al., 2019; Dupnock & Deshusses, 2019; Dupnock & Deshusses, 2020; Thema et al., 2021)
	Cattle manure	(Ashraf et al., 2020; Dahl Jonson et al., 2020; Sieborg et al., 2020; Ashraf et al., 2021)
	Digestate	(Burkhardt et al., 2015; Porte et al., 2019; Jensen et al., 2021; Tsapekos et al., 2021; Ghofrani-Isfahani et al., 2022)
	Reject water (supernatant from digested sewage sludge)	(Strübing et al., 2019; Feickert Fenske et al., 2023a; Kamravamanesh et al., 2023)
Syngas	Defined nutrient medium	(Asimakopoulos et al., 2019; Asimakopoulos et al., 2021a; Asimakopoulos et al., 2021b)
	Digestate	(Andreides et al., 2022; Ali et al., 2024; Goonesekera et al., 2024; Bilgiç et al., 2025)

When targeting upscaling, a cheap, readily available nutrient source should be used. The use of defined media at pilot or industrial scale will necessitate significant preparation time and imply higher operational costs. Non-defined nutrient media, such as digestates or reject water from digested sewage sludge at wastewater treatment plants (WWTPs), provide a widely distributed nutrient source containing most of the required nutrient elements, thereby synergizing with existing biogas plants as well as WWTPs.

A recent study by Andreides et al. (2022) demonstrated that digestate can serve as a nutrient source for TBR syngas biomethanation; however, little

information is currently available on the optimal, maximum, and minimum levels of macronutrients and trace elements in such systems with mixed microbial consortia.

Numerous variables, such as the quantity of methanogens, the liquid recirculation regime, and nutrient bioavailability, may influence the required nutrient concentrations (Grimalt-Alemany et al., 2017; Feickert Fenske et al., 2023c). The following sections provide a more detailed overview of the current understanding of essential macronutrients and trace elements, as well as their threshold concentrations in TBR syngas biomethanation systems.

3.7.1 Macronutrients

The typical macronutrients required by methanogens include nitrogen (commonly supplied as ammonium, NH_4^+), sulfur, and sodium (Kamravamanesh et al., 2023). NH_4^+ supports biomass development and additionally acts as a buffer (Dupnock & Deshusses, 2019). Several studies have shown that NH_4^+ concentrations decline over time during TBR biomethanation (e.g., Kamravamanesh et al., 2023), which negatively affects H_2 consumption (Ashraf et al., 2021) and pH stability (Thema et al., 2021). At elevated temperatures and/or high pH, the equilibrium between NH_4^+ and NH_3 (free ammonia) shifts toward the latter, leading to severe inhibition of methanogenesis in AD (Chen et al., 2008). Optimum NH_4^+ concentrations in the TBR liquid are reported to range from 60 mg/L (Thema et al., 2021) to 1000 mg/L (Dupnock & Deshusses, 2019). High biomethanation performance was observed by Ashraf et al. (2021), Jønson et al. (2022), and Feickert Fenske et al. (2023a) when NH_4^+ concentrations in the process liquid ranged from 300 mg/L to 800 mg/L. Sulfur is another critical macronutrient element for methanogens, as they cannot utilize organic sulfur compounds and therefore rely primarily on sulfide (S^{2-}) for their metabolism (Shakeri Yekta et al., 2023). Sulfur has been identified as a limiting factor by several studies, and sodium sulfide (Na_2S) has therefore been used as a supplement to maintain sufficient sulfur availability (Rachbauer et al., 2016; Dupnock & Deshusses, 2017; Strübing et al., 2017; Strübing et al., 2018; Asimakopoulos et al., 2019; Dupnock & Deshusses, 2019; Strübing et al., 2019; Asimakopoulos et al., 2020; Thema et al., 2021). Strübing et al. (2017) assumed growth-limiting conditions for methanogenic archaea when the S^{2-} concentration in the process liquid was below 0.02 mM (0.64 mg S^{2-}/L). However, dissolved S^{2-} in the liquid phase is in equilibrium with H_2S in the

gas phase and can precipitate trace elements such as Fe, Ni, and Co (Feickert Fenske et al., 2023a), thereby reducing their bioavailability.

Feickert Fenske et al. (2023a) further hypothesized that different sulfur sources could enhance nutrient bioavailability and assessed the potential of using H_2S from biogas to meet methanogens' sulfur requirements. When H_2S was applied as the sole sulfur source, only half of the H_2S content in the biogas was detected in the resulting gas at high gas conversion rates (Feickert Fenske et al., 2023a). The H_2S concentration in the process liquid was only 0.01 mM, reflecting the low biogas H_2S concentration of 200 ppm. Consequently, Na_2S was added to achieve high biomethanation performance and to provide sufficient sulfur for microbial activity.

3.7.2 Trace Elements

Trace elements must be present at low concentrations for methanogens to grow. Fe, Ni, Co, and molybdenum (Mo) are commonly identified as the most essential trace elements for biomethanation (Feickert Fenske et al., 2023c). These elements can form chemical complexes with S^{2-}, which decreases their bioavailability. Fe is typically the most abundant trace element, followed by Ni, Co, and Mo. Dupnock and Deshusses (2019) suggested an optimal Fe concentration of 2 mg/L for H_2/CO_2 biomethanation, while Ashraf et al. (2021) reported a minimum value of 1.5 mg/L for syngas conversion. Kamravamanesh et al. (2023) reported comparably high Fe concentrations (>100 mg/L) that declined with increasing gas loads.

Other trace elements, such as zinc, tungsten, and boron, were detected in the defined nutrient media used in several experiments and were occasionally reported as relevant for methanogens (Rachbauer et al., 2016; Asimakopoulos et al., 2019). However, the literature remains inconclusive regarding which trace elements are necessary or can enhance biomethanation. Additions of Fe, Ni, Co, and Mo have been shown to increase CH_4 concentrations during H_2/CO_2 biomethanation (Kamravamanesh et al., 2023), whereas supplementation of zinc, copper, tungsten, and manganese had no significant effect.

It is important to note that when trace elements are added, the metal bonds of other trace elements may be replaced, making them accessible to methanogens once again (Salazar-Batres & Moreno-Andrade, 2025). Therefore, the addition of inexpensive trace elements with high binding

affinities, such as Fe, can be used to enhance the bioavailability of critical metals (e.g., Ni and Co) in TBR systems.

3.8 Syngas Biomethanation in Trickle-Bed Reactors

3.8.1 Choice and Supply Rate of Nutrient Media

The nutrient addition rate, often characterized by hydraulic retention time (HRT), is a key operational parameter that influences TBR syngas biomethanation. Across studies using non-defined nutrient media, a wide range of HRTs (5–31 d) has been applied, depending on reactor configuration and medium characteristics. For instance, Andreides et al. (2022) operated a 1 L TBR at an HRT of 5 days with no adverse effects on conversion rates despite suboptimal Fe concentrations, indicating that the biofilm's nutrient uptake capacity was not saturated. Conversely, Ali et al. (2024) and Goonesekera et al. (2024) used higher HRTs of 31.5 and 20 days, respectively. While Ali et al. (2024) reported stable performance, Goonesekera et al. (2024) observed decreased CH_4 productivity and CO conversion, which were subsequently improved by trace element supplementation.

Nevertheless, comparisons between studies based solely on the applied HRTs remain complicated because this parameter is strongly depending on the TBR setup — particularly the liquid reservoir volume. Transferring HRT and liquid reservoir volume into a new parameter that also accounts for the daily nutrient medium supply rate (NMSR) relative to the total packed bed volume could improve the comparability among studies in the literature.

3.8.2 Liquid Recirculation

Liquid recirculation is a defining feature of TBR operation that directly influences nutrient delivery and gas–liquid mass transfer (Feickert Fenske et al., 2023c). The recirculated liquid trickles over the packed bed, supplying nutrients to biofilm-embedded microbes while potentially impeding gas diffusion due to increased liquid film thickness (Sieborg et al., 2021). Therefore, optimizing the frequency and duration of liquid recirculation is essential for efficient syngas conversion and CH_4 productivity.

Both continuous and intermittent recirculation regimes have been explored (Asimakopoulos et al., 2021b; Bilgiç et al., 2025). Lower

recirculation rates or intermittent operations generally enhance gas–liquid mass transfer by reducing the liquid film thickness over the biofilm, thereby improving substrate accessibility. Previous studies have reported that CO-utilizing microorganisms are particularly sensitive to mass transfer limitations (Jensen et al., 2021). Each recirculation occasion can produce a temporary inhibitory effect on gas–liquid mass transfer, likely due to the transient coverage of the biofilm by nutrient liquid (Sieborg et al., 2021).

Importantly, the optimal recirculation regime depends on carrier material characteristics. Carrier liquid hold-up capacity (or water-binding capacity), which is influenced by porosity and surface area, determines how frequently recirculation is required. Clay-based carriers with high surface areas (up to ca. 1,000 m^2/m^3) can retain more liquid, enabling less frequent recirculation (e.g., once per day). In contrast, plastic carriers require more frequent recirculation due to their lower water hold-up capacity (Jensen et al., 2021).

Overall, effective liquid recirculation regimes in TBRs must consider not only the nutrient medium and applied syngas loads but also the physical properties of the carrier material. While continuous recirculation is not always necessary, the frequency and duration of trickling events should be optimized to maximize gas–biofilm contact and minimize disturbance in syngas conversion.

3.8.3 Change of Syngas Composition

Syngas composition plays a central role in determining the efficiency of biomethanation in TBRs, particularly in relation to conversion rates, CH_4 productivity, and the final quality of the product gas. The inhibitory effect of high H_2 partial pressure on CO_2 and CO conversion underscores the vital balance that syngas biomethanation optimization requires (Braga Nan et al., 2020; Li et al., 2021).

The Syngas Quality Index (SQI), introduced by Asimakopoulos et al. (2021a), serves as a helpful metric for defining target compositions. An SQI of 4 represents the optimal stoichiometric ratio of syngas components (H_2, CO, and CO_2) for complete conversion to CH_4.

However, due to energy losses associated with microbial growth and metabolic activity, an SQI above 4 should theoretically be selected for complete conversion of CO and CO_2. Yet, it is crucial to note that excessively high H_2 partial pressures can actually inhibit the biological conversion of

CO_2 and CO, counteracting the intended benefits and limiting CH_4 productivity.

Thus, further product gas upgrading may be necessary to achieve biomethane purities above 95 % and to fulfil other requirements — such as CO_2 limits — for injection into local or national gas grids. Ultimately, optimizing the syngas composition through gasification process control or subsequent conditioning (e.g., H_2 addition) is essential to ensure that TBR biomethanation produces gas streams meeting application-specific quality standards.

4. Methodology

This thesis is based on laboratory-scale experiments using two different TBR setups. Setup A consisted of a mesophilic 35 L TBR that was used exclusively in Paper I. Setup B comprised a thermophilic 5 L TBR that was employed in Papers II–IV. In Paper II, two identical TBR of this type were operated in parallel.

The main characteristics distinguishing the two TBR setups are summarized in Tables 3 and 4. Detailed descriptions of the materials and methods are provided in Papers I–IV.

Table 3. Characteristics of TBR setups A and B (Part I).

	Setup A	**Setup B**		
	Paper I	**Paper II**	**Paper III**	**Paper IV**
Volume (active packed bed) [L]	35		5	
Volume liquid reservoir [L]	5		1	
H:D ratio[1]	6		25	
Carrier material	Hiflow® ring 15–7, polypropylene, specific area 313 m^2/m^3	AnoxKaldnes K1 500, polyethylene, specific area 500 m^2/m^3		
Temperature [°C]	37 ± 1		56 ± 1	
Syngas composition				
H_2 [%]	56	40	40	40–71
CO [%]	30	30	30	30–14
CO_2 [%]	14	20	20	20–10
N_2 [%]	0	10	10	10–5
Total operation time [d]	862	381	282	126

[1] H:D ratio defines the correlation between height and diameter of a TBR.

Table 4. Characteristics of TBR setups A and B (Part II).

	Setup A	Setup B		
	Paper I	**Paper II**	**Paper III**	**Paper IV**
Liquid recirculation	Intermittent	Intermittent	Intermittent	Intermittent
Average Liquid Load [$L/(L_{pbv} \cdot d)$]	9.8	6.4	0.4–8.5	3.2
Inoculum	Digestate from mesophilic manure-based lab-scale digester	Mixture of four different digestates from thermophilic and mesophilic large-scale digesters (different substrates)		
Nutrient Media	Defined basal medium, reject water, diluted digestates	Reject water and diluted manure-based digestate	Diluted manure-based digestate	Diluted manure-based digestate
Nutrient Supplements	NH_4Cl, Na_2S, $NaSO_4$, Na_2CO_3	Na_2S KH_2PO_4	–	Na_2S

4.1 TBR Setup

Both TBR setups were constructed from acid-proof stainless steel and installed in a movable container together with all associated equipment. Both TBR setups were operated with intermittent liquid recirculation under different regimes and in a counter-current configuration, where the syngas entered the reactor below the packed bed and flowed upward, meeting the liquid that trickled downward through the column.

The different nutrient media utilized were supplied to the TBRs in a semi-continuous manner. In Paper I, nutrient addition was performed approximately once per week by adding a defined volume and simultaneously removing the same amount from the liquid reservoir to maintain a constant liquid volume. In Papers II–IV, the nutrient media were

pumped into the liquid reservoir 4–6 times per day, while the liquid volume was reduced to 1 L every 3–4 days.

Product gases were collected at the top of the TBR and passed through a condensed water trap, followed by a volume measurement, a gas dome, and a gas composition analyzer (CH_4, CO_2, CO, O_2, H_2) using an ETG MCA 100 Syn Biogas Multigas Analyzer (ETG Risorse e Tecnologia; Chivasso, Italy). Syngas flow rates were controlled via calibrated mass flow regulators (MFRs; Aalborg DPC17; Orangeburg, USA).

To enable carrier sampling, both TBR setups were equipped with larger sampling ports (Figs. 5–8). Volumetric data obtained from the MFRs and drum meters were manually recorded on working days.

4.1.1 TBR Setup A

The reactor in setup A had a total volume of 49 L, including head space and liquid reservoir, with an inner diameter of 215 mm and a total height of 1,344 mm (Fig. 5). The packed bed volume (pbv) was 35 L, and the liquid reservoir integrated in the column had a volume of 5 L (Tab. 3). A schematic visualization of TBR setup A is shown in Figure 5.

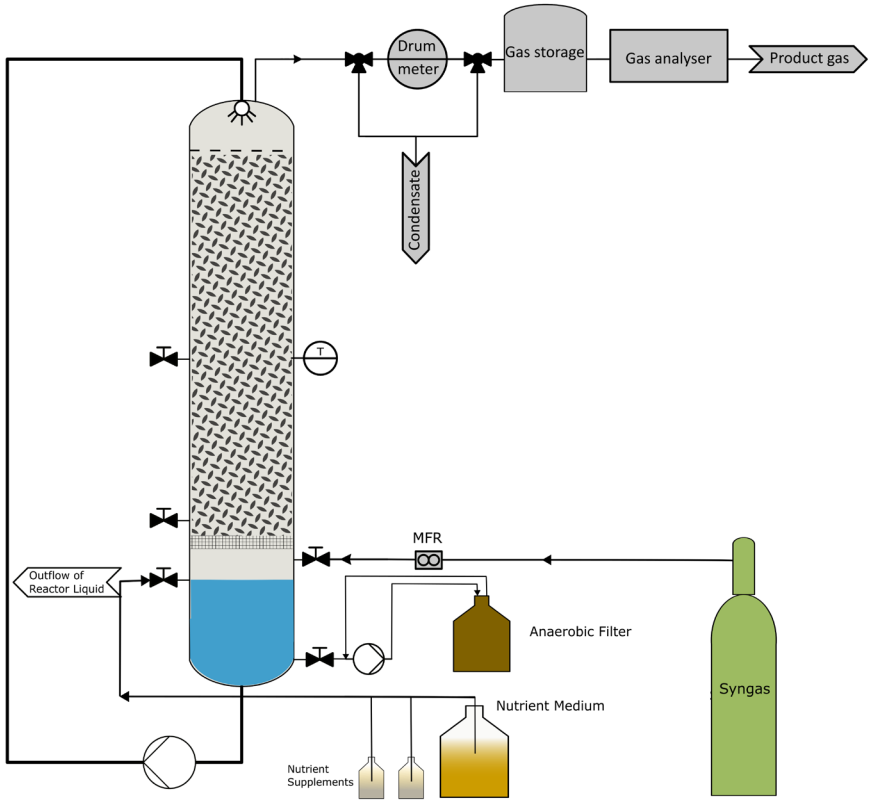

Figure 5. TBR setup A with V_{pbv} = 35 L and anaerobic filter (AF, day 200–862) used in Paper I.

The liquid phase was recirculated using a hose pump in intermittent mode, with 5 s of pumping followed by 37 s of stop time, resulting in an average flow of approximately 14.3 L/h and a liquid load of 9.8 L/(L_{pbv}·d).

After around 200 days of operation, an additional reactor — an anaerobic filter (AF) — was installed. The nutrient liquid from the bottom of the TBR was recirculated through the AF in an upflow configuration (Fig. 5). The purpose of installing the AF was to extend the hydraulic retention time for the nutrient liquid to recirculate and to promote the degradation of accumulated volatile fatty acids (VFAs). The AF was constructed from polyvinyl chloride and had a total active volume of 1.5 L (height = 190 mm, diameter = 100 mm). It was filled with the same type of inoculum and carrier

as the TBR; gas produced from this reactor was not collected. Figure 6 shows the assembled TBR setup A with all associated equipment (Paper I).

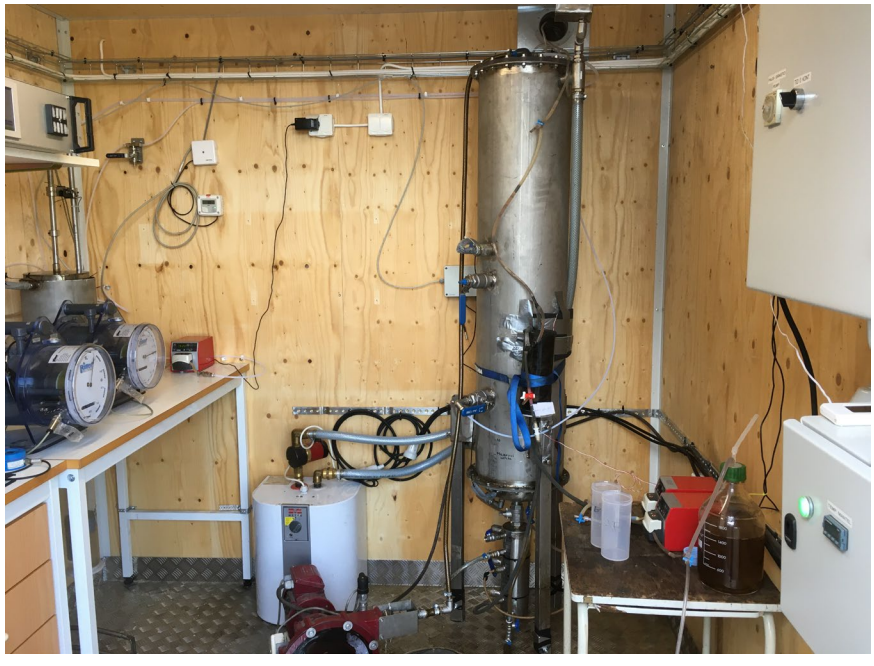

Figure 6. TBR setup A (V_{pbv} = 35 L) with assembled equipment.

4.1.2 TBR Setup B

Each TBR in setup B had a total volume of 7.5 L, including a liquid reservoir of up to 2 L, with an inner diameter of 72 mm and a total height of 1,782 mm. For biofilm growth, polyethylene carrier material was used, resulting in a total packed bed volume (pbv) of 5 L. The schematic visualization of TBR setup B is shown in Figure 7, while Figure 8 shows a photograph of the fully assembled setup during operation (Papers II–IV).

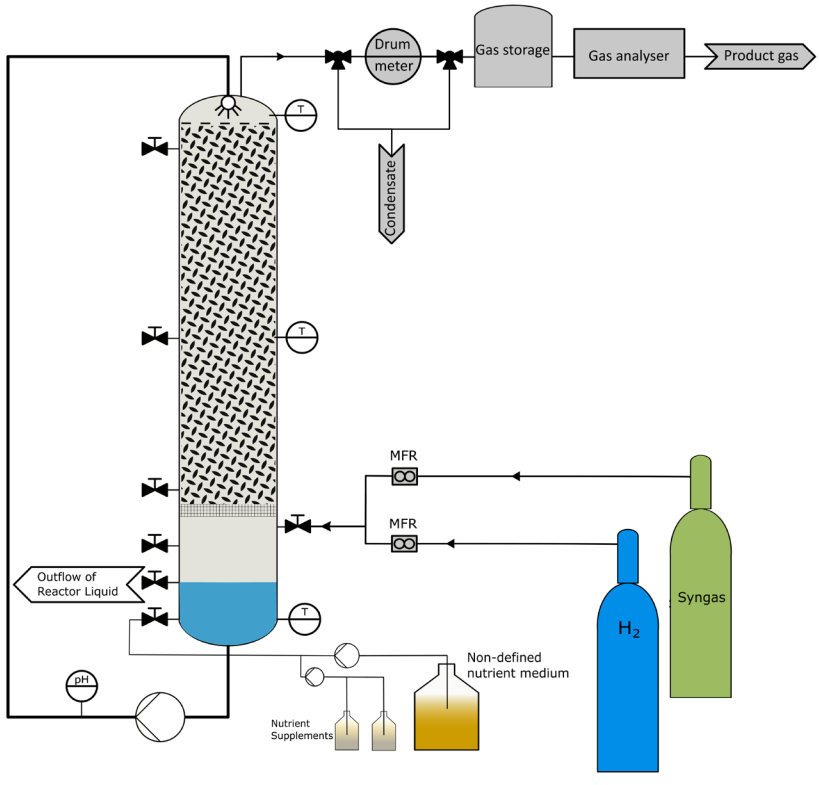

Figure 7. TBR setup B with V_{pbv} = 5 L used in Papers II–IV. Nutrient supplements were added only for TBR 2 in Paper II (day 209–382) and in Paper IV (day 774–824). Additional H_2 was only supplied in Paper IV (day 698–824).

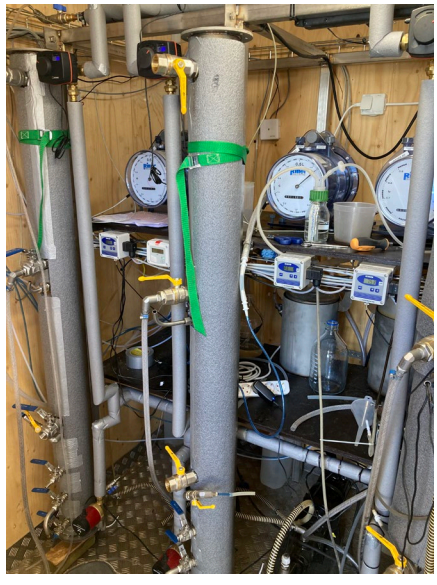

Figure 8. TBR setup B (V_{pbv} = 5 L) during operation (Papers II–IV).

4.2 Inoculum and Syngas

The inocula used in the TBRs were various digestates originating from either mesophilic lab-scale reactors (setup A) or mesophilic and thermophilic large-scale reactors operated on different substrates (setup B). In Paper I, several inocula were screened before selection; further details are provided in Papers I and II.

After inoculation, TBR setup A was gradually adapted to the syngas mixture used, which comprised 56 % H_2, 30 % CO, and 14 % CO_2. This composition corresponded to the expected target syngas from the WoodRoll® process developed by the industrial project partner Cortus Energy AB (Höganäs, Sweden).

TBR setup B was operated with a different syngas composition — 40 % H_2, 30 % CO, 20 % CO_2, and 10 % N_2 — to mimic the thermochemical conversion of forestry biomass as processed by the GoBiGas project (Gothenburg, Sweden) (Larsson et al., 2019). Nitrogen (N_2) was used as an inert placeholder for CH_4 originating from the gasification process. In Paper IV, the syngas composition was altered by increasing the H_2 concentration,

which consequently reduced the relative proportions of CO, CO_2, and N_2 (Tab. 2).

4.3 Nutrient Media

Different nutrient media were used across the operation of the TBRs. Detailed information on the nutrient media characteristics, pretreatment procedures, sampling occasions, etc., is provided in Papers I–IV. Table 5 summarizes the key chemical characteristics of the nutrient media used before their application in the TBRs.

Table 5. Characteristics of different nutrient media utilized in Papers I–IV

	Unit	Defined Media	Digestate[1]	Reject water[2]	Digestate[3]	Reject water[4]
Used in Paper		I	I	I	II–IV	II
pH	–	7.2	7.9	7.8	8.5–8.7	8.2–8.5
Alkalinity	mg $CaCO_3$/L	2,320	9,080	1,000–3,600	5,000–8,800	7,300
VFA (total)	g/L	NA	0.1–0.3	NA	0.1–0.2	0.4
NH_4^+	mg/L	405*	300–1,430	560–800	200–1,100	740
SO_4^{2-}	mg/L	–*	147–441	320	150–380	10
PO_4^{3-}	mg/L	5*	NA	NA	20–70	2

[1] Digestate from thermophilic AD operated mainly on food waste, Uppsala, Sweden
[2] Reject water from the digested sewage sludge from a WWTP in Höganäs, Sweden
[3] Digestate from agricultural AD operated mainly on manure, Lövsta, SLU, Uppsala, Sweden
[4] Reject water from digested sewage sludge from a WWTP in Uppsala, Sweden
* Based on recipes described in Paper I and Westerholm et al. (2010). Sulfur source was Na_2S (240 mg/L)
NA – not analyzed

For TBR setup A (Paper I), three different nutrient media were used: defined medium, digestate from a thermophilic biogas plant (Uppsala, Sweden) operated on mixed food waste, and reject water (from digested sewage sludge) from a municipal WWTP (Höganäs, Sweden). Prior to application, one unit of the utilized digestate was mixed with two units of deionized

water. These nutrient media were added to the same reactor in the order listed above over the total operation time of 862 days.

For TBR setup B (Paper II–IV), digestate from a mesophilic biogas plant primarily operated on manure (Lövsta, SLU, Uppsala, Sweden) was used as nutrient medium for TBR1. The digestate was sieved (1 mm) and diluted (1:1) with tap water before application to the TBR to reduce the risk of clogging in the TBR column and associated TBR equipment (e.g., pumps and hoses). Reject water from the digested sewage sludge treatment at the WWTP in Uppsala (Sweden) was used for TBR2, which was operated until day 382 (Paper II). No sterilization of the non-defined nutrient media was performed.

Nutrient supplements providing N (NH_4Cl), S (Na_2S, $NaSO_4$), and P (KH_2PO_4), as well as Na_2CO_3 to increase buffer capacity, were added to the TBRs as described in the following section and in Papers I, II, and IV.

4.4 TBR operation

4.4.1 TBR operation Setup A

After the start-up and acclimatization phase, the TBR operation was divided into three main periods according to the nutrient medium applied. Each period was further subdivided into two sub-phases based on significant operational adjustments, the installation of the AF, or changes in nutrient flow and composition. The main operational periods are summarized below, while further details are provided in Paper I.

Start-up and acclimatization (day -129–0)

During this phase, the microbial community was gradually adapted to the reactor conditions and syngas. A defined nutrient medium (Westerholm et al., 2010) was supplied at a low flow rate, and the inlet gas composition ($CO:N_2$ ratio of 15:85) was adjusted to enrich CO-consuming bacteria.

Defined medium (day 0–241)

Day 0 marked the start of this operational period, during which syngas with the target industrial composition (56 % H_2, 30 % CO, and 14 % CO_2) was introduced. Volatile fatty acids (VFAs) began to accumulate, prompting the installation of an AF. To address possible nutrient limitations and increase

the buffer capacity, additional sulfur (Na_2S) and nitrogen (NH_4Cl) sources were supplied to the TBR.

Digestate (day 241–441)

The nutrient medium was switched to diluted digestate. An initially high flow rate was later reduced as operation progressed. Additional sulfur (Na_2S or $NaSO_4$) was periodically supplemented to support gas conversion when performance began to decline.

Reject water (day 442–662)

Reject water was used as the nutrient medium, and its addition rate was gradually decreased over time. Supplementation of sulfur (Na_2S or $NaSO_4$) and sodium bicarbonate (Na_2CO_3) was applied to maintain reactor performance and stabilize pH levels.

4.4.2 TBR operation Setup B

Based on the insights from Paper I, the decision was made to place greater focus on developing the H_2 and CO conversion rates and maintaining them above a certain threshold. To prevent VFA accumulation in the reactor liquid and avoid process instabilities, operational guidelines were established to maintain H_2 and CO conversion rates above 90–95 %. Additionally, to reduce syngas consumption, the TBR packed bed volume was reduced from 35 L to 5 L. The operational temperature was also changed from mesophilic (setup A) to thermophilic (56 ± 1 °C) in setup B to improve CH_4 productivity and the conversion rates of H_2 and CO.

Paper II - comparison of digestate and reject water (day 0–381)

Operation commenced with the inoculation of two identical TBRs (day 0), followed by a gradual increase in syngas load. During the start-up period (until day 62), no external nutrient sources were added to the TBRs, and only internal recirculation of the inoculum was performed. Thereafter, the reactors were operated on diluted digestate (TBR1) and reject water (TBR2).

Their operation was categorized into several periods based on the applied HRTs of the nutrient media (15 d and 7.5 d) and the addition of nutrient supplements (Paper II). TBR1 and TBR2 were operated for 370 and 381 days, respectively. Following this period, TBR1 remained in operation for subsequent studies (Papers III and IV), whereas TBR2 was terminated.

For TBR1, aside from the addition of diluted digestate, no further nutrient solution was added. In contrast, TBR2 received additional S and P starting on days 209 and 308, respectively.

The nutrient liquid was intermittently recirculated with 20 s of pumping every 10 min (144 d^{-1}) at an average flow rate of 40 L/h. This resulted in a nutrient liquid load of 6.4 L/(L_{pbv}·d) (Tab. 2).

Paper III - Nutrient medium supply rate and liquid recirculation regime (day 381–665)

In this study, only TBR1 was used, as it demonstrated more stable operation and higher CH_4 productivity than TBR2.

The first part of the experiments (until day 564) assessed different nutrient medium supply rates (NMSRs), ranging from 11 to 22 mL/(L_{pbv}·d), corresponding to HRTs of 8.9 d to 18 d.

In the second part (until day 665), the liquid recirculation regime was evaluated by changing its frequency (8, 16, 32, 48 d^{-1}) and duration (20, 40, 80 s), applying liquid loads between 0.4 and 8.5 L/(L_{pbv}·d) (Tab. 2).

Paper IV - Increase of H_2 concentration (day 665–824)

Before the start of the study, a conversion recovery period of 33 d was conducted, during which both the HRT and syngas loads were reduced, while liquid recirculation was increased.

For Paper IV, the liquid recirculation was set to a liquid load of 3 L/(L_{pbv}·d), with a frequency of 72 d^{-1} and 20 s on-time.

The experimental phase began on day 698 by changing the inflow syngas composition, increasing the H_2 share while reducing the concentrations of CO, CO_2, and N_2 (Tab. 2). On day 774, S supplementation was initiated by adding 10 mL/d of a 1 g/L Na_2S solution.

4.5 Analytical methods and sampling

Across all studies, process liquid was regularly withdrawn from the liquid reservoir for chemical and microbial analyses — at least once a week in Paper I and typically every 3–4 days in Papers II–IV. Carrier material was sampled at selected time points, typically in connection with operational changes such as shifts in nutrient media or the beginning and end of specific study periods.

Ammonium (NH_4^+), sulfate (SO_4^{2-}), and phosphate (PO_4^{3-}) concentrations were analyzed using a spectrophotometer (Spectroquant® Nova 60A photometer; MilliporeSigma, Burlington, Massachusetts, United States) and Supelco reagent test kits (Merck, Darmstadt, Germany). Total alkalinity was calculated as the amount of acid required to lower the sample pH to 4.4 by titration with an automatic titrator (TitraLab® AT1000 series; Hach, Düsseldorf, Germany). Concurrently, pH was measured with a Hanna HI83141 pH meter (Woonsocket, Rhode Island, United States).

VFAs were analyzed by high-performance liquid chromatography as described by Westerholm et al. (2012). The concentration of H_2S was regularly measured using Kitagawa Gas Detector Tubes No.120SD (Komyo Rikagaku Kogyo, Japan). Micronutrients and trace elements were analyzed externally by an accredited laboratory according to SS-EN ISO 17294-2:2016 and SS-EN ISO 11885:2009.

4.6 Microbial analyses

DNA extraction for microbial community analysis was performed on both liquid samples and carrier biofilms collected from the TBRs. Carrier samples were occasionally scraped and pooled to obtain enough biomass. Detailed methodological information is provided in Papers I–IV.

All DNA extractions were performed using the FastDNA Spin Kit for Soil (MP Biomedicals, France) with minor modifications, such as extended centrifugation (10 min at 14,000 RCF), matrix settling, and an additional cleaning step with humic acid wash solution containing guanidine thiocyanate to remove polymerase chain reaction (PCR) inhibitors.

Carrier biofilm extractions were often performed in triplicate or quadruplicate to collect enough material.

Sequencing libraries targeting the 16S rRNA gene were prepared using Illumina MiSeq (2 × 300 bp) by SciLifeLab (Stockholm, Sweden) or Novogene (Munich, Germany), following the protocols established by Westerholm et al. (2018). Paired-end reads were trimmed (typically to 250–300 bp), processed using the DADA2 pipeline in R (various versions), and truncated the forward and reverse reads at positions 240/180bp and 160/200bp, respectively.

Amplicon sequence variants (ASVs) were aligned using MAFFT or DECIPHER, and phylogenetic trees were constructed using FastTree or

phangorn. Community structures were visualized and analyzed using weighted UniFrac-based Principal Coordinate Analysis (PCoA). Data analysis and visualization were performed in RStudio using phyloseq and a suite of other R packages (e.g., ggplot2, plotly, vegan, lattice).

ASV identities were further confirmed via BLAST against the NCBI database, acknowledging that short read lengths (ca. 250–300 bp) limit species-level resolution. Raw sequence data were deposited in NCBI under project IDs PRJNA796200, PRJNA1276488, PRJNA1275821, PRJNA1345548, and PRJNA1268893.

In Paper II, quantitative PCR (qPCR) targeting the mcrA gene was used to quantify methanogens using specific primers (mcrA-F3/mcrA-rev). DNA standards were prepared by cloning PCR-amplified fragments into vectors and sequencing the inserts.

4.7 Performance Indicators

The average inflow-based hydraulic retention time (HRT) of the nutrient media [d] was calculated based on the addition rate of fresh nutrient medium V_M [L/d] to the reactor and the total liquid volume V_L in the reactor (1 L), as follows:

$$HRT = \frac{V_L}{V_M} \qquad \text{(Eq. 1)}$$

To enable comparability of the nutrient addition strategies among the literature, the nutrient medium supply rate (NMSR) [mL/(L_{pbv}·d)] was calculated by dividing the addition rate of fresh nutrient medium [mL/d] by the total packed bed volume (V_{pbv} = 5 L) of the TBR (Eq. 2).

$$NMSR = \frac{V_M}{V_{pbv}}/1000 \qquad \text{(Eq. 2)}$$

The methane evolution rate (MER) [L/(L_{pbv}·d)] was calculated as shown in Eq. 3, where F_{out} [L/(L_{pbv}·d)] denotes the total normalized product gas flow rate (1013.15 mbar, 273.15 K) including moisture and c_{CH4} represents the CH_4 fraction in the product gas originating from the conversion of H_2, CO, and CO_2.

$$MER = F_{out} * c_{CH4} \qquad \text{(Eq. 3)}$$

The conversion rate [%] of H_2 and CO was calculated according to Eq. 4, where F_i *in* is the normalized flow rate of the respective gas component in the inlet gas [L/(L_{pbv}·d)] and F_i *out* is the normalized flow rate of the same component in the product gas from the TBR.

$$conversion\ rate = \frac{F_i\ in - F_i\ out}{F_i\ in} * 100 \qquad \text{(Eq. 4)}$$

The inflow-based gas retention time (GRT) [h] was defined as the average residence time of the gas within the packed bed volume, assuming no gas conversion, according to Eq. 5, where V_{pbv} is the active packed bed reactor volume [mL] and F_{in} is the total normalized inflowing gas flow rate [mL/h].

$$GRT = \frac{V_{pbv}}{F_{in}} \qquad \text{(Eq. 5)}$$

5. Results

5.1 Nutrient Media Management

5.1.1 Assessment of Defined and Non-Defined Media (Paper I)

After the inoculation and adaptation phase, the final syngas mixture (56 % H_2, 30 % CO, 14 % CO_2) was applied to the TBR using a defined nutrient medium with an NMSR of 4 mL/(L_{pbv}·d), corresponding to an HRT of 35 d. During the first period, the syngas inflow rate varied between 1.1 and 3.3 L/(L_{pbv}·d) and was adjusted based on H_2 and CO conversion rates (Fig. 9a). The highest MER reached up to 0.9 L/(L_{pbv}·d) (Fig. 9b). Despite decreasing syngas loads, the VFA concentration in the TBR liquid increased to over 1.8 g/L, leading to the decision to install an anaerobic filter (AF) to increase the HRT and thereby enhance VFA consumption. However, alongside increasing syngas loads in period 1B, VFAs again rose to levels above 3.7 g/L (Fig. 9c).

In period 2, the nutrient medium was changed to diluted digestate, initially with an NMSR of 29 mL/(L_{pbv}·d), corresponding to an HRT of 5 d. Syngas loads were slightly increased to approximately 4 L/(L_{pbv}·d), which led to MERs of 0.9–1.1 L/(L_{pbv}·d). In period 2B, the NMSR was reduced to 6 mL/(L_{pbv}·d) (HRT of 25 d), while syngas loads were increased, resulting in lower conversion rates but no increase in CH_4 productivity. To address the assumed S limitation, Na_2S or Na_2SO_4 was added during period 2B, improving syngas conversion and CH_4 productivity without VFA accumulation.

In period 3, reject water was used as the nutrient medium at NMSRs of 11 and 6 mL/(L_{pbv}·d), corresponding to HRTs of 12.5 and 25 d, respectively. At both NMSRs, S supplementation was required to maintain stable process performance. The applied syngas loads and MERs reached approximately 5 L/(L_{pbv}·d) and 1–1.2 L/(L_{pbv}·d), respectively (Fig. 9). Sodium carbonate (Na_2CO_3) was added to counteract pH drops below 6.4. No VFA accumulation was observed during this period.

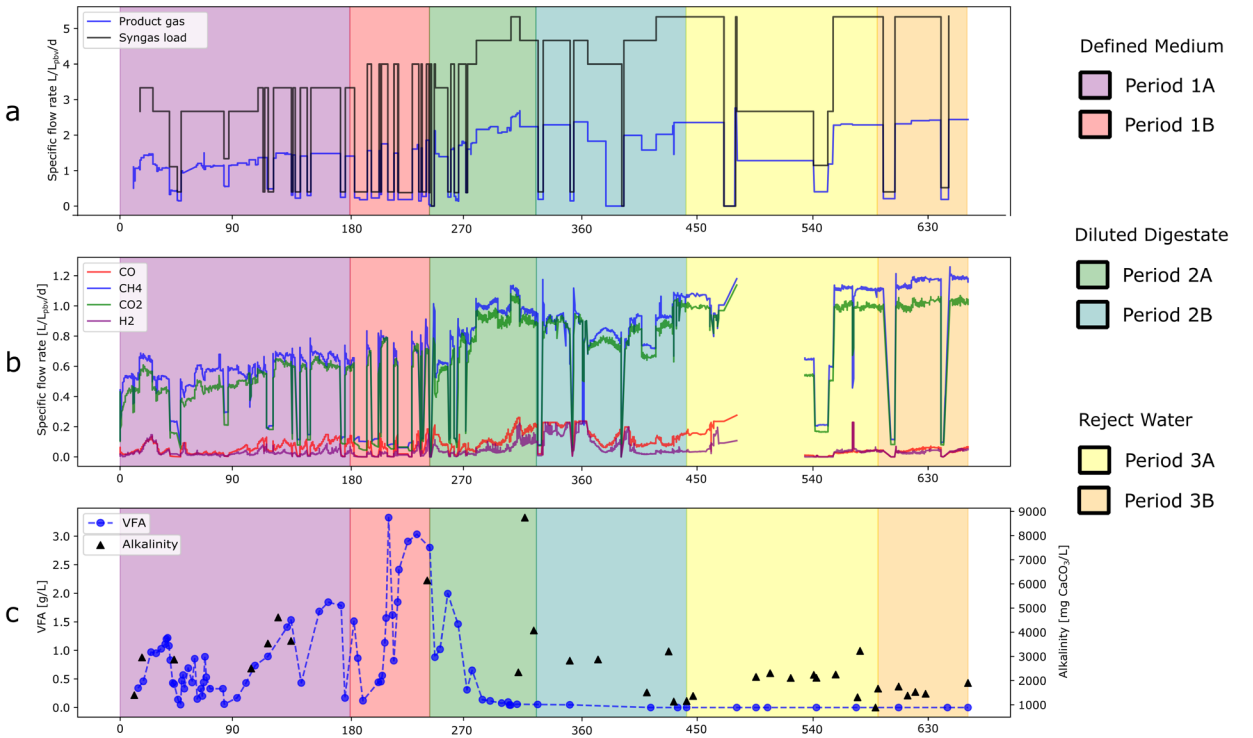

Figure 9. Process data from Paper I. (a) Syngas load (black) and product gas flow rate; (b) Specific outflow gas rates. The gap seen in period 3A was due to a gas analyzer malfunction; (c) Total volatile fatty acids (VFAs) concentration and alkalinity.

In the microbial community, the acetogen *Sporomusa sphaeroides* and the methanogen *Methanobacterium bryantii* were identified as the core functional microorganisms throughout the operation in Paper I. The community composition responded strongly to changes in the nutrient media used and operational conditions, including VFA accumulation and pH changes. The increase of *Acetobacterium* in period 3 indicates a shift toward enhanced acetate production under more stabilized conditions.

5.1.2 Comparison of Digestate and Reject Water as Nutrient Media (Paper II)

To prevent VFA accumulation in the reactor liquid and avoid process instabilities, TBR setup B was operated in accordance with guidelines to maintain H_2 and CO conversion rates above a defined threshold (>90 % in Paper II). The operating temperature was shifted from mesophilic (setup A) to thermophilic (56 ± 1 °C) in setup B.

After inoculation of TBR1 and TBR2, both reactors achieved >99 % H_2 and CO conversion rates during the 62-day start-up period without any external nutrient addition (Fig. 10b). At a syngas load of approximately 5.3 L/(L_{pbv}·d) and a corresponding MER of approximately 0.9 L/(L_{pbv}·d), nutrient concentrations, alkalinity, and H_2S levels in the product gas decreased (Fig. 11), indicating nutrient limitation.

In TBR1, diluted digestate was added from day 62 with an NMSR of 13 mL/(L_{pbv}·d) (HRT 15 d). H_2 and CO conversion rates initially remained high but later declined as NH_4^+ and alkalinity dropped at around day 110 (Fig. 10). To counteract this, the NMSR was increased to 27 mL/(L_{pbv}·d) (HRT 7.5 d), which restored nutrient levels and raised H_2 and CO conversion rates back to >99 %. Subsequently, the syngas load was gradually increased to 28 L/(L_{pbv}·d), resulting in a maximum MER of 4.5 L/(L_{pbv}·d) (Fig. 10). The later decline in H_2 and CO conversion rates was unlikely due to macronutrient limitations, as sufficient levels of N, P, and S were detected in the TBR liquid and product gas (Fig. 11) at an NMSR of 27 mL/(L_{pbv}·d). Instead, decreased conversion was likely caused by limitations in gas–liquid mass transfer at higher syngas loads or shorter GRTs (Fig. 10a).

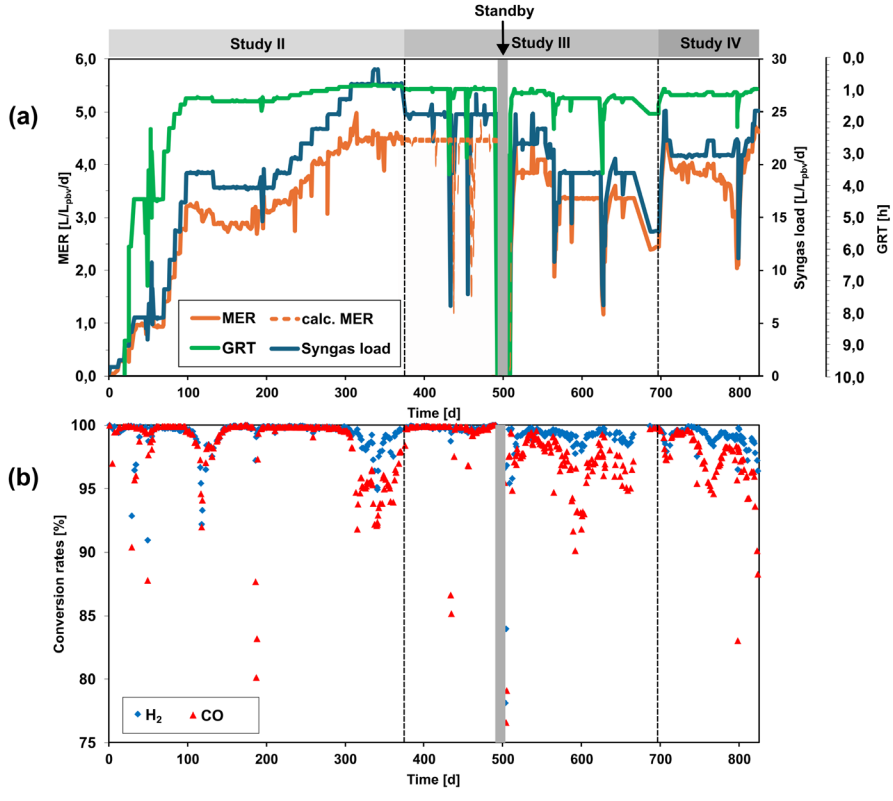

Figure 10. TBR1: (a) Development of syngas load, GRT*, and MER; (b) H_2 and CO conversion rates.

*TBR1 started with a GRT of 35 d, which is beyond the scale.

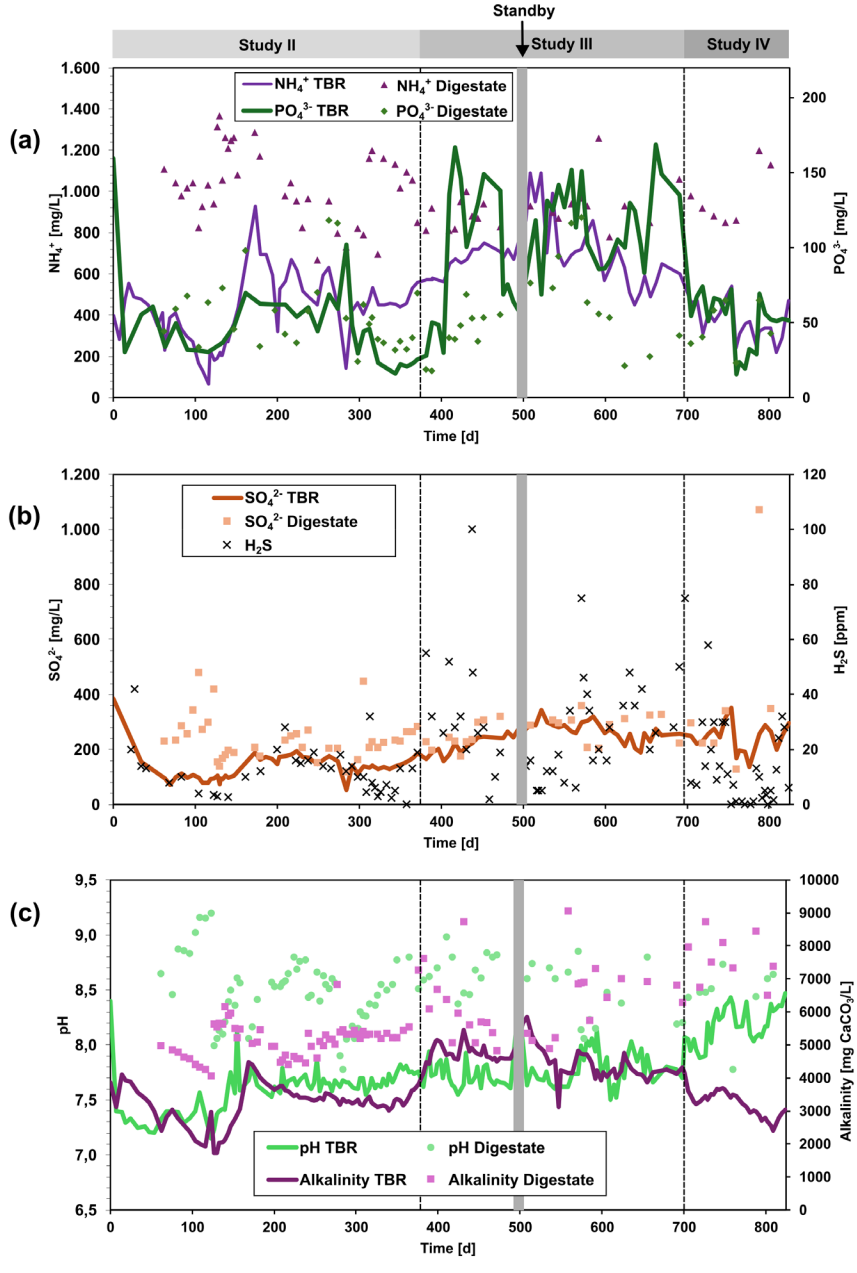

Figure 11. TBR1: a) NH_4^+ and PO_4^{3-} levels of TBR liquid and digestate; (b) SO_4^{2-} levels of TBR liquid and digestate, and H_2S concentration in the product gas; (c) pH and alkalinity of TBR liquid and digestate.

For TBR2, the inoculation and the start-up period were conducted identically to those of TBR1. Reject water was supplied to TBR2 from day 62 at an NMSR of 13 mL/(L_{pbv}·d) (HRT 15 d). As observed for TBR1, declining nutrient concentrations and alkalinity likely caused a reduction of H_2 and CO conversion rates by day 100 (Fig. 12). From day 109 onward, the NMSR was increased to 27 mL/(L_{pbv}·d) (HRT 7.5 d). However, H_2 conversion rates remained low (85–90 %) until the syngas load was reduced (Fig. 12). Despite the increased NSMR, liquid concentrations of S and P remained low due to their low levels in the reject water, resulting in the absence of H_2S in the product gas and a recurring decline in H_2 conversion between days 160–170. The maximum MER in that period was approximately 1 L/(L_{pbv}·d).

On day 209, Na_2S supplementation was initiated, which increased bioavailable S levels and improved H_2 and CO conversion rates. The syngas load was gradually increased; however, CO conversion declined slightly at higher syngas loads of 15 L/(L_{pbv}·d), corresponding to a MER of 2.2 L/(L_{pbv}·d), around day 300.

Due to a suspected P limitation, KH_2PO_4 supplementation began on day 308. Only after increasing its concentration tenfold on day 341 did PO_4^{3-} levels rise (Fig. 13), improving CO conversion rates and resulting in a maximum MER of 3.1 L/(L_{pbv}·d).

Even with S and P supplementation, the use of reject water as a nutrient medium did not achieve the same H_2 and CO conversion rates or MER as digestate (TBR1).

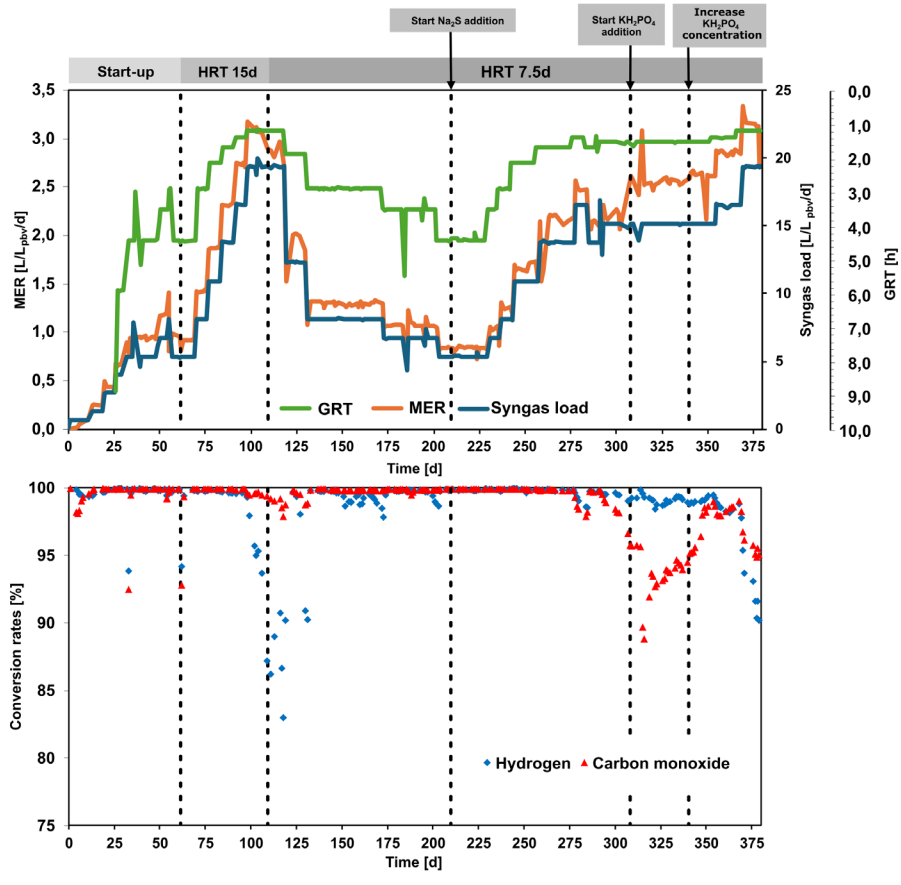

Figure 12. TBR2: (a) Development of syngas load, GRT*, and MER; (b) H_2 and CO conversion rates; (c) NH_4^+ and PO_4^{3-} levels of TBR liquid and reject water; (d) SO_4^{2-} levels of TBR liquid and reject water, and H_2S concentration in product gas; (e) pH and alkalinity of TBR liquid and reject water.

*TBR2 started with a GRT of 35 d, which is beyond the scale.

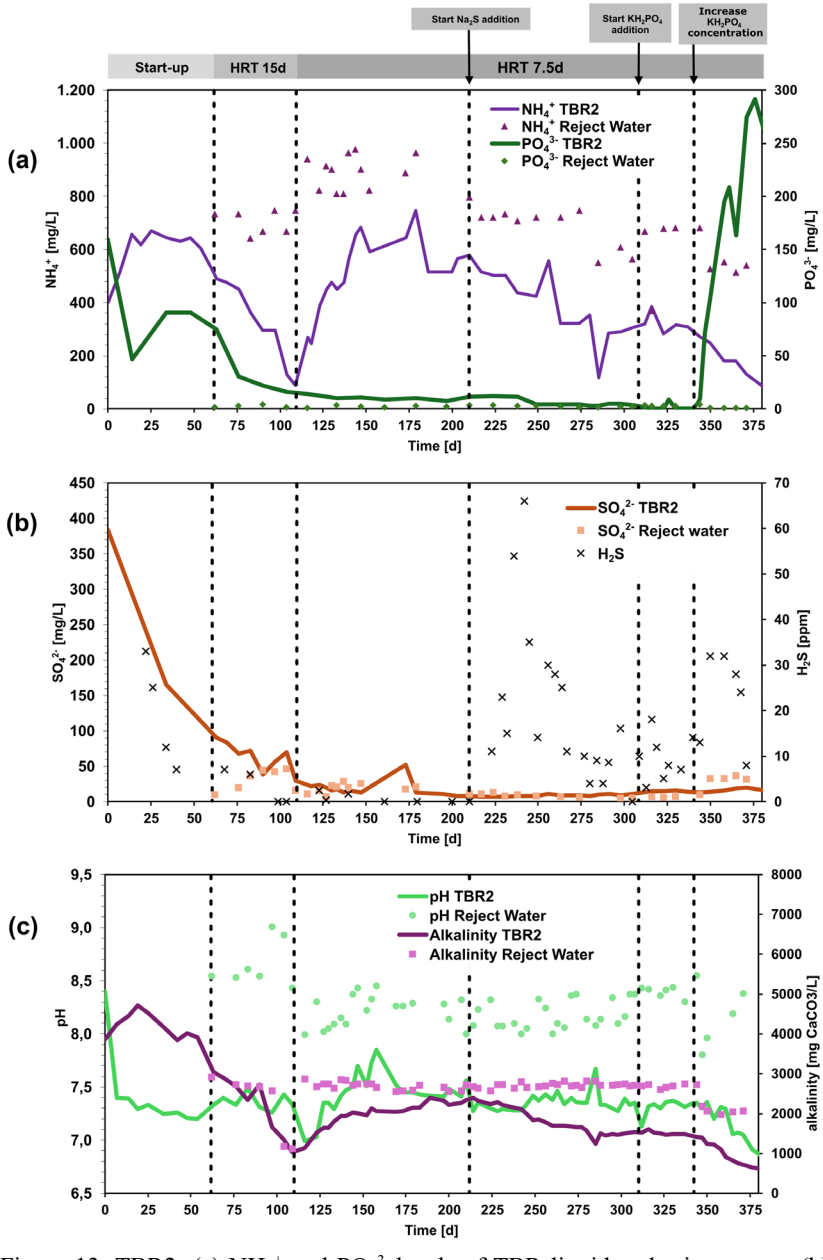

Figure 13. TBR2: (a) NH_4^+ and PO_4^{3-} levels of TBR liquid and reject water; (b) SO_4^{2-} levels of TBR liquid and reject water, and H_2S concentration in product gas; (c) pH and alkalinity of TBR liquid and reject water.

Microbial community analyses of both the liquid phase and carrier biofilms revealed no major differences between TBR1 and TBR2, despite the utilization of different nutrient media and operational variations (i.e., syngas load, H_2 and CO conversion rates, and MER). Although minor differences were observed in the liquid-phase communities during the early stages, both reactors gradually developed similar microbial compositions over time (Paper II). *Methanothermobacter* was the most abundant methanogen in both TBRs, while potential SAOBs, including the genera *Syntrophaceticus* and *Thermacetogenium*, predominated the bacterial community.

5.1.3 Nutrient Medium Supply Rate and Liquid Recirculation Regime (Paper III)

As a result of the findings from Paper II, the operation of TBR2 was terminated, and the long-term experiment continued using only TBR1 with diluted digestate as the nutrient medium to assess the influence of NMSR and the liquid recirculation regime on syngas biomethanation performance.

Operation of TBR1 continued under the guideline to maintain H_2 and CO conversion rates above 95 %.

Nutrient Medium Supply Rate

In the first part of this study, the NMSR was gradually reduced from 22 to 11 mL/(L_{pbv}·d), corresponding to an increase in HRT from 8.9 d to 18 d by day 472. Despite this, high H_2 and CO conversion rates (>99 %) were maintained under stable conditions and a consistent syngas load (24–25 L/(L_{pbv}·d)) (Fig. 10a). The achieved MERs (ca. 4.3 L/(L_{pbv}·d)) were calculated based on syngas load and H_2 and CO conversion rates due to a malfunction of the drum meter. Between operation days 494 and 503 (at NMSR 11 mL/(L_{pbv}·d), the TBR was operated in standby mode for instrument maintenance and repair. Subsequently, H_2 and CO conversion rates remained below previous levels, with a maximum MER of approximately 4.1 L/(L_{pbv}·d). Although no obvious macronutrient limitation was detected, it was hypothesized that the low NMSR reduced biomethanation performance. Therefore, the NMSR was increased to 14 mL/(L_{pbv}·d), corresponding to an HRT of 14.5 d, to evaluate whether an accelerated NMSR would improve biomethanation performance. This adjustment gradually recovered H_2 and CO conversion rates to >99 %. A

final increase in syngas load led to a slight decline in the conversion rates, suggesting that system limits were being approached.

Liquid Recirculation Regime

The effect of liquid recirculation on H_2 and CO conversion rates was systematically evaluated from day 565 onward. The recirculation frequency was reduced from 144 d^{-1} to 8 d^{-1}, while the duration was increased from 20 s to 80 s. Despite H_2 and CO conversion rates initially remaining high, reducing the recirculation duration to 20 s caused CO conversion to decrease to approximately 90 %, which only partially recovered with increased frequency (Fig. 10). Stable CO conversion above 96 % was achieved again with a recirculation duration of 40 s at frequencies of 16 d^{-1} and higher. By day 665, at a frequency of 48 d^{-1}, H_2 and CO conversion stabilized at approximately 99 % for H_2 and 96 % for CO. High-resolution (24 h) monitoring confirmed that recirculation frequency directly influenced CO concentration patterns in the product gas (Fig. 14), while recirculation duration had negligible impact. H_2 conversion remained largely unaffected throughout the trial. However, lower liquid loads likely limited nutrient supply to the biofilm, resulting in reduced biomethanation performance, with maximum MERs stabilizing around 3.4 $L/(L_{pbv} \cdot d)$ (Fig. 10a).

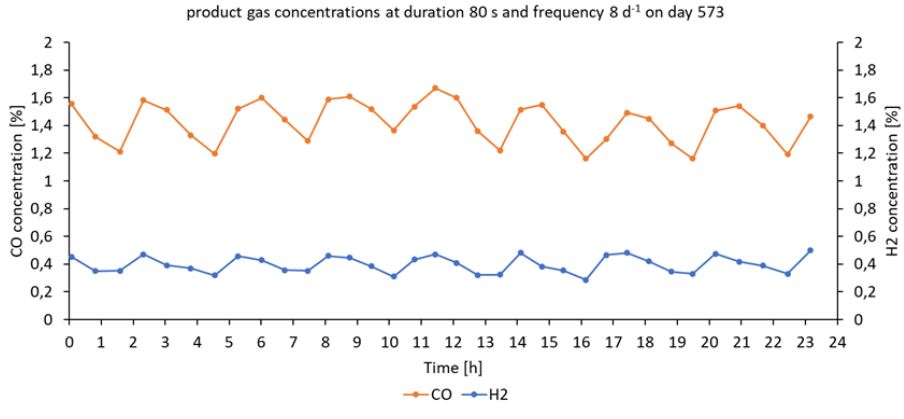

Figure 14. Influence of recirculation occasions on the H_2 and CO conversion rates within 24 hours (presented as H_2 and CO concentrations in the product gas) at a recirculation duration of 80 s and at a recirculation frequency of 8 d^{-1}.

Microbial Community

The microbial community remained stable despite variations in NSMRs and liquid recirculation regimes. Clear differences were observed between the nutrient medium and TBR microbial communities. *Methanothermobacter* dominated the archaeal population, while diverse bacterial taxa, including Aggregatilineales, Haloplasma, and *Syntrophaceticu*s, persisted throughout, showing some spatial variation in abundance along the TBR column.

5.2 Change of Syngas Composition (Paper IV)

This study was conducted under the same major operational guideline as in Paper III, i.e., to maintain high H_2 and CO conversion rates (>95 %). The experiment commenced on day 698, following a 33-day recovery period including reduced syngas loads, more frequent liquid recirculation, and increased NMSR. These adjustments resulted in complete conversion of H_2 and CO and an MER of 2.4 L/(L_{pbv}·d), with a CH_4 percentage of 30 % in the product gas (Figs. 15 and 16).

To increase the CH_4 concentration by changing the inlet syngas composition, pure H_2 was added and gradually increased to 11.5 L/(L_{pbv}·d), raising the total syngas load to approximately 25 L/(L_{pbv}·d) and the H_2 share to 67 %. This led to an increase in CH_4 concentration to 57 % (Fig. 15), but slightly reduced H_2 and CO conversion rates (Fig. 16). Reducing the H_2 load restored complete conversion.

Changing the approach to maintain a stable total syngas load (20–21 L/(L_{pbv}·d)) while gradually increasing the H_2 concentration — reaching a peak of 73 % — resulted in reduced H_2 and CO conversion rates. With 71 % H_2 in the feed, conversion rates recovered to above 95 %, resulting in CH_4 concentrations of 63–66 % and MERs up to 4 L/(L_{pbv}·d). A temporary increase in syngas load to 22 L/(L_{pbv}·d) caused a minor reduction in conversion efficiency. Despite adequate macronutrient levels in the TBR liquid, H_2S concentration in the product gas was very low (Fig. 16b), suggesting S limitation. Consequently, Na_2S supplementation began on day 774, although this did not enhance CO conversion.

After resolving a drum meter malfunction, further increases in syngas load raised the MER to a maximum of 4.7 L/(L_{pbv}·d). However, conversion rates declined to 96 % for H_2 and 88 % for CO, with CH_4 concentrations around 56 % in the product gas. Overall, H_2 supplementation improved both

MER and CH_4 content, but conversion challenges emerged, notably at high H_2 concentrations. S supplementation did not substantially enhance biomethanation performance, and the final MER reached 4.7 $L/(L_{pbv} \cdot d)$, with CH_4 concentrations ranging between 63–67 % (or 84–90 % when accounting for inert N_2 in the syngas as a placeholder for CH_4).

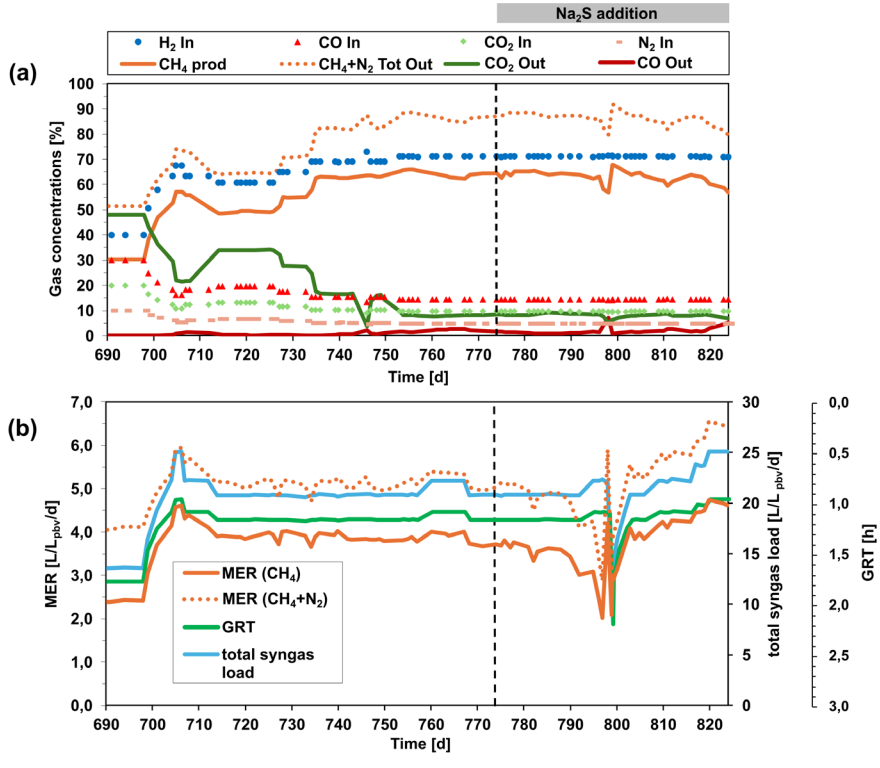

Figure 15. Influence of a changing syngas composition. Na_2S addition started on day 774. (a) Composition of syngas and product gas; (b) Development of total syngas load (incl. H_2 flow rate), GRT, and MER (with and without consideration of N_2).

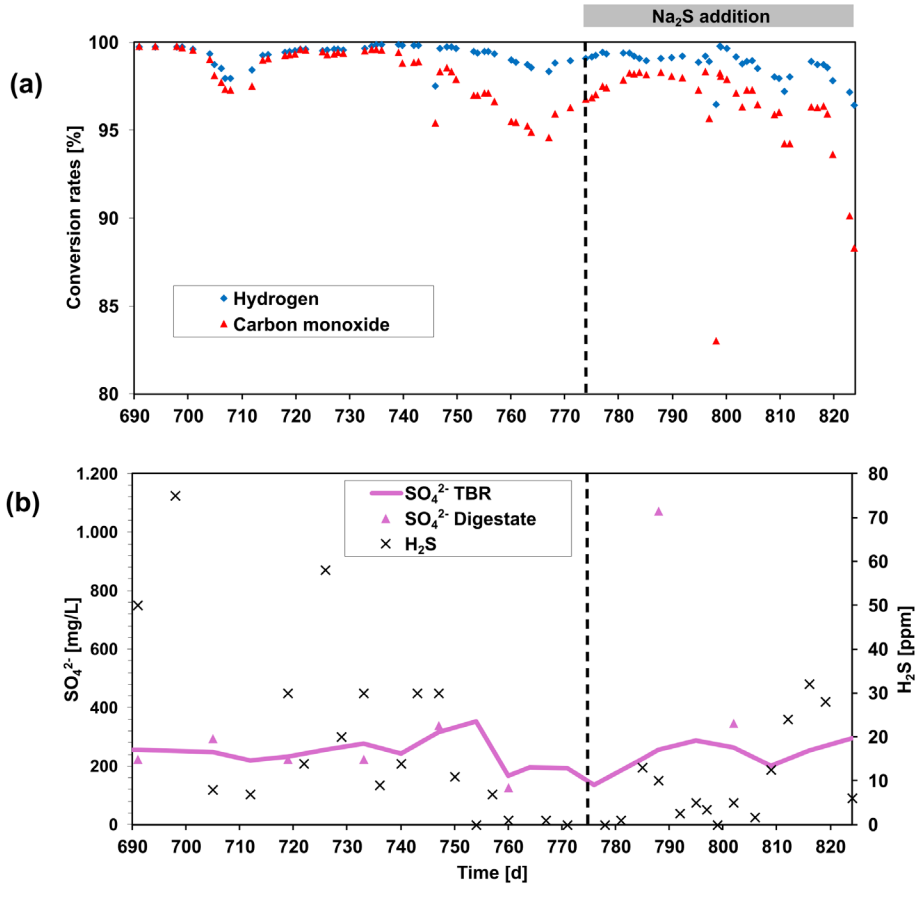

Figure 16. Influence of changing syngas composition. Na_2S addition started on day 774. (a) H_2 and CO conversion rates; (b) SO_4^{2-} levels of TBR liquid and reject water, and H_2S concentration in product gas.

As observed in Papers II and III, the microbial community remained largely stable, exhibiting similar structures in both the liquid phase and carrier biofilms, despite the elevated H_2 concentration in the syngas. The archaeal community was dominated by the genus *Methanothermobacter*. The bacterial community was predominantly composed of members of the phylum Bacillota, with carrier biofilms also hosting genera such as *Acetomicrobium* and *Thermacetogenium*, indicating a more diverse bacterial community compared to the liquid phase.

6. Discussion

6.1 Nutrient Media Composition and Supply

Across all studies, one of the most consistent findings was the key role of nutrient medium type and its addition rate on TBR performance. In Paper I, the use of a defined medium resulted in only moderate process efficiency and quickly revealed limitations in buffering capacity, which led to VFA accumulation and process instability. Process limitations were reached at a comparatively low MER of 0.9 L/(L_{pbv}·d), contrasting with other studies that used similar defined media. For instance, Asimakopoulos et al. (2020) reported MERs of 1.9 L/(L_{pbv}·d) under mesophilic conditions in 180 mL TBRs with high-specific-area plastic carriers (800 m^2/m^3) and continuous liquid recirculation, while even higher values (4.6 L/(L_{pbv}·d)) were achieved under thermophilic conditions. When scaling up to a 5 L TBR, Asimakopoulos et al. (2021b) achieved the highest reported MER of 9.4 L/(L_{pbv}·d) using a configuration and syngas composition comparable to TBR setup B in this thesis.

Although the defined nutrient medium compositions in Asimakopoulos et al. (2021b) and Paper I were relatively similar, some key differences existed — for example, K_2HPO_4 concentrations of 7 mg/L in Paper I versus 303 mg/L in Asimakopoulos et al. (2021b), and Na_2S concentrations of 240 mg/L and 78 mg/L, respectively. It is therefore unlikely that the reduced performance in Paper I was caused by the defined nutrient medium itself. Instead, operational factors such as the use of low-specific-area carriers (313 m^2/m^3) and inadequate control of key process parameters (H_2 and CO conversion rates, pH) were likely responsible. Maintaining high syngas loads during inhibited conversion promoted VFA accumulation and process instability.

Transitioning to non-defined substrates such as diluted digestate and reject water enabled higher syngas loads and improved MERs. This is in line with other studies confirming the suitability of non-defined nutrient media for syngas biomethanation (Ashraf et al., 2020; Kamravamanesh et al., 2023; Ali et al., 2024; Goonesekera et al., 2024). In Paper I, MERs up to 1.3 L/(L_{pbv}·d) were achieved under mesophilic conditions, but only when S levels — essential for methanogenic enzyme synthesis — were satisfactorily managed. This aligns with earlier reports highlighting the positive impact of

S supplementation on biomethanation of syngas (Figueras et al., 2021) and H_2/CO_2 (Dupnock & Deshusses, 2019; Thema et al., 2021).

The importance of sufficient nutrient supply was further underscored in Paper II, where the reject water–operated TBR2 reached less than 25 % of the biomethanation performance of the digestate-operated TBR1. Benefiting from higher nutrient concentrations, TBR1 reached MERs up to 4.5 $L/(L_{pbv} \cdot d)$, whereas TBR2 suffered from persistent sulfur and phosphorus deficiencies, even after supplementation. This finding highlights the need for adequate macronutrient concentrations, regardless of the nutrient medium used. For instance, NH_4^+, essential for protein and enzyme synthesis in methanogens, is typically required at minimum concentrations between 60 mg/L (Thema et al., 2021) and 1,000 mg/L (Dupnock & Deshusses, 2019) — a range maintained throughout this thesis. Phosphorus, required for ATP synthesis, should be supplied at 1–2 mg/L (Gu et al., 2022) to preserve an optimal C:N:P ratio of 100:3:1 (Gerardi, 2003). In Paper I, P levels were not monitored, whereas in Papers II–IV, digestate-fed TBRs maintained 15–166 mg PO_4^{3-}/L, well above the minimum requirement. In contrast, reject water–fed TBR2 showed strong P limitation (0.1–0.5 mg PO_4^{3-}/L). Although P supplementation improved H_2 and CO conversion, excessive dosing caused a sharp increase in PO_4^{3-} levels, which may have disrupted the methanogen–bacteria balance (Mancipe-Jiménez et al., 2017). Even with S and P supplementation, the reject water–fed TBR achieved a MER of only 3.1 $L/(L_{pbv} \cdot d)$, lower than the digestate-fed TBR. Comparable findings were reported by Kamravamanesh et al. (2023), who observed MERs up to 2.6 $L/(L_{pbv} \cdot d)$ when trace elements were added to reject water.

Sulfur availability is particularly critical as shortages inhibit biomethanation performance (Thema et al., 2021), but recovery is rapid once liquid-phase concentrations exceed 6.4 mg/L (Strübing et al., 2017). Conversely, excessive sulfide (S^{2-}) can precipitate trace elements, lowering their bioavailability and impeding enzyme synthesis. As S^{2-} and H_2S equilibrate between the liquid and gas phases, maintaining 5–30 ppm H_2S in the product gas is recommended to balance sufficiency and avoid inhibition.

Digestate has repeatedly proven to be an adequate nutrient source (Andreides et al., 2022; Ali et al., 2024; Goonesekera et al., 2024; Bilgiç et al., 2025). In Paper II, its sole use supported MERs up to 4.5 $L/(L_{pbv} \cdot d)$, among the highest reported under thermophilic conditions. Goonesekera et al. (2024) achieved similar MERs (4.3 $L/(L_{pbv} \cdot d)$) using digestate in a 1 L

TBR. The highest reported MER to date (9.5 $L/(L_{pbv} \cdot d)$) was reported by Asimakopoulos et al. (2021b) in a 5 L TBR; however, this was achieved using a defined nutrient medium.

In Paper III, it was demonstrated that reducing the NMSR (and thereby increasing HRT) of diluted digestate did not impair H_2 and CO conversion, indicating that the nutrient composition provided was adequate. Overall, across all TBR setups, nutrient sufficiency emerged as the key factor for stable and efficient syngas conversion at high gas loads. However, the results do not allow a generalized conclusion on whether digestate is better than reject water, as both substrates exhibit substantial variability in nutrient composition depending on their origin and treatment processes. Consequently, each potential nutrient medium should be characterized to verify its suitability for TBR-based syngas biomethanation. While trace element supplementation can improve biomethanation, it may increase operational costs at larger scales. These could potentially be mitigated by using non-defined nutrient media — such as liquid organic waste streams, like digestates — which typically contain sufficient concentrations of essential macronutrients and trace elements if the digestates' origin is a well-balanced, stable AD process.

6.2 Process Parameters as Levers for Stability and Improvement

Process parameters such as temperature, nutrient medium supply rate, and liquid recirculation are key factors that affect the performance of TBR syngas biomethanation. Their influence is interconnected, determining the balance among microbial activity, gas–liquid mass transfer, and overall CH_4 productivity.

Temperature has consistently been shown to strongly influence syngas biomethanation efficiency (Grimalt-Alemany et al., 2019). Two studies have specifically examined the effects of temperature in TBR systems. Operating a 180 mL TBR at low GRTs (0.6 h), Asimakopoulos et al. (2020) achieved maximum MERs of 1.9 and 4.6 $L/(L_{pbv} \cdot d)$ under mesophilic and thermophilic conditions, respectively. The maximum MERs under thermophilic conditions were accompanied by low H_2 and CO conversion rates (89 % and 73 %, respectively). At 37 °C, the H_2 and CO conversion rates were even lower (40 %). In another study, utilizing a 1 L TBR,

Andreides et al. (2022) achieved maximum MERs of 1.5 and 2.1 L/(L_{pbv}·d) at 35 °C and 55 °C, respectively. Here, CO conversion increased from 82 % under mesophilic to >99 % under thermophilic conditions, while H_2 conversion remained high (97–99 %) at both temperatures. Despite the higher theoretical MER expected from higher H_2 share in the syngas, the performance observed in Paper I under mesophilic conditions was lower, with MERs of 0.9 L/(L_{pbv}·d) for defined nutrient medium and 1.2 L/(L_{pbv}·d) for digestate in a 35 L TBR. The higher performance reported by Asimakopoulos et al. (2020) was likely due to the use of carrier materials with a higher specific surface area for biofilm growth (800 m^2/m^3), compared to the 313–320 m^2/m^3 carriers used in Paper I and by Andreides et al. (2022).

Over the last few years, a clear trend has emerged toward operating at elevated temperatures in both syngas and H_2/CO_2 biomethanation, as higher CH_4 productivity is associated with enhanced methanogenic activity despite lower gas solubility (Asimakopoulos et al., 2020; Feickert Fenske et al., 2023c). Under thermophilic conditions, the highest reported MERs were reached with up to 9.5 L/(L_{pbv}·d) for syngas in a 5 L TBR (Asimakopoulos et al., 2021b) and 15.4 L/(L_{pbv}·d) for H_2/CO_2 in a 58 L TBR (Strübing et al., 2017), both using defined nutrient media. Consequently, for this thesis, temperature was increased from mesophilic to thermophilic conditions when starting TBR setup B for the experiments in Papers II–IV. This temperature shift improved process performance and stability, consistent with literature observations.

The nutrient medium supply rate plays a critical role in maintaining microbial activity, buffering capacity, and biofilm stability in TBR biomethanation systems (Feickert Fenske et al., 2023c). However, comparisons across studies are complicated by differences in reactor configuration, liquid reservoir volume, and nutrient composition of the digestates used. To standardize this, Paper III employed NMSR (mL/(L_{pbv}·d)) as a comparative parameter, which ranged from 11 to 22. Efficient H_2 and CO conversion (>99 %) was achieved at an NMSR of 14 mL/(L_{pbv}·d), corresponding to an HRT of 14 d. This aligns with previous reports where nutrient limitations have generally not been observed even at lower NMSRs, provided macronutrient concentrations were satisfactory (Asimakopoulos et al., 2020; Andreides et al., 2022). Nevertheless, suboptimal NMSRs can lead to reduced gas conversion, as reported in Paper I, and may also limit trace element availability (Goonesekera et al., 2024). In

Paper III, reduced performance at lower NMSRs (11 mL/(L_{pbv}·d)) could indicate trace-element depletion or operational issues such as solids accumulation. Thus, while macronutrients may remain adequate at relatively low NMSRs, micronutrient supply and reactor hydrodynamics must also be considered. Overall, these findings underscore the importance of balancing nutrient retention time and reactor hydrodynamics for efficient TBR syngas biomethanation.

Another key operational parameter is liquid recirculation (trickling), which affects both nutrient distribution and gas–liquid mass transfer. High biomethanation performance has been achieved under both continuous (Asimakopoulos et al., 2021b; Goonesekera et al., 2024) and intermittent (Dahl Jonson et al., 2020; Sieborg et al., 2020) recirculation modes. Lower recirculation rates can improve mass transfer by reducing the liquid film thickness over the biofilm, thereby enhancing substrate availability (Burkhardt et al., 2015; Sieborg et al., 2021). However, finding a balance is vital. Intermittent recirculation has been shown to disrupt syngas conversion, particularly for CO, due to its lower solubility and slower mass transfer compared to H_2 (Asimakopoulos et al., 2021a; Paniagua et al., 2022). In Paper III, lower recirculation frequencies decreased overall biomethanation performance, with CO conversion being more strongly affected than conversion of H_2 (Fig. 14). Similar findings have been reported in other TBR studies, where trickling once per day was insufficient to supply sufficient nutrients to lower reactor zones, leading to decreased performance (Tsapekos et al., 2021). Moreover, Jensen et al. (2021) reported that each recirculation event caused transient reductions in H_2 conversion (from 99 to 79 %), requiring extended recovery times. Conversely, increased liquid recirculation rates have been shown to enhance mass transfer and CH_4 productivity in some cases (Ullrich & Lemmer, 2018; Goonesekera et al., 2024), although very high flow rates may alter hydrodynamics unfavorably and reduce MERs (Ashraf et al., 2021). Noteworthy, the recirculation regime must also account for the liquid hold-up capacity of the carrier material, which varies significantly between plastics and more porous carriers such as clay (Jensen et al., 2021). For the plastic carriers used throughout this thesis, frequent short recirculation intervals (>48 d^{-1}, 20 s duration) appeared to represent an optimal balance, ensuring adequate nutrient delivery while minimizing adverse mass transfer effects.

Overall, the results confirm that syngas biomethanation in TBRs is highly sensitive to process parameters. Mesophilic temperatures provide stable but moderate MERs, while thermophilic conditions enable higher yields but may require stricter control of nutrient and mass transfer regimes. Adequate nutrient medium supply — covering both macro- and micronutrients — is essential to sustain high conversion rates. Finally, liquid recirculation should be optimized based on carrier type, syngas composition, and applied syngas loads to balance nutrient availability and gas–liquid mass transfer limitations. These parameters must be carefully integrated into future process designs to maximize CH_4 productivity and reactor stability.

6.3 Syngas Composition and Conversion Dynamics

Paper IV assessed the in-situ addition of pure H_2 to increase CH_4 concentration in the product gas, which significantly influences gas quality and the pathway of further utilization. H_2 supplementation was conducted using two strategies: (i) increasing both the H_2 share in syngas and the total syngas load, and (ii) raising the H_2 share while maintaining a nearly constant syngas load.

In the first approach, the observed decline in H_2 and CO conversion was probably caused by excessive syngas loads (25 $L/(L_{pbv} \cdot d)$), corresponding to GRTs below 1 h, rather than high H_2 partial pressures (67 % H_2). This interpretation was supported by later results showing that syngas biomethanation proceeded successfully even at higher H_2 shares. GRTs below 1 h have been reported to limit gas–liquid mass transfer (Asimakopoulos et al., 2019). Bilgiç et al. (2025) likewise reported limited H_2 and CO conversion (60–80 %) in thermophilic 0.9 L TBRs at higher GRTs of 1.2–1.5 h. However, although GRTs below 1 h were also applied in Paper II, H_2 and CO conversion rates >95 % were achieved. In the second approach, where syngas loads remained nearly constant (20–21 $L/(L_{pbv} \cdot d)$), reduced conversion was attributed to elevated H_2 partial pressure, which limited the feasible H_2 share to approximately 71 % while maintaining >95 % H_2 and CO conversion. This is in accordance with findings that high H_2 pressures can inhibit methanogenic and acetogenic pathways (Cazier et al., 2015; Li et al., 2021).

In Paper IV, macronutrient concentrations remained above the critical thresholds identified in Paper II, and increasing S^{2-} availability due to Na_2S

supplementation did not improve conversion. Thus, it is more likely that high H_2 partial pressures, combined with high syngas loads and low GRTs, reduced syngas biomethanation performance compared to the higher performance seen in Paper II, rather than any limitation in nutrient availability.

Syngas composition strongly shapes the quality of the TBR product gas, particularly CH_4 concentration. Throughout Papers II–IV, N_2 in the syngas was used as a placeholder for CH_4 originating from gasification — initially 10 %, reduced to 4.8 % due to H_2 addition in Paper IV. Accounting for this placeholder, the maximum MER (CH_4+N_2) reached approximately 5.4 L/(L_{pbv}·d), while the final CH_4 concentration was 84–88 %, with >95 % H_2 and CO conversion rates. At lower syngas loads (GRT 1.7 h; MER (CH_4+N_2) ca. 3.8 L/(L_{pbv}·d)), conversion rates exceeded 98 % for both H_2 and CO, and CH_4 concentration reached up to 91 % (including N_2). Compared to other H_2-supplemented studies on thermophilic syngas biomethanation, these CH_4 concentrations were slightly lower than those reported by Asimakopoulos et al. (2021a), who achieved 97 % CH_4 in a 180 mL TBR with defined nutrient medium, but comparable to Bilgiç et al. (2025), who obtained CH_4 concentrations up to 90 % in a 0.9 L TBR using digestate as nutrient medium.

However, CO_2 levels remained >6 % in Paper IV, suggesting that further product gas upgrading would be required to meet grid or fuel specifications. Optimizing inlet syngas composition toward an ideal Syngas Quality Index (SQI) of 4, as shown by Asimakopoulos et al. (2021a), could enhance CH_4 quality. In Paper IV, the SQI reached 3.55, with lower H_2 (71.1 %), higher CO (14.4 %), and similar CO_2 (9.5 %) and N_2 (4.8 %) contents compared with those reported by Asimakopoulos et al. (2021a). However, Paper IV focused on maximizing MER, applying syngas loads of 20–25 L/(L_{pbv}·d) (GRTs 1–1.2 h), whereas Asimakopoulos et al. (2021a) used lower syngas loads and longer GRTs (1.5–3 h), achieving full conversion but a lower MER (ca. 2.6 L/(L_{pbv}·d)). This aligns with the findings of Paper IV, where a reduced GRT of 1.7 h was applied, resulting in the highest CH_4 concentration of the trial and high H_2 and CO conversion rates. Overall, longer GRTs (>2 h) appear beneficial for maintaining H_2 and CO conversion rates >99 % during H_2-supplemented syngas biomethanation.

Future advances in process performance may be realized through optimized reactor configurations. A particularly promising strategy is the

two-stage system, first proposed by Andreides et al. (2021), in which a syngas biomethanation unit (CSTR) was coupled with an upgrading unit (TBR). In this configuration, supplemental H_2 addition in the TBR enabled conversion of residual CO and CO_2 to CH_4, resulting in a final CH_4 concentration of approximately 95 %. More recently, Aruleeswaran et al. (2025) evaluated a similar concept under thermophilic conditions, operating two serially connected 0.7 L TBRs on digestate as nutrient medium. The two-stage TBR design outperformed the single-reactor system, increasing MER from 4.6 to 6.1 L/(Lpbv·d), driven by targeted hydrogenotrophic methanogenesis in the second TBR and producing gas with approximately 95 % CH_4 purity. In contrast, Paper IV demonstrated that direct (in-situ) H_2 supplementation inhibited CO conversion, yielding gas of substandard quality for grid injection or fuel utilization. The two-stage concept mitigates this by fostering a more specialized microbial community: hydrogenotrophic methanogens dominate in the second reactor, while CO consumers — more sensitive to H_2 partial pressure — are primarily in the first. This design allows operation at higher syngas loads (lower GRTs) and provides enhanced operational flexibility under fluctuating renewable H_2 supply.

6.4 Microbial Community: Stability despite Operational Dynamics

The microbial community structures under both mesophilic and thermophilic conditions demonstrated remarkable stability, with slightly higher diversity observed at lower temperature (Paper I). Repeated exposure to CO-containing syngas led to an enrichment of *Methanothermobacter spp*. Within the methanogenic community, reflecting their greater physiological and/or syntrophic tolerance to CO compared with other methanogens. This enrichment represents a gradual selection from an initially more diverse community rather than an abrupt taxonomic shift. The dominance of *Methanothermobacter*, particularly in reactors operating under high CO partial pressures, is supported not only by their inherent abilities metabolic capacities but also by syntrophic interactions with SAOBs, which mitigate CO toxicity and maintain stable syngas biomethanation (Diender et al., 2016; Goonesekera et al., 2024).

6.4.1 Archaeal Communities

Under mesophilic conditions, the archaeal community was dominated by an ASV identified as *Methanobacterium bryanti*. This strictly hydrogenotrophic methanogen utilizes only H_2/CO_2 and cannot use CO or formate (Benstead et al., 1991). The dominance of the genus *Methanobacterium* aligns with observations from other mesophilic syngas biomethanation systems (Aryal et al., 2021; Li et al., 2021). Mesophilic reactors generally exhibit greater archaeal diversity than those operated at higher temperatures, typically including *Methanobacterium*, *Methanosaeta*, and *Methanosarcina*. This broader diversity reflects the coexistence of both hydrogenotrophic and acetoclastic methanogenic pathways active at lower temperatures. In Paper I, *Methanosarcina* was detected only on the biocarriers, which were likely linked to acetate consumption. However, this can only be assumed, as *Methanosarcina* can also use H_2/CO_2.

Under thermophilic conditions, the methanogenic community was dominated by *Methanothermobacter*, most closely related to *M. marburgensis*, which is a hydrogenotrophic methanogen capable of utilizing both H_2/CO_2 and CO for CH_4 formation (Diender et al., 2016). The prevalence of *Methanothermobacter* is consistent with previous studies on thermophilic syngas biomethanation (Asimakopoulos et al., 2019; Ali et al., 2024; Goonesekera et al., 2024). *Methanothermobacter* species are well adapted to high temperatures through a combination of energy-conservation mechanisms, thermostable cell structures, and resistance to CO inhibition. Their high H_2 affinity further enhances their competitiveness, although it is not exclusive to thermophilic adaptation (Thauer et al., 2008). Consequently, they typically outcompete other methanogens during long-term thermophilic TBR operation, reaching high relative abundances. This dominance is supported by the prevailing substrate conditions: under thermophilic and H_2/CO_2-rich operation, acetate availability is low due to the predominance of hydrogenotrophic methanogenesis, thereby limiting ecological niches for acetoclastic methanogens. Accordingly, *Methanosarcina* was mainly detected on biocarriers, likely functioning as acetate consumers in localized microenvironments where acetate accumulates (Guneratnam et al., 2017). The reduced microbial diversity observed under thermophilic conditions thus reflects both kinetic selection and thermodynamic favorability toward hydrogenotrophic pathways, rendering acetoclastic methanogens less competitive.

6.4.2 Bacterial Communities

The bacterial communities were generally more diverse and less dominated by a single genus than the methanogenic communities, yet remained relatively stable despite operational changes.

At lower temperatures (Paper I), one ASV was identified as *Sporomusa sphaeroides*, showing a high relative abundance throughout the operation of TBR setup A. Members of the genus *Sporomusa* are acetogens known to produce acetate primarily via H_2/CO_2 utilization, thereby competing with methanogens for substrate. However, they are typically inhibited by CO (Bengelsdorf et al., 2018b).

Under thermophilic conditions (Papers II–IV), no known acetogens were detected, consistent with previous findings in both syngas and H_2/CO_2 biomethanation, where acetogens dominate under mesophilic conditions but decline above 50 °C (Liu et al., 2016; Aryal et al., 2021). At higher temperatures, hydrogenotrophic methanogenesis and SAO instead become the dominant pathways (Hattori, 2008; Westerholm et al., 2019). Increasing temperature reduces the thermodynamic favorability of acetogenesis due to lower Gibbs free energy yields and fast H_2 consumption by methanogens, which decreases dissolved H_2 concentrations (Hattori, 2008). Nevertheless, certain carboxydotrophic acetogens, such as *Desulfitibacter* and *Desulfitobacterium*, were identified in thermophilic TBR liquid samples. These genera are known for their relatively high CO tolerance compared to most methanogens (Nielsen et al., 2006; Villemur et al., 2006), which may explain their persistence in syngas biomethanation systems. However, their activity in the thermophilic TBR setup B (Papers II–IV) was likely limited due to suboptimal growth conditions and competition with hydrogenotrophic methanogens such as *Methanothermobacter*, which can also utilize CO at moderate concentrations.

Acetate conversion likely proceeded via SAO, supported by the consistent detection of *Syntrophaceticus*, *Thermacetogenium*, and other potential SAOBs, such as MBA03 and DTU014, during operation of thermophilic TBR setup B (Papers II–IV). This is in line with findings from other H_2/CO_2 and syngas biomethanation studies (Porte et al., 2019; Kamravamanesh et al., 2023; Ali et al., 2024). These organisms oxidize acetate in syntrophy with hydrogenotrophic methanogens, such as *Methanothermobacter*, which maintain low H_2 partial pressures, essential for the thermodynamic feasibility of SAO (Hattori et al., 2005; Westerholm et

al., 2019). The detection of SAOBs on the bottom biocarriers near the syngas inlet further supports this syntrophic relationship and is consistent with the findings of Goonesekera et al. (2024).

6.4.3 Role of Heterotrophic and Fermentative Bacteria

Although syngas biomethanation primarily relies on autotrophic pathways, heterotrophic and fermentative bacteria likely play supporting roles. The presence of fermenting bacteria such as *Tepidimicrobium*, *Acetomicrobium*, and *Symbiobacterium* suggests that heterotrophic fermentation contributed to acetate formation when organic substrates from the nutrient liquid (digestate) were available. Elevated H_2 concentration can shift fermentation patterns toward more reduced end-products, such as propionate and butyrate (Miceli et al., 2016), which may explain the detection of propionate degraders such as *Cloacimonetes* in Paper IV.

Hydrogenogenic bacteria may also indirectly support methanogenesis by scavenging residual organic carbon and releasing H_2, thereby further stabilizing syngas biomethanation during periods of CO inhibition or temporary substrate fluctuations caused by reduced syngas loads. The observed ASV *Thermotogales sp*. SRI-15, known to include thermophilic fermenters that produce acetate, CO_2, and H_2 (Reysenbach et al., 2001; Zannoni & De Philioois, 2014), exemplifies this role.

6.4.4 Influence of Nutrient Media and Operational Parameters

The results of Paper I illustrated that the selection of nutrient source further influenced community dynamics. When switching from the defined nutrient medium to digestate, several thermophilic microorganisms — such as *Defluviitoga* — originating from the nutrient source were identified during a period with a high nutrient medium supply rate. However, during long-term operation with manure-based digestate (Papers II–IV), no measurable influence of the digestate community on the established TBR community was observed. Digestates and reject water provide a complex mixture of organic substrates, trace elements, and buffering capacity, which can stimulate heterotrophic microorganisms while maintaining stable methanogenic communities (Burkhardt et al., 2015; Goonesekera et al., 2024). Increasing the H_2 concentration in the syngas did not substantially change the archaeal or bacterial communities, suggesting that the microbial consortium maintained both functional and structural resilience. This finding

aligns with Li et al. (2021), who reported only minor community shifts under elevated H_2 conditions during syngas biomethanation.

6.4.5 Concluding Microbiological Remarks

The combination of thermophilic conditions, diverse non-defined nutrient media, and efficient H_2 consumption fostered a stable and robust microbial consortium dominated by hydrogenotrophic methanogens and their syntrophic partners. Overall, these findings highlight the metabolic efficiency and resilience of TBRs for syngas biomethanation.

7. Implementation Outlook and Future Research Perspectives

To date, TBR syngas biomethanation has only been investigated at laboratory scale. However, the results obtained so far are promising and encourage further development toward large-scale implementation. Moving toward commercial application will require careful consideration of several technical, regulatory, and economic aspects.

7.1 Implementation Outlook

From a technical perspective, the gasification process itself must be considered when assessing the potential for large-scale implementation. In Sweden, the GoBiGas project and Cortus AB have demonstrated biomass gasification at energy outputs of 20 and 6 MW syngas, respectively (Larsson et al., 2019; Mesfun et al., 2022). Comparable plant sizes, with thermal inputs of 8.4 and 22.8 MW, have been used by Menin et al. (2022) to evaluate the techno-economic feasibility of syngas biomethanation. Based on the reported syngas compositions and the lower heating values (LHV) for H_2, CO, and CH_4, the corresponding daily syngas flows from the Cortus and GoBiGas gasifiers would be approximately 53,000 and 148,000 m^3, respectively. Assuming complete conversion under thermophilic conditions with a syngas load of 25 $L/(L_{pbv} \cdot d)$, as achieved in Paper II, the associated syngas biomethanation would require TBR volumes of roughly 2,100 and 5,900 m^3, respectively.

The product gases from both systems would theoretically contain a 45–48 % CH_4 and a high CO_2 share, requiring additional H_2 supplementation of approximately 47,000 m^3/d (Cortus) and 69,000 m^3/d (GoBiGas) to achieve maximum CH_4 concentrations. This demand depends on the initial syngas; for instance, Cortus syngas has a higher H_2 share (56 %), whereas GoBiGas targets a higher overall LHV. Nutrient medium requirements would range between 30 and 120 m^3/d of diluted digestate, assuming an NMSR of 14 $mL/(L_{pbv} \cdot d)$ based on results from Paper III. These estimates do not account for potential scaling effects, which are expected to substantially reduce reactor volume, H_2 demand, and nutrient requirements.

Large-scale implementation, however, introduces additional technical challenges, particularly related to reactor cooling and the management of metabolic water. Based on the syngas compositions used in this thesis, complete conversion would generate approximately 0.4–0.5 L H_2O per m^3 CH_4 produced. Following microbial uptake, this metabolic water can dilute the liquid phase, lowering buffer capacity and nutrient concentrations in the TBR liquid, thereby reducing its suitability for use as a fertilizer. In addition, potential syngas impurities from biomass gasification, such as residual hydrocarbons, may complicate downstream processing and handling of the liquid effluent.

Long-term operational experience with TBRs provides valuable insights into practical implementation and process stability. Systems operated with non-defined nutrient media, such as digestate, are more prone to clogging and channel formation than those supplied with defined nutrient media. Digestate typically contains suspended solids and organic residues that can accumulate within the packing material, reducing gas–liquid mass transfer. Furthermore, discontinuous nutrient medium supply and liquid recirculation may promote biofilm formation and clogging in hoses, pumps, and valves, leading to severe malfunctions and process failure. Such issues may be less pronounced at larger scales due to reactor design and dimensions, but regular maintenance remains essential.

Over extended operation, fine sediments and particles in digestate can accumulate in the TBR and partially block the reactor bed, forming dead zones that reduce the total active reactor volume and impair biomethanation efficiency. Periodic maintenance routines — such as partial drainage, flushing, or mechanical cleaning — are therefore recommended to maintain efficient performance. Furthermore, fluctuations in microbial activity due to biomass detachment or washout may occur, making periodic re-inoculation beneficial for maintaining stable H_2 and CO conversion and overall reactor performance.

In industrial operation, this could be addressed through a parallel TBR configuration, in which multiple units operate simultaneously but in staggered cycles — for example, five reactors running continuously while one undergoes maintenance or re-inoculation. Such a setup would enable quasi-continuous operation and ensure process robustness, even under varying substrate or nutrient conditions.

Regarding large-scale implementation, one key issue is the utilization and classification of the product gas. Due to H_2 addition (Paper IV), the product gas reached a Wobbe Index of approximately 45 MJ/m^3, exceeding grid injection thresholds in several European countries (Thema et al., 2019). However, further upgrading would be required to meet CO_2 and CO concentration limits.

Another critical aspect concerns the legal classification of the final product gas when substantial amounts of external H_2 are supplied. In the conventional case — where syngas originates exclusively from biomass without exogenous H_2 — the resulting CH_4 is classified as biomethane. Biomethane is well established in current regulatory frameworks and generally benefits from support mechanisms such as tax exemptions, grid injection incentives, and renewable energy certificates. However, the limited inherent H_2 content in syngas results in a low CH_4-concentrated product gas, thereby restricting its utilization options.

Increasing H_2 supplementation shifts the product's legal status. When the added H_2 is produced via water electrolysis powered by renewable electricity, the resulting CH_4 is more accurately categorized as e-methane or synthetic methane/synthetic natural gas (SNG) — a renewable fuel of non-biological origin (RFNBO) (European Union, 2023). At low levels of H_2 addition, the product gas may still be considered as biomethane enriched with renewable H_2, but due to stoichiometric constraints, higher supplementation levels are necessary to achieve CH_4 concentrations suitable for grid injection or vehicle fuel. Consequently, the product gas is likely to be categorized as e-methane under RFNBO regulations.

Currently, there is no clearly defined threshold at which a hybrid product transitions from "bio" to "synthetic" and legal definitions do not explicitly address such mixed production routes. Moreover, these regulations remain somewhat restrictive, as the electricity used for H_2 production must be fully renewable, with biomass-derived or nuclear electricity explicitly excluded (eFuel alliance, 2025).

This "biomethane vs. e-methane" ambiguity affects both market value and economic viability, as it determines qualification for subsidies and other incentives. While e-methane may benefit from emerging support schemes for RFNBOs, it could lose access to well-established biomethane incentives. Hence, the financial competitiveness of hybrid systems will depend strongly on future regulatory interpretation. Harmonizing the EU framework for

biomethane and RFNBOs will be crucial to attract investment and reduce Europe's dependency on imported fossil energy sources.

7.2 Future Research Perspectives

Although TBR-based syngas biomethanation was first explored in the early 1990s (Klasson et al., 1990; Kimmel et al., 1991; Klasson et al., 1992), it remains an emerging technology. Early studies used defined microbial consortia rather than mixed communities, and substantial progress has only been achieved within the past decade. Following these pioneering efforts, nearly 30 years passed before Danish research groups at SDU and DTU conducted further studies on TBR syngas biomethanation (Ashraf et al., 2020; Asimakopoulos et al., 2021b). Our research group began exploring this topic in 2018, starting a 35 L TBR operated on various nutrient media (Paper I), followed by another long-term experiment using smaller 5 L TBRs. Despite the increasing number of scientific publications on this subject during the past seven years, considerable potential remains for further development and optimization of this technology.

Process upscaling represents the next critical step. A pilot-scale 800 L TBR has already been demonstrated for H_2/CO_2 biomethanation (Feickert Fenske et al., 2023a), yet similar pilot-scale trials for syngas biomethanation are still lacking. Scaling efforts are likely constrained by design challenges such as the height-to-diameter (H:D) ratio. This parameter likely affects liquid recirculation, gas–liquid mass transfer, and microbial distribution. Reported H:D ratios between 5 and 10 in laboratory systems will likely need to be reduced to enable feasible pilot- or industrial-scale operation.

Thermal and hydraulic conditions also warrant further research. Operation under elevated, potentially hyperthermophilic conditions (70–80 °C) could enhance reaction kinetics and enable the partial utilization of internally generated heat, thereby reducing external heating demand. At larger scales, syngas biomethanation becomes an exothermic process, requiring active reactor cooling to maintain a constant temperature (Jønson et al., 2022).

TBR pressure optimization has not yet been explored within syngas biomethanation. While higher pressures can improve gas solubility and potentially enhance conversion, they may also intensify CO inhibition. Similarly, liquid recirculation rates strongly influence both performance and

energy consumption. As shown in Paper III, the recirculation regime must be carefully matched to the biocarrier's physical characteristics to ensure adequate nutrient supply and gas–liquid mass transfer.

Carrier material selection offers additional optimization potential. Clay-based materials have demonstrated superior mass-transfer performance compared to plastic or cellulose-based materials (Jensen et al., 2021). Promoting homogeneous and stable biofilm formation across the carrier surface will be essential for successful scale-up.

To further increase CH_4 concentration, coupling two TBRs in series has been proposed: the first TBR focuses on CO conversion, followed by a second TBR with H_2 addition for CO_2 conversion, to achieve CH_4 levels above 95 %. In such a configuration, distinct microbial communities would likely develop in each reactor, enabling higher gas loads and CH_4 production rates.

The microbial community development in TBRs remains another promising research direction. Most previous studies have focused on the suspended communities in the reactor liquid, whereas biofilm-associated communities on biocarriers remain underexplored despite their critical role in process performance and long-term stability.

Beyond methane, TBR syngas bioconversion could target alternative products such as acetic acid, longer-chain VFAs, or higher alcohols, thereby broadening the technology’s industrial potential.

Finally, to complement these technical advances, techno-economic assessments and life-cycle assessments of the integrated gasification–syngas biomethanation process are essential. Such analyses will help identify key design and operational parameters that affect cost-effectiveness and sustainability while guiding policy alignment and industrial implementation.

8. Conclusions

Syngas biomethanation in trickle-bed reactors (TBRs) has proven to be a robust and efficient process under both mesophilic and thermophilic conditions, achieving methane evolution rates (MERs) up to 4.5 L/(L_{pbv}·d) with high H_2 and CO conversion rates (>90 %) at elevated temperature. Long-term studies demonstrated stable operation using a variety of nutrient sources, including defined media, digestate, and reject water. However, nutrient availability — particularly phosphorus and sulfur — emerged as a critical determinant of process performance. Nutrient deficiencies led to reduced H_2 and CO conversion rates and impaired process stability, while supplementation restored activity. Nevertheless, gas–liquid mass transfer limitations were also identified as potential bottlenecks.

Operational strategies concerning nutrient medium supply rate (NMSR) and liquid recirculation frequency strongly influenced reactor performance. Reduced nutrient addition or limited liquid recirculation caused gradual declines in H_2 and CO conversion rates, whereas adequate supply and distribution maintained high biomethanation activity. Similarly, variations in syngas composition, including elevated H_2 partial pressures, affected acetogenic activity and acetate conversion. These findings highlight the importance of carefully balancing gas retention times and syngas composition to optimize CH_4 productivity.

Despite process-dependent differences in performance, microbial community structures across all studies converged towards similar and stable consortia dominated by hydrogenotrophic methanogens such as *Methanothermobacter* or *Methanobacterium*, together with syntrophic acetate-oxidizing bacteria (*Syntrophaceticus*, *Thermacetogenium*, *Tepidanaerobacter*) and acetogens such as *Sporomusa*. Community composition remained relatively stable, with observed performance shifts primarily linked to differences in microbial activity rather than shifts in abundance or taxonomy.

Collectively, these findings highlight the potential of TBRs as a reliable reactor configuration for syngas biomethanation. High CH_4 productivity can be sustained when key operational parameters — nutrient supply, liquid recirculation, syngas composition, and gas retention times — are carefully managed. The resilience and adaptability of the microbial community further

support the feasibility of TBR-based syngas biomethanation for long-term and scalable applications.

Overall, this work advances the understanding of process–microorganism interactions in TBR syngas biomethanation and provides a framework for upscaling toward continuous, resource-efficient CH_4 production.

References

Ali, R., Samadi, H., Yde, L. & Ashraf, M.T. (2024). Carbon monoxide conversion by anaerobic microbiome in a thermophilic trickle bed reactor. *Biochemical Engineering Journal,* 212. https://doi.org/10.1016/j.bej.2024.109492

Andreides, D., Bautista Quispe, J.I., Bartackova, J., Pokorna, D. & Zabranska, J. (2021). A novel two-stage process for biological conversion of syngas to biomethane. *Bioresour Technol,* 327, 124811. https://doi.org/10.1016/j.biortech.2021.124811

Andreides, D., Stransky, D., Bartackova, J., Pokorna, D. & Zabranska, J. (2022). Syngas biomethanation in countercurrent flow trickle-bed reactor operated under different temperature conditions. *Renewable Energy,* 199, 1329-1335. https://doi.org/10.1016/j.renene.2022.09.072

Angelidaki, I., Treu, L., Tsapekos, P., Luo, G., Campanaro, S., Wenzel, H. & Kougias, P.G. (2018). Biogas upgrading and utilization: Current status and perspectives. *Biotechnol Adv,* 36(2), 452-466. https://doi.org/10.1016/j.biotechadv.2018.01.011

Arantes, A.L., Alves, J.I., Stams, A.J.M., Alves, M.M. & Sousa, D.Z. (2018). Enrichment of syngas-converting communities from a multi-orifice baffled bioreactor. *Microbial Biotechnology,* 11(4), 639-646. https://doi.org/10.1111/1751-7915.12864

Aruleeswaran, A., Ashraf, M.T., Ali, R. & Yde, L. (2025). Integration of two trickle-bed reactors in series for enhanced biomethane production from syngas. *ChemRxiv,* Pre-Print. https://doi.org/https://doi.org/10.26434/chemrxiv-2025-5v2fm-v2

Aryal, N., Odde, M., Petersen, C.B., Ottosen, L.D.M. & Kofoed, M.V.W. (2021). Methane production from syngas using a trickle-bed reactor setup. *Bioresource Technology,* 333. https://doi.org/ARTN 12518310.1016/j.biortech.2021.125183

Ashraf, M.T., Sieborg, M.U., Yde, L., Rhee, C., Shin, S.G. & Triolo, J.M. (2020). Biomethanation in a thermophilic biotrickling filter — pH control and lessons from long-term operation. *Bioresource Technology Reports,* 11. https://doi.org/10.1016/j.biteb.2020.100525

Ashraf, M.T., Yde, L., Triolo, J.M. & Wenzel, H. (2021). Optimizing the dosing and trickling of nutrient media for thermophilic biomethanation in a biotrickling filter. *Biochemical Engineering Journal,* 176. https://doi.org/10.1016/j.bej.2021.108220

Asimakopoulos, K., Gavala, H.N. & Skiadas, I.V. (2018). Reactor systems for syngas fermentation processes: A review. *Chemical Engineering Journal,* 348, 732-744. https://doi.org/10.1016/j.cej.2018.05.003

Asimakopoulos, K., Gavala, H.N. & Skiadas, I.V. (2019). Biomethanation of Syngas by Enriched Mixed Anaerobic Consortia in Trickle Bed Reactors. *Waste*

and Biomass Valorization, 11(2), 495-512. https://doi.org/10.1007/s12649-019-00649-2

Asimakopoulos, K., Grimalt-Alemany, A., Lundholm-Høffner, C., Gavala, H.N. & Skiadas, I.V. (2021a). Carbon Sequestration Through Syngas Biomethanation Coupled with H2 Supply for a Clean Production of Natural Gas Grade Biomethane. *Waste and Biomass Valorization,* 12(11), 6005-6019. https://doi.org/10.1007/s12649-021-01393-2

Asimakopoulos, K., Kaufmann-Elfang, M., Lundholm-Høffner, C., Rasmussen, N.B.K., Grimalt-Alemany, A., Gavala, H.N. & Skiadas, I.V. (2021b). Scale up study of a thermophilic trickle bed reactor performing syngas biomethanation. *Applied Energy,* 290. https://doi.org/10.1016/j.apenergy.2021.116771

Asimakopoulos, K., Łężyk, M., Grimalt-Alemany, A., Melas, A., Wen, Z., Gavala, H.N. & Skiadas, I.V. (2020). Temperature effects on syngas biomethanation performed in a trickle bed reactor. *Chemical Engineering Journal,* 393. https://doi.org/10.1016/j.cej.2020.124739

Bengelsdorf, F.R., Beck, M.H., Erz, C., Hoffmeister, S., Karl, M.M., Riegler, P., Wirth, S., Poehlein, A., Weuster-Botz, D. & Durre, P. (2018a). Bacterial Anaerobic Synthesis Gas (Syngas) and CO2+H2 Fermentation. *Adv Appl Microbiol,* 103, 143-221. https://doi.org/10.1016/bs.aambs.2018.01.002

Bengelsdorf, F.R., Beck, M.H., Erz, C., Hoffmeister, S., Karl, M.M., Riegler, P., Wirth, S., Poehlein, A., Weuster-Botz, D. & Dürre, P. (2018b). Chapter Four - Bacterial Anaerobic Synthesis Gas (Syngas) and CO2+H2 Fermentation. In: Sariaslani, S. & Gadd, G.M. (eds) *Advances in Applied Microbiology*. (103). Academic Press. 143-221. [2023-03-17 13:18:42]

Benstead, J., Archer, D.B. & Lloyd, D. (1991). Formate utilization by members of the genus Methanobacterium. *Archives of Microbiology,* 156(1), 34-37. https://doi.org/10.1007/BF00418184

Bilgiç, B., Andersen, T.O., Abera, G.B., Sposób, M., Feng, L. & Horn, S.J. (2025). Syngas biomethanation using trickle bed reactor, impact of external hydrogen addition at high loading rate. *Bioresource Technology Reports*. https://doi.org/10.1016/j.biteb.2025.102197

Blumberg, T., Morosuk, T. & Tsatsaronis, G. (2017). A Comparative Exergoeconomic Evaluation of the Synthesis Routes for Methanol Production from Natural Gas. *Applied Sciences,* 7(12). https://doi.org/10.3390/app7121213

Börjesson, P., Lundgren, J., Ahlgren, S. & Nyström, I. (2016). *Dagens och framtidens hållbara biodrivmedel– i sammandrag*. (The Swedish Knowledge Centre for Renewable Transportation Fuels).

Braga Nan, L., Trably, E., Santa-Catalina, G., Bernet, N., Delgenès, J.-P. & Escudié, R. (2020). Biomethanation processes: new insights on the effect of a high H2 partial pressure on microbial communities. *Biotechnology for Biofuels,* 13(1), 141. https://doi.org/10.1186/s13068-020-01776-y

Bu, F., Dong, N., Kumar Khanal, S., Xie, L. & Zhou, Q. (2018). Effects of CO on hydrogenotrophic methanogenesis under thermophilic and extreme-thermophilic conditions: Microbial community and biomethanation pathways. *Bioresour Technol,* 266, 364-373. https://doi.org/10.1016/j.biortech.2018.03.092

Burkhardt, M. & Busch, G. (2013). Methanation of hydrogen and carbon dioxide. *Applied Energy,* 111, 74-79. https://doi.org/10.1016/j.apenergy.2013.04.080

Burkhardt, M., Jordan, I., Heinrich, S., Behrens, J., Ziesche, A. & Busch, G. (2019). Long term and demand-oriented biocatalytic synthesis of highly concentrated methane in a trickle bed reactor. *Applied Energy,* 240, 818-826. https://doi.org/10.1016/j.apenergy.2019.02.076

Burkhardt, M., Koschack, T. & Busch, G. (2015). Biocatalytic methanation of hydrogen and carbon dioxide in an anaerobic three-phase system. *Bioresource Technology,* 178, 330-333. https://doi.org/10.1016/j.biortech.2014.08.023

Cazier, E.A., Trably, E., Steyer, J.P. & Escudie, R. (2015). Biomass hydrolysis inhibition at high hydrogen partial pressure in solid-state anaerobic digestion. *Bioresour Technol,* 190, 106-13. https://doi.org/10.1016/j.biortech.2015.04.055

Chatzis, A., Gkotsis, P. & Zouboulis, A. (2024). Biological methanation (BM): A state-of-the-art review on recent research advancements and practical implementation in full-scale BM units. *Energy Conversion and Management,* 314. https://doi.org/10.1016/j.enconman.2024.118733

Chen, Y., Cheng, J.J. & Creamer, K.S. (2008). Inhibition of anaerobic digestion process: a review. *Bioresour Technol,* 99(10), 4044-64. https://doi.org/10.1016/j.biortech.2007.01.057

Dahl Jonson, B., Ujarak Sieborg, M., Tahir Ashraf, M., Yde, L., Shin, J., Shin, S.G. & Mi Triolo, J. (2020). Direct inoculation of a biotrickling filter for hydrogenotrophic methanogenesis. *Bioresour Technol,* 318, 124098. https://doi.org/10.1016/j.biortech.2020.124098

Dhakal, N. & Acharya, B. (2021). Syngas Fermentation for the Production of Bio-Based Polymers: A Review. *Polymers (Basel),* 13(22). https://doi.org/10.3390/polym13223917

Diender, M., Pereira, R., Wessels, H.J., Stams, A.J. & Sousa, D.Z. (2016). Proteomic Analysis of the Hydrogen and Carbon Monoxide Metabolism of Methanothermobacter marburgensis. *Frontiers in Microbiology,* 7, 1049. https://doi.org/10.3389/fmicb.2016.01049

Diender, M., Stams, A.J. & Sousa, D.Z. (2015). Pathways and Bioenergetics of Anaerobic Carbon Monoxide Fermentation. *Frontiers in Microbiology,* 6, 1275. https://doi.org/10.3389/fmicb.2015.01275

Dolfing, J. (2014). Thermodynamic constraints on syntrophic acetate oxidation. *Appl Environ Microbiol,* 80(4), 1539-41. https://doi.org/10.1128/AEM.03312-13

Dupnock, T.L. & Deshusses, M.A. (2017). High-Performance Biogas Upgrading Using a Biotrickling Filter and Hydrogenotrophic Methanogens. *Appl Biochem Biotechnol,* 183(2), 488-502. https://doi.org/10.1007/s12010-017-2569-2

Dupnock, T.L. & Deshusses, M.A. (2019). Detailed investigations of dissolved hydrogen and hydrogen mass transfer in a biotrickling filter for upgrading biogas. *Bioresour Technol,* 290, 121780. https://doi.org/10.1016/j.biortech.2019.121780

Dupnock, T.L. & Deshusses, M.A. (2020). Biological Co-treatment of H(2)S and reduction of CO(2) to methane in an anoxic biological trickling filter upgrading biogas. *Chemosphere,* 256, 127078. https://doi.org/10.1016/j.chemosphere.2020.127078

EBA (2024a). *Gasification - Diversification of biomass processing and waste utilisation*. EBA. Gasification: diversification of biomass processing and waste utilisation - European Biogas Association

EBA (2024b). *Mapping - e-methane plants and technologies* EBA. https://www.europeanbiogas.eu/publication/mapping-e-methane-plants-and-technologies/

eFuel alliance (2025). *Analysis of the EU, UK, and US Approaches to Regulatory Frameworks for RFNBOs*. eFuel alliance. 20250618_eFA_Paper_Comparison_Production-Rules_EU-UK-US.pdf

Energigas Sverige (2025). *Produktion av biogas och rötrester och dess användning år 2024*. Stockholm, Sweden. Produktion av biogas och rötrester och dess användning år 2024 - Energigas Sverige

Energimyndigheten (2025). *Tillförsel av energi*. https://www.energimyndigheten.se/energisystemet/tillforsel/#anchor_60112

European Union. *Directive (EU) 2023/2413 of the European Parliament and of the Council of 18 October 2023 amending Directive (EU) 2018/2001*. https://eur-lex.europa.eu/eli/dir/2023/2413/oj

Feickert Fenske, C., Kirzeder, F., Strubing, D. & Koch, K. (2023a). Biogas upgrading in a pilot-scale trickle bed reactor - Long-term biological methanation under real application conditions. *Bioresour Technol,* 376, 128868. https://doi.org/10.1016/j.biortech.2023.128868

Feickert Fenske, C., Md, Y., Strubing, D. & Koch, K. (2023b). Preliminary gas flow experiments identify improved gas flow conditions in a pilot-scale trickle bed reactor for H(2) and CO(2) biological methanation. *Bioresour Technol,* 371, 128648. https://doi.org/10.1016/j.biortech.2023.128648

Feickert Fenske, C., Strubing, D. & Koch, K. (2023c). Biological methanation in trickle bed reactors - a critical review. *Bioresour Technol,* 385, 129383. https://doi.org/10.1016/j.biortech.2023.129383

Figueras, J., Benbelkacem, H., Dumas, C. & Buffiere, P. (2021). Biomethanation of syngas by enriched mixed anaerobic consortium in pressurized agitated

column. *Bioresour Technol,* 338, 125548. https://doi.org/10.1016/j.biortech.2021.125548

Figueras, J., Benbelkacem, H., Dumas, C. & Buffiere, P. (2023). Syngas biomethanation: Study of process performances at high syngas flow rate in pressurized stirred column. *Bioresource Technology,* 376. https://doi.org/10.1016/j.biortech.2023.128936

Garcia-Casado, S., Munoz, R. & Lebrero, R. (2025). Towards syngas biorefineries: The potential of microbial consortia for syngas valorisation. *Biotechnol Adv,* 85, 108699. https://doi.org/10.1016/j.biotechadv.2025.108699

Gerardi, M.H. (2003). *The Microbiology of Anaerobic Digesters*. Wiley. https://books.google.se/books?id=QzzENAEACAAJ

Ghofrani-Isfahani, P., Tsapekos, P., Peprah, M., Kougias, P., Zervas, A., Zhu, X., Yang, Z., Jacobsen, C.S. & Angelidaki, I. (2022). Ex-situ biogas upgrading in thermophilic trickle bed reactors packed with micro-porous packing materials. *Chemosphere,* 296, 133987. https://doi.org/10.1016/j.chemosphere.2022.133987

Goonesekera, E.M., Grimalt-Alemany, A., Thanasoula, E., Yousif, H.F., Krarup, S.L., Valerin, M.C. & Angelidaki, I. (2024). Biofilm mass transfer and thermodynamic constraints shape biofilm in trickle bed reactor syngas biomethanation. *Chemical Engineering Journal,* 500. https://doi.org/10.1016/j.cej.2024.156629

Götz, M., Lefebvre, J., Mörs, F., McDaniel Koch, A., Graf, F., Bajohr, S., Reimert, R. & Kolb, T. (2016). Renewable Power-to-Gas: A technological and economic review. *Renewable Energy,* 85, 1371-1390. https://doi.org/10.1016/j.renene.2015.07.066

Grimalt-Alemany, A., Łężyk, M., Kennes-Veiga, D.M., Skiadas, I.V. & Gavala, H.N. (2019). Enrichment of Mesophilic and Thermophilic Mixed Microbial Consortia for Syngas Biomethanation: The Role of Kinetic and Thermodynamic Competition. *Waste and Biomass Valorization,* 11(2), 465-481. https://doi.org/10.1007/s12649-019-00595-z

Grimalt-Alemany, A., Skiadas, I.V. & Gavala, H.N. (2017). Syngas biomethanation: state-of-the-art review and perspectives. *Biofuels, Bioproducts and Biorefining,* 12(1), 139-158. https://doi.org/10.1002/bbb.1826

Gu, W., Muller, A.L., Deutzmann, J.S., Williamson, J.R. & Spormann, A.M. (2022). Growth rate-dependent coordination of catabolism and anabolism in the archaeon Methanococcus maripaludis under phosphate limitation. *ISME J,* 16(10), 2313-2319. https://doi.org/10.1038/s41396-022-01278-9

Guneratnam, A.J., Ahern, E., FitzGerald, J.A., Jackson, S.A., Xia, A., Dobson, A.D.W. & Murphy, J.D. (2017). Study of the performance of a thermophilic biological methanation system. *Bioresour Technol,* 225, 308-315. https://doi.org/10.1016/j.biortech.2016.11.066

Hattori, S. (2008). Syntrophic acetate-oxidizing microbes in methanogenic environments. *Microbes Environ,* 23(2), 118-27. https://doi.org/10.1264/jsme2.23.118

Hattori, S., Galushko, A.S., Kamagata, Y. & Schink, B. (2005). Operation of the CO dehydrogenase/acetyl coenzyme A pathway in both acetate oxidation and acetate formation by the syntrophically acetate-oxidizing bacterium Thermacetogenium phaeum. *J Bacteriol,* 187(10), 3471-6. https://doi.org/10.1128/JB.187.10.3471-3476.2005

Hjort, A. (2019). *Potentialen för biogas och bio-SNG i Sverige*. Stockholm. https://doi.org/SBN 978-91-7883-026-8

Hurst, K.M. & Lewis, R.S. (2010). Carbon monoxide partial pressure effects on the metabolic process of syngas fermentation. *Biochemical Engineering Journal,* 48(2), 159-165. https://doi.org/10.1016/j.bej.2009.09.004

IEA-Bioenergy (2022). *Valuable (by-)products of gasification*. Valuable (by-)products of gasification – Bioenergy

Industrins Biogaskommission (2025). *Mer biogas till industrin - Åtgärdspaket för industrins materialomställning och konkurrenskraft*. Industrins-Biogaskommission. https://doi.org/https://biogaskommissionen.se/Media/yeqcywc4/ibk_mer-biogas-till-industin-_a-lo.pdf

IPCC (2014). *Climate Change 2014: Synthesis Report. Contribution of Working Groups I, II and III to the Fifth Assessment Report of the Intergovernmental Panel on Climate Change* Geneva, Switzerland: IPCC.

Jensen, M.B., Poulsen, S., Jensen, B., Feilberg, A. & Kofoed, M.V.W. (2021). Selecting carrier material for efficient biomethanation of industrial biogas-CO2 in a trickle-bed reactor. *Journal of CO2 Utilization,* 51, 101611. https://doi.org/10.1016/j.jcou.2021.101611

Jønson, B.D., Tsapekos, P., Tahir Ashraf, M., Jeppesen, M., Ejbye Schmidt, J. & Bastidas-Oyanedel, J.R. (2022). Pilot-scale study of biomethanation in biological trickle bed reactors converting impure CO(2) from a Full-scale biogas plant. *Bioresour Technol,* 365, 128160. https://doi.org/10.1016/j.biortech.2022.128160

Joshua Abioye, K., Rajamanickam, R., Ogunjinmi, T., Paul, S., Selvasembian, R. & Ighalo, J.O. (2025). Advancements in biomass waste conversion to sustainable biofuels via gasification. *Chemical Engineering Journal,* 505. https://doi.org/10.1016/j.cej.2024.159151

Kamravamanesh, D., Rinta Kanto, J.M., Ali-Loytty, H., Myllärinen, A., Saalasti, M., Rintala, J. & Kokko, M. (2023). Ex-situ biological hydrogen methanation in trickle bed reactors: Integration into biogas production facilities. *Chemical Engineering Science,* 269. https://doi.org/10.1016/j.ces.2023.118498

Khalid, H., Raza Amin, F., Gao, L., Chen, L., Chen, W., Javed, S. & Li, D. (2024). Syngas conversion to biofuels and biochemicals: a review of process engineering and mechanisms. *Sustainable Energy & Fuels,* 8(1), 9-28. https://doi.org/10.1039/D3SE00916E

Khosravani, H., Meshksar, M., Rahimpour, H.R. & Rahimpour, M.R. (2023). Chapter 1 - Introduction to syngas products and applications. In:

Rahimpour, M.R., Makarem, M.A. & Meshksar, M. (eds) *Advances in Synthesis Gas: Methods, Technologies and Applications*. (3). Elsevier. 3-25. https://doi.org/https://doi.org/10.1016/B978-0-323-91878-7.00014-9

Kimmel, D.E., Klasson, K.T., Clausen, E.C. & Gaddy, J.L. (1991). Performance of trickle-bed bioreactors for converting synthesis gas to methane. *Applied Biochemistry and Biotechnology,* 28(1), 457. https://doi.org/10.1007/BF02922625

Klasson, K.T., Ackerson, M.D., Clausen, E.C. & Gaddy, J.L. (1992). Bioconversion of synthesis gas into liquid or gaseous fuels. *Enzyme and Microbial Technology,* 14(8), 602-608. https://doi.org/10.1016/0141-0229(92)90033-K

Klasson, K.T., Cowger, J.P., Ko, C.W., Vega, J.L., Clausen, E.C. & Gaddy, J.L. (1990). Methane production from synthesis gas using a mixed culture of R. rubrum, M. barkeri, and M. formicicum. *Applied Biochemistry and Biotechnology,* 24(1), 317-328. https://doi.org/10.1007/BF02920256

Kumar, K.K., Cema, G., Ziembinska-Buczynska, A., Hassan, G.K., Hellal, M.S. & Surmacz-Gorska, J. (2025). Sustainable biomethane production from waste biomass: challenges associated with process optimization in improving the yield. *Environ Sci Pollut Res Int*. https://doi.org/10.1007/s11356-024-35864-5

Larsson, A., Gunnarsson, I. & tengberg, F. (2019). *The GoBiGas Project - Demonstration of the production of Biomethane from Biomass via Gasification*. AB, G.E.

Lee, M.J. & Zinder, S.H. (1988). Hydrogen Partial Pressures in a Thermophilic Acetate-Oxidizing Methanogenic Coculture. *Applied and Environmental Microbiology,* 54(6), 1457-1461. https://doi.org/doi:10.1128/aem.54.6.1457-1461.1988

Li, C., Zhu, X. & Angelidaki, I. (2020). Carbon monoxide conversion and syngas biomethanation mediated by different microbial consortia. *Bioresour Technol,* 314, 123739. https://doi.org/10.1016/j.biortech.2020.123739

Li, C., Zhu, X. & Angelidaki, I. (2021). Syngas biomethanation: effect of biomass-gas ratio, syngas composition and pH buffer. *Bioresour Technol,* 342, 125997. https://doi.org/10.1016/j.biortech.2021.125997

Liu, R., Hao, X. & Wei, J. (2016). Function of homoacetogenesis on the heterotrophic methane production with exogenous H2/CO2 involved. *Chemical Engineering Journal,* 284, 1196-1203. https://doi.org/10.1016/j.cej.2015.09.081

Lönnqvist, T., Sanches-Pereira, A. & Sandberg, T. (2015). Biogas potential for sustainable transport – a Swedish regional case. *Journal of Cleaner Production,* 108, 1105-1114. https://doi.org/10.1016/j.jclepro.2015.07.036

Luo, G., Wang, W. & Angelidaki, I. (2013). Anaerobic digestion for simultaneous sewage sludge treatment and CO biomethanation: process performance and microbial ecology. *Environ Sci Technol,* 47(18), 10685-93. https://doi.org/10.1021/es401018d

Mancipe-Jiménez, D.C., Costa, C. & Márquez, M.C. (2017). Methanogenesis inhibition by phosphorus in anaerobic liquid waste treatment. *Waste Treatment and Recovery,* 2(1), 1-8. https://doi.org/10.1515/lwr-2017-0001

Menin, L., Asimakopoulos, K., Sukumara, S., Rasmussen, N.B.K., Patuzzi, F., Baratieri, M., Gavala, H.N. & Skiadas, I.V. (2022). Competitiveness of syngas biomethanation integrated with carbon capture and storage, power-to-gas and biomethane liquefaction services: Techno-economic modeling of process scenarios and evaluation of subsidization requirements. *Biomass and Bioenergy,* 161. https://doi.org/10.1016/j.biombioe.2022.106475

Mesfun, S., Engvall, K. & Toffolo, A. (2022). Electrolysis Assisted Biomass Gasification for Liquid Fuels Production. *Frontiers in Energy Research,* 10. https://doi.org/10.3389/fenrg.2022.799553

Miceli, J.F., 3rd, Torres, C.I. & Krajmalnik-Brown, R. (2016). Shifting the balance of fermentation products between hydrogen and volatile fatty acids: microbial community structure and function. *Fems Microbiology Ecology,* 92(12). https://doi.org/10.1093/femsec/fiw195

Milledge, J., Smith, B., Dyer, P. & Harvey, P. (2014). Macroalgae-Derived Biofuel: A Review of Methods of Energy Extraction from Seaweed Biomass. *Energies,* 7(11), 7194-7222. https://doi.org/10.3390/en7117194

Minchener, A.J. (2005). Coal gasification for advanced power generation. *Fuel,* 84(17), 2222-2235. https://doi.org/10.1016/j.fuel.2005.08.035

Molino, A., Chianese, S. & Musmarra, D. (2016). Biomass gasification technology: The state of the art overview. *Journal of Energy Chemistry,* 25(1), 10-25. https://doi.org/10.1016/j.jechem.2015.11.005

Neto, A.S., Wainaina, S., Chandolias, K., Piatek, P. & Taherzadeh, M.J. (2025). Exploring the Potential of Syngas Fermentation for Recovery of High-Value Resources: A Comprehensive Review. *Curr Pollut Rep,* 11(1), 7. https://doi.org/10.1007/s40726-024-00337-3

Nielsen, M.B., Kjeldsen, K.U. & Ingvorsen, K. (2006). Desulfitibacter alkalitolerans gen. nov., sp. nov., an anaerobic, alkalitolerant, sulfite-reducing bacterium isolated from a district heating plant. *Int J Syst Evol Microbiol,* 56(Pt 12), 2831-2836. https://doi.org/10.1099/ijs.0.64356-0

Paniagua, S., Lebrero, R. & Munoz, R. (2022). Syngas biomethanation: Current state and future perspectives. *Bioresour Technol,* 358, 127436. https://doi.org/10.1016/j.biortech.2022.127436

Poehlein, A., Zeldes, B., Flaiz, M., Boer, T., Luschen, A., Hofele, F., Baur, K.S., Molitor, B., Kroly, C., Wang, M., Zhang, Q., Fan, Y., Chao, W., Daniel, R., Li, F., Basen, M., Muller, V., Angenent, L.T., Sousa, D.Z. & Bengelsdorf, F.R. (2025). Advanced aspects of acetogens. *Bioresour Technol,* 427, 131913. https://doi.org/10.1016/j.biortech.2024.131913

Porte, H., Kougias, P.G., Alfaro, N., Treu, L., Campanaro, S. & Angelidaki, I. (2019). Process performance and microbial community structure in thermophilic trickling biofilter reactors for biogas upgrading. *Science of the*

Total Environment, 655, 529-538. https://doi.org/10.1016/j.scitotenv.2018.11.289

Rachbauer, L., Voitl, G., Bochmann, G. & Fuchs, W. (2016). Biological biogas upgrading capacity of a hydrogenotrophic community in a trickle-bed reactor. *Applied Energy,* 180, 483-490. https://doi.org/10.1016/j.apenergy.2016.07.109

Rauch, R., Hofbauer, H., Bosch, K., Siefert, I., Aichernig, C., Tremmel, H., Voigtländer, K., Koch, R. & Lehner, R. (2004). Steam gasification of biomass at CHP plant in Güssing - Status of the demonstration plant. *2nd World Conference and Technology Exhibition on Biomass for Energy, Industry and Climate Protection,* Rome, Italy.

Ren, J., Liu, Y.-L., Zhao, X.-Y. & Cao, J.-P. (2020). Methanation of syngas from biomass gasification: An overview. *International Journal of Hydrogen Energy,* 45(7), 4223-4243. https://doi.org/10.1016/j.ijhydene.2019.12.023

Reysenbach, A.-L., Huber, R., Stetter, K.O., Davey, M.E., MacGregor, B.J. & Stahl, D.A. (2001). Phylum BII. Thermotogae phy. nov. In: Boone, D.R., Castenholz, R.W. & Garrity, G.M. (eds) *Bergey's Manual® of Systematic Bacteriology: Volume One: The Archaea and the Deeply Branching and Phototrophic Bacteria*. New York, NY: Springer New York. 369-387. https://doi.org/10.1007/978-0-387-21609-6_19

Salazar-Batres, K.J. & Moreno-Andrade, I. (2025). Review of the Effects of Trace Metal Concentrations on the Anaerobic Digestion of Organic Solid Waste. *BioEnergy Research,* 18(1). https://doi.org/10.1007/s12155-025-10826-y

Sancho Navarro, S., Cimpoia, R., Bruant, G. & Guiot, S.R. (2016). Biomethanation of Syngas Using Anaerobic Sludge: Shift in the Catabolic Routes with the CO Partial Pressure Increase. *Frontiers in Microbiology,* 7, 1188. https://doi.org/10.3389/fmicb.2016.01188

Sander, R. (2023). Compilation of Henry's law constants (version 5.0.0) for water as solvent. *Atmospheric Chemistry and Physics,* 23(19), 10901-12440. https://doi.org/10.5194/acp-23-10901-2023

SCB (2023). *Marken i Sverige*. https://www.scb.se/hitta-statistik/sverige-i-siffror/miljo/marken-i-sverige/

Shakeri Yekta, S., Svensson, B.H., Skyllberg, U. & Schnurer, A. (2023). Sulfide in engineered methanogenic systems - Friend or foe? *Biotechnol Adv,* 69, 108249. https://doi.org/10.1016/j.biotechadv.2023.108249

Sieborg, M.U., Jensen, M.B., Jensen, B. & Kofoed, M.V.W. (2021). Effect of minimizing carrier irrigation on H2 conversion in trickle bed reactors during ex situ biomethanation. *Bioresource Technology Reports,* 16. https://doi.org/10.1016/j.biteb.2021.100876

Sieborg, M.U., Jønson, B.D., Ashraf, M.T., Yde, L. & Triolo, J.M. (2020). Biomethanation in a thermophilic biotrickling filter using cattle manure as nutrient media. *Bioresource Technology Reports,* 9. https://doi.org/10.1016/j.biteb.2020.100391

Sipma, J., Lens, P.N.L., Stams, A.J.M. & Lettinga, G. (2003). Carbon monoxide conversion by anaerobic bioreactor sludges. *Fems Microbiology Ecology,* 44(2), 271-277. https://doi.org/10.1016/S0168-6496(03)00033-3

SOU (2019:63). *Mer biogas! För ett hållbart Sverige*. (Elanders Sverige AB). Stockholm 2019. https://doi.org/ISBN 978-91-38-25002-0

Stams, A.J.M., Teusink, B. & Sousa, D.Z. (2019). Ecophysiology of Acetoclastic Methanogens. In: Stams, A.J.M. & Sousa, D. (eds) *Biogenesis of Hydrocarbons*. Cham: Springer International Publishing. 1-14. https://doi.org/10.1007/978-3-319-53114-4_21-1

Strübing, D., Huber, B., Lebuhn, M., Drewes, J.E. & Koch, K. (2017). High performance biological methanation in a thermophilic anaerobic trickle bed reactor. *Bioresoure Technology,* 245(Pt A), 1176-1183. https://doi.org/10.1016/j.biortech.2017.08.088

Strübing, D., Moeller, A.B., Mossnang, B., Lebuhn, M., Drewes, J.E. & Koch, K. (2019). Load change capability of an anaerobic thermophilic trickle bed reactor for dynamic H2/CO2 biomethanation. *Bioresoure Technology,* 289, 121735. https://doi.org/10.1016/j.biortech.2019.121735

Strübing, D., Moeller, A.B., Mößnang, B., Lebuhn, M., Drewes, J.E. & Koch, K. (2018). Anaerobic thermophilic trickle-bed reactor as a promising technology for flexible, demand-oriented H2/CO2 biomethanation. *Applied Energy,* 232, 543-554. https://doi.org/10.1016/j.apenergy.2018.09.225

Taqvi, S.A.A., Kazmi, B., Naqvi, S.R., Juchelková, D. & Bokhari, A. (2024). State-of-the-Art Review of Biomass Gasification: Raw to Energy Generation. *ChemBioEng Reviews,* 11(4). https://doi.org/10.1002/cben.202400003

Thauer, R.K., Kaster, A.K., Seedorf, H., Buckel, W. & Hedderich, R. (2008). Methanogenic archaea: ecologically relevant differences in energy conservation. *Nat Rev Microbiol,* 6(8), 579-91. https://doi.org/10.1038/nrmicro1931

Thema, M., Weidlich, T., Hörl, M., Bellack, A., Mörs, F., Hackl, F., Kohlmayer, M., Gleich, J., Stabenau, C., Trabold, T., Neubert, M., Ortloff, F., Brotsack, R., Schmack, D., Huber, H., Hafenbradl, D., Karl, J. & Sterner, M. (2019). Biological CO2-Methanation: An Approach to Standardization. *Energies,* 12(9). https://doi.org/10.3390/en12091670

Thema, M., Weidlich, T., Kaul, A., Bollmann, A., Huber, H., Bellack, A., Karl, J. & Sterner, M. (2021). Optimized biological CO2-methanation with a pure culture of thermophilic methanogenic archaea in a trickle-bed reactor. *Bioresource Technology,* 333, 125135. https://doi.org/10.1016/j.biortech.2021.125135

Thunman, H., Gustavsson, C., Larsson, A., Gunnarsson, I. & Tengberg, F. (2019). Economic assessment of advanced biofuel production via gasification using cost data from the GoBiGas plant. *Energy Science & Engineering,* 7(1), 217-229. https://doi.org/10.1002/ese3.271

Tsapekos, P., Treu, L., Campanaro, S., Centurion, V.B., Zhu, X., Peprah, M., Zhang, Z., Kougias, P.G. & Angelidaki, I. (2021). Pilot-scale biomethanation in a trickle bed reactor: Process performance and microbiome functional reconstruction. *Energy Conversion and Management,* 244. https://doi.org/10.1016/j.enconman.2021.114491

Ullrich, T. & Lemmer, A. (2018). Performance enhancement of biological methanation with trickle bed reactors by liquid flow modulation. *GCB Bioenergy,* 11(1), 63-71. https://doi.org/10.1111/gcbb.12547

Ullrich, T., Lindner, J., Bar, K., Mors, F., Graf, F. & Lemmer, A. (2018). Influence of operating pressure on the biological hydrogen methanation in trickle-bed reactors. *Bioresour Technol,* 247, 7-13. https://doi.org/10.1016/j.biortech.2017.09.069

Villemur, R., Lanthier, M., Beaudet, R. & Lepine, F. (2006). The Desulfitobacterium genus. *FEMS Microbiol Rev,* 30(5), 706-33. https://doi.org/10.1111/j.1574-6976.2006.00029.x

Wainaina, S., Horvath, I.S. & Taherzadeh, M.J. (2018). Biochemicals from food waste and recalcitrant biomass via syngas fermentation: A review. *Bioresour Technol,* 248(Pt A), 113-121. https://doi.org/10.1016/j.biortech.2017.06.075

Westerholm, M., Dolfing, J. & Schnurer, A. (2019). Growth Characteristics and Thermodynamics of Syntrophic Acetate Oxidizers. *Environ Sci Technol,* 53(9), 5512-5520. https://doi.org/10.1021/acs.est.9b00288

Westerholm, M., Hansson, M. & Schnurer, A. (2012). Improved biogas production from whole stillage by co-digestion with cattle manure. *Bioresour Technol,* 114, 314-9. https://doi.org/10.1016/j.biortech.2012.03.005

Westerholm, M., Isaksson, S., Karlsson Lindsjö, O. & Schnürer, A. (2018). Microbial community adaptability to altered temperature conditions determines the potential for process optimisation in biogas production. *Applied Energy,* 226, 838-848. https://doi.org/10.1016/j.apenergy.2018.06.045

Westerholm, M., Roos, S. & Schnurer, A. (2010). Syntrophaceticus schinkii gen. nov., sp. nov., an anaerobic, syntrophic acetate-oxidizing bacterium isolated from a mesophilic anaerobic filter. *FEMS Microbiol Lett,* 309(1), 100-4. https://doi.org/10.1111/j.1574-6968.2010.02023.x

Xu, N., Liu, S., Xin, F., Zhou, J., Jia, H., Xu, J., Jiang, M. & Dong, W. (2019). Biomethane Production From Lignocellulose: Biomass Recalcitrance and Its Impacts on Anaerobic Digestion. *Front Bioeng Biotechnol,* 7, 191. https://doi.org/10.3389/fbioe.2019.00191

Yasin, M., Jeong, Y., Park, S., Jeong, J., Lee, E.Y., Lovitt, R.W., Kim, B.H., Lee, J. & Chang, I.S. (2015). Microbial synthesis gas utilization and ways to resolve kinetic and mass-transfer limitations. *Bioresour Technol,* 177, 361-74. https://doi.org/10.1016/j.biortech.2014.11.022

Youngsukkasem, S., Chandolias, K. & Taherzadeh, M.J. (2015). Rapid bio-methanation of syngas in a reverse membrane bioreactor: membrane

encased microorganisms. *Bioresour Technol,* 178, 334-340. https://doi.org/10.1016/j.biortech.2014.07.071

Zannoni, D. & De Philioois, R. (2014). *Microbial BioEnergy: Hydrogen Production*. https://doi.org/DOI 10.1007/978-94-017-8554-9

Zhao, Y., Haddad, M., Cimpoia, R., Liu, Z. & Guiot, S.R. (2013). Performance of a Carboxydothermus hydrogenoformans-immobilizing membrane reactor for syngas upgrading into hydrogen. *International Journal of Hydrogen Energy,* 38(5), 2167-2175. https://doi.org/10.1016/j.ijhydene.2012.11.038

Popular Science Summary

Imagine turning biomass, such as forestry residues, into clean, renewable energy using microbes — *syngas biomethanation* holds this promise. This process uses specialized microorganisms to convert syngas — a mixture of hydrogen, carbon monoxide, and carbon dioxide derived from the thermal gasification of biomass — into biomethane, a green fuel that can replace fossil natural gas. This dissertation explored strategies to optimize this conversion using trickle-bed reactors (TBRs), in which gases and liquids flow over beds packed with microbes that do the work.

Over several years, lab-scale TBRs were operated under various conditions to understand the factors that make the system run efficiently and robustly. Different nutrient sources were tested, such as digestate from biogas plants and wastewater byproducts. Nutrient availability, notably sulfur and phosphorus, was found to play a key role in sustaining microbial activity. How reactor settings affect the process was also assessed, including how often liquid is recirculated, how quickly nutrients are supplied, and even how the syngas composition affects conversion. Increasing the hydrogen share in the inlet gas, for example, boosted biomethane output but only up to a certain point, after which the microbes struggled to keep up.

The study revealed valuable insights into the biological and operational limits of syngas biomethanation using TBR. It showed that fine-tuning reactor conditions and nutrient inputs can significantly boost methane production, paving the way for more efficient renewable gas systems. Ultimately, this work brings us one step closer to turning recalcitrant biomass into sustainable energy, contributing to a cleaner and more circular energy future.

Populärvetenskaplig Sammanfattning

Tänk dig att omvandla biomassa som skogsavfall till ren, förnybar energi med hjälp av mikrober – det är vad syngasbiometanisering lovar. Denna process använder speciella mikroorganismer för att omvandla syntesgas – en blandning av väte, koloxid och koldioxid som man får från termisk förgasning av biomassa – till biometan, ett grönt bränsle som kan ersätta fossil naturgas. Denna avhandling undersökte hur man kan optimera denna omvandling med hjälp av droppbädsreaktorer (TBR), där gaser och vätskor strömmar över en bädd fyllda med mikroorganismer som utför arbetet.

Under flera år kördes TBR i laboratorieskala under olika förhållanden för att förstå vad som gör att systemet fungerar effektivt och robust. Olika näringskällor testades, såsom rötrester från biogasanläggningar och biprodukter från avloppsvatten. Det visade sig att tillgången på näringsämnen, särskilt svavel och fosfor, spelar en viktig roll för att upprätthålla den mikrobiella aktiviteten. Hur styrningen av reaktorn påverkar processen undersöktes också, till exempel hur ofta vätskan recirkuleras, hur snabbt näringsämnen tillförs och till och med hur sammansättningen av själva syntesgasen påverkar omvandlingen. Att öka andelen väte i inloppsgasen ökade till exempel biometanproduktionen, men bara upp till en viss punkt, varefter mikroberna hade svårt att hålla jämna steg.

Studien gav värdefulla insikter om de biologiska och driftsmässiga begränsningarna för biometanisering av syntesgas med hjälp av TBR. Den visade sig att finjustering av reaktorförhållanden och näringstillförsel kan öka metanproduktionen avsevärt, vilket banar väg för effektivare system för förnybar gas. I slutändan tar detta arbete oss ett steg närmare att omvandla svårnedbrytbar biomassa till hållbar energi, vilket bidrar till en renare och mer cirkulär energiframtid.

Acknowledgements

The PhD thesis was funded by the Swedish Energy Agency (Energimyndigheten) [149656-1].

First and foremost, I would like to express my sincere gratitude to my main supervisor, Åke Nordberg, for his continuous guidance, encouragement, and insightful discussions throughout this work. I cannot imagine reaching this point without you. Your contributions, enthusiasm, and belief in the project and me have left a lasting impact.
I am equally grateful to my co-supervisor, Anna Schnürer, for her valuable feedback during the experiments, her support, and her motivation to broaden my perspective on microbiological aspects. My sincere thanks also go to Leticia Pizzul for her co-supervision, endless lessons in the lab, constructive feedback, and, most importantly, for keeping me on track with the right amount of pressure (the red book will never be forgotten). I would also like to thank Leandro Janke, who was part of the supervisory team until the second year, for his early input and engagement.
Special thanks go to George B. Cheng, a great collaborator and co-author, for his constructive approach and patience in handling last-minute figure revisions under tight deadlines. Your positive energy made our joint work both productive and enjoyable.
I am deeply appreciative of all my colleagues at RISE, Uppsala, who have been generous with their time and always ready to share tips and tricks for practical lab work — and for the Swedish practice during lunch and fika breaks. In particular, I would like to thank Karin, Henrik, Johan, and Anders for their help with data analysis, their constant technical support, and for making the experiments run (more or less) smoothly.
I am also grateful to my fellow PhD students for accepting me as a comrade — despite joining the group later than most — and for the shared frustrations, encouragement, and good moments that made this journey more rewarding.
My heartfelt thanks go to my friends and family for their constant belief in me, for keeping me grounded, and for reminding me of life beyond research.
To my beloved daughters, who bring joy and perspective to every single day — I'm so proud to be your daddy.

And finally, to my wife — your love, patience, and unwavering support have been my greatest source of strength and motivation. This achievement is as much yours as it is mine.

I

Applied Microbiology and Biotechnology (2022) 106:5317–5333
https://doi.org/10.1007/s00253-022-12035-5

ENVIRONMENTAL BIOTECHNOLOGY

Microbial community development during syngas methanation in a trickle bed reactor with various nutrient sources

George Cheng[1] · Florian Gabler[2,3] · Leticia Pizzul[3] · Henrik Olsson[3] · Åke Nordberg[2,3] · Anna Schnürer[1]

Received: 3 February 2022 / Revised: 13 June 2022 / Accepted: 16 June 2022 / Published online: 8 July 2022

Abstract

Microbial community development within an anaerobic trickle bed reactor (TBR) during methanation of syngas (56% H_2, 30% CO, 14% CO_2) was investigated using three different nutrient media: defined nutrient medium (241 days), diluted digestate from a thermophilic co-digestion plant operating with food waste (200 days) and reject water from dewatered digested sewage sludge at a wastewater treatment plant (220 days). Different TBR operating periods showed slightly different performance that was not clearly linked to the nutrient medium, as all proved suitable for the methanation process. During operation, maximum syngas load was 5.33 L per L packed bed volume (pbv) & day and methane (CH_4) production was 1.26 L CH_4/L_{pbv}/d. Microbial community analysis with Illumina Miseq targeting 16S rDNA revealed high relative abundance (20–40%) of several potential syngas and acetate consumers within the genera *Sporomusa*, *Spirochaetaceae*, *Rikenellaceae* and *Acetobacterium* during the process. These were the dominant taxa except in a period with high flow rate of digestate from the food waste plant. The dominant methanogen in all periods was a member of the genus *Methanobacterium*, while *Methanosarcina* was also observed in the carrier community. As in reactor effluent, the dominant bacterial genus in the carrier was *Sporomusa*. These results show that syngas methanation in TBR can proceed well with different nutrient sources, including undefined medium of different origins. Moreover, the dominant syngas community remained the same over time even when non-sterilised digestates were used as nutrient medium.

Key points

- *Independent of nutrient source, syngas methanation above 1 L/L_{pbv}/D was achieved.*
- *Methanobacterium and Sporomusa were dominant genera throughout the process.*
- *Acetate conversion proceeded* via *both methanogenesis and syntrophic acetate oxidation.*

Keywords Methanation · Syngas · Microbial community · *Sporomusa* · *Methanobacterium* · Trickling bed reactor

Introduction

Anaerobic digestion is a well-established and well-known process-based technology for treatment of different types of organic waste streams, such as sewage sludge, manure or food waste, while producing renewable energy (biogas) and a nutrient-rich digestate that can be used as fertiliser (Kougias and Angelidaki 2018). Among possible substrates for biogas production, plant biomass residues, such as straw, represent a huge global resource with great potential (Paul and Dutta 2018). However, such materials are currently rather under-used in biogas reactors due to limited applicability within the conventional digestion process (Hendriks and Zeeman 2009; Paul and Dutta 2018). One way to tap the potential of such materials can be thermal gasification to syngas, followed by conversion to methane (Ren et al. 2020).

The composition of syngas varies depending on biomass type and gasification conditions, but it mainly consists of methane (CH_4), carbon dioxide (CO_2), hydrogen (H_2) and carbon monoxide (CO), with very low concentrations of nitrogen (N_2) and oxygen (O_2) and trace gases in varying amounts (Ciliberti et al. 2020). Although syngas can be

✉ Anna Schnürer
anna.schnurer@slu.se

[1] Department of Molecular Science, Biocenter SLU, Box 7015, 750 07 Uppsala, Sweden

[2] Department of Energy and Technology, SLU, Box 7032, 750 07 Uppsala, Sweden

[3] Department of Biorefinery and Energy, RISE, Box 7033, 750 07 Uppsala, Sweden

combusted directly, conversion to an established biofuel, such as methane, offers synergies with existing infrastructure for energy storage and distribution (Ren et al. 2020). Methanation of syngas can be performed by chemical catalytic methods or biologically (biomethanation) using methanogenic archaea (Ren et al. 2020). Biomethanation has the advantage that it can be carried out at ambient operating conditions (low pressure, low temperature) (Asimakopoulos et al. 2020b; Aryal et al. 2021; Wegener Kofoed et al. 2021). Moreover, compared with the chemical conversion process biomethanation is more robust to impurities, such as tar or hydrogen sulphide (H_2S) (Grimalt-Alemany et al. 2018). Based on this, biomethanation is estimated to be more cost-efficient than chemical catalytic conversion (Benjaminsson et al. 2013).

One challenge for the biomethanation process is gas–liquid transfer. Among different reactor systems available, the trickle bed reactor (TBR) can be considered an efficient technology for producing biomethane from syngas (Sposob et al. 2021). The TBR consists of a column packed with carrier material with high surface area, for immobilisation of microbial biomass. A liquid nutrient medium to support microbial growth and activity is sprinkled at the top of the TBR and trickles over the carrier material to the bottom of the reactor, while input gas flows in a counter-current or co-current direction. Rate-limiting mass transfer of gases is circumvented in TBR, since the carrier material provides a large surface area for interactions between gas, liquid and biofilm (Sposob et al. 2021). However, combining TBR and biomethanation is a relatively new concept and parameters indicating a stable continuous process and high output have not yet been identified (Grimalt-Alemany et al. 2017).

Acetogenesis and methanogenesis are two main essential microbial routes during methanation of syngas or H_2/CO_2 (Grimalt-Alemany et al. 2018), although syntrophic acetate oxidation (SAO) can also be part of the process (Sancho Navarro et al. 2016) (Fig. 1). Hydrogenotrophic methanogens convert H_2 and CO_2 to CH_4, but the same substrates can be used by acetogens for the production of acetate, creating competition for H_2. In addition, CO can be used by acetogenic bacteria (Arantes et al. 2020) but can also be converted by some methanogens (Ferry 2010; Sancho Navarro et al. 2016). Based on thermodynamics and substrate affinities, methanogens have an advantage over acetogens as they can use lower levels of dissolved hydrogen (reviewed in Wegener Kofoed et al. 2021). However, acetogens become more competitive at lower operating temperatures (Fu et al. 2019), higher hydrogen levels (Liu et al. 2016) and high or low pH values, which inhibit methanogens (Voelklein et al. 2019). Acetate can be consumed by acetoclastic methanogens to produce methane or oxidised to H_2/CO_2 by syntrophic acetate-oxidising bacteria. The latter process is preferentially operating under low partial pressures of hydrogen

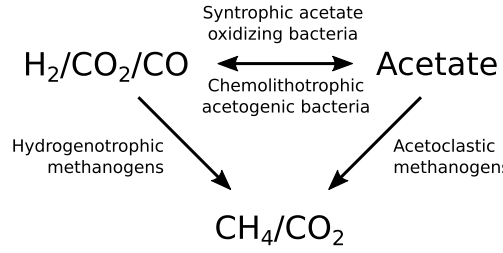

Fig. 1 Groups of microbes involved in methanation of syngas. Hydrogenotrophic methanogens converting H_2/CO_2 to methane (CH_4) also compete with chemolithotrophic acetogenic bacteria that consume H_2/CO_2 to produce acetate. Acetate is consumed by either acetoclastic methanogens for CH_4 production or syntrophic acetate oxidising bacteria to produce H_2/CO_2

and carbon dioxide and thus are likely to have a negligible role during methanation of syngas. However, under certain conditions syntrophic acetate oxidation can be enabled and compete with acetoclastic methanogenesis, such as during low P_{CO2} levels (< 0.01 atm), which improves the thermodynamics of this metabolic route (Grimalt-Alemany et al. 2020a), and high P_{CO} concentrations, which inhibits acetate utilising methanogens (Sancho Navarro et al. 2016).

To ensure high microbiological activity and growth during conversion of gases, such as syngas or H_2/CO_2, it is important to supply sufficient amounts of nutrients with the liquid medium (Wegener Kofoed et al. 2021). It is well known that, in addition to carbon and energy sources represented by the process gases, microorganisms (including methane producers) also need other macronutrients and micronutrients, such as nitrogen (N), phosphorus (P), sulphur (S) and various salts and trace metals (Jarrell and Kalmokoff 1988). Several previous studies have examined syngas methanation in laboratory-scale TBR operating with different defined nutrient media (Burkhardt et al. 2015; Asimakopoulos et al. 2020a, b). For full-scale application, there is a need for more accessible and economically feasible nutrient sources, such as manure, digestate or reject water from sludge processing in wastewater treatment plants (WWTP). The use of such undefined nutrient media has mainly been evaluated for biomethanation of H_2/CO_2, during operation in batch or continuous mode (Kougias and Angelidaki 2018; Sieborg et al. 2020; Tsapekos et al. 2021), and for biomethanation of syngas in a TBR in batch mode (Aryal et al. 2021). To our knowledge, only one previous study has used a non-defined nutrient source during continuous operation of a TBR for syngas methanation (Figueras et al. 2021).

The biological processes involved in syngas conversion have been investigated in many studies and have been shown to be influenced by different parameters, such as type of reactor and carrier, composition of the gas, environmental

parameters such as temperature, and liquid recirculating rates and nutrient composition (for reviews, see Grimalt-Alemany et al. 2017; Aryal et al. 2021; Li et al. 2021; Sposob et al. 2021; Tsapekos et al. 2021). Other determinants of process efficiency, such as microbial community structure and abundance as influenced by operating parameters, have been less thoroughly investigated and the links between operational settings and performance and the microbial community are not fully understood. The few microbiological analyses that have been performed have mainly focused on methanation from H_2/CO_2 (Sposob et al. 2021; Tsapekos et al. 2021) and less on syngas, and most studies have been performed at thermophilic temperatures, using defined medium (Li et al. 2020a, 2021; Andreides et al. 2021; Aryal et al. 2021). The aim of the present study was to extend knowledge on the microbiology of syngas methanation and, more specifically, to investigate the influence of different nutrient media on microbial community development during long-term operation of a mesophilic TBR. The work formed part of a larger research project and was performed over 3 years in a succession of periods utilising defined and complex nutrient medium, represented by digestate from a food waste–based biogas plant and reject waster from a WWTP. The syngas used in the study was designed to mimic the expected composition of syngas according to an industrial partner, Cortus Energy Ltd.

Material and methods

Screening and selection of inoculum

Initial screening of syngas consumption capacity, using digestate from three different mesophilic biogas reactors (a, b, c), was performed to select a suitable microbial inoculum for the start-up of the TBR. Reactors a and b were mesophilic laboratory-scale reactors, operating with cow manure and mixed food waste, respectively. Operation and performance of these reactors have been described elsewhere, as manure-based Reactor A_{ref} in Ahlberg-Eliasson et al. (2021) and food waste reactor GR2 in Westerholm et al. (2015), respectively. The third inoculum was taken from a full-scale reactor (c), located at Uppsala WWTP, operating with a mix of secondary and primary sludge at mesophilic temperature (37 °C), using an organic load of 2 g volatile solids/L day and a hydraulic retention time of 18 days. The volatile solid concentration (% of wet weight) in inoculum from reactor a, b and c was 6.1, 2.9 and 1.5%, respectively. Each inoculum was incubated at 37 °C for 7 days to remove excess gas from endogenous material and then 200 mL of inoculum was transferred to each of 12 serum bottles (539.5 mL) under flushing with nitrogen gas. The bottles were sealed with butyl rubber stoppers and aluminium caps and filled with different gases to one of the following concentrations (%) at a final pressure of 1.5 atm: (i) CO/N_2 (15/85%); (ii) $CO/H_2/CO_2/N_2$ (15/28/7/50%); (iii) H_2/CO_2 (28/72%); (iv) N_2 (100%), with three replicates per gas composition. The gases used were synthetic mixtures supplied by Air Liquide (Paris, France). The bottles were then incubated at 37 °C for 10 days on a shaking table at 200 rpm (Orbitron, Infors, Bottmingen, Switzerland). Gas compositional analyses were performed after 1, 2, 3, 7, 8 and 10 days. On each sampling occasion, the pressure was measured (model GMH3111; Greisinger Electronics, Regenstauf, Germany) and a 5 mL gas sample (at normal pressure) was taken with a plastic syringe. The gas was analysed by gas chromatography (see below). Based on the initial screening of syngas consumption (Fig. S1), inoculum from the manure-based reactor (reactor a) was selected as the inoculum source.

Digestate collected from reactor a (inoculum A) was filtered through a 2-mm mesh to remove large particles, after which 1.25 L was diluted with defined mineral medium (Westerholm et al. 2010) to reach a final volume of 5 L. The diluted digestate was transferred under flushing (N_2) to two plastic containers (20 L), each filled with 17.5 L plastic carrier (Hiflow® ring 15–7 plastic; height 15 mm, specific area 313 m^2/m^3, density 80 kg/m^3, void fraction 91%). The containers were closed and incubated anaerobically at 37 °C for 7 days, with manual shaking twice every day. This incubation was intended to reduce the level of organic matter in the inoculum, decrease background CH_4 production and initiate biofilm development on the carrier before filling the TBR.

Source of nutrients

During operation of the TBR, three different nutrient sources were used: defined medium (M1); digestate from a thermophilic biogas plant (Uppsala, Sweden) operating with mixed food waste (Grim et al. 2015) (M2); and reject water from dewatered digestate from a biogas unit at a WWTP (Höganäs, Sweden) operating with mixed primary and activated sludge (M3). Medium M1 was prepared as described previously (Westerholm et al. 2010) and consisted of phosphate/bicarbonate buffer supplemented with salt, trace metals, vitamins and reducing agents (e.g. cysteine-hydrochloric acid (HCl) and sodium sulphide (NaS_2)). These reducing agents also represented the only S source in the medium, with a total S concentration of 135 mg/L. The N source in the medium was ammonium chloride (NH_4Cl), with an ammonium-N concentration of 400 mg/L. The pH of M1 was 7.2–7.4. Medium M2 was prepared by mixing one volume unit of digestate with two volume units of deionised water. The resulting liquid was passed through a cloth to remove particles. No sterilisation of the liquid was performed. This diluted solution had a pH of 8.5–8.6, total alkalinity of 2249–3057 mg/L and an ammonium-N

concentration of 300–670 mg/L. Sulphur was analysed as sulphate and the concentration was 50–60 mg/L. The reject water medium (M3) was dewatered but not sterilised at the WWTP and no further treatment was done before its use as nutrient medium for the TBR. The pH was 7.6–7.9, the total alkalinity was 2676–3871 mg $CaCO_3$/L and the concentration of ammonium-N and S was 560–800 mg/L and 107 mg/L, respectively. Additional supplements were added to the media as described in section TBR Operation

TBR and anaerobic filter

The TBR was constructed from acid-proof stainless steel (Fig. 2) and was placed in a movable container together with all associated equipment (Fig. S2). The reactor had a total volume of 49 L, including head space and liquid reservoir, an inner diameter of 215 mm and a total height of 1344 mm. The reactor was filled with the inoculated carrier to a total packed bed volume (pbv) of 35 L. A grid plate spreader (5 mm pores) was placed 80 mm above the bottom of the reactor, creating a reservoir in which a volume of nutrient medium (max. 8 L) could be contained and collected. Liquid from this reservoir was manually removed on a regular basis and replaced with fresh nutrient medium. The liquid was recirculated with a hose pump (FPSH 15, 0.37 kW; Valisi, Rozzano, Italy) from the reservoir to the top of the reactor, where it was sprinkled over the packed bed and trickled back to the liquid reservoir. The pump was operated in semi-continuous batch mode with 5 s of pumping followed by 37 s of stop time, giving an average flow of approximately 14.3 L/h. At the top of the reactor, two stainless steel grid plate spreaders were positioned to distribute the nutrient liquid (Fig. 2, Fig. S2d). Syngas was added through a port in the lower part of the reactor (Fig. 2) to meet the liquid coming from the top, thus operating in a counter-current manner. At the top of the reactor, the gas was collected and the volume was measured by a drum meter (TG 0.5; Ritter, Germany). Samples for chemical and microbiological analyses of the liquid were taken at position 6 in Fig. 2. The composition of the outgoing gas (CH_4, CO_2, CO, O_2, H_2) was analysed by a ETG MCA 100 Syn Biogas Multigas Analyzer (ETG Risorse e Tecnologia, Chivasso, Italy). The reactor was heated to 37 °C by a water jacket and the temperature in the reactor was logged using a temperature probe (Tinytag View 2; Gemini Data loggers, Chichester, United Kingdom). The temperature was 36–38 °C during the entire operating period of the TBR. After around 200 days of operation, an additional reactor (anaerobic filter, AF) was installed, through which nutrient liquid from the bottom of the TBR was recycled in an upflow manner (Fig. 2, Fig. S2d). The aim was for the AF to prolong the retention time for the nutrient liquid recirculate and by doing so allow more time for degradation of accumulated volatile fatty acids (VFA) in the nutrient liquid. This reactor was made of plastic and had a total/active volume of 1.5 L (height 190 mm, diameter 100 mm). The AF was filled with the same type of inoculum and carrier as the TBR and the same procedure as for TBR inoculation was used, with an incubation period of 14 days before filling the AF. The gas from this reactor was not collected.

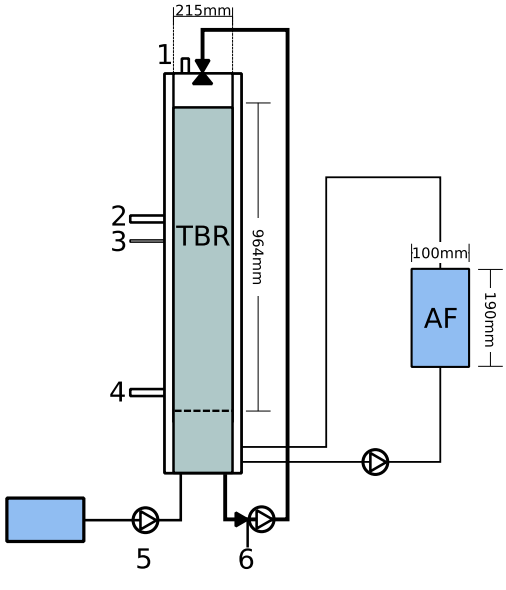

Fig. 2 Schematic diagram of the trickle bed reactor (TBR) and anaerobic filter (AF). 1: Outlet for product gas. 2: Carrier sampling port. 3: Position of temperature probe. 4: Syngas inflow. 5: Inflow of liquid nutrient medium. 6: Sampling port for microbial analysis

TBR operation

The TBR was operated for a total of 862 days. The initial 129 days of operation were devoted to start-up and acclimatisation of the process. Thereafter, TBR operation was divided into different main periods based on the nutrient medium used (Table 1). Each main operating period was in turn divided in two sub-phases (A and B) based on major operational changes, installation of the AF or changes in flow or composition of the nutrient medium (Table 1). The gases used throughout TBR operation were synthetic mixtures (Air Liquide, Paris, France). The different periods are described briefly below and summarised in Table 1 and Supplementary Material.

Start-up and acclimatisation (129 days) During this period, the biomass was allowed to adjust to the prevailing conditions in the reactor and to the syngas. Defined nutrient

Table 1 Description of the different operating periods in the trickle bed reactor (TBR) process

Phase name	Period dates	Days of operation[a]	Nutrient solution[b]	Feed rate[c] (mL/day)	Gas composition[d] (%)	Description
Start-up	2018/06/01–2018/07/26	− 129 (56)	M1[e]	140	CO: 15 N_2: 85	Initiation of reactor and enrichment of CO-utilising microorganisms
Acclimatisation	2018/07/27–2018/10/07	− 73 (73)	M1[e]	140	CO: 15 CO_2: 7 H_2: 28 N_2: 50	Change of gas mixture towards industrial-like gas composition and acclimatisation
Period 1A	2018/10/08–2019/04/04	0–179 (179)	M1[e]	140	CO: 30 CO_2: 14 H_2: 56	Change of gas mixture to simulate syngas produced by Cortus Energy. This gas mixture was used in the following periods
Period 1B	2019/04/05–2019/06/05	180–241 (62)	M1[e]	140	CO: 30 CO_2: 14 H_2: 56	Addition of a small anaerobic filter (AF) reactor to alleviate accumulating VFA levels. The small reactor was used to the end of the process
Period 2A	2019/06/06–2019/08/27	242–324 (83)	M2[f]	1000	CO: 30 CO_2: 14 H_2: 56	Change in liquid nutrient feed stabilisation and feed rate
Period 2B	2019/08/28–2019/12/22	325–441 (117)	M2[f]	1000→200	CO: 30 CO_2: 14 H_2: 56	Gradually decrease in liquid feeding throughout phase
Period 3A	2019–12-23– 2020/05/19	442–590 (149)	M3[g]	400	CO: 30 CO_2: 14 H_2: 56	Change in liquid nutrient feed and feed rate
Period 3B	2020/05/20–2020/07/29	591–661 (71)	M3[g]	200	CO: 30 CO_2: 14 H_2: 56	Nutrient feed rate reduced to 200 mL

[a]Operating time set to zero at the start of period 1; days in brackets represent the number of operation days for each period

[b]Recirculated liquid nutrient solution

[c]Feeding rate of liquid nutrient medium

[d]Composition of ingoing gas mixture

[e]Defined nutrient medium

[f]Digestate from a co-digestion plant, operated under thermophilic conditions, digesting sorted household food waste with organic food waste from larger kitchens, stores and food distributors

[g]Digestate from a wastewater treatment plant, operated under mesophilic conditions, digesting sludge from the wastewater treatment process and minor fractions of different sludges from the food processing industry

medium (M1) was used at a low flow rate (140 mL/day) and the inlet gas composition was initially CO/N_2 (15/85), to enrich CO-consuming bacteria. Thereafter, the gas composition was changed to CO/CO_2/H_2/N_2, representing 15, 7, 28 and 50%, respectively, in order to add CO_2 and H_2 while maintaining the same partial pressure of CO.

Period 1 (241 days) The start of this operating period was defined as Day 0. In this period, the reactor was fed syngas with the target composition expected by the industrial partner (Cortus Energy), which was 30% CO, 14% CO_2 and 56% H_2. The defined nutrient medium (M1) at an average inflow rate of 140 mL/d was used throughout. During operation, VFA were produced quickly in response to increasing syngas inflow, so an AF was installed (phase 1B) and process liquid from the TBR reservoir was recirculated through the TBR (Fig. 1). To evaluate possible nutrient limitation as a cause of VFA accumulation and decreasing gas consumption, additional N (NH_4Cl; Fisher Chemicals, Göteborg, Sweden) and S (NaS_2 and cysteine-HCl; Merck, Darmstadt, Germany) were also added at the end of period 1A and during period 1B (see Supplementary Material).

Period 2 (200 days) In this period, the nutrient medium was changed to digestate from the industrial food waste biogas plant (M2). In the initial phase (2A), a high flow of

nutrients was supplied (1000 mL/day), while in the second phase (2B), this was gradually reduced to 200 mL/day. In phase 2B, additional S (NaS_2 or $NaSO_4$, Merck, Darmstadt, Germany) was added (Table 1, Supplementary Material) in an attempt to mitigate decreasing syngas consumption rate.

Period 3 (220 days) In this period, the nutrient medium was changed to reject water from dewatered digested WWTP sewage sludge (M3)**,** initially at a flow rate of 400 mL/day (phase 3A) and later reduced to 200 mL/day (phase 3B). In addition, extra S (NaS_2 or $NaSO_4$, Merck, Darmstadt, Germany) was added throughout the whole operating period (Supplementary Material) and in phase 3B, sodium bicarbonate (Na_2CO_3) was added to enhance the alkalinity and mitigate a trend of decreasing pH (Supplementary Material).

Analytical methods

In the screening experiments with different inocula, the gas composition was analysed by gas chromatography according to Westerholm et al. (2012). Short-chain VFA (C2-C6) were quantified by ion-exclusion chromatography according to Westerholm et al. (2012). Process pH was measured with a Hanna instrument HI83141 (Woonsocket, Rhode Island, United States). Ammonium and sulphate were analysed with a spectrophotometer (Spectroquant® Nova 60A photometer; MilliporeSigma, Burlington, MA, USA) with reagent test kits from the series Supelco (Merck, Darmstadt, Germany). The total alkalinity was calculated as the amount of acid required to bring the sample to pH 4.4. Titration was carried out with an automatic titrator (TitraLab® AT1000 series; Hach, Düsseldorf, Germany).

Microbial analysis

Samples for DNA extraction were withdrawn from the recirculated liquid on a weekly basis from sampling port 6 as shown in Fig. 2, and on a few occasions, samples of carrier were taken from the TBR and microbial material was scraped off the carrier using a small spatula. DNA was extracted from 200 µL of liquid sample using the FastDNA Spin Kit for Soil (MPBiomedicals, Illkirch-Graffenstaden, France) according to the manufacturer's protocol with an additional cleaning step with guanidine thiocyanate (Danielsson et al. 2017). DNA was also extracted from the ingoing nutrient medium by concentrating 4 mL of sample by centrifugation and dissolving the cell pellet obtained in 200 µL of the supernatant. The samples were initially extracted in triplicate but, after preliminary sequence analysis showing no significant variations between triplicate extractions, single extractions were done in order to allow analysis of more samples. Sequencing libraries were generated by SciLifeLab, in Stockholm, Sweden, using Illumina MiSeq (2 × 300 bp) targeting 16S rDNA. To cover both bacteria and archaea, the amplification was done using the forward primer 515′F and reverse primer 806R, as described previously (Westerholm et al. 2018). The paired end reads were processed with Cutadapt version 1.13, removing the aforementioned primers and adapters on forward and reverse reads (GTGBCAGCMGCCGCGGTAA and GACTACHVGGGTATCTAATCC, respectively) and filtering based on quality and trimming reads to 300 bp. The trimmed reads were processed with Division Amplicon Denoising Algorithm2 (DADA2) version 1.16.0 in Rstudio running R version 4.1.1, as described by Westerholm et al. (2018), with forward and reverse reads truncated at positions 240 and 160, respectively. Microbial classification was performed using the SILVA reference database v. 132. The data were organised with *phyloseq* v1.32.0 (McMurdie and Holmes 2013) into a single data object that was subsequently used for graphic generation in RStudio v1.4.1717 (RStudio Team 2020) running R v4.1.1. The following R packages were used for visualisation of the microbial data: ggplot v2 3.3.5, data.table v1.13.4, plotly v4.9.2.1, lattice v0.20.45, permut v0.9.5, vegan v2.5.7, readxl v1.3.1, plyr v1.8.6, grid v4.1.1 and ggtext v0.1.1. The amplicon sequence variants (ASV) were submitted to the Basic Local Alignment Search Tool (BLAST) algorithm provided by the National Center for Biotechnology Information (NCBI), The sequences obtained by Illumina sequencing are too short (~250–300 bp) to clearly reveal the identity of the engaged microorganisms on species level. However, ASVs showing 100% identity with a known organism are in the presentation referred to the putative species name. Raw sequence data have been deposited in NCBI PRJNA796200.

Results

Selection of inoculum

Evaluation of different sources of inoculum for methane production from different gas mixtures (H_2/CO_2, CO/N_2 or $H_2/CO_2/CO$; see Fig. S1) before the start-up of the TBR process revealed that the consumption/production patterns of the different inocula did not differ significantly. However, CO consumption rate, with or without H_2 and CO_2, was highest for the inoculum from the manure-based biogas reactor (reactor a; see Fig. S1), and therefore, inoculum A was chosen for the TBR.

TBR operation: process and microbiology

Period 1

Throughout period 1, the syngas inflow fluctuated between 1.11 and 3.33 $L/L_{pbv}/d$, depending on the consumption

efficiency (Fig. 3a). During periods of high syngas gas outflow, the inflow was decreased to match the rate of consumption. In line with the variation in inflow, the total biogas outflow for the period ranged from 0.041 to 1.86 $L/L_{pbv}/d$, with higher values towards the end of the period (Fig. 3a). The CH_4 content in the gas was around 50%, resulting in an output range of 0.06–0.91 L CH_4 $/L_{pbv}/d$ (mean 0.60 L $CH_4/L_{pbv}/d$) for the period (Fig. 3b). VFA accumulation and pH declines were observed early in operation (Fig. 3c) and the gas inflow was temporarily stopped/lowered on a number of occasions to mitigate further accumulation and decreasing pH. Once VFA were consumed, normal syngas inflow was resumed. However, with an increase in the gas inflow rate, it was no longer possible to control VFA levels, which increased continuously to values as high as 3.7 g/L by the end of period 1B (Fig. 3c, Supplementary Material). The VFA present were mainly represented by acetic and propionic acid, with propionic acid initially making up 71–96%, but with a higher proportion of acetic acid in the later phase (59–99%) (Supplementary Material).

The microbial community in the starting inoculum was characterised by high relative abundance of phylum *Firmicutes* (57.0%), dominated by uncultivated members of genus *MBA03* (15.5%) and genus *Sedimentibacter* (7.7%) and phylum *Bacteriodetes* (24.0%), mainly dominated by unknown members of family *Rikenellaceae* (11.9%) (Fig. 4, Fig. S3a). During the stabilisation phase, these two phyla continued to show high relative abundance, accompanied by emergence

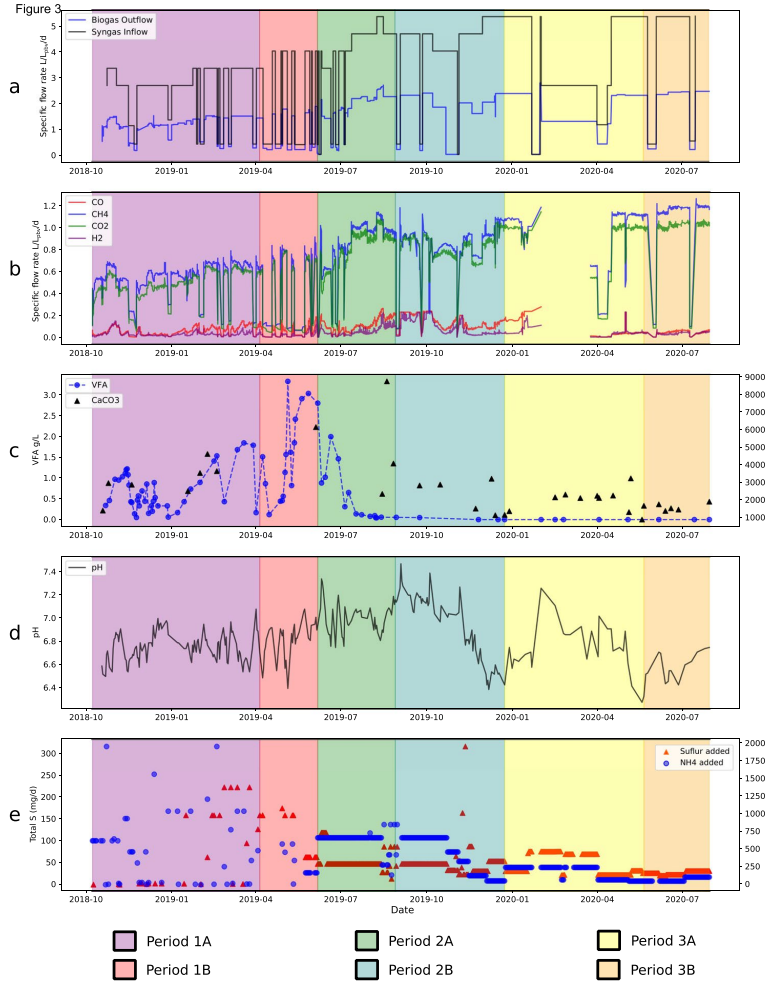

Fig. 3 Process data from trickle bed reactor (TBR) operation during three periods (1–3) operating with different nutrient medium: 1) defined medium (M1) 2) dewatered digestate from a thermophilic biogas plant operating with food waste (M2) and 3) reject water from a biogas plant at a wastewater treatment plant (M3). Each period was further divided into two sub phases (A,B) based on major changes in operating parameters, such as flow rate of nutrient medium (see Table 1). **a** Specific syngas inflow (black) and biogas outflow rate (blue). **b** Specific outflow gas rate. The gap seen in period 3A was due to gas analyser malfunction. **c)** Total volatile fatty acids (VFA) concentration and alkalinity. **d** pH. **e** Total amount of sulphur (S) and ammonium nitrogen (NH4-N) added via nutrient medium and by additional supply via external source. For details, see Supplementary Material

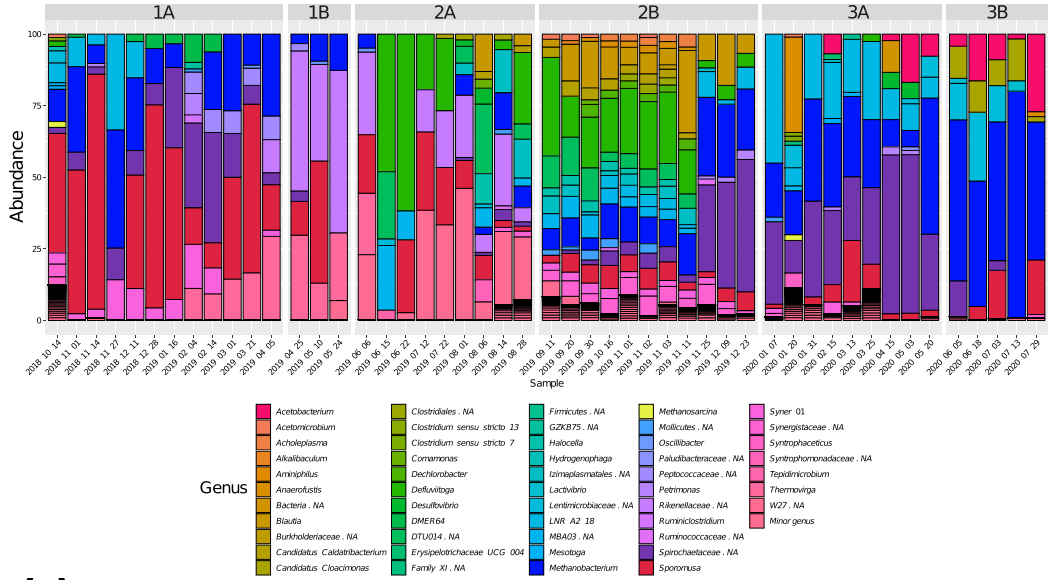

Fig. 4 Microbial community structure at genus level during trickle bed reactor (TBR) operation in three periods (1–3) operating with different nutrient medium: (1) defined mineral medium (M1) (2) dewatered digestate from a thermophilic biogas plant operating with food waste (M2) and (3) reject water from a biogas plant at a wasterwater treatment plant (M3). Each operating period was further divided into two sub-phases (A,B) based on major changes in operating parameters, such as flow rate of nutrient medium (see Table 1)

of phylum *Syngergistetes* (31.6–50.2%), primarily composed of unknown members of family *Synergistaceae*. The abundance of methanogens (phylum *Euryarchaeota*) was very low in this initial phase of operation and they represented less than < 1% of the total community. However, in period 1, when the H_2 level in the syngas was increased, the relative abundance of *Euryarchaeota* increased rapidly and for most samples the value was between 10 and 35% (Fig. S3a). Phylum *Euryarchaeota* was represented mainly by one amplicon sequence variant (ASV), which according to a BLAST search in NCBI corresponded to the putative species *Methanobacterium bryantii* (100% similarity). The bacterial community during period 1 also changed compared with that in the stabilisation/acclimatisation phase. Relative abundance of phylum *Bacteriodetes* was initially low but increased when the VFA content was high, represented by two genera within family *Rikenellaceae*, genus DMER64 (1–7%) in period 1A and an unknown genus in period 1B (11–50%). Genus *DMER64* was mainly abundant when propionate represented a major part of the VFA, while the unknown genus was more abundant when propionate level decreased. Phylum *Firmicutes* and phylum *Syngergistetes* showed significant shifts compared with the stabilisation/acclimatisation phase. Throughout period 1, *Firmicutes* was dominated by a member within genus *Sporomusa*, reaching values between 8 and 90% (Fig. 4). A BLAST search of this ASV showed 100% similarity to the putative species *Sporomusa sphaeroides*. Within *Syngergistetes*, genus *Thermovirga* showed an increasing trend over the period. In addition, phylum *Cloacimonetes* and phylum *Spirochaetes* were present during this period, represented mainly by genus *LNR_A2-18* and an unknown member within genus *Spirochaetaceae*, respectively. Genus *LNR_A2-18* initially increased to a high level (~23%) in the beginning of period 1A but showed a significant drop just before the start of VFA accumulation (late December 2018) and thereafter remained at low abundance throughout the rest of period 1. *Spirochaetaceae* showed increased relative abundance with a concurrent decrease in relative abundance of *LNR_A2-18*, and represented up to 35% of the community in period 1A, after which this ASV also decreased in abundance. At the time of the decrease, a shift in VFA composition towards a higher level of acetate relative to propionate was seen.

Period 2

In period 2, the recirculated nutrient solution was changed from the defined medium (M1) to the digestate from the thermophilic biogas plant operating with mixed food waste (M2) and the nutrient solution feeding rate was increased to

1000 mL/day. The syngas inflow rate in period 2A was initially kept at the same level as in period 1B but, as the VFA level was significantly lower than in period 1, the rate was gradually increased to around 4 L/L_{pbv}/d. In line with this increase, the volume of outgoing methane also increased, to reach values of around 0.9–1.10 L CH_4/L_{pbv}/d by the end of period 2A (Fig. 3b). However, towards the end of period 2A, a rise in the outflow levels of CO and H_2 was observed (Fig. 3b), resulting in a decrease in production of CH_4. The decreasing trend in CH_4 production continued during the beginning of period 2B, although VFA were not detected, and the average pH was around 7.2. From the middle to the end of period 2B, the nutrient solution feeding rate was gradually decreased to 200 mL/day, which led to a gradual decrease in NH_4-N and S supply (Fig. 3c). In an attempt to improve syngas conversion efficiency, which was assumed to be limited by S availability, S was added to the process (Fig. 3e, Supplementary Material). This strategy improved syngas conversion, allowing syngas inflow rate to be increased to 5 L/L_{pbv}/d and resulting in an increase in CH_4 production to around 1.1 L/L_{pbv}/d without any accumulation of VFA, although with a decrease in pH to ~ 6.5 (Fig. 3d).

The change of nutrient solution (from M1 to M2) had a major effect on microbial community composition. At the beginning of period 2A, members from the thermophilic phylum *Thermotogae* appeared in high relative abundance, along with *Firmicutes* (Fig. S4a). This community composition mainly reflected the composition of the dewatered digestate used as the nutrient source (Fig. S3a). Phylum *Thermotogae* was represented by genus *Defluviitoga* within the family *Petrotogaceae* (48–56%) and *Firmicutes* were represented by unknown members within two main orders, *DTU014* (6.28–23.49%) and MBA03 (12.36–23.61%). These families stayed in the system until the end of period 2A (Fig. S4b), when the feeding rate of the nutrient medium was reduced to 200 mL/day. In addition, period 2A showed high abundance of phylum *Cloacimonetes* (Fig. S4a), which was not observed in the nutrient solution. This phylum was represented by family *W27* and reached relative abundance values of 17–42% by the end of period 2A (after the decrease in VFA), after which it quickly decreased in period 2B. Moreover, *Sporomusa sphaeroides*, established in period 1 and not present in the digestate, maintained its presence throughout period 2, initially at high relative abundance (~ 20%) but stabilising at lower levels (1.6–6.6%) from the middle of period 2A to the end of period 2B. *Methanobacterium bryantii*, the only methanogen identified in period 2, as in period 1, was present throughout but with increasing relative abundance values towards the end, representing 21–27% of the microbial community (Fig. 4). The community at the end of period 2B was also characterised by high abundance of a member within the genus *Spirochaetaceae* (30–46%), the same species that was dominant in the late stages of period 1.

Period 3

In period 3, the nutrient source was switched to reject water from the mesophilic wastewater treatment plant (M3). The feed rate was 400 mL/d during period 3A and decreased to 200 mL/day during period 3B (Table 1). During the whole of period 3, the process was supported with additional S. In addition, sodium hydrogen carbonate ($NaHCO_3$) was added to mitigate decreasing pH values, as low as 6.4 during period 3B (Fig. 3e, Supplementary Material). In period 3A, the syngas inflow was initially continued at the same rate as in the previous period, i.e. 5 L/L_{pbv}/d, resulting in biogas and methane production of around 2 and 1 L/L_{pbv}/d, respectively (Fig. 3a). However, due to problems with the gas analyser, no data were obtained for the outgoing gas for some time and therefore the syngas inflow was decreased to 2.67 L/L_{pbv}/d in order to avoid the risk of overloading. When the functionality of the gas analyser was restored, the syngas inflow rate was again set to the previous level, which resulted in similar CH_4 production values as before. In period 3B, syngas conversion was maintained at a high level, which led to an average CH_4 production rate of 1.15 L/L_{pbv}/d. No VFAs were observed during operation in period 3 (Fig. 3c).

The use of the new medium (M3) in period 3 had little or no influence on the community composition compared with that in period 2. The relative abundance of *Methanobacterium bryantii*, the dominant methanogen, increased in period 3 compared with period 2 and reached values of 21–45% for most of the samples analysed (Fig. 4). For bacteria, the relative abundance of the previously observed member within the genus *Spirochaetaceae* was initially maintained at a similar level as observed in period 2B, but it decreased gradually when the nutrient flow rate decreased in period 3B, to reach values of 2–3% at the end (Fig. 4). *Sporomusa sphaeroides* was initially high in period 3 but decreased during the pH decrease and then recovered towards the end of period 3B, reaching values of around 10%. In addition, at the end of period 3B, the relative abundance of a member within genus *Acetobacterium* increased and it became one of the most abundant species at the end, representing ~ 31% (Fig. 4). A BLAST search in NCBI showed 100% similarity with the putative species *Acetobacterium wieringae*. In addition, genus LNR_A2-18 (phylum *Cloacimonetes*) was present in high relative abundance (5–26%) throughout period 3. This ASV was the same as that previously identified in high relative abundance in period 1. Another unknown member within this phylum was also identified in period 3B and showed increasing abundance towards the end, representing 12% of the total community. This increase in abundance was the opposite of the decreasing trend seen for *Sporomusa sphaeroides* during the stage of decreasing pH.

Microbial analysis of carrier samples

Carrier samples were taken on only four occasions and only from one position (Fig. 2), due to the difficulty in removing the carrier without causing process disturbance. Independent of sampling time, *Firmicutes* was one of the most highly abundant phyla on the carrier samples, with relative abundance ranging from 37 to 92%, primarily represented by *Sporomusa* at the genus level (Fig. 5). *Euryarchaeota* was present in all carrier samples (Fig. S5), represented mainly by *Methanobacterium* (3–36%), but at the final carrier sampling point in the process (phase 2B), *Methanosarcina* (4%) was also detected (Fig. 5). Phylum *Synergistetes* (4–30%) maintained a presence on the carrier through the four sampling points (Fig. S5) and was comprised mainly of genus *Syner-01* (3–19%) and *Thermovirga* (5–10%) at the first three sampling points. At the final sampling point in period 2B, an unknown genus in *Syngeristaceae* (0.21%) was observed together with *Acetomicrobium* (2.2%) and *Aminobacterium* (0.49%) (Fig. S5). At the final sampling point, there was also comparatively high relative abundance of Bacteroidetes (15%), represented by genus *Fermentimonas* (3%, family *Dysgonomonadaceae*) and a genus belonging to family *Lentimicrobiaceae* (7%) (Fig. 5, Fig. S5b). The ASV belonging to the *Sporomusa* found on all carrier samples was identified as *Sporomusa sphaeroides*, with 99.2% similarity in a BLAST search. The ASV for *Methanosarcina* showed 99.2% similarity with *Methanosarcina flavescens.*

Discussion

Selection of start-up inoculum

The inoculum for the TBR was chosen from an initial screening of three different digestates. The selection of digestate was based on the processes having different microbial communities and dominance of different methane-producing pathways, potentially influencing syngas consumption capacity. It is known that microbial community structure in processes operating with sludge, manure and food waste is different and statistically distinct, mostly driven by differences in ammonia levels (Sundberg et al. 2013; De Vrieze et al. 2015). The food waste reactor (reactor b), operating at a high ammonia level (0.5–0.9 g NH_3/L), was shown to have high abundance of the hydrogentrophic methanogen *Methanoculleus bourgensis* (genus *Methanomicrobiales*) and different known syntrophic acetate-oxidising bacteria, and dominance of methane production via SAO (Westerholm et al. 2015). In the reactor operating with manure (reactor a), quantification of methanogens by qPCR illustrated dominance of order *Methanosarcinaceae* and *Methanobacteriales* and lower levels of *Methanomicrobiales*, suggesting a mix of methylotrophic and hydrogenotrophic methanogenesis. Analysis of the inoculum from the WWTP plant (reactor c) in a previous study showed it to be dominated by the acetoclastic genus *Methanosaeta,* a strict acetoclastic methanogen (Liu et al. 2017). The highest methane production from syngas was seen for inoculum A (from the manure-based

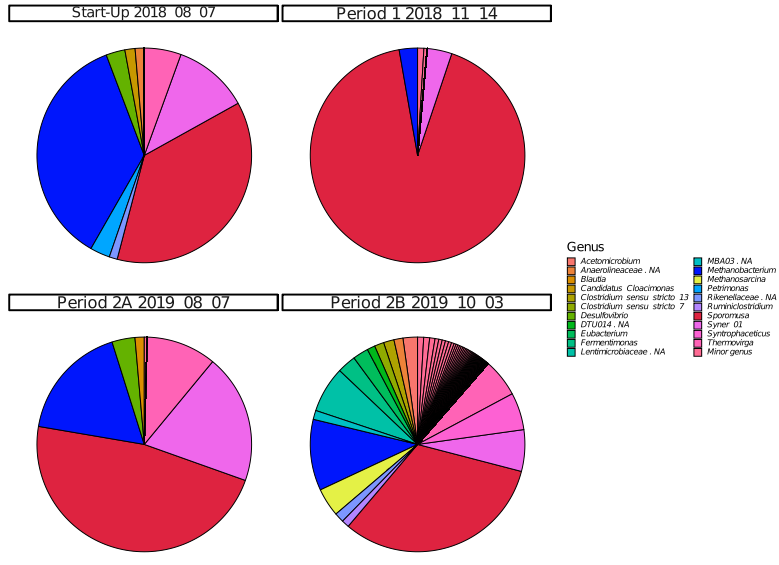

Fig. 5 Microbial community structure on genus level in biofilm recovered from plastic carriers in the trickle bed reactor (TBR) in the start-up phase and in operating periods 1 and 2. Carrier samples taken in period 2B were sequenced in triplicate. Carrier samples taken in start-up, period 1 and period 2A were sequenced without replicates, due to lack of extracted material

reactor), which could have been caused by factors such as (i) the presence of both methylotrophic and hydrogenotrophic methanogenesis, since hydrogenotrophic methanogens mainly utilise hydrogen during syngas methanation but acetate can be produced via acetogenesis from CO, requiring acetoclastic methanogens for further conversion to methane and (ii) high abundance of order *Methanobacteriales*, as several studies on biomethanation in TBR have shown enrichment of methanogens within this order, such as genus *Methanobacterium* and *Methanothermobacter*, indicating importance for biomethanation in such reactors (Aryal et al. 2021; Sposob et al. 2021). Previous studies on syngas methanation in TBR have used inoculum from biogas processes operating with manure (Aryal et al. 2021) and sludge (Grimalt-Alemany et al. 2020; Figueras et al. 2021; Li et al. 2021), or a mix of both (Asimakopoulos et al. 2020a), as well as syngas- or H_2-enriched cultures (Asimakopoulos et al. 2020b, 2021; Sieborg et al. 2020) and defined cultures comprising just a few organisms (Kimmel et al. 1991; Klasson et al. 1992). No obvious trends have emerged that some inocula are more suitable than others. Some thermophilic processes have even been initiated with mesophilic inocula but have still resulted in well-functioning processes (Kimmel et al. 1991; Grimalt-Alemany et al. 2020; Li et al. 2020b). However, for methanation of CO_2 with H_2, inoculation with enriched culture is reported to shorten the lag phase during start-up (Sposob et al. 2021). Microbiological studies of continuously operated TBR have observed a complete change in syngas-enriched communities compared with the inoculum and high adaptive capacity, likely due to intrinsic biological diversity (Asimakopoulos et al. 2020a; Grimalt-Alemany et al. 2020). Such a change was also observed in the present study and is discussed further below in the section 'Microbial communities in the trickle bed reactor'.

Methane productivity and VFA accumulation

Previous studies on productivity during biomethanation in TBR have reported different values, influenced by different parameters such as reactor design, carrier material, inflow gas composition and rate, nutrient composition and loading rate, gas injection, operating time and inoculum source (Asimakopoulos et al. 2020a; Grimalt-Alemany et al. 2020b; Aryal et al. 2021; Sposob et al. 2021). For methanation of gas composed of only H_2 and CO_2, values of around 1.17–3.1 L_{CH4}/L/d during mesophilic (38–40 °C) operation have been reported (Burkhardt and Busch 2013; Burkhardt et al. 2015; Rachbauer et al. 2016). During thermophilic operations, considerably higher values, up to 8.85–15.4 L_{CH4}/L/d, have been reported (Strübing et al. 2017; Lemmer and Ullrich 2018). For methanation from syngas, values between 0.21–1.90 and 1.88–9.46 L_{CH4}/L/d for mesophilic (Grimalt-Alemany et al. 2018) and thermophilic conditions, respectively, have been reported. The higher productivity at higher temperatures is suggested to relate to higher conversion efficiencies resulting from increased methanogenic activity and abundance (Lemmer and Ullrich 2018; Asimakopoulos et al. 2020b). The TBR in the present study was operated under mesophilic conditions, and methane production was in line with that in previous studies operating at this temperature, reaching maximum values of 0.9–1.2 L_{CH4}/L_{pbv}/d. Production efficiency was lowest at the beginning of the process (period 1), mainly caused by difficulties in increasing the load of syngas due to accumulation of organic acids and low pH values. Accumulation of VFA indicates imbalances between the microbiological steps in digestion, with acid formation rate exceeding methanogenesis. Instances of acid accumulation have been observed previously during methanation of syngas, particularly in response to increasing levels of H_2 in the syngas, and it is believed to be caused by inhibition of syntrophic acid conversion (Li et al. 2021). The acids produced in the present study were initially composed of both acetate and propionate but shifted towards a higher fraction of acetate at the end of the period. Acetate is the main product of acetogenesis, but none of the acetogenic carboxydotrophs isolated to date can produce propionate. However, in addition to acetate, acetogens can also produce ethanol and small amounts of butyrate, butanol and 2,3-butanediol, which in turn can be converted by other bacteria to propionate (Moreira et al. 2021). Organic acids were degraded in the second period of operation in this study (period 2), which allowed a higher syngas load and initially resulted in slightly increased methane productivity. Degradation of propionate proceeds via syntrophic collaboration and results in formation of acetate and hydrogen, which if present in high levels can block further degradation (Westerholm et al. 2021). Hydrogen is used by methanogens, but acetate can be converted via acetoclastic methanogens or via SAO (Westerholm et al. 2021; Sancho Navarro et al. 2016). No acetoclastic methanogens were detected in period 1, which might explain why acetate accumulated, although accumulation could also have been caused by decreased hydrogenotrophic methanogenic activity, causing problems for acetate degradation via SAO. Methanogenic activity can be inhibited by CO, VFA and low pH (Luo et al. 2013; Sancho Navarro et al. 2016; Grimalt-Alemany et al. 2018), which all appeared at the same time in period 1. The relative abundance of methanogens was lowest in periods 1B and 2A, which could have resulted in less efficient acid degradation. The improved VFA conversion observed in period 2 could have been caused by factors such as (i) acclimatisation of the methanogenic community to inhibiting conditions; (ii) installation of the anaerobic filter, prolonging the time for degradation and/

or (iii) the change of nutrient medium, providing buffering capacity and additional nutrients for improved microbial growth or providing new microbes, including acetate-degrading microorganisms.

Effect of nutrient source

Among the various parameters influencing the methanation processes and the activity of the microorganisms involved, the nutrient source is of crucial importance. For economic feasibility of full-scale applications, finding a cheap nutrient source is essential (Wegener Kofoed et al. 2021). Ideally, the nutrient medium should supply macronutrients and micronutrients, as well as buffering agents that can help to stabilise the pH in the event of acid formation (Sposob et al. 2021). For biological CO_2 methanation, including TBR, several different non-defined cheap nutrient sources, such as digestate from different biogas processes and manure, have been evaluated and have been shown to be economically feasible for both mesophilic and thermophilic operation (for reviews, see Sposob et al. 2021; Wegener Kofoed et al. 2021). However, many previous studies have used defined nutrient medium for syngas methanation (Grimalt-Alemany et al. 2018; Asimakopoulos et al. 2020a, 2021; Grimalt-Alemany et al. 2020) and only a few have evaluated non-defined nutrients sources, mostly in batch systems (Ács et al. 2019; Aryal et al. 2021). To our knowledge, only one previous study has used a undefined nutrient source during continuous operation of a TBR for syngas methanation (Figueras et al. 2021). The batch reactors were operated under mesophilic conditions and with digestate from manure and wastewater processes and methane production reached only 0.15–0-22 L CH_4/L/d. However, during continuous operation with dewatered WWTP digestate for more than 70 days under thermophilic conditions (55 °C), methane production values of 6.8 mmol $CH_4/L_{reactor}$/h, corresponding to 3.65 L L_{CH4}/L_{pbv}/d, have been reported (Figueras et al. 2021). This is three-fold the value obtained in the present study when using a similar nutrient source (in period 3 of operation). A likely explanation for the higher productivity is thus the higher temperature rather than the nutrient source, and possibly the higher pressure (~4 atm) applied in the previous study (Figueras et al. 2021) than in the present study (1.5 atm).

There is currently no consensus on the medium composition and origin that represent the best nutrient source for a biomethanation process (Wegener Kofoed et al. 2021). Nutrients suggested to be of specific importance for methanation from both H_2/CO_2 and syngas include macronutrients such as N, S and P and various trace elements, all of importance for methanogenic activity (Strübing et al. 2017; Li et al. 2020b; Figueras et al. 2021; Wegener Kofoed et al. 2021). According to the results in this and other studies, undefined nutrient sources of different origins can work well for biomethanation, offering the possibility to establish full-scale sustainable processes using cheap nutrient sources. A possible drawback/limitation with such nutrient sources is the need for pre-treatments to remove particles and to prevent growth of unintended microorganisms potentially also producing biogas from additional carbon sources (Sposob et al. 2021). In the present study, a shift was made from a defined nutrient medium to two different types of digestate. Neither of these digestates was sanitised before use, but the digestate from the food waste biogas plant (M2) had to be filtered before use. The process showed better performance during operation with the undefined nutrient sources than with the defined medium, with no acid accumulation and with the possibility for higher syngas loads. However, the defined medium was used in the initial phase of TBR operation and it cannot be concluded that this medium was less beneficial for the process, since process stabilisation and biofilm development may not have been complete. The periods with undefined medium occasionally suffered from low pH (with no VFA accumulation), particularly when the nutrient flow rate was lowered, leading to additional need for buffering capacity. Moreover, during most of the TBR operating time, the process was supported by additional S, in all phases, indicating a need for additional nutrients. During methanation of syngas in the study by Figueras et al. (2021), supplementation with additional S (Na_2S) was found to be beneficial for the process. Similar findings were made in a previous study on biomethanation from H_2/CO_2 at thermophilic temperature using a TBR (Strübing et al. 2017). Strübing et al. (2017) suggested that sulphur deficiency could be caused by the loss of sulphide in the off-gas due to trickling of the liquid. These previously observed positive effects of sulphide addition were confirmed in the present study, where supplementation with additional sulphide was found to be beneficial for the conversion efficiency in periods 1A, 1B and 3A. Methanogens mainly use sulphide as a sulphur source, but some can also assimilate cysteine (Liu et al. 2012), and both were present in the defined medium (M1) in this study. In periods 2B and 3B, addition of sulphate instead was evaluated (Supplementary Material). Sulphate is not used directly by methanogens but can be converted to sulphide by sulphate-reducing bacteria present in the recycled nutrient medium. No obvious difference in methane productivity related to S source was however seen in this study.

Microbial communities in the TBR

Methanogenic community

Throughout the process, independent of nutrient medium, one dominant methanogen was observed, represented by one ASV showing 100% similarity with *Methanobacterium*

bryantii. Even though the digestate-based nutrient sources (M2 and M3) were not sterilised, methanogens from these sources did not establish in the process. Nutrient medium M2 was derived from a thermophilic biogas process, which might explain why no methanogens from this medium established in the mesophilic TBR. However, transition from thermophilic to mesophilic conditions with inoculum from the same biogas plant as M2 has been shown to be possible, illustrating the presence of mesophilic methanogenic species in this biogas plant (Westerholm et al. 2018). Nutrient medium M3 was derived from a mesophilic biogas plant, but both M2 and M3 showed little to no abundance of methanogens (representing less than 1% of the whole community), possibly also explaining the low contribution of methanogens to the methanation process in the TBR. The dominant methanogen, identified as *Methanobacterium bryantii*, is a hydrogenotrophic methanogen using H_2/CO_2, but not formate (Benstead et al. 1991). It is unclear whether this bacterium can use CO, but other members within this genus, e.g. the thermophilic *Methanobacterium thermoautotrophicus*, can grow with CO as the sole energy source, although at very low growth rates (Ferry 2010). Members within the genus *Methanobacterium* have been found to dominate in several other studies on biomethanation in TBR at both mesophilic and thermophilic temperatures (Rachbauer et al. 2017; Porté et al. 2019) and in other processes during ex situ and in situ biomethanation of H_2 and syngas (Li et al. 2020a; Aryal et al. 2021; Jiang et al. 2021; Braga Nan et al. 2022). In line with results in the present study, this genus has also been found on carrier biofilm (Rachbauer et al. 2017; Thapa et al. 2021). Moreover, in several studies it has been observed under mesophilic conditions together with the hydrogenotrophic genus *Methanoculleus* and is suggested to be more crucial of the two in restoring efficiency after starvation periods and VFA accumulation, while also being decisive for efficient biomethanation due to high hydrogen consumption rates (Logroño et al. 2021; Braga Nan et al. 2022). *Methanoculleus*, a known partner during SAO and prevailing under low hydrogen concentrations (Westerholm et al. 2016), was not detected in the present study. In addition to *Methanobacterium*, genus *Methanosarcina* was observed in low relative abundance on the carrier biofilm in period 2B. In BLAST searches, this ASV was identified as *Methanosarcina flavescens*, a methanogen utilising both acetate and H_2/CO_2 for growth, and also methanol and methylamines (Kern et al. 2016). Establishment of this genus in period 2 could have occurred via the nutrient medium, as it has been identified previously at low abundance in the biogas plant from which the digestate originated (Westerholm et al. 2018). However, the genus could not be detected in the nutrient solution M2 (Fig. S3). In the process, *Methanosarcina* sp. could have used either acetate or H_2/CO_2, or both, but its enrichment in period 2B after the observed decrease in acetate concentration suggests that it acted as an acetoclastic methanogen. However, members of this genus, including *M. flavescens*, may be able to shift their metabolism from acetate to H_2 in response to increasing partial pressure of H_2, making them more competitive for hydrogen (Thapa et al. 2021). Thus, it is possible that *M. flavescens* acted as a hydrogenotrophic methanogen in the present study, together with *Methanobacterium*. Moreover, it is possible that *M. flavescens* used CO, as several species within genus *Methanosarcina* have been demonstrated to have this ability (Oelgeschläger and Rother 2008). In line with the results in this study, *M. flavescens* was recently identified at higher abundance in biofilm than in the liquid phase during in situ biogas upgrading in an anaerobic TBR treating thermal post-treated digestate (Thapa et al. 2021).

Bacterial community

The AVS identified as *Sporomusa sphaeroides* showed high abundance throughout the operation. This genus is known to utilise H_2 and CO_2, why it seems likely that this acetogen competed with the methanogen for its substrate. Some species within genus *Sporomusa* can also utilise CO, however, not *S. sphaeroides* (see review by Bengelsdorf et al. 2018). The end product of *Sporomusa* is mainly acetate, but *S. sphaeroides* can also produce small amount of ethanol (Möller et al. 1984). In addition to *Sporomusa*, one unknown member of *Spirochaetaceae* was highly abundant in the first phase of period 1. Members within *Spirochaetaceae* have been proposed to be involved in syntropic acid degradation, specifically acetate, together with methanogens (Wang et al. 2019). The abundance of this genus decreased/increased with observed acetate accumulation/consumption, indicating involvement in syntrophic acetate degradation also in this study. In the period with high VFA levels, increasing abundance of family *Rikenellaceae* and genera *Thermovirga* was also observed. Members within *Thermovirga* cannot use H_2/CO_2 or fatty acids but utilise proteinaceous substrate and amino acids, including cysteine, while producing acetate as the end product (Dahle and Birkeland 2006). This bacterium likely contributed to production of acetate, using yeast extract and/or the cysteine used as a reducing agent in nutrient medium M1. The abundance of this genus decreased to < 1% when the nutrient medium was changed in periods 2 and 3, but it was still found in biofilm on carrier samples from period 2, suggesting that also the digestates supported growth of this genus. Family *Rikenellaceae* contains several different genera, and species isolated so far can ferment carbohydrates or proteins and grow on yeast extract, while producing acetate and propionate and also H_2 and CO_2 and other acids (Krieg et al. 2010; Abe et al. 2012; Graf 2014; Su et al. 2014). Members of this family have been found previously in batch reactors fed with syngas (Aryal et al. 2021). In

the present study, family *Rikenellaceae* was represented by two different genera, one of which (genus DMER64) is suggested to be a potential syntrophic propionate degrader (Lee et al. 2019). This is in line with the decreased abundance of this genus with decreasing propionate concentration. This genus possibly took over the role of propionate degrader from genus LNR_A2_18, within family *Cloacimonadaceae*, that was initially present in the TBR. This family is suggested to act also as a syntrophic propionate degrader and its disappearance has been shown to be accompanied by an increase in propionate (as in the present study) and to be an indicator of process disturbance (Klang et al. 2019; Singh et al. 2021).

In period 2A, a drastic change in microbial community composition was seen. An immediate rise in several well-known thermophilic microorganisms was observed, i.e. genus *Defluviitoga* (phylum Thermotogae) and order MBA03 and DTU014 (phylum Firmicutes). This composition was very much influenced by the microbial composition of the nutrient medium, which changed in period 2 to thermophilic food waste digestate at a high flow rate. The observed organisms were highly abundant in the nutrient medium per se, and is also common in thermophilic biogas reactors (Westerholm et al. 2018; Dyksma et al. 2020). It has been suggested that members within these taxonomic groups perform carbohydrate fermentation and do not have the ability to use gaseous substrates, so most likely, they did not contribute to the methanation process. However, in contrast, genus W27, within family *Cloacimonadaceae*, was highly abundant in period 2A and not detected in the nutrient medium. As mentioned earlier, members within this taxonomic group are suggested to be involved in propionate degradation (Westerholm et al. 2021). However, it is difficult to predict the role of genus W27 in the present study, as it was highly abundant in period 2A after VFA had been degraded and disappeared in phase 2B. The high nutrient flow rate may have supplied the process with substrates for bacteria producing propionate, but kept to a low level by the genus W27. In period 2B, when the nutrient flow was reduced, there might not have been enough substrate to maintain the growth of this organism at a high level. In period 2B, no accumulation of acids was seen and the process appeared to be more stable than in period 1 (with defined nutrient medium). Degradation of propionate, and acetate, via syntrophic reactions, only proceeds at low P_{H2}, and thus, the observed improved VFA degradation could potentially have been caused by a more efficient H_2 turnover in period 2B as compared to 2A. However, looking at the hydrogen level in the gas out flow illustrated small differences in this regard between the periods. The more complex medium M2 may instead have allowed for more efficient acetate turnover by enrichment of the potential acetate oxidiser *Spirochaetaceae*. The improved acetate conversion might also be explained by the establishment of this organism on the carrier biofilm, which was observed in period 2B, but not 2A. However, in periods 1 and 2A, other members within phylum *Synergistetes*, also representing potential acetate oxidisers, were observed.

In period 3, when the nutrient solution was changed to digestate from a mesophilic wastewater biogas system, the microbial community initially maintained the same composition as at the end of period 2B, with dominance of *Methanobacterium*, *Sporomusa* and *Spirochaetaceae*. Approaching the end of period 3A, the *Spirochaetaceae* genus even became dominant in the community (55.5%). In addition, the potential propionate-degrading LNR_A2-18 (phylum *Cloacimonetes*) reappeared in the community. The high abundance of these two organisms likely contributed to the low acid level in this period of operation. However, on entering period 3B, *Spirochaetaceae* decreased in abundance (12.4–3.3%), possibly coinciding with a drop in pH since it is suggested to be favoured by slightly basic conditions (Lee et al. 2013). Moreover, in this period, an increased abundance of *Acetobacterium wieringae* was observed. This species can grow and produce acetate while consuming CO_2 and H_2 (Braun and Gottschalk 1982; Poehlein et al. 2016). A recently isolated novel strain of *Acetobacterium wieringae* is also able to grow on carbon monoxide (100% CO), producing mainly acetate as the end product (Arantes et al. 2020). Thus, in this phase of TBR operation, CO might have been used by this organism. The CO-utilising organisms in operating periods 1 and 2 were not identified, but the member within *Sporomusa* found in both periods could have been a CO utiliser.

In conclusion, methanation of syngas (56% H_2, 30% CO, 14% CO_2) in a TBR during long-term operation (862 days) was possible using different nutrient sources (defined nutrient medium, dewatered digestate from a thermophilic biogas plant treating food waste and reject water from a biogas plant at a wastewater treatment plant). The process reached maximum methane production levels of 0.9–1.15 $L/L_{PBV}/d$, with some variation during operation, which corresponded to similar production levels as observed before at mesophilic conditions. The process showed some imbalance with accumulation of VFA in period 1, when the defined nutrient medium was used. However, concentrations declined in later operating periods with undefined medium and after introduction of an anaerobic filter to prolong nutrient recycling time.

For the microbial community, the overall trend within each period with different nutrient medium was stabilisation towards the same dominant species by the end of the period. Thus, the community was altered at the start of each period with the change in nutrient source, but after some time, it returned to the composition established prior to the change in nutrient medium. The main microbes observed included *Methanobacterium*, as the dominant methanogen, and the acetogen *Sporomusa*, as a dominant bacterial genus, both in liquid and on the carriers. These are both using hydrogen

and carbon dioxide, while producing mainly methane and acetate, respectively, and have commonly been detected in various biomethanation processes before. Acetate was likely mainly converted via syntrophic acetate oxidation by an abundant representative within the genus *Spirochaetaceae* but could also have been directly converted to methane via *Methanosarcina*, present on the carriers. *Acetobacterium* also appeared later in the process and represent a potential CO-consuming acetogen.

Supplementary Information The online version contains supplementary material available at https://doi.org/10.1007/s00253-022-12035-5.

Acknowledgements The authors acknowledge Simon Isaksson for the assistance with DNA extraction.

Author contribution ÅN and AS contributed to the study conception and design. Material preparation, data collection and analysis were performed by FG, LP, HO and GC. The first draft of the manuscript was written by AS and GC and all authors commented on previous versions of the manuscript. All authors have read and approved the final manuscript.

Funding Open access funding provided by Swedish University of Agricultural Sciences. This project was funded by the Swedish Energy Agency [45261–1] and Formas (2018–01341), and by participating partners, Cortus Energy, Sveaskog, Höganäs kommun, Gasum, Wärtsilä Biogas Systems, KTH, RISE and SLU, all acknowledged for their active contributions to the project.

Data availability The sequence data generated and analysed from this study is made available in NCBI repository in BioProject PRJNA796200.

Declarations

Ethics approval No human or animal participants were involved in this study.

Consent for publication All authors have read and approved the final manuscript.

Conflict of interest The authors declare no competing interests.

References

Abe K, Ueki A, Ohtaki Y, Kaku N, Watanabe K, Ueki K (2012) *Anaerocella delicata* gen. nov., sp. nov., a strictly anaerobic bacterium in the phylum *Bacteroidetes* isolated from a methanogenic reactor of cattle farms. J Gen Appl Microbiol 58(6):405–412. https://doi.org/10.2323/jgam.58.405

Ács N, Szuhaj M, Wirth R, Bagi Z, Maróti G, Rákhely G, Kovács KL (2019) Microbial community rearrangements in power-to-biomethane reactors employing mesophilic biogas digestate. Front Energy Res 7:132. https://doi.org/10.3389/fenrg.2019.00132

Ahlberg-Eliasson K, Westerholm M, Isaksson S, Schnürer A (2021) Anaerobic digestion of animal manure and influence of organic loading rate and temperature on process performance, microbiology, and methane emission from digestates. Front Energy Res 9:683. https://doi.org/10.3389/fenrg.2021.740314

Andreides D, Bautista Quispe JI, Bartackova J, Pokorna D, Zabranska J (2021) A novel two-stage process for biological conversion of syngas to biomethane. Bioresour Technol 327:124811. https://doi.org/10.1016/j.biortech.2021.124811

Arantes AL, Moreira JPC, Diender M, Parshina SN, Stams AJM, Alves MM, Alves JI, Sousa DZ (2020) Enrichment of anaerobic syngas-converting communities and isolation of a novel carboxydotrophic *Acetobacterium wieringae* strain JM. Front Microbiol 11:58. https://doi.org/10.3389/fmicb.2020.00058

Aryal N, Odde M, Petersen CB, Ottosen LDM, Kofoed MVW (2021) Methane production from syngas using a trickle-bed reactor setup. Bioresour Technol 333:125183. https://doi.org/10.1016/j.biortech.2021.125183

Asimakopoulos K, Gavala HN, Skiadas IV (2020a) Biomethanation of syngas by enriched mixed anaerobic consortia in trickle bed reactors. Waste Biomass Valorization 11(2):495–512. https://doi.org/10.1007/s12649-019-00649-2

Asimakopoulos K, Łężyk M, Grimalt-Alemany A, Melas A, Wen Z, Gavala HN, Skiadas IV (2020b) Temperature effects on syngas biomethanation performed in a trickle bed reactor. Chem Eng J 393.https://doi.org/10.1016/j.cej.2020.124739

Asimakopoulos K, Kaufmann-Elfang M, Lundholm-Høffner C, Rasmussen NBK, Grimalt-Alemany A, Gavala HN, Skiadas IV (2021) Scale up study of a thermophilic trickle bed reactor performing syngas biomethanation. Appl Energy 290.https://doi.org/10.1016/j.apenergy.2021.116771

Bengelsdorf FR, Beck MH, Erz C, Hoffmeister S, Karl MM, Riegler P, Wirth S, Poehlein A, Weuster-Botz D, Durre P (2018) Bacterial anaerobic synthesis gas (syngas) and CO2+H2 fermentation. Adv Appl Microbiol 103:143–221. https://doi.org/10.1016/bs.aambs.2018.01.002

Benjaminsson G, Benjaminsson J, Rudberg RB (2013) Power to gas – a technical review. SGC Rapport (2013:284). http://www.sgc.se/ckfinder/userfiles/files/SGC284_eng.pdf

Benstead J, Archer DB, Lloyd D (1991) Formate utilization by members of the genus *Methanobacterium*. Arch Microbiol 156(1):34–37. https://doi.org/10.1007/BF00418184

Braga Nan L, Trably E, Santa-Catalina G, Bernet N, Delgenes J-P, Escudie R (2022) Microbial community redundance in biomethanation systems lead to faster recovery of methane production rates after starvation. Sci Total Environ 804:150073. https://doi.org/10.1016/j.scitotenv.2021.150073

Braun M, Gottschalk G (1982) *Acetobacterium wieringae* sp. nov., a new species producing acetic acid from molecular hydrogen and carbon dioxide. Zbl Bakt Mik Hyg I C 3(3):368–376. https://doi.org/10.1016/S0721-9571(82)80017-3

Burkhardt M, Busch G (2013) Methanation of hydrogen and carbon dioxide. Appl Energy 111:74–79. https://doi.org/10.1016/j.apenergy.2013.04.080

Burkhardt M, Koschack T, Busch G (2015) Biocatalytic methanation of hydrogen and carbon dioxide in an anaerobic three-phase system. Bioresour Technol 178:330–333. https://doi.org/10.1016/j.biortech.2014.08.023

Ciliberti C, Biundo A, Albergo R, Agrimi G, Braccio G, de Bari I, Pisano I (2020) Syngas derived from lignocellulosic biomass gasification as an alternative resource for innovative bioprocesses. Processes 8(12). https://doi.org/10.3390/pr8121567

Dahle H, Birkeland N-K (2006) *Thermovirga lienii* gen. nov., sp. nov., a novel moderately thermophilic, anaerobic, amino-acid-degrading bacterium isolated from a North Sea oil well. Int J Syst Evol Microbiol 56(7):1539–1545. https://doi.org/10.1099/ijs.0.63894-0

Danielsson R, Dicksved J, Sun L, Gonda H, Müller B, Schnürer A, Bertilsson J (2017) Methane production in dairy cows correlates with rumen methanogenic and bacterial community structure. Front Microbiol 8:226. https://doi.org/10.3389/fmicb.2017.00226

De Vrieze J, Saunders AM, He Y, Fang J, Nielsen PH, Verstraete W, Boon N (2015) Ammonia and temperature determine potential clustering in the anaerobic digestion microbiome. Water Res 75:312–323. https://doi.org/10.1016/j.watres.2015.02.025

Dyksma S, Jansen L, Gallert C (2020) Syntrophic acetate oxidation replaces acetoclastic methanogenesis during thermophilic digestion of biowaste. Microbiome 8(1):105. https://doi.org/10.1186/s40168-020-00862-5

Ferry JG (2010) CO in methanogenesis. Ann Microbiol 60(1):1–12. https://doi.org/10.1007/s13213-009-0008-5

Figueras J, Benbelkacem H, Dumas C, Buffiere P (2021) Biomethanation of syngas by enriched mixed anaerobic consortium in pressurized agitated column. Bioresour Technol 338:125548. https://doi.org/10.1016/j.biortech.2021.125548

Fu B, Jin X, Conrad R, Liu H, Liu H (2019) Competition between chemolithotrophic acetogenesis and hydrogenotrophic methanogenesis for exogenous H2/CO2 in anaerobically digested sludge: impact of temperature. Front Microbiol 10:2418. https://doi.org/10.3389/fmicb.2019.02418

Graf J (2014) The family *Rikenellaceae*. (The Prokaryotes.). Springer, Berlin, Heidelberg. https://doi.org/10.1007/978-3-642-38954-2_134

Grim J, Malmros P, Schnürer A, Nordberg Å (2015) Comparison of pasteurization and integrated thermophilic sanitation at a full-scale biogas plant – heat demand and biogas production. Energy 79:419–427. https://doi.org/10.1016/j.energy.2014.11.028

Grimalt-Alemany A, Asimakopoulos K, Skiadas IV, Gavala HN (2020a) Modeling of syngas biomethanation and catabolic route control in mesophilic and thermophilic mixed microbial consortia. Appl Energy 262:114502. https://doi.org/10.1016/j.apenergy.2020.114502

Grimalt-Alemany A, Łężyk M, Kennes-Veiga DM, Skiadas IV, Gavala HN (2020b) Enrichment of mesophilic and thermophilic mixed microbial consortia for syngas biomethanation: the role of kinetic and thermodynamic competition. Waste Biomass Valorization 11(2):465–481. https://doi.org/10.1007/s12649-019-00595-z

Grimalt-Alemany A, Skiadas IV, Gavala HN (2018) Syngas biomethanation: state-of-the-art review and perspectives. Biofuel Bioprod Bioresour 12(1):139–158. https://doi.org/10.1002/bbb.1826

Grimalt-Alemany A, Skiadas IV, Gavala HN (2017) Syngas biomethanation: state-of-the-art review and perspectives. Biofuel Bioprod Bioresour 12(1):139–158. https://doi.org/10.1002/bbb.1826

Hendriks AT, Zeeman G (2009) Pretreatments to enhance the digestibility of lignocellulosic biomass. Bioresour Technol 100(1):10–18. https://doi.org/10.1016/j.biortech.2008.05.027

Jarrell KF, Kalmokoff ML (1988) Nutritional requirements of the methanogenic *archaebacteria*. Can J Microbiol 34(5):557–576. https://doi.org/10.1139/m88-095

Jiang H, Wu F, Wang Y, Feng L, Zhou H, Li Y (2021) Characteristics of in-situ hydrogen biomethanation at mesophilic and thermophilic temperatures. Bioresour Technol 337:125455. https://doi.org/10.1016/j.biortech.2021.125455

Kern T, Fischer MA, Deppenmeier U, Schmitz RA, Rother M (2016) *Methanosarcina flavescens* sp. nov., a methanogenic archaeon isolated from a full-scale anaerobic digester. Int J Syst Evol Microbiol 66(3):1533–1538. https://doi.org/10.1099/ijsem.0.000894

Kimmel DE, Klasson KT, Clausen EC, Gaddy JL (1991) Performance of trickle-bed bioreactors for converting synthesis gas to methane. Appl Biochem Biotechnol 28(1):457. https://doi.org/10.1007/BF02922625

Klang J, Szewzyk U, Bock D, Theuerl S (2019) Nexus between the microbial diversity level and the stress tolerance within the biogas process. Anaerobe 56:8–16. https://doi.org/10.1016/j.anaerobe.2019.01.003

Klasson KT, Ackerson MD, Clausen EC, Gaddy JL (1992) Bioconversion of synthesis gas into liquid or gaseous fuels. Enzyme Microb Technol 14(8):602–608. https://doi.org/10.1016/0141-0229(92)90033-K

Kougias PG, Angelidaki I (2018) Biogas and its opportunities—a review. Front Environ Sci Eng 12(3):14. https://doi.org/10.1007/s11783-018-1037-8

Krieg NR, Ludwig W, Euzéby J, Whitman WB (2010) Phylum XIV. Bacteroidetes phyl. nov. In: Krieg NR, Staley JT, Brown DR, Hedlund BP, Paster BJ, Ward NL, Ludwig W, Whitman WB (eds) Bergey's Manual® of Systematic Bacteriology: Volume Four The Bacteroidetes, Spirochaetes, Tenericutes (Mollicutes), Acidobacteria, Fibrobacteres, Fusobacteria, Dictyoglomi, Gemmatimonadetes, Lentisphaerae, Verrucomicrobia, Chlamydiae, and Planctomycetes. Springer, New York, pp 25–469 [2021-12-26 13:21:45]

Lee J, Koo T, Yulisa A, Hwang S (2019) Magnetite as an enhancer in methanogenic degradation of volatile fatty acids under ammonia-stressed condition. J Environ Manage 241:418–426. https://doi.org/10.1016/j.jenvman.2019.04.038

Lee S-H, Park J-H, Kang H-J, Lee Y, Lee T, Park H-D (2013) Distribution and abundance of Spirochaetes in full-scale anaerobic digesters. Bioresour Technol 145.https://doi.org/10.1016/j.biortech.2013.02.070

Lemmer A, Ullrich T (2018) Effect of different operating temperatures on the biological hydrogen methanation in trickle bed reactors. Energies 11(6):1344. https://doi.org/10.3390/en11061344

Li C, Zhu X, Angelidaki I (2020a) Carbon monoxide conversion and syngas biomethanation mediated by different microbial consortia. Bioresour Technol 314:123739. https://doi.org/10.1016/j.biortech.2020.123739

Li Y, Wang Z, He Z, Luo S, Su D, Jiang H, Zhou H, Xu Q (2020b) Effects of temperature, hydrogen/carbon monoxide ratio and trace element addition on methane production performance from syngas biomethanation. Bioresour Technol 295:122296. https://doi.org/10.1016/j.biortech.2019.122296

Li C, Zhu X, Angelidaki I (2021) Syngas biomethanation: effect of biomass-gas ratio, syngas composition and pH buffer. Bioresour Technol 342:125997. https://doi.org/10.1016/j.biortech.2021.125997

Liu R, Hao X, Wei J (2016) Function of homoacetogenesis on the heterotrophic methane production with exogenous H2/CO2 involved. Chem Eng J 284:1196–1203. https://doi.org/10.1016/j.cej.2015.09.081

Liu T, Sun L, Müller B, Schnürer A (2017) Importance of inoculum source and initial community structure for biogas production from agricultural substrates. Bioresour Technol 245:768–777. https://doi.org/10.1016/j.biortech.2017.08.213

Liu Y, Beer LL, Whitman WB (2012) Methanogens: a window into ancient sulfur metabolism. Trends Microbiol 20(5):251–258. https://doi.org/10.1016/j.tim.2012.02.002

Logroño W, Popp D, Nikolausz M, Kluge P, Harms H, Kleinsteuber S (2021) Microbial communities in flexible biomethanation of

hydrogen are functionally resilient upon starvation. Front Microbiol 12:123. https://doi.org/10.3389/fmicb.2021.619632

Luo G, Wang W, Angelidaki I (2013) Anaerobic digestion for simultaneous sewage sludge treatment and co biomethanation: process performance and microbial ecology. Environ Sci Technol 47(18):10685–10693. https://doi.org/10.1021/es401018d

McMurdie PJ, Holmes S (2013) phyloseq: an R package for reproducible interactive analysis and graphics of microbiome census data. PLoS ONE 8(4):e61217. https://doi.org/10.1371/journal.pone.0061217

Möller B, Oßmer R, Howard BH, Gottschalk G, Hippe H (1984) *Sporomusa*, a new genus of gram-negative anaerobic bacteria including *Sporomusa sphaeroides* spec. nov. and *Sporomusa ovata* spec. nov. Arch Microbiol 139(4):388–396. https://doi.org/10.1007/BF00408385

Moreira JPC, Diender M, Arantes AL, Boeren S, Stams AJM, Alves MM, Alves JI, Sousa DZ (2021) Propionate production from carbon monoxide by synthetic cocultures of *Acetobacterium wieringae* and Propionigenic Bacteria. Appl Environ Microbiol. https://doi.org/10.1128/AEM.02839-20

Oelgeschläger E, Rother M (2008) Carbon monoxide-dependent energy metabolism in anaerobic bacteria and archaea. Arch Microbiol 190(3):257–269. https://doi.org/10.1007/s00203-008-0382-6

Paul A, Dutta A (2018) Challenges and opportunities of lignocellulosic biomass for anaerobic digestion. Resour Conserv Recycl 130:164–174. https://doi.org/10.1016/j.resconrec.2017.12.005

Poehlein A, Bengelsdorf FR, Schiel-Bengelsdorf B, Daniel R, Dürre P (2016) Genome sequence of the acetogenic bacterium *Acetobacterium wieringae DSM 1911T*. Genome Announc. https://doi.org/10.1128/genomeA.01430-16

Porté H, Kougias PG, Alfaro N, Treu L, Campanaro S, Angelidaki I (2019) Process performance and microbial community structure in thermophilic trickling biofilter reactors for biogas upgrading. Sci Total Environ 655:529–538. https://doi.org/10.1016/j.scitotenv.2018.11.289

Rachbauer L, Beyer R, Bochmann G, Fuchs W (2017) Characteristics of adapted hydrogenotrophic community during biomethanation. Sci Total Environ 595:912–919. https://doi.org/10.1016/j.scitotenv.2017.03.074

Rachbauer L, Voitl G, Bochmann G, Fuchs W (2016) Biological biogas upgrading capacity of a hydrogenotrophic community in a trickle-bed reactor. Appl Energy 180:483–490. https://doi.org/10.1016/j.apenergy.2016.07.109

Ren J, Liu Y-L, Zhao X-Y, Cao J-P (2020) Methanation of syngas from biomass gasification: an overview. Int J Hydrogen Energy 45(7):4223–4243. https://doi.org/10.1016/j.ijhydene.2019.12.023

RStudio Team (2020) RStudio: Integrated Development for R. RStudio, PBC, Boston, MA. http://www.rstudio.com/

Sancho Navarro S, Cimpoia R, Bruant G, Guiot SR (2016) Biomethanation of Syngas using anaerobic sludge: shift in the catabolic routes with the CO partial pressure increase. Front Microbiol 7:1188. https://doi.org/10.3389/fmicb.2016.01188

Sieborg MU, Jønson BD, Ashraf MT, Yde L, Triolo JM (2020) Biomethanation in a thermophilic biotrickling filter using cattle manure as nutrient media. Bioresour Technol Rep 9:100391. https://doi.org/10.1016/j.biteb.2020.100391

Singh A, Müller B, Schnürer A (2021) Profiling temporal dynamics of acetogenic communities in anaerobic digesters using next-generation sequencing and T-RFLP. Sci Rep 11(1):13298. https://doi.org/10.1038/s41598-021-92658-2

Sposob M, Wahid R, Fischer K (2021) Ex-situ biological CO2 methanation using trickle bed reactor: review and recent advances. Rev Environ Sci Biotechnol 20(4):1087–1102. https://doi.org/10.1007/s11157-021-09589-7

Strübing D, Huber B, Lebuhn M, Drewes JE, Koch K (2017) High performance biological methanation in a thermophilic anaerobic trickle bed reactor. Bioresour Technol 245:1176–1183. https://doi.org/10.1016/j.biortech.2017.08.088

Su X-L, Tian Q, Zhang J, Yuan X-Z, Shi X-S, Guo R-B, Qiu Y-L (2014) *Acetobacteroides hydrogenigenes gen.* nov., sp. nov., an anaerobic hydrogen-producing bacterium in the family *Rikenellaceae* isolated from a reed swamp. Int J Syst Evol Microbiol 64(9):2986–2991. https://doi.org/10.1099/ijs.0.063917-0

Sundberg C, Al-Soud WA, Larsson M, Alm E, Yekta SS, Svensson BH, Sørensen SJ, Karlsson A (2013) 454 pyrosequencing analyses of bacterial and archaeal richness in 21 full-scale biogas digesters. FEMS Microb Ecol 85(3):612–626. https://doi.org/10.1111/1574-6941.12148

Thapa A, Park J-G, Yang H-M, Jun H-B (2021) In-situ biogas upgrading in an anaerobic trickling filter bed reactor treating a thermal post-treated digestate. J Environ Chem Eng 9(6):106780. https://doi.org/10.1016/j.jece.2021.106780

Tsapekos P, Treu L, Campanaro S, Centurion VB, Zhu X, Peprah M, Zhang Z, Kougias PG, Angelidaki I (2021) Pilot-scale biomethanation in a trickle bed reactor: process performance and microbiome functional reconstruction. Energy Convers Manage 244.https://doi.org/10.1016/j.enconman.2021.114491

Voelklein MA, Rusmanis D, Murphy JD (2019) Biological methanation: Strategies for in-situ and ex-situ upgrading in anaerobic digestion. Appl Energy 235:1061–1071. https://doi.org/10.1016/j.apenergy.2018.11.006

Wang H-Z, Lv X-M, Yi Y, Zheng D, Gou M, Nie Y, Hu B, Nobu MK, Narihiro T, Tang Y-Q (2019) Using DNA-based stable isotope probing to reveal novel propionate- and acetate-oxidizing bacteria in propionate-fed mesophilic anaerobic chemostats. Sci Rep 9(1):17396. https://doi.org/10.1038/s41598-019-53849-0

Wegener Kofoed MV, Jensen MB, Mørck Ottosen LD (2021) Chapter 12 - Biological upgrading of biogas through CO2 conversion to CH4. In: Aryal N, Mørck Ottosen LD, Wegener Kofoed MV, Pant D (eds) Emerging technologies and biological systems for biogas upgrading. Academic Press; pp 321–362. [2022–01–12 08:38:14]

Westerholm M, Calusinska M, Dolfing J (2021) Syntrophic propionate-oxidizing bacteria in methanogenic systems. FEMS Microbiol Rev:fuab057. https://doi.org/10.1093/femsre/fuab057

Westerholm M, Hansson M, Schnürer A (2012) Improved biogas production from whole stillage by co-digestion with cattle manure. Bioresour Technol 114:314–319. https://doi.org/10.1016/j.biortech.2012.03.005

Westerholm M, Isaksson S, Karlsson Lindsjö O, Schnürer A (2018) Microbial community adaptability to altered temperature conditions determines the potential for process optimisation in biogas production. Appl Energy 226:838–848. https://doi.org/10.1016/j.apenergy.2018.06.045

Westerholm M, Moestedt J, Schnürer A (2016) Biogas production through syntrophic acetate oxidation and deliberate operating strategies for improved digester performance. Appl Energy 179:124–135. https://doi.org/10.1016/j.apenergy.2016.06.061

Westerholm M, Müller B, Isaksson S, Schnürer A (2015) Trace element and temperature effects on microbial communities and links to biogas digester performance at high ammonia levels. Biotechnol Biofuels 8(1):154. https://doi.org/10.1186/s13068-015-0328-6

Westerholm M, Roos S, Schnürer A (2010) *Syntrophaceticus schinkii* gen. nov., sp. nov., an anaerobic, syntrophic acetate-oxidizing bacterium isolated from a mesophilic anaerobic filter. FEMS Microbiol Lett 309(1):100–104. https://doi.org/10.1111/j.1574-6968.2010.02023.x

II

Bioresource Technology 435 (2025) 132893

Contents lists available at ScienceDirect

Bioresource Technology

journal homepage: www.elsevier.com/locate/biortech

Comparative evaluation of digestate and reject water as nutrient media for syngas biomethanation in thermophilic trickle-bed reactors☆

Florian Gabler [a,b,*], George Cheng [c], Leticia Pizzul [b], Anna Schnürer [c], Åke Nordberg [a]

[a] Department of Energy and Technology, SLU, Box 7032, 750 07 Uppsala, Sweden
[b] Department of Biorefinery and Energy, RISE, Box 7033, 750 07 Uppsala, Sweden
[c] Department of Molecular Science, BioCenter SLU, Box 7015, 750 07 Uppsala, Sweden

HIGHLIGHTS

- High Methane Evolution Rate (4.5 L/(L_{pbv}·d)) achieved using digestate as nutrient.
- High H_2 and CO conversion rates (>95 %) attained using digestate as sole medium.
- Adding S and P to reject water improved MER from 1.0 to 3.1 L/(L_{pbv}·d).
- *Methanothermobacter* was the most abundant methanogen in both reactors.
- Syntrophic acetate oxidation was a key function for efficient gas conversion.

GRAPHICAL ABSTRACT

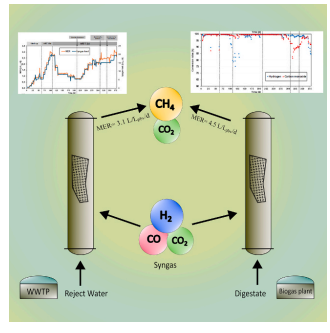

ARTICLE INFO

Keywords:
Biosyngas
Hydrogen
Carbon Monoxide
Sulfur
Microbial Community
Phosphorus

ABSTRACT

Syngas biomethanation facilitates the utilization of thermal gasification products. This study evaluated the performance of two liquid organic waste streams (manure-based digestate and reject water from digested sewage sludge) as nutrient media in thermophilic trickle-bed reactors (TBRs) over more than one year. Digestate achieved a Methane Evolution Rate (MER) of 4.5 L/(L_{pbv}·d) with the highest so far published H_2 and CO conversion rates (>95 %). Reject water only led to a maximum MER of 1.0 L/(L_{pbv}·d), while the addition of sulfur and phosphorus to the reject water resulted in improved MER of up to 3.1 L/(L_{pbv}·d). The microbial analysis illustrated a similar microbial community structure and methanogenic abundance for both TBRs, with *Methanothermobacter* as the dominating methanogen both in the liquid phase and biofilm of the carriers. Carbon monoxide was likely converted to both methane and acetate.

☆ This article is part of a special issue entitled: 'Innovative Biogasprocess' published in Bioresource Technology.

* Corresponding author at: Department of Energy and Technology, SLU, Box 7032, 750 07, Uppsala, Sweden.
E-mail address: florian.gabler@slu.se (F. Gabler).

https://doi.org/10.1016/j.biortech.2025.132893
Received 31 January 2025; Received in revised form 25 June 2025; Accepted 25 June 2025
Available online 25 June 2025

1. Introduction

Syngas originating from the thermochemical conversion of biomass is typically comprised of hydrogen (H_2), carbon monoxide (CO), carbon dioxide (CO_2), and additional gases like nitrogen (N_2) and methane (CH_4). Syngas can be utilized as an energy source, but is also used as an intermediate product for the further processing of high-value products like CH_4 or acetate (Aryal et al., 2021; Andreides et al., 2024). The route for CH_4 production from syngas can turn a variety of low-biodegradable and recalcitrant biomass, like lignocellulosic material or municipal waste, into a versatile energy carrier, increasing synergies with current gas infrastructure for energy storage and distribution (Ren et al., 2020).

Both chemical and biological processes can be used for the methanation of syngas: chemical methanation through catalytic mechanisms or biomethanation mediated by methanogenic archaea (Ren et al., 2020). Compared to chemical-catalytic methods, biomethanation offers the advantage of operating under mild conditions, such as low pressures and temperatures (Grimalt-Alemany et al., 2017). Additionally, biomethanation is more resilient to contaminants like tar and hydrogen sulfide (H_2S) than chemical conversion (Grimalt-Alemany et al., 2017).

During syngas biomethanation, hydrogenotrophic methanogens convert H_2 and CO_2 to CH_4 at a broad temperature range, but the same substrates can be utilized by acetogens for the production of acetate, creating competition for H_2. Methanogens have an advantage over acetogens as they can metabolize lower levels of dissolved hydrogen, due to thermodynamics and substrate affinities (Wegener Kofoed et al., 2021). However, at higher hydrogen levels, acetogens become more competitive for H_2 than methanogens (Liu et al., 2016). The produced acetate can be directly converted into CH_4 by acetoclastic methanogens or via H_2 and CO_2 through a complex biocatalytic reaction chain involving syntrophic acetate-oxidizing (SAO) bacteria and hydrogenotrophic methanogens (Westerholm et al., 2019). Due to thermodynamic restrictions, the SAO conversion route can only function at very low hydrogen partial pressures (Westerholm et al., 2019).

CO can be directly converted to CH_4 by a few hydrogenotrophic methanogens. Between 55 °C and 70 °C, CO is usually converted to CO_2 by carboxydotrophic hydrogenogens (biological water-to-gas shift) (Sipma et al., 2003). The pathway through intermediate products dominates CO conversion due to the favorable thermodynamic conditions of CO-converting bacteria as compared to direct CO transformation by carboxydotrophic hydrogenogens (Sancho Navarro et al., 2016). High CO partial pressure can potentially limit biomethanation because of its toxicity to methanogens and its competition with H_2 as an electron donor.

The slow kinetics of methanogens and the temperature-dependent low liquid–gas mass transfer limit CH_4 productivity. Despite lower gas solubility at higher temperatures, the biological conversion of syngas is faster at 55 °C compared to 37 °C due to higher microbial activity under thermophilic conditions (Sipma et al., 2003). To circumvent mass transfer limitations, the trickle-bed reactor (TBR) is a viable reactor design for biomethanation (Feickert Fenske et al., 2023b). TBRs are gas-tight columns filled with carrier material covered by microbes, over which a nutrient liquid is trickled at different frequencies. The carriers provide a high specific surface (in relation to the reactor volume) for the biofilm to grow on, strengthening the gas–liquid phase boundary interaction (Strübing et al., 2017).

It is essential to supply enough nutrients with the liquid medium to develop microbial activity and growth while either converting syngas or only H_2 and CO_2, which represent carbon and energy sources (Wegener Kofoed et al., 2021). Both macro- and micronutrients that are essential for microbial activity, such as nitrogen (N), sulfur (S), phosphorus (P), and various salts and trace elements, should be present. Several studies have examined biomethanation using a defined nutrient media (Burkhardt et al., 2015; Rachbauer et al., 2016; Asimakopoulos et al., 2019). However, more accessible and economically feasible nutrient sources such as digestate, manure, or reject water from sludge processing at wastewater treatment plants (WWTP) are needed for process upscaling.

The utilization of such non-defined nutrient media, especially digestate or manure, has been assessed satisfactorily for the biomethanation of H_2 and CO_2 (Feickert Fenske et al., 2023b). For the biomethanation of syngas, the use of digestate as a nutrient source has seen interest in recent years (Aryal et al., 2021; Figueras et al., 2021; Andreides et al., 2022a; Cheng et al., 2022; Ali et al., 2024; Goonesekera et al., 2024). Another representative of non-defined media is reject water, which contains high levels of N. For TBR biomethanation systems, reject water as a nutrient medium has only been assessed in three previous studies. The studies by Kamravamanesh et al. (2023) and Feickert Fenske et al. (2023a) used reject water for TBR biomethanation of H_2 and CO_2 and added trace elements stock solutions, whereas the study of Cheng et al. (2022) indicated that the addition of Na_2S to the reject water increases syngas conversion rates and CH_4 productivity. However, there is a need for more comprehensive studies of the digestate and reject water macronutrient supply using the same TBR setup and inoculum for comparison of syngas conversion and CH_4 productivity, to identify potential nutrient limitations.

The objective of the present study was to assess and compare H_2 and CO conversion, and the CH_4 production of syngas biomethanation in continuous long-term (ca. one year) operated thermophilic TBR (V_{pbv} = 5 L) using either digestate or reject water as the nutrient media. Furthermore, indications of performance limitations caused by shortages of S and P in reject water were studied by the supplementation of these macronutrients. Moreover, an additional objective was to study the long-term development of the microbial community with a focus on potential differences depending on the nutrient media.

2. Materials and methods

2.1. Inoculum and syngas

To achieve a broad microbial spectrum covering both mesophilic and thermophilic conditions, a mixture of 4 different digestates was used as inoculum: (A) digestate from the thermophilic digestion of agricultural substrates and municipal food waste (More Biogas Småland AB, Läckeby, Sweden), (B) digestate from thermophilic municipal food waste digestion (Uppsala Vatten och avfall AB, Sweden), (C) digestate from mesophilic manure-based digestion (SLU, Lövsta, Uppsala, Sweden), and (D) digestate from mesophilic sewage sludge digestion (Uppsala Vatten och avfall AB, Sweden). Before mixing, the digestates were filtered through a mesh column (4/2/1 mm) to remove large particles and were subsequently stored for a degassing period of three weeks at 55 °C (digestates A and B) or 37 °C (digestates C and D). The digestates were combined in equal proportions of 25 vol%, and the final mixture was used as inoculum. The characterization of the inoculum is presented in Table S1 (supplementary Material). The utilized syngas was an artificial mixture supplied by Air Liquide (Paris, France) with 40 % H_2, 30 % CO, 20 % CO_2, and 10 % N_2, which can reflect an industrial syngas mixture according to the GoBiGas project, utilizing forestry biomass as gasification substrate (Larsson et al., 2019).

2.2. Nutrient media

The characterization of both nutrient media is presented in Table S1 (SM). The digestate was collected from a mesophilic biogas reactor (SLU, Lövsta, Uppsala, Sweden), mainly operating with manure from pigs and cows. Batches of approximately 60 L were collected at the beginning of the trial, and on day 126 for subsequent storage at 2 °C. Before application to the reactor, the digestate was filtered through a mesh column (4/2/1 mm), diluted with 50 % tap water to reduce the risk of clogging in the reactor, and subsequently stored at 6–8 °C before it was added to the reactor.

Reject water from the sewage sludge dewatering process at a

wastewater treatment plant (WWTP) in Uppsala, Sweden, was collected as two batches of approximately 60 L each at the beginning of the trial and on day 115; these were subsequently long-term stored at 2 °C. The reject water was not filtered or diluted before being added to the reactor. As for digestate, the reject water was moved to a 6–8 °C fridge before addition to the reactor.

2.3. Trickle-bed reactor setup

Two identical acid-proof stainless-steel TBRs were constructed and placed in a movable container together with all associated equipment (Fig. 1). The reactors had a total volume of 7.5 L (an inner diameter of 72 mm and a total height of 1782 mm), including a liquid reservoir of 1 L, which was separated from the packed bed with a grid installed at a height of 504 mm from the bottom. A similar H:D ratio has been used by e.g. Asimakopoulos et al. (2021). For biofilm growth, polyethylene carrier material AnoxKaldnes K1 500 (10 mm diameter, surface area 500 m^2/m^3, density 1.2 g/m^3) was used to create a total packed bed volume (pbv) of 5 L. The nutrient liquid was intermittently recirculated using a progressive cavity pump (Nova Rotors, MN 015–1, 0.6 kW; Sossano, VI, Italy) from the reservoir to the top of the reactor, where it was sprinkled over a perforated metal distribution plate and then trickled downwards through the packed bed to the liquid reservoir. Intermittent liquid trickling was chosen to reduce gas–liquid mass transfer limitations (Sieborg et al., 2021; Goonesekera et al., 2024). The pumps for liquid recirculation were operated with a frequency exchanger in semi-continuous mode with 20 s of pumping every 10 min at an average flow of 40 L/h, recirculating 222 mL per trickling occasion and resulting in a nutrient liquid load of 6.4 $L/(L_{pbv} \cdot d)$. The fresh nutrient medium was pumped into the liquid reservoir 4 to 6 times per day using peristaltic pumps (WMC, 200 Series, Southwick, UK), depending on operational conditions within the corresponding periods. Nutrient supplements were added using adjustable peristaltic pumps (Aalborg TPUA-010005, Orangeburg, US).

The syngas load was controlled by a calibrated mass flow regulator (MFR, Aalborg DPC17; Orangeburg, US) and was continuously added through a port between the liquid reservoir and the packed bed (Fig. 1) to meet the liquid coming from the top, thus operating in a counter-current manner. There was no significant overpressure applied to the TBRs. At the top of the reactor and above the packed bed, the product gas was collected, and after passing a condensed water trap, its volume was measured using a drum meter (TG 0.5; Ritter, Germany) before passing a second condensed trap and entering the gas storage. The composition of the product gas was analyzed for CH_4, CO_2, CO, O_2, and H_2 using an ETG MCA 100 Syn Biogas Multigas Analyzer (ETG Risorse e Tecnologia, Chivasso, Italy) in batches of ca. 3 L from the gas storage. The concentration of H_2S was followed regularly using Kitagawa Gas Detector Tubes No.120SD (Komyo Rikagaku Kogyo, Japan).

The reactors were equipped with three larger ports to allow sampling of carrier material at the top, middle and bottom of the packed bed (Fig. 1). Both TBRs were heated by a water jacket and the temperature in the reactors was logged using three digital temperature sensors at the bottom, middle and top of the TBRs. The nominal temperature monitored in the middle of the TBR was 56 ± 1°C for the entire experiment. A pH electrode (Greisinger GPHU 014 MP-BNC pH electrode, Regenstauf, Germany) was placed in line with the outer recirculation circuit just after the recirculation pump (Fig. 1). Operational control of all pumps was achieved through a microcontroller and software by Arduino (Version 1.8.15; Italy). For the data collection of gas composition, pH, and temperature, the software LabVIEW (National Instruments, Austin,

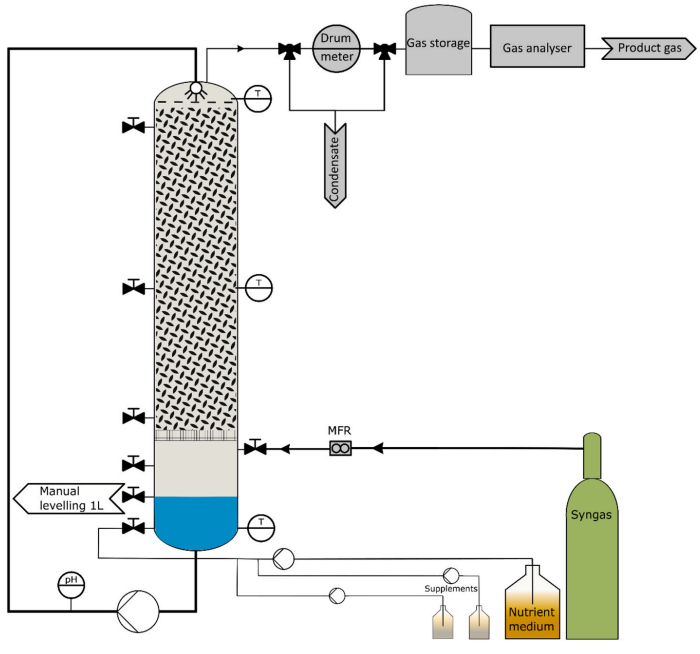

Fig. 1. Process and instrumentation scheme of the trickle-bed reactor (TBR) design. Syngas was supplied to the TBR from a gas cylinder using a mass flow regulator. The liquid medium was intermittently recirculated from the liquid reservoir (V = 1 L) to the top of the trickle bed column. The gas flow was in a counter-current direction to the trickling liquid from bottom to top. The product gas left the reactor at the top, followed by a water trap, volume measurement, and gas dome. Fresh nutrient medium and supplements were pumped intermittently into the liquid reservoir using a peristaltic pump.

US) was used. Volumetric data originating from the MFRs and drum meters was manually documented on working days.

2.4. Process operation

Both reactors were flushed with N_2 (flow rate 20 mL/min) for 24 h before inoculation. The initial 62 days of operation (start-up) were devoted to inoculation of the reactors, which started with the addition of 1.7 L of inoculum to each TBR, followed by a stepwise increase of syngas load (Fig. 2a and 3a). During the start-up period (until day 62), no external nutrient sources were added to the TBRs, and only internal and intermittent (as described in section 2.3) recirculation of the inoculum was performed to establish biofilm growth and adaptation to the environment. Thereafter, the reactors were operated on fresh diluted digestate (TBR1) and reject water (TBR2). Their operation was categorized in several periods based on the hydraulic retention time (HRT) for the nutrient media and the addition of nutritional supplements, as summarised in Table S1, SM. Both TBRs started with an HRT of 15 d, which was based on prior experiences of using non-defined nutrient media for syngas biomethanation. Due to the unstable operation of TBR2 and to assess S and P shortages in the reactor liquid, supplementary sulfur (Na_2S, Merck, Darmstadt/Germany) and phosphorous (KH_2PO_4, Merck, Darmstadt/Germany) were added to TBR2 (Table 1). TBR1 and TBR2 were operated for a total of 370 days and 381 days, respectively.

The major operational guideline applied was to maintain high H_2 and CO conversion rates (above 90 %) throughout the experiment. The adjustment of process parameters such as syngas load or nutrient addition rate was based on the development of H_2 and CO conversion rates, accompanied by changes in the methane evolution rate (MER).

2.5. Sampling and analytical methods

Process liquid was manually removed from the liquid reservoir regularly (every 3–4 days) and was used for chemical and microbial analyses. Analyses of ammonium (NH_4^+) and sulfate (SO_4^{2-}) were conducted straight after sampling from the TBRs, whereas samples used for analyses of phosphate (PO_4^{3-}), volatile fatty acids (VFA) and microbial community were stored at −18 °C. Carriers from the TBRs were sampled on two occasions (day 210 and the end of the trial, i.e. day 371 for TBR1 and day 382 for TBR2) by opening the valves at the top, middle and bottom of the reactor (Fig. 1) while flushing with N_2 (5 mL/min) followed by replacement with fresh carriers.

NH_4^+, SO_4^{2-}, and PO_4^{3-} were analysed using a spectrophotometer (Spectroquant® Nova 60A photometer; MilliporeSigma, Burlington, Massachusetts, United States) with reagent test kits from the series Supelco (Merck, Darmstadt, Germany). Total alkalinity was calculated as the amount of acid required to bring the sample to pH 4.4 based on titration with an automatic titrator (TitraLab® AT1000 series; Hach, Düsseldorf, Germany). Concurrently, pH was measured using a Hanna instrument HI83141 (Woonsocket, Rhode Island, United States). Volatile fatty acids were analyzed through high-performance liquid chromatography according to Westerholm et al. (2012).

Table 1
Chronology of operational changes of TBR1 and TBR2 during the comparison of their syngas biomethanation performance.

Duration [d]	TBR1	TBR2
0	Start inoculation; only internal recirculation	
62	Addition of diluted digestate(HRT 15 d)	Addition of reject water (HRT 15 d)
109		Increase nutrient addition rate (HRT 7.5 d)
117	Increase nutrient addition rate (HRT 7.5 d)	
209		Addition of Na_2S (20 mL/d with 1 g/L)
308		Addition of Na_2S (10 mL/d with 1 g/L) + KH_2PO_4 10 mL/d with 0.8 g/L
341		Increase concentration of KH_2PO_4 to 8 g/L
370	End	
381		End

2.6. Microbial sequencing and analysis

DNA extraction was completed using the FastDNA Spin Kit for Soil (MPBiomedicals, Illkirch-Graffenstaden, France) with 2 mL of the liquid sample following the manufacturer's instructions, with the following modifications: step 7 (10 min centrifugation at 14,000 RCF), step 9 (10 min of matrix settling), and an additional cleaning step between steps 11 and 12 with humic acid. The same extraction kit was used for the carrier biofilm samples. Before following manufacturer's instructions, the following steps were performed: 1. add 978 μL of sodium phosphate buffer and 122 μL of microtubule buffer to a Lysing Matrix E Tube; 2. resuspend the solution in the Lysis Matrix E Tube and transfer all the contents to a 5 mL Eppendorf tube; 3. select a representative carrier from the sample and place into the 5 mL tube; 4. vortex continuously at low speed for 1 min; 5. remove the carrier from the 5 mL tube; and 6. transfer everything from the 5 mL tube back into the Lysing Matrix E tube, then continue from step 3 of the manufacturer's instructions. Sequencing libraries were prepared and generated by SciLifeLab, Stockholm, Sweden, using Illumina MiSeq (2x300 bp) targeting 16S rDNA as described previously (Westerholm et al., 2018). Adapters were removed from the paired-end reads using Cutadapt version 1.13 on the forward and reverse reads (GTGBCAGCMGCCGCGGTAA and GACTACHVGGGTATCTAATCC, respectively) and filtered based on quality and trimmed reads to 250 bp. The trimmed reads were processed using Division Amplicon Denoising Algorithm2 (DADA2) version 1.16.0 in RStudio running R version 4.3.1, as described by Westerholm et al. (2018), with forward and reverse reads truncated at positions 240 and 160, respectively. The SILVA reference database v. 138 was used for microbial classification. The data was organized using phyloseq v1.44.0 (McMurdie & Holmes, 2013) in a single data object. The DADA2 analysis was completed on the UPPMAX high-performance computing cluster. The single data object created was visualized in R Studio 2024.09.1 (RStudio Team, 2021) running R v4.4.1. The following R packages were installed for the visualization of the microbial data: ggplot v3.5.1, data.table v1.15.4, plotly v4.10.4, lattice v0.22.6, permute v0.9.7, vegan v2.6.6.1, readxl v1.4.3, plyr v1.8.9, grid v4.4.1 and ggtext v0.1.2. Weighted principal coordinate analysis (PCoA) was calculated using the UniFrac method (Lozupone & Knight, 2005) based on the maximum-likelihood phylogenetic tree generated with FastTree (v2.1.11) (options –nt, −gtr, −gamma were used) using an alignment of all the amplicon sequence variants (ASV) with MAFFT (v7.526). To determine potential species similarity, the ASVs were submitted to the Basic Local Alignment Search Tool (BLAST) algorithm provided by the National Center for Biotechnology Information (NCBI). Raw sequence data have been deposited in NCBI PRJNA1268893.

To quantify the total amount of methanogens, a qPCR was performed using the primers mcrA-rev (CGTTCATBGCGTAGTTVGGRTAGT) and mcrA-F3 (CTTGAARMTCACTTCGGTGGWTC) (Steinberg & Regan, 2008; Cisek et al., 2022). The fragment amplification was completed using Thermo Fisher Scientific QuantStudio 5 programed to run at 98 °C/10 s, 56 °C/30 s, 72 °C/30 s, 35 cycles. For the construction of DNA standards for methanogens, the methanogens were amplified from environmental manure samples using primers mcrA-rev and mcrA-F3. The mcrA genes amplified were PCR purified using Qiagen (QIAquick PCR Purification Kit) and cloned into the pGEM-T Easy Vector System (Promega) and transformed into competent *Escherichia coli* cells following the manufacturer's instructions. Plasmids were extracted using QIAprep spin miniprep kit (Qiagen, Hilden, Germany) and sent to Macrogen for sequencing using Macrogen's standard primers M13F-pUC

(−40) and M13R-pUC (−40).

2.7. Calculations

The average inflow-based hydraulic retention time of the nutrient media was calculated based on the addition of fresh nutrient medium V_M (L/d) to the reactor and the total liquid volume V_L in the reactor (1 L), as follows:

$$HRT = \frac{V_L}{V_M} \quad (1)$$

The methane evolution rate (MER) was calculated as shown in Eq. (2). Here, F_{out} ($L/(L_{pbv}\cdot d)$) is defined as the total normalized product gas flow rate (1013.15 mbar, 273.15 K) including moisture and c_{CH4} is the CH_4 composition in the product gas.

$$MER = F_{out} * c_{CH4} \quad (2)$$

The conversion rate (%) of H_2 and CO was respectively calculated according to Eq. (3), where F_i *in* is the normalized flow rate of the specific gas compartment in the inlet gas ($L/(L_{pbv}\cdot d)$) and F_i *out* is the normalized flow rate of it in the product gas at the outlet of the TBR.

$$conversionrate = \frac{F_i in - F_i out}{F_i in} * 100 \quad (3)$$

The inflow-based gas retention Time (GRT) was defined as the average time for the gas to stay in the packed bed volume without conversion of the gases according to Eq. (4), where V_{pbv} is the active packed bed reactor volume (mL), and F_{in} is the total normalized inflowing gas load (mL/h).

$$GRT = \frac{V_{pbv}}{F_{in}} \quad (4)$$

3. Results

3.1. The effect of nutrient media on process parameters

The results in this section are described based on the operational periods for each reactor (Table 1). As a result of the major operational guideline to maintain high H_2 and CO conversion rates, no periods of VFA accumulation (< 0.6 g/L) were observed during the entire operation of 370 and 381 days for TBR1 and TBR2, respectively (Fig. S2a; supplementary material).

3.1.1. Start-up – without nutrient medium addition

The operation process during the start-up period was identical for TBR1 and TBR2. Straight after inoculation with the digestate mixture, syngas was applied to the reactors. During the first 62 days, the syngas load was increased stepwise (usually every 7–10 days), depending on H_2 and CO conversion, up to a final syngas load of ca. 5.3 $L/(L_{pbv}\cdot d)$ (GRT 4.5 h; Fig. 2a and 3a). This resulted in a MER of ca. 0.9 $L/(L_{pbv}\cdot d)$, while conversion rates for both H_2 and CO (Fig. 2b and 3b) were very high (>99 %). In both TBRs, PO_4^{3-} declined from 160 mg/L to 35–70 mg/L, whereas NH_4^+ remained stable at around 400 mg/L in TBR1 and slightly increased to 500–600 mg/L in TBR2 (Fig. 2c and 3c). The alkalinity declined from 4000 to 3000 mg $CaCO_3$/L, and the pH dropped from 8.5 to around 7.3 in both reactors (Fig. 2e and 3e). Furthermore, the concentration of SO_4^{2-} decreased from 385 to 90–95 mg/L (Fig. 2d and 3d), and H_2S in product gas declined below 10 ppm, indicating reduced bioavailability of sulfur in the form of sulfide (S^{2-}) in both reactors.

3.1.2. Trickle-bed reactor 1 – Digestate as nutrient medium

3.1.2.1. Hydraulic Retention Time 15 d. After the start-up phase, diluted digestate was added to TBR1 from day 62, at an HRT of 15 d, i.e., with the addition of 65–70 ml nutrient medium/d. The decreasing SO_4^{2-} concentration observed during the start-up phase was stabilized at ca. 100 mg/L, and the H_2S level in the product gas stabilized at ca. 5–10 ppm (Fig. 2d) during the continuous addition of digestate. The syngas load was increased stepwise between day 60 and day 100 (Fig. 2a) up to 19 $L/(L_{pbv}\cdot d)$ (GRT 1.25 h), while conversion rates for H_2 and CO were

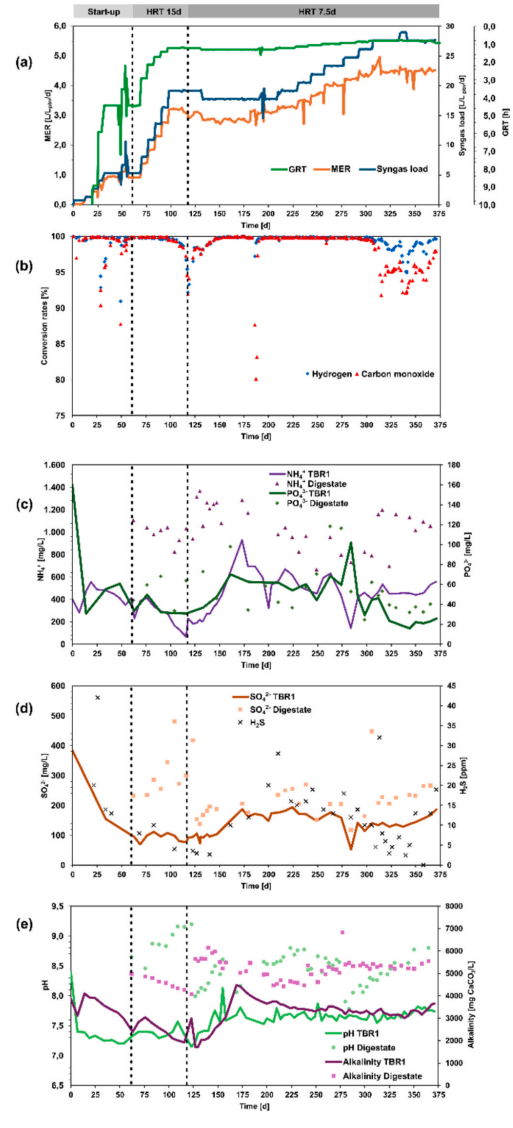

Fig. 2. TBR1: (a) Development of syngas load, gas retention time (GRT)* and Methane Evolution Rate (MER), (b) H_2 and CO conversion rates, (c) NH_4^+ and PO_4^{3-} levels of TBR liquid and digestate, (d) SO_4^{2-} levels of TBR liquid and digestate, and H_2S concentration in product gas, and (e) pH and alkalinity of TBR liquid and digestate. *TBR1 started with GRT of 35d which is beyond the scale.

kept close to 100 %. During periods of full conversion of H_2 and CO, the product gas of the TBR was comprised of 29 % CH_4 and 48 % CO2 with 22 % N_2 (Fig. S2b; SM). On day 100, MER was ca. 3.2 L/(L_{pbv}·d) (Fig. 2a). A slight drop in H_2 and CO conversion rates was detected from day 100. The conversion rates for H_2 and CO declined simultaneously (Fig. 2b) and in parallel with decreasing NH_4^+ levels from 230 mg/L on day 62 to 65 mg/L on day 116 (Fig. 2c). This was alongside a decrease in alkalinity to 1900 mg $CaCO_3$/L on day 116 with pH stability between 7.3–7.5. To overcome this negative trend, the addition of the nutrient medium was increased by 100 %, decreasing the HRT from 15 to 7.5 d on day 117.

3.1.2.2. Hydraulic Retention Time 7.5 d. The increased addition of the nutrient medium led to increasing concentrations of NH_4^+, SO_4^{2-} and PO_4^{3-} and the conversion rates of H_2 and CO increased from 92-95 % on day 117 to nearly full conversion around day 145 (Fig. 2b). The concentrations of NH_4^+ increased to > 900 mg/L on day 174 followed by a decrease, finally reaching a steady state between 400–600 mg/L until the end of the trial on day 371 (Fig. 2c). Furthermore, PO_4^{3-} concentrations rose from 35 to 70 mg/L on day 161, followed by a steady state until day 285 and a declining trend down to 15 mg/L on day 350, likely connected to increased syngas loads at this time. At HRT 7.5 d, stable alkalinity and SO_4^{2-} concentrations were observed, which were above 3000 mg $CaCO_3$/L and 150 mg/L, respectively. H_2S concentrations in the product gas were usually between 5 and 30 ppm (Fig. 2d), indicating sufficient S supply with the liquid medium.

On day 210, the strategy of stepwise increasing the syngas load was continued up to the maximum MER of 4.5 L/(L_{pbv}·d) on day 306 (Fig. 2a). The corresponding syngas load was 27–28 L/(L_{pbv}·d) (GRT 0.9 h) and both H_2 and CO were converted by > 99 %. With a further increase of syngas load, the conversion rates began to drop to 95–99 % and 95–97 % for H_2 and CO, respectively. During this time, the MER remained constant at approximately 4.5 L/(L_{pbv}·d). Thus, syngas load above 28 L/(L_{pbv}·d) (GRT 0.8 h) did not lead to higher MER, but rather to declining H_2 and CO conversion rates. In general, the potential contribution of CH_4 in the diluted digestate was assessed to be negligible. The maximum daily production based on the highest supply rate (HRT 7.5 d) and residual methane potential (20 ml/g VS) only resulted in ca. 2 mL CH_4/d when the daily CH_4 production was above 15 L/d.

3.1.3. Trickle-bed reactor 2 – Reject water as nutrient medium

3.1.3.1. Hydraulic Retention Time 15 d. The addition of reject water as nutrient medium (HRT 15 d) started simultaneously with the addition of digestate to TBR1 on day 62. Identically to TBR1, the syngas load was increased stepwise up to ca. 19–20 L/(L_{pbv}·d) (GRT 1.25 h) within this period (Fig. 3a), reaching a maximum MER of ca. 3.1 L/(L_{pbv}·d) on day 100 with conversion rates of 97 % and > 99 % for H_2 and CO, respectively. As for TBR1 and during periods of full conversion of H_2 and CO, the product gas of the TBR was comprised of 29 % CH_4 and 48 % CO2 with 22 % N_2 (Fig. S2c; SM). There was a clear decreasing trend in macronutrient concentrations, which negatively affected the H_2 and CO conversion rates. NH_4^+ concentration decreased from 500 to 90 mg/L, and PO_4^{3-} declined from 75 to 10 mg/L within this period (Fig. 3c). Besides the drop in alkalinity from 3000 to 1000 mg $CaCO_3$/L (Fig. 3e), a decline in H_2S in the product gas was observed. From day 100 onwards, no H_2S was detected in the product gas, while the H_2 conversion rate was reduced to ca. 86 %. In contrast to TBR1, CO conversion changed very little at that time, remaining stable above 98 % (Fig. 3b). The low concentration of macronutrients and, additionally, the absence of H_2S indicated the need for an increase in nutrient feeding (in line with TBR1). On day 109, the nutrient medium addition was doubled to ca. 133 mL/d, which reduced HRT from 15 d to 7.5 d.

3.1.3.2. Hydraulic Retention Time 7.5 d. The increased supply of nutrients at the beginning of this period did not have an immediate effect on the conversion of H_2 (low rates between 83–91 %) in comparison to TBR1. To restore the H_2 conversion rates and avoid VFA accumulation, the syngas load was stepwise reduced from 19.5 L/(L_{pbv}·d) on day 117 to 8 L/(L_{pbv}·d) (GRT 3 h) on day 130. This measure finally led to

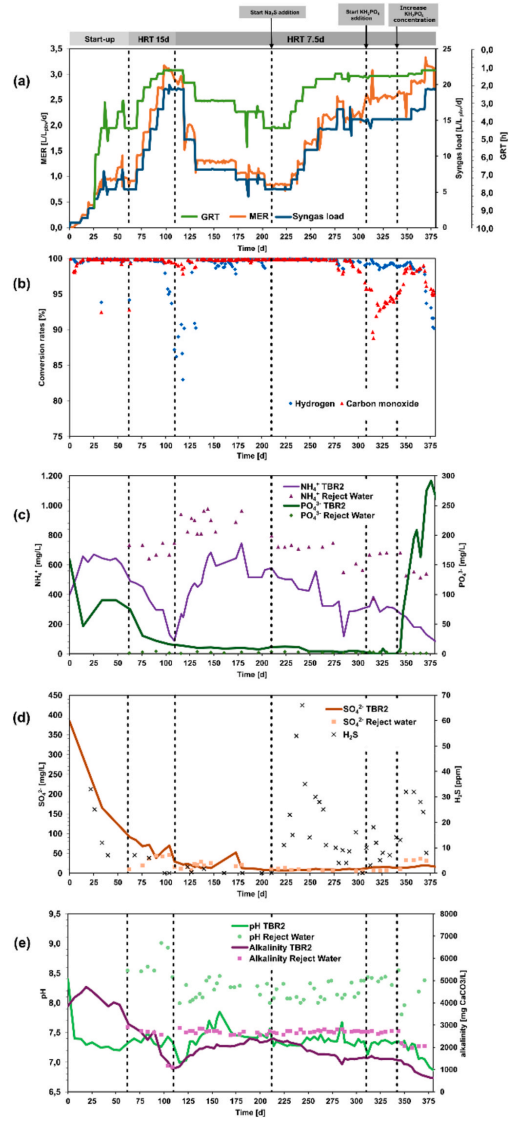

Fig. 3. TBR2: (a) Development of syngas load, gas retention time (GRT)* and Methane Evolution Rate (MER), (b) H_2 and CO conversion rates, (c) NH_4^+ and PO_4^{3-} levels of TBR liquid and reject water, (d) SO_4^{2-} levels of TBR liquid and reject water, and H_2S concentration in product gas, and (e) pH and alkalinity of TBR liquid and reject water *TBR2 started with GRT of 35d which is beyond the scale.

improved conversion rates of both H_2 and CO. Up to day 150 the concentration of NH_4^+ recovered and reached 600–700 mg/L (Fig. 3c). However, SO_4^{2-} and PO_4^{3-} remained at low levels despite the increased nutrient solution addition in this period, likely because the reject water itself was very low in SO_4^{2-} and PO_4^{3-} (Fig. 3c and 3d). From day 160 onwards, no H_2S was detected in the product gas and H_2 conversion rates dropped again, as seen earlier at HRT 15 d, leading to another decrease in syngas load to 6–7 L/(L_{pbv}·d) (GRT 3.6 h) with a corresponding maximum MER of 1.1 L/(L_{pbv}·d) from day 175 onwards (Fig. 3a). Based on the very low concentration of SO_4^{2-} and PO_4^{3-}, the decision to add supplemental nutrients in the next period was taken.

3.1.3.3. Hydraulic Retention Time 7.5 d with Na_2S addition. The addition of 20 ml Na_2S solution (1 g/L) per day started on day 209 to mitigate declining H_2 and CO conversion rates, and an immediate response by the system was observed. H_2S was detectable at levels of 10–30 ppm in the product gas, and the conversion rates of H_2 and CO were close to 100 %, allowing a stepwise increase of the syngas load. From day 250 onwards, the Na_2S addition was reduced to 10 mL/d because H_2S concentrations above 30 ppm in the product gas indicated overfeeding (Fig. 3d and Table 1). Between day 209 and day 308, NH_4^+ decreased from 580 to 300 mg/L, while the added reject water also had lower NH_4^+ levels (Fig. 3c). Syngas loads were increased up to 14–15 L/(L_{pbv}·d) (GRT 1.6 h) around day 300 (Fig. 3a). With this syngas load, the conversion rates began to drop slightly to 98 % and 96 % for H_2 and CO, respectively (Fig. 3b), and MER increased to around 2.5 L/(L_{pbv}·d) at the end of that period. Interestingly, the CO conversion was affected more than the H_2 conversion, which differed from the declining conversion rates observed between days 100 and 125, where only the H_2 conversion was affected. In comparison to TBR1, the MER and H_2 and CO conversion rates were lower, and the low PO_4^{3-} concentration (2–4 mg/L) in the liquid phase of TBR2 indicated that P could be a limiting factor.

3.1.3.4. Hydraulic Retention Time 7.5 d with Na_2S and KH_2PO_4 addition. On day 308, a daily addition of 10 ml KH_2PO_4 solution (0.8 g/L) started as a second supplement besides Na_2S. However, the concentration of PO_4^{3-} in TBR2 liquid did not increase and the CO conversion rates stayed low (88–94 %) (Fig. 3b). MERs did not exceed levels above 2.6 L/(L_{pbv}·d) (Fig. 3a). From day 341, the concentration of the KH_2PO_4 solution was increased ten-times (8 g/L) and PO_4^{3-} levels in the nutrient liquid raised from 0.5 to more than 250 mg/L at the end of the trial (day 381). Consequently, increasing CO conversion rates were observed, and syngas loads were increased above 16 L/(L_{pbv}·d) (GRT 1.5 h). At this load, MER was 2.9 L/(L_{pbv}·d) with still proper H_2 and CO conversion rates (>98 %) (Fig. 3a and 3b). Between day 341 and 381, the alkalinity declined from 1200 to 600 mg $CaCO_3$/L, pH decreased from 7.3 to 6.9 (Fig. 3e) and NH_4^+ decreased from 300 to 100 mg/L (Fig. 3c). A final approach in increasing syngas loads up to 19 L/(L_{pbv}·d) (GRT 1.2 h), was responded with decreasing conversion rates (90–95 %) of both H_2 and CO with a corresponding maximum MER of 3.1 L/(L_{pbv}·d) (Fig. 3a and b).

3.2. Effect of nutrient media on microbial community development

The analysis of the microbial community composition in the liquid phase and on the carriers showed that there were no obvious differences between TBR1 and TBR2, despite the differences in syngas load, H_2 and CO conversion rates, and MER. The communities in the liquid phase were slightly different in the early phase of operation, but over time each reactor gradually transformed towards similar compositions (Fig. 4). The difference between the starting communities and the final communities in each reactor are mostly explained by principal coordinate 1, which accounts for 62.5 % of the variation.

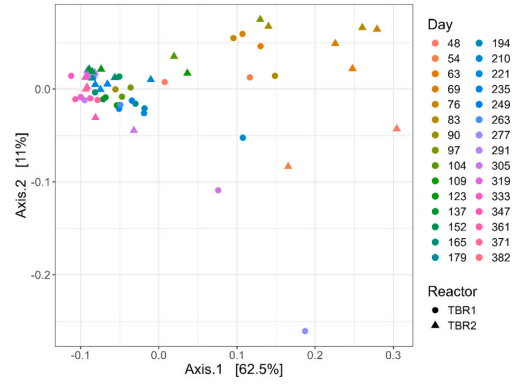

Fig. 4. Weighted principal coordinates analysis plot highlighting the microbial community development in the liquid phases of TBR1 (circles) and TBR2 (triangles) with colors indicating the sampling day.

3.2.1. Archaea

The methanogen belonging to *Methanothermobacter* was the primary methanogen in both TBR1 and TBR2 (Fig. 5). The NCBI BLAST result of the amplicon sequence variance (ASV) revealed the methanogen to be *Methanothermobacter marburgensis* with 100 % query coverage and 100 % identity. The relative abundance (RA) of this ASV gradually increased towards the end of the operation in both TBR1 and TBR2 (Fig. 5). In TBR1, the initial level was 17–39 %, while the RA was 69–92 % at the end of the operation (Tab. S3; SM). In TBR2, the corresponding values were 1–15 % and 78–84 %, respectively (Fig. 5, Tab. S3; SM). Alongside *Methanothermobacter* in TBR1, two additional methanogens, one belonging to *Methanobacterium* and one representing an unknown genus of *Methanobacteriales*, were present throughout the operation at comparably lower RA (1–5 %) (Fig. 5, Tab. S3; SM). The same methanogens were initially seen in TBR2 at similar RA (1–12 %) but disappeared (<1%) after 210 days of operation. The ASV for *Methanobacterium* was *Methanobacterium formicicum* at 100 % query coverage and 100 % identity. The ASV for *Methanobacteriales* was matched to three different species of *Methanothermobacter*, *M. marburgensis*, *M. thermautotrophicus*, and *M. defluvii*, all with 100 % query coverage and 98 % identity. The qPCR analysis of methanogens in the liquid phase revealed that the quantity of the methanogens was initially higher in TBR2 between days 83–123 (Fig. 5, SM). Over time, the abundance of the total methanogens equaled the same amount.

The methanogenic community on the carriers from each reactor, independent of their reactor position, reflected a similar composition to that of the liquid phase, with some minor differences (Fig. S4; SM). The methanogen ASVs on the carriers in TBR1 belonged to the dominating *Methanothermobacter* (5–83 %); *Methanobacterium* was also detected (1–2.8 %) (Fig. S4; SM). However, a small percentage of *Methanosarcina* (1–7 %) (Fig. S4; SM) was detected on the carriers. TBR2 primarily had *Methanothermobacter* (25–77 %) and *Methanobacterium* (1–9 %), the former being the dominant methanogen (Tab. S3; SM).

The qPCR analysis showed that the abundance of the total methanogens in the liquid fluctuated between $1.8x10^5$ to $5.8x10^5$ gene copies/L in TBR1 and $6.4x10^4$ to $1.2x10^6$ gene copies/L in TBR2. The abundance of the total methanogens near the end of the operation of both reactors was similar (Fig. S5; SM). There was a major increase of methanogens in TBR2 compared to TBR1 (Fig. S5; SM) within the operational period with HRT 15 d, when the syngas load was stepwise increased in TBR2 (Fig. 3a). Afterwards, when the syngas load was again decreased, the abundance dropped below that of TBR1 (Fig. S5; SM). Another dip in methanogenic abundance in TBR2 was seen around the

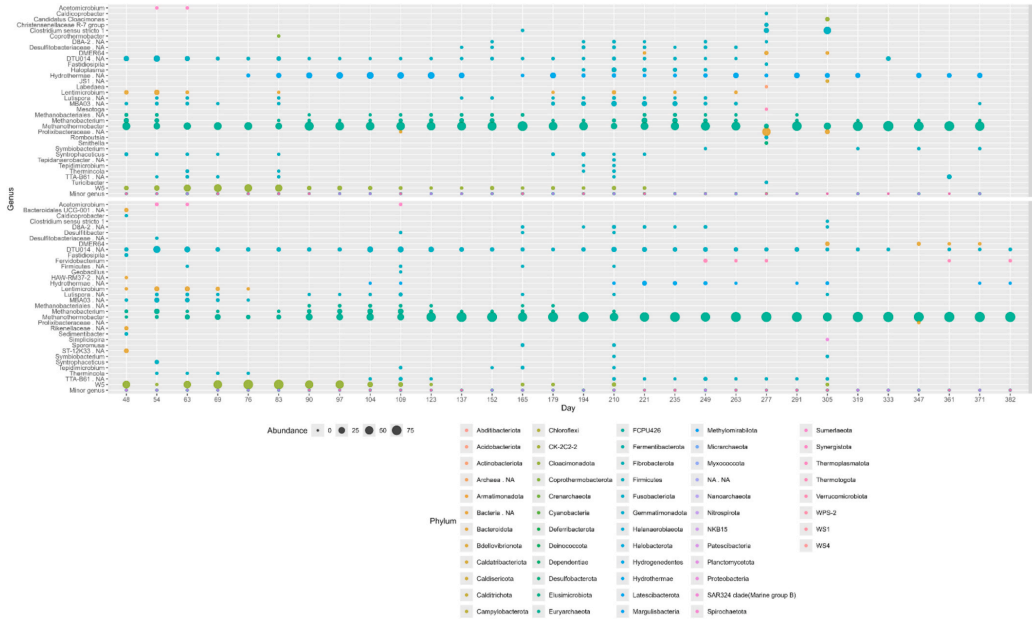

Fig. 5. Bubble plot of the relative abundance of the microbial community composition in the liquid phase of TBR1 (top plot) and TBR2 (bottom plot). The x-axis indicates the day of the sampling. The phylum level is depicted by the color of the bubbles and the genus is presented on the y-axis.

same time as the second decrease in the syngas load. However, the level increased to a similar level in TBR1 from day 250 after the addition of Na_2S into TBR2 on day 209.

3.2.2. Bacteria

The bacterial communities in the liquid phase of TBR1 and TBR2 also showed similar structures (Fig. 5). Both reactors showed a relatively high presence of an ASV belonging to the genus *W5* at the beginning of the operation, but this species gradually decreased over time. A similarly decreasing trend was seen for an ASV belonging to the order *DTU014*, but with some slight differences between the reactors at the end of the operation, with a higher RA in TBR2. This ASV was similar to an unidentified thermophilic *Eubacterium ST12* with 100 % query coverage and 97 % identity. A clear difference was seen between the reactors for an ASV belonging to the phylum *Hydrothermae*, which was recovered in TBR1 throughout many of the days of operation but only during a short period in TBR2. The BLAST result of this ASV revealed its closest relative to be *Thermotogales* sp. SRI-15 with 100 % query coverage and 96 % identity. Another ASV appeared mainly in TBR1 and shared 95 % identity in 100 % query coverage to *Syntrophaceticus schinkii*. An ASV belonging to *MBA03* was seen during the early phase of operation in both TBR1 and TBR2, whereafter it disappeared from TBR2 while fluctuating at low RA throughout the entire operation of TBR1.

In the carrier communities, the composition shared similarities to the liquid phase of the reactors. The abundance was slightly different between levels in the reactor, but with no consistency between reactors and sampling occasions. The carriers in TBR1 showed the presence of *DTU014* (2–10 %), *Hydrothermae* (1–40 %), *MBA03* (1–4 %), *Syntrophaceticus* (1–7 %), and *W5* (1–72 %) (Tab. S3 and Fig. S4; SM). On TBR2 carriers, similar groups of microbes were identified, including *DTU014* (1–9 %), *Hydrothermae* (2–10 %), *MBA03* (1 %), *Syntrophaceticus* (1 %), and *W5* (2–4 %). Additionally, an ASV belonging to the genus *Thermacetogenium* was recovered in TBR1 (6 %), which was BLASTed to be 99.2 % similar to Thermacetogenium phaeum over 100 % query coverage.

4. Discussion

4.1. The effect of nutrient media composition on syngas biomethanation

Among macronutrients, NH_4^+ is a crucial nutrient, especially for methanogens (protein synthesis, enzymatic activity), contributing to buffer capacity and maintaining a stable pH (Dupnock & Deshusses, 2019; Kamravamanesh et al., 2023). The reported minimum NH_4^+ levels vary for TBR biomethanation systems, ranging between 60 mg/L (Thema et al., 2021) and 1000 mg/L (Dupnock & Deshusses, 2019). For TBR1, utilizing digestate as the nutrient medium, low NH_4^+ concentrations of 65 mg/L were analyzed at the end of the operation period with HRT 15 d and were most likely responsible for declining H_2 and CO conversion rates (Fig. 2b). Due to increased nutrient medium addition (HRT 7.5 d), suggested NH_4^+ levels above 400 mg/L (Feickert Fenske et al., 2023a) were ensured to maintain high CH_4 productivity in combination with nearly complete conversion of H_2 and CO in TBR1.

For TBR2, a decline in NH_4^+ and SO_4^{2-} could be observed at HRT 15 d. Additionally, H_2S was no longer detected in the product gas towards the end of this period. Shortages of N and S were the most likely reasons for the observed decreasing conversion rates. From day 110 to 125, the H_2 conversion rate decreased to 82–95 %, while the CO conversion remained over 98 %. The lack of available S likely inhibited the hydrogenotrophic methanogens, causing an accumulation of H_2 in TBR2. During the same period, TBR1 showed a decrease in the conversion rate of both H_2 and CO to 92 % but only with a decreased concentration of NH_4^+. The increased inflow of reject water (HRT 7.5 d) had a positive impact on the NH_4^+ levels in the reactor liquid, which increased from day 109 onwards. The rising NH_4^+ concentration was also influenced by declining syngas loads, which were drastically reduced from 20 to 6 $L/(L_{pbv} \cdot d)$ (Fig. 3a) to maintain high H_2 and CO conversion

rates, resulting in lower microbial nutrient consumption. With increasing syngas loads starting around day 230, the trend in NH_4^+ concentration decreased again, maintaining lower concentrations (100–350 mg/L) after day 280. This indicates that the HRT should be further decreased to generally ensure NH_4^+ levels of around 400 mg/L.

Phosphorus is essential for methanogenesis (i.e., ATP synthesis via the acetyl-CoA pathway), ensuring an optimal C:N:P relation for methanogens of 100:3:1 (Gerardi, 2003) with the minimum concentration reported to be 1–2 mg/L (Gu et al., 2022). Severe inhibition of methanogenesis is documented at a PO_4^{3-} concentration above 2300 mg/L (Lackner et al., 2020). In TBR1, no PO_4^{3-} shortages were observed because its concentration varied between 20–100 mg/L throughout the entire operation. In TBR2, on the other hand, PO_4^{3-} was comparatively low, with concentrations below 10 mg/L from day 240 onwards and remaining at concentrations below 2 mg/L between days 312 and 343. A decrease in H_2 and CO conversion rate, starting on day 275, may be associated with limited PO_4^{3-} availability. The PO_4^{3-} concentration of the utilized reject water varied between 1–4 mg/L throughout the experiment (Fig. 3c), thus, likely not providing enough essential P. During the first phase of adding a KH_2PO_4 solution (0.8 g/L), the PO_4^{3-} levels in the TBR2 liquid did not change and remained below 1 mg/L. Still, the conversion rates of CO improved, suggesting a positive effect on PO_4^{3-} availability and microbial activity. However, after a ten-fold increase in the amount of PO_4^{3-} added to TBR2 from day 341 onwards, the PO_4^{3-} concentration in the reactor liquid increased rapidly within a short time. It can be assumed that this had an inhibitory effect on the H_2 and CO conversion performance in line with reports from Mancipe-Jiménez et al. (2017), who reported a sudden increase from 3.3 to 33 mg P/L (101.2 mg/L of PO_4^{3-}) in phosphorus concentration in anaerobic waste treatment. This imbalanced the equilibrium between bacteria and methanogens, causing a decrease in methanogenic activity. Concerning the present study, this explains why TBR2 did not achieve the same performance as TBR1 despite S and P supplementation. Additionally, the observed decline in H_2 and CO conversion rates from day 368 to 381 can be directly linked to an increased syngas load (16.5 to 19 $L/(L_{pbv}\cdot d)$). Nevertheless, in future P-optimizing studies of biomethanation, the application of supplementary P should be applied carefully. However, based on our results, the PO_4^{3-} concentration in the TBR liquid should be above 20 mg/L to maintain high conversion of H_2 and CO.

The addition of Na_2S to TBR2 raised the availability of S_2 in the reactor and, thus, hydrogenotrophic methanogens were able to metabolize H_2 and CO_2 to a higher degree, which was in line with several previous studies (Rachbauer et al., 2016; Strübing et al., 2017; Asimakopoulos et al., 2019; Dupnock & Deshusses, 2019; Thema et al., 2021). S^{2-} is essential for methanogens, more specifically for the biosynthesis of coenzymes involved in the final step of methanogenesis (methyl-CoM reductase) and for the biosynthesis of Fe-S clusters, which are found in other enzymes involved in H_2 oxidation/ CO_2 reduction and electron transport. Under S^{2-} shortages, the biomethanation performance is inhibited (Thema et al., 2021) but can recover quickly when the S_2 concentration is above 0.02 mM (6.4 mg/L) (Strübing et al., 2017). However, when S^{2-} is in excess, it can precipitate trace elements (i.e. Fe, Ni and Co), which are essential for many enzymes and for microbial activity. Therefore, the addition of Na_2S should be used with caution to circumvent process failure. It can be recommended to follow the H_2S concentration in the product gas maintaining levels between 5–30 ppm.

In contrast to the present study, Kamravamanesh et al. (2023) did not see macronutrient limitation for the reject water per se, but still proposed the addition of trace elements to maintain high H_2 conversion rates. The addition of trace elements was shown to improve H_2 and CO conversion and CH_4 productivity when using digestate as a nutrient medium (Goonesekera et al., 2024). However, information about minimum concentrations of trace elements is scarce and varies among the available literature. Iron is of great importance for methanogens, and sufficient Fe levels are reported to be above 1.5 or 2 mg/L in the nutrient liquid (Dupnock & Deshusses, 2019; Ashraf et al., 2021). In the present study, the Fe concentration of the diluted digestate was 14 mg/L (Tab. S1; SM), indicating a sufficient supply of this specific element, whereas in reject water, only 4 mg/L were analysed, which may be a limiting factor. However, for other important trace elements such as Co, Mo, Ni, and Zn, the concentrations in the digestate were considerably higher compared to the reject water (Tab. S1; SM), making it a potent alternative to defined nutrient media. Still, it is unclear to what extent those elements are present in a bioavailable form to be metabolized by the microbial community. For future research, micronutrients should be considered as an important threshold for continuous syngas biomethanation systems.

4.2. The performance of hydrogen and carbon monoxide conversion and methane production using trickle-bed reactors

Studies of biomethanation using only H_2 and CO_2 have achieved MERs between 1 and 15 $L/(L_{pbv}\cdot d)$, depending on several operational parameters, such as temperature, H_2:CO_2 ratio, and applied pressure (Burkhardt & Busch, 2013; Strübing et al., 2017; Porte et al., 2019; Feickert Fenske et al., 2023a). However, MERs for syngas biomethanation are expected to be lower for stochiometric reasons, as the presence of CO potentially limits the production of CH_4 (Sancho Navarro et al., 2016). In the present study, TBR1 showed a maximum MER of 4.5 $L/(L_{pbv}\cdot d)$, maintaining H_2 and CO conversion rates above 95 % during long-term (ca. one year) experimentation. To the best knowledge of the authors, there are currently only two studies of syngas biomethanation using TBR that show higher MERs. Asimakopoulos et al. (2021) operated a 5 L TBR under thermophilic conditions with a defined basal nutrient medium (HRT 8 d) and achieved a MER of up to 9.5 $L/(L_{pbv}\cdot d)$ with conversion rates of 97 % and 76 % for H_2 and CO, respectively. Goonesekera et al. (2024) documented a maximum MER of 5.3 $L/(L_{pbv}\cdot d)$ using digestate (HRT 20 d) with supplementary trace elements using a thermophilic 1 L TBR and achieving "full H_2 and CO conversion". Without the addition of trace elements, the latter study achieved slightly lower MERs (4.3 $L/(L_{pbv}\cdot d)$) compared to the present study, maintaining lower conversion rates for H_2 (<90 %) and CO (<80 %). Furthermore, Asimakopoulos et al. (2021) and Goonesekera et al. (2024) used a syngas composition with higher H_2 shares (45 and 65 %, respectively) and lower shares of CO (20 and 17 %, respectively) and CO_2 (25 and 13 %, respectively) in comparison to the present study (40 % H_2, 30 % CO, 20 % CO_2 and 10 % N_2). Additionally, other than using a defined basal medium as the nutrient source, Asimakopoulos et al. (2021) applied a pH control, and the liquid recirculation was continuous. Another major difference from the present study was the choice of carrier material. The specific surface of the carriers within our study was 500 m^2/m^3, which was identical to the one in Goonesekera et al. (2024), whereas Asimakopoulos et al. (2021) used a packing material with 800 m^2/m^3.

Regarding studies using digestate as a nutrient medium without supplementary nutrient addition, Andreides et al. (2022b) documented a MER of 2.1 $L/(L_{pbv}\cdot d)$ using a 1 L TBR under thermophilic conditions when investigating the influence of temperature for syngas biomethanation at an HRT of 6 d. With only CO as the sole carbon source, Ali et al. (2024) achieved a MER of 0.99 $L/(L_{pbv}\cdot d)$, continuously utilising digestate within a 0.7 L TBR.

In TBR1, from day 300 onwards, the conversion rates for H_2 and CO decreased to 95–99 % and 92–97 %, respectively. This was likely caused by reaching the maximum syngas load capacity during prevailing conditions. Limiting factors concerning macronutrient levels could not be determined because no shortages in the trickling liquid or lack of sulfur (i.e., H_2S in the product gas) were observed at that time. The decline in conversion rates was most likely connected to low gas retention times in the reactor caused by gas–liquid mass transfer limitations (Asimakopoulos et al., 2019; Dupnock & Deshusses, 2019; Jensen et al., 2021). At syngas loads of 27–30 $L/(L_{pbv}\cdot d)$, the gaseous retention time in the TBR was between 0.8 to 0.9 h, and in combination with the specific area of the chosen carriers, it might have limited the gas–liquid mass

transfer. Consequently, higher syngas loads at the end of this final period did not result in higher CH_4 productivity but only in lower H_2 and CO conversion rates. Still, the addition of trace elements as done by Goonesekera et al. (2024), seems to be a reasonable option to further increase MERs while maintaining high conversion rates for digestate-driven syngas biomethanation systems.

In comparison to TBR1, the assessment of reject water as a nutrient medium in TBR2 was characterized by lower MERs during periods of sole reject water feeding (maximum MER up to 1 L/(L_{pbv}·d)). This aligns with previous findings of Cheng et al. (2022), achieving a MER of 1 L/(L_{pbv}·d) during continuous syngas biomethanation in a mesophilic 35 L TBR. Under thermophilic conditions with H_2 and CO_2 as the only gaseous substrate, another study observed MERs of up to 2.6 L/(L_{pbv}·d) using trace element-modified reject water as a nutrient medium in an 8.3 L TBR (Kamravamanesh et al., 2023). In the present study, a higher MER of 3.1 L/(L_{pbv}·d) and H_2 and CO conversion rates above 91 % were achieved for reject water with supplements for S and P. To our knowledge, this is the highest MER observed for biomethanation using reject water as a nutrient medium. However, to reach even higher MER while maintaining H_2 and CO conversion rates in the same order of magnitude as digestate, additional supplements such as trace elements will be required, as shown in Kamravamanesh et al. (2023).

4.3. Microbial community development

The syngas biomethanation process relies on a mixed microbial consortium involving both bacteria and archaea. Key groups in the process include hydrogenotrophic and acetoclastic methanogens, acetogens, and SAOBs, which were all found in the present study. Interestingly, even though the reactors showed differences in performance depending on the nutrient source, no major differences were seen in the community structure or methanogenic abundance in the liquid phase (Fig. 5) or on the carriers (Fig. S4; SM), suggesting that the difference in MER between TBR1 and TBR2 was mainly related to the activity of the communities and not to the community members per se.

In line with other studies on thermophilic syngas biomethanation, CH_4 was mostly produced by hydrogenotrophic methanogens (Asimakopoulos et al., 2019; Goonesekera et al., 2024). *Methanothermobacter* was the dominant methanogen, followed by *Methanobacterium* in both the liquid phases and on the carriers, and both groups have been seen to dominate the archaeal community in biomethanation systems with both H_2/CO_2 and syngas (Grimalt-Alemany et al., 2019; Goonesekera et al., 2024). The *Methanothermobacter* ASV was closely identified as *M. marburgensis*, which has been shown to effectively utilize both syngas and even to grow on CO as the sole substrate (Diender et al., 2016). While *M. thermautotrophicus* is typically the dominant methanogen in thermophilic biomethanation processes, its CO consumption can be limited at higher concentrations of CO, particularly without a carboxydotrophic partner, such as *Carboxydothermus hydrogenoformans* (Diender et al., 2016). However, while *M. marburgensis* prefers to use H_2/CO_2, this methanogen exhibits better CO utilization compared to *M. thermautotrophicus* (Diender et al., 2016), which likely explains its dominance in the presently investigated reactors.

Both reactors showed low levels of acetate or other VFAs during the whole period of operation (Fig. 2a, SM), suggesting that acetate was efficiently consumed. Acetate can be produced both by the conversion of CO or of H_2 and CO_2 via homoacetogenesis, which has been shown to be competitive with methanogenesis under some conditions, such as high gas load (Liu et al., 2016). Acetogens are also typically more tolerant to CO compared to methanogens, even those using CO (Alves et al., 2013). In addition, acetate can also be produced by fermenting bacteria growing on decaying biomass, as shown in several studies on biomethanation (Grimalt-Alemany et al., 2019; Laguillaumie et al., 2022). In the present study, only one known acetogen, genus *Sporomusa*, occasionally appeared in the liquid phase of both reactors, and no obvious acetogens were found on the carriers. However, several known heterotrophic acetate-producing microbial groups, such as *Acetomicrobium, Coprothermobacter,* and *Lentimicrobium*, were present in low abundance. These genera have been found before in syngas-fed processes (Luo et al., 2013; Li et al., 2021; Laguillaumie et al., 2022; Ali et al., 2024). Another potential acetate producer was represented by the ASV belonging to the candidatus phylum Hydrothermae, present only in TBR1 in both the liquid and on the carriers. This ASV is most closely identified with *Thermotogales* sp. *SRI-15*, which belongs to the order *Thermotogales*, is known to include thermophilic fermenting members producing acetate, CO_2, and H_2 (Reysenbach et al., 2001). Both reactors also initially showed a high abundance of an ASV belonging to *W5* (family *Cloacimonadaceae*), suggested to be a syntrophic propionate degrader producing acetate and H_2 as end products (Dyksma & Gallert, 2019). Interestingly, while acetate was likely formed, no acetate-consuming methanogens were identified in the liquid. However, *Methanosarcina* sp. was identified on the carriers in TBR1 but in lower relative abundance compared to *Methanothermobacter* sp. Species within *Methanosarcina* can use acetate, but some can also use H_2/CO_2 and CO (Rother et al., 2007; Luo et al., 2013), and thus their presence is not solely associated with acetate. In line with this, a previous study showed *Methanosarcina barkeri,* combined with *Methanothermobacter thermautotrophicus,* to be involved in CO biomethanation in a thermophilic CSTR reactor (Luo et al., 2013). Representatives in the genus *Methanosarcina* have been found before in both mesophilic and thermophilic syngas biomethanation processes (Aryal et al., 2021; Goonesekera et al., 2024). Acetate can also be consumed, in addition to methanogens, by syntrophic acetate-oxidizing bacteria (SAOB). In the present study, an ASV was closely related to a known SAOB (*S. schinkii*). This ASV was found in the liquid in both reactors, with higher abundances in TBR1. This SAOB has been observed previously in thermophilic biogas processes (Singh et al., 2023) and is suggested to play a key role in reaching efficient syngas conversion combined with *Methanothermobacter* (Ali et al., 2024). In addition, the carriers in TBR 1 indicated the presence of an ASV belonging to *Thermacetogenium*, matched to *Thermacetogenium phaeum*, known to convert acetate when partnered with hydrogenotrophic methanogens like *M. thermautotrophicus* (Hattori et al., 2005). However, *T. phaeum* can also take the role of an acetogen, converting H_2/CO_2 into acetate. Thus, its role in the present TBR reactors cannot be completely clarified. Moreover, two potential SAOBs were also present in both reactors, *DTU014* (Dyksma et al., 2020; Kamravamanesh et al., 2023) and family *MBA03* (Kamravamanesh et al., 2023), in both the liquid and carriers.

The finding of genus *Methanosarcina* only on the carriers was in line with a recent study by Goonesekera et al. (2024), who found this methanogen mainly present on carriers at the bottom of the TBR. The authors proposed a spatial specialisation in the carrier biofilm, with hydrogenotrophic methanogens in the top and acetate utilizers, methanogens, and SAOB at the bottom. Such spatial separation could not be determined in the present paper. Here, *Methanosarcina* was instead detected in the middle and at the top of the reactor, and SAOB and hydrogenotrophic methanogens were found at all levels. It is possible that these differences could be related to the counter-current operation of the TBRs in the present study, while the previous study by Goonesekera et al. (2024) used a co-current operation. However, to address differences and spatial distribution, more samples would be required. In the present study, the number of sampling occasions was limited, as removing carriers was challenging, and each sampling led to the introduction of oxygen and a reduction of syngas conversion.

4.4. Perspectives on syngas biomethanation

Considering the implementation of TBR syngas biomethanation on a production scale, there would be a synergy between establishing gasification of forest residues integrated with biogas plants, where digested residues can be utilized as nutrient media for TBRs. Furthermore, the combination of conventional biogas and biomethanised syngas will

increase the total gas flow, which can lead to a more cost-effective upgrading process to biomethane. The increased gas flow will further potentially facilitate the conversion to liquified biomethane. Digestates originating from well-functioning digestion processes likely contain all essential nutrients, as both AD and biomethanation are closely related microbial processes. Still, digestates likely must be processed (phase separation, dilution) before their utilisation as nutrient media. Reject water from dewatered digested sewage sludge shows lower concentrations of essential nutrients in general due to, for example, the use of polymers during dewatering. However, if a co-digestion plant and a WWTP are located close to each other, the option of using reject water for dilution of digestate instead of fresh water might be an option, as reject water generally contains relatively high concentrations of ammonium. This could facilitate the optimization of *N*-supply, reducing the nutrient addition rate needed and increasing process stability.

To further increase the MER with high syngas conversion using digestate as a nutrient source, further process parameters should be studied and optimized, including trace element supply, conditioning before use, carrier characteristics (e.g., liquid hold-up capacity), and liquid recirculation regimes.

5. Conclusions

Biomethanation of syngas was studied over a year in two identical trickle-bed reactors (TBRs) using diluted manure-based digestate and reject water from digested sewage sludge as non-defined nutrient sources, respectively. A maximum methane evolution rate (MER) of 4.5 $L/(L_{pbv}\cdot d)$ was achieved with digestate, maintaining H_2 and CO conversion rates above 95 %. In contrast, the specific reject water used in this study, characterized by low concentrations of phosphate and sulfate, resulted in only 1 $L/(L_{pbv}\cdot d)$, but supplementation with sulfur and phosphorus improved stability and conversion, reaching 3.1 $L/(L_{pbv}\cdot d)$ with H_2 and CO conversion over 91 %. These findings highlight the importance of key macronutrient availability for efficient syngas biomethanation, though further enhancement may require trace element supplementation. However, as digestate and reject water compositions might vary due to its origin and processing, these results should not be generalized beyond the specific nutrient media used in this study. Despite nutrient source differences, microbial community structures were similar in both reactors, with only minor variations due to the nutrient media. Methanogen abundance remained constant, suggesting MER differences were due to activity rather than community composition. The syngas-converting community was dominated by *Methanothermobacter* and included syntrophic acetate-oxidizing bacteria like *Syntrophaceticus* and *Thermacetogenium*.

CRediT authorship contribution statement

Florian Gabler: Writing – original draft, Visualization, Formal analysis, Data curation, Conceptualization. **George Cheng:** Writing – review & editing, Visualization, Formal analysis, Data curation. **Leticia Pizzul:** Writing – review & editing, Supervision, Funding acquisition, Conceptualization. **Anna Schnürer:** Writing – review & editing, Supervision, Funding acquisition, Conceptualization. **Åke Nordberg:** Writing – review & editing, Supervision, Funding acquisition, Conceptualization.

Declaration of competing interest

The authors declare that they have no known competing financial interests or personal relationships that could have appeared to influence the work reported in this paper.

Acknowledgments

This project was funded by the Swedish Energy Agency [149656-1] and Formas (2018-01341). The authors acknowledge Vasiliki Tsamadou for assistance with DNA extraction.

Appendix A. Supplementary data

Supplementary data to this article can be found online at https://doi.org/10.1016/j.biortech.2025.132893.

Data availability

The sequencing data generated and analyzed in this study are available in the NCBI repository under BioProject accession number PRJNA1268893.

References

Ali, R., Samadi, H., Yde, L., Ashraf, M.T., 2024. Carbon monoxide conversion by anaerobic microbiome in a thermophilic trickle bed reactor. Biochem. Eng. J. 212. https://doi.org/10.1016/j.bej.2024.109492.

Alves, J.I., Stams, A.J.M., Plugge, C.M., Madalena Alves, M., Sousa, D.Z., 2013. Enrichment of anaerobic syngas-converting bacteria from thermophilic bioreactor sludge. FEMS Microbiol. Ecol. 86 (3), 590–597. https://doi.org/10.1111/1574-6941.12185.

Andreides, D., Fliegerova, K.O., Pokorna, D., Zabranska, J., 2022a. Biological conversion of carbon monoxide and hydrogen by anaerobic culture: Prospect of anaerobic digestion and thermochemical processes combination. Biotechnol. Adv. 58, 107886. https://doi.org/10.1016/j.biotechadv.2021.107886.

Andreides, D., Lopez Marin, M.A., Zabranska, J., 2024. Selective syngas fermentation to acetate under acidic and psychrophilic conditions using mixed anaerobic culture. Bioresour. Technol. 394, 130235. https://doi.org/10.1016/j.biortech.2023.130235.

Andreides, D., Stransky, D., Bartackova, J., Pokorna, D., Zabranska, J., 2022b. Syngas biomethanation in countercurrent flow trickle-bed reactor operated under different temperature conditions. Renew. Energy 199, 1329–1335. https://doi.org/10.1016/j.renene.2022.09.072.

Aryal, N., Odde, M., Petersen, C.B., Ottosen, L.D.M. & Kofoed, M.V.W. (2021). Methane production from syngas using a trickle-bed reactor setup. *Bioresource Technology,* 333. https://doi.org/ARTN 12518310.1016/j.biortech.2021.125183.

Ashraf, M.T., Yde, L., Triolo, J.M., Wenzel, H., 2021. Optimizing the dosing and trickling of nutrient media for thermophilic biomethanation in a biotrickling filter. Biochem. Eng. J. 176. https://doi.org/10.1016/j.bej.2021.108220.

Asimakopoulos, K., Gavala, H.N., Skiadas, I.V., 2019. Biomethanation of Syngas by Enriched mixed Anaerobic Consortia in Trickle Bed Reactors. Waste Biomass Valoriz. 11 (2), 495–512. https://doi.org/10.1007/s12649-019-00649-2.

Asimakopoulos, K., Kaufmann-Elfang, M., Lundholm-Hoffner, C., Rasmussen, N.B.K., Grimalt-Alemany, A., Gavala, H.N., Skiadas, I.V., 2021. Scale up study of a thermophilic trickle bed reactor performing syngas biomethanation. Appl. Energy 290. https://doi.org/10.1016/j.apenergy.2021.116771.

Burkhardt, M., Busch, G., 2013. Methanation of hydrogen and carbon dioxide. Appl. Energy 111, 74–79. https://doi.org/10.1016/j.apenergy.2013.04.080.

Burkhardt, M., Koschack, T., Busch, G., 2015. Biocatalytic methanation of hydrogen and carbon dioxide in an anaerobic three-phase system. Bioresour. Technol. 178, 330–333. https://doi.org/10.1016/j.biortech.2014.08.023.

Cheng, G., Gabler, F., Pizzul, L., Olsson, H., Nordberg, A., Schnurer, A., 2022. Microbial community development during syngas methanation in a trickle bed reactor with various nutrient sources. Appl. Microbiol. Biotechnol. 106 (13–16), 5317–5333. https://doi.org/10.1007/s00253-022-12035-5.

Cisek, A.A., Bak, I., Stefanska, I., Binek, M., 2022. Selection and optimization of high-yielding DNA isolation protocol for quantitative analyses of methanogenic archaea. Microorganisms 10 (3). https://doi.org/10.3390/microorganisms10030523.

Diender, M., Pereira, R., Wessels, H.J., Stams, A.J., Sousa, D.Z., 2016. Proteomic Analysis of the Hydrogen and Carbon Monoxide Metabolism of Methanothermobacter marburgensis. Front. Microbiol. 7, 1049. https://doi.org/10.3389/fmicb.2016.01049.

Dupnock, T.L., Deshusses, M.A., 2019. Detailed investigations of dissolved hydrogen and hydrogen mass transfer in a biotrickling filter for upgrading biogas. Bioresour. Technol. 290, 121780. https://doi.org/10.1016/j.biortech.2019.121780.

Dyksma, S., Gallert, C., 2019. Candidatus Syntrophosphaera thermopropionivorans: a novel player in syntrophic propionate oxidation during anaerobic digestion. Environ. Microbiol. Rep. 11 (4), 558–570. https://doi.org/10.1111/1758-2229.12759.

Dyksma, S., Jansen, L., Gallert, C., 2020. Syntrophic acetate oxidation replaces acetoclastic methanogenesis during thermophilic digestion of biowaste. Microbiome 8 (1), 105. https://doi.org/10.1186/s40168-020-00862-5.

Feickert Fenske, C., Kirzeder, F., Strubing, D., Koch, K., 2023a. Biogas upgrading in a pilot-scale trickle bed reactor - long-term biological methanation under real application conditions. Bioresour. Technol. 376, 128868. https://doi.org/10.1016/j.biortech.2023.128868.

Feickert Fenske, C., Strubing, D., Koch, K., 2023b. Biological methanation in trickle bed reactors - a critical review. Bioresour. Technol. 385, 129383. https://doi.org/10.1016/j.biortech.2023.129383.

Figueras, J., Benbelkacem, H., Dumas, C., Buffiere, P., 2021. Biomethanation of syngas by enriched mixed anaerobic consortium in pressurized agitated column. Bioresour. Technol. 338, 125548. https://doi.org/10.1016/j.biortech.2021.125548.

Gerardi, M.H. (2003). *The Microbiology of Anaerobic Digesters*. Wiley. https://books.google.se/books?id=QzzENAEACAAJ.

Goonesekera, E.M., Grimalt-Alemany, A., Thanasoula, E., Yousif, H.F., Krarup, S.L., Valerin, M.C., Angelidaki, I., 2024. Biofilm mass transfer and thermodynamic constraints shape biofilm in trickle bed reactor syngas biomethanation. Chem. Eng. J. 500. https://doi.org/10.1016/j.cej.2024.156629.

Grimalt-Alemany, A., Łężyk, M., Kennes-Veiga, D.M., Skiadas, I.V., Gavala, H.N., 2019. Enrichment of Mesophilic and Thermophilic mixed Microbial Consortia for Syngas Biomethanation: the Role of Kinetic and Thermodynamic Competition. Waste Biomass Valoriz. 11 (2), 465–481. https://doi.org/10.1007/s12649-019-00595-z.

Grimalt-Alemany, A., Skiadas, I.V., Gavala, H.N., 2017. Syngas biomethanation: state-of-the-art review and perspectives. Biofuels Bioprod. Biorefin. 12 (1), 139–158. https://doi.org/10.1002/bbb.1826.

Gu, W., Muller, A.L., Deutzmann, J.S., Williamson, J.R., Spormann, A.M., 2022. Growth rate-dependent coordination of catabolism and anabolism in the archaeon Methanococcus maripaludis under phosphate limitation. ISME J. 16 (10), 2313–2319. https://doi.org/10.1038/s41396-022-01278-9.

Hattori, S., Galushko, A.S., Kamagata, Y., Schink, B., 2005. Operation of the CO dehydrogenase/acetyl coenzyme a pathway in both acetate oxidation and acetate formation by the syntrophically acetate-oxidizing bacterium Thermacetogenium phaeum. J. Bacteriol. 187 (10), 3471–3476. https://doi.org/10.1128/JB.187.10.3471-3476.2005.

Jensen, M.B., Poulsen, S., Jensen, B., Feilberg, A., Kofoed, M.V.W., 2021. Selecting carrier material for efficient biomethanation of industrial biogas-CO2 in a trickle-bed reactor. J. CO2 Util. 51, 101611. https://doi.org/10.1016/j.jcou.2021.101611.

Kamravamanesh, D., Rinta Kanto, J.M., Ali-Loytty, H., Myllärinen, A., Saalasti, M., Rintala, J., Kokko, M., 2023. Ex-situ biological hydrogen methanation in trickle bed reactors: Integration into biogas production facilities. Chem. Eng. Sci. 269. https://doi.org/10.1016/j.ces.2023.118498.

Lackner, N., Wagner, A.O., Markt, R., Illmer, P., 2020. pH and Phosphate induced shifts in carbon flow and microbial community during thermophilic anaerobic digestion. Microorganisms 8 (2). https://doi.org/10.3390/microorganisms8020286.

Laguillaumie, L., Rafrafi, Y., Moya-Leclair, E., Delagnes, D., Dubos, S., Sperandio, M., Paul, E., Dumas, C., 2022. Stability of ex situ biological methanation of H2/CO2 with a mixed microbial culture in a pilot scale bubble column reactor. Bioresour. Technol. 354, 127180. https://doi.org/10.1016/j.biortech.2022.127180.

Larsson, A., Gunnarsson, I. & tengberg, F. (2019). *The GoBiGas Project - Demonstration of the production of Biomethane from Biomas via Gasification*. AB, G.E.

Li, C., Zhu, X., Angelidaki, I., 2021. Syngas biomethanation: effect of biomass-gas ratio, syngas composition and pH buffer. Bioresour. Technol. 342, 125997. https://doi.org/10.1016/j.biortech.2021.125997.

Liu, R., Hao, X., Wei, J., 2016. Function of homoacetogenesis on the heterotrophic methane production with exogenous H2/CO2 involved. Chem. Eng. J. 284, 1196–1203. https://doi.org/10.1016/j.cej.2015.09.081.

Lozupone, C., Knight, R., 2005. UniFrac: a new phylogenetic method for comparing microbial communities. Appl. Environ. Microbiol. 71 (12), 8228–8235. https://doi.org/10.1128/AEM.71.12.8228-8235.2005.

Luo, G., Wang, W., Angelidaki, I., 2013. Anaerobic digestion for simultaneous sewage sludge treatment and CO biomethanation: process performance and microbial ecology. Environ. Sci. Technol. 47 (18), 10685–10693. https://doi.org/10.1021/es401018d.

Mancipe-Jiménez, D.C., Costa, C., Márquez, M.C., 2017. Methanogenesis inhibition by phosphorus in anaerobic liquid waste treatment. Waste Treat. Recovery 2 (1), 1–8. https://doi.org/10.1515/lwr-2017-0001.

McMurdie, P.J., Holmes, S., 2013. phyloseq: an R Package for Reproducible Interactive Analysis and Graphics of Microbiome Census Data. PLoS One 8 (4), e61217. https://doi.org/10.1371/journal.pone.0061217.

Porte, H., Kougias, P.G., Alfaro, N., Treu, L., Campanaro, S., Angelidaki, I., 2019. Process performance and microbial community structure in thermophilic trickling biofilter reactors for biogas upgrading. Sci. Total Environ. 655, 529–538. https://doi.org/10.1016/j.scitotenv.2018.11.289.

Rachbauer, L., Voitl, G., Bochmann, G., Fuchs, W., 2016. Biological biogas upgrading capacity of a hydrogenotrophic community in a trickle-bed reactor. Appl. Energy 180, 483–490. https://doi.org/10.1016/j.apenergy.2016.07.109.

Ren, J., Liu, Y.-L., Zhao, X.-Y., Cao, J.-P., 2020. Methanation of syngas from biomass gasification: an overview. Int. J. Hydrogen Energy 45 (7), 4223–4243. https://doi.org/10.1016/j.ijhydene.2019.12.023.

Reysenbach, A.-L., Huber, R., Stetter, K.O., Davey, M.E., MacGregor, B.J. & Stahl, D.A. (2001). Phylum BII. Thermotogae phy. nov. In: Boone, D.R., Castenholz, R.W. & Garrity, G.M. (eds) *Bergey's Manual® of Systematic Bacteriology: Volume One : The Archaea and the Deeply Branching and Phototrophic Bacteria*. New York, NY: Springer New York. 369-387. https://doi.org/10.1007/978-0-387-21609-6_19.

Rother, M., Oelgeschlager, E., Metcalf, W.M., 2007. Genetic and proteomic analyses of CO utilization by Methanosarcina acetivorans. Arch. Microbiol. 188 (5), 463–472. https://doi.org/10.1007/s00203-007-0266-1.

Sancho Navarro, S., Cimpoia, R., Bruant, G., Guiot, S.R., 2016. Biomethanation of Syngas using Anaerobic Sludge: Shift in the Catabolic Routes with the CO Partial pressure increase. Front. Microbiol. 7, 1188. https://doi.org/10.3389/fmicb.2016.01188.

Sieborg, M.U., Jensen, M.B., Jensen, B., Kofoed, M.V.W., 2021. Effect of minimizing carrier irrigation on H2 conversion in trickle bed reactors during ex situ biomethanation. Bioresour. Technol. Rep. 16. https://doi.org/10.1016/j.biteb.2021.100876.

Singh, A., Schnurer, A., Dolfing, J., Westerholm, M., 2023. Syntrophic entanglements for propionate and acetate oxidation under thermophilic and high-ammonia conditions. ISME J. 17 (11), 1966–1978. https://doi.org/10.1038/s41396-023-01504-y.

Sipma, J., Lens, P.N.L., Stams, A.J.M., Lettinga, G., 2003. Carbon monoxide conversion by anaerobic bioreactor sludges. FEMS Microbiol. Ecol. 44 (2), 271–277. https://doi.org/10.1016/S0168-6496(03)00033-3.

Steinberg, L.M., Regan, J.M., 2008. Phylogenetic comparison of the methanogenic communities from an acidic, oligotrophic fen and an anaerobic digester treating municipal wastewater sludge. Appl. Environ. Microbiol. 74 (21), 6663–6671. https://doi.org/10.1128/AEM.00553-08.

Strübing, D., Huber, B., Lebuhn, M., Drewes, J.E., Koch, K., 2017. High performance biological methanation in a thermophilic anaerobic trickle bed reactor. Bioresource Technology 245 (Pt A), 1176–1183. https://doi.org/10.1016/j.biortech.2017.08.088.

Thema, M., Weidlich, T., Kaul, A., Bollmann, A., Huber, H., Bellack, A., Karl, J., Sterner, M., 2021. Optimized biological CO2-methanation with a pure culture of thermophilic methanogenic archaea in a trickle-bed reactor. Bioresour. Technol. 333, 125135. https://doi.org/10.1016/j.biortech.2021.125135.

Wegener Kofoed, M.V., Jensen, M.B., Mørck Ottosen, L.D., 2021. Biological upgrading of biogas through CO2 conversion to CH4. In: In: *Emerging Technologies and Biological Systems for Biogas Upgrading*, pp. 321–362. https://doi.org/10.1016/b978-0-12-822808-1.00012-x.

Westerholm, M., Dolfing, J., Schnurer, A., 2019. Growth Characteristics and Thermodynamics of Syntrophic Acetate Oxidizers. Environ. Sci. Technol. 53 (9), 5512–5520. https://doi.org/10.1021/acs.est.9b00288.

Westerholm, M., Hansson, M., Schnurer, A., 2012. Improved biogas production from whole stillage by co-digestion with cattle manure. Bioresour. Technol. 114, 314–319. https://doi.org/10.1016/j.biortech.2012.03.005.

Westerholm, M., Isaksson, S., Karlsson Lindsjö, O., Schnürer, A., 2018. Microbial community adaptability to altered temperature conditions determines the potential for process optimisation in biogas production. Appl. Energy 226, 838–848. https://doi.org/10.1016/j.apenergy.2018.06.045.

III

Bioresource Technology Reports 32 (2025) 102353

Contents lists available at ScienceDirect

Bioresource Technology Reports

journal homepage: www.sciencedirect.com/journal/bioresource-technology-reports

Influence of nutrient medium supply rate and liquid recirculation regime on syngas biomethanation in thermophilic trickle-bed reactor

Florian Gabler [a,b,*], George Cheng [c], Leticia Pizzul [b], Anna Schnürer [c], Åke Nordberg [a]

[a] Department of Energy and Technology, SLU, Box 7032, 750 07, Uppsala, Sweden
[b] Department of Biorefinery and Energy, RISE, Box 7033, 750 07, Uppsala, Sweden
[c] Department of Molecular Science, BioCenter SLU, Box 7015, 750 07, Uppsala, Sweden

ARTICLE INFO

Keywords:
Biosyngas
Digestate
Hydraulic retention time
Trickling
Syntrophic acetate oxidation
Methanothermobacter

ABSTRACT

Syngas biomethanation enables the use of recalcitrant biomass or waste for methane production. To reveal knowledge on the importance of nutrient medium supply rate (NMSR) and liquid recirculation regime, a thermophilic 5 L trickle-bed reactor was operated for 283 days. Efficient and stable operation with >99 % H_2 and CO conversion rates was achieved at a minimum NMSR of 14 mL/(L_{pbv}·d) and 1 h gas retention time, yielding a maximum methane evolution rate (MER) of 4.3 L/(L_{pbv}·d). Reduced intermittent liquid recirculation resulted in lowered MERs (max. 3.4 L/(L_{pbv}·d)) with CO conversion more affected by low recirculation frequencies than H_2 conversion. The microbial analysis revealed a similar microbial community structure across all experimental phases, dominated by *Methanothermobacter* in both liquid and carrier biofilm. CO was likely converted to methane and acetate, with syntrophic acetate-oxidizing bacteria metabolizing acetate to H_2 and CO_2, supporting efficient hydrogenotrophic methanogenesis.

1. Introduction

Covering the demand for biomethane (CH_4) within the near future is a central challenge of the European bioeconomy. To enhance CH_4 production without increasing pressure on the existing competition of energy vs. food, it is necessary to broaden the technological availability for biomethane production. Lignocellulosic-rich substrates (e.g., forestry residues) can currently not be used within traditional large-scale anaerobic digestion but can be thermochemically converted to syngas, which is typically comprised of hydrogen (H_2), carbon monoxide (CO), carbon dioxide (CO_2), and additional gases like nitrogen (N_2) and CH_4. Syngas serves not only as an energy source but also as an intermediate for producing high-value compounds such as methane, acetate, and liquid fuels (Neto et al., 2025). The process of syngas conversion into a useful energy carrier (CH_4) is attractive, as it allows the conversion of different types of low-degradable biomass, i.e., lignocellulosic material. This method improves the alignment with current gas infrastructure, thus promoting energy transport and storage (Ren et al., 2020). Syngas methanation can be achieved through either chemical or biological pathways: catalytic methanation via chemical processes under high temperature and pressure using metal catalysts such as nickel or iron, whereas biomethanation is a biological process mediated by microorganisms of the domains Bacteria and Archaea (Ren et al., 2020). In contrast to catalytic methods, biomethanation operates under more moderate circumstances such as reduced pressures and temperatures, rendering it a more energy-efficient option (Grimalt-Alemany et al., 2017; Asimakopoulos et al., 2020). Furthermore, in contrast to chemical catalysts, microorganisms showed higher robustness to fluctuating gas load and pollutants, like tar and hydrogen sulfide (H_2S) (Grimalt-Alemany et al., 2017).

The dominant microorganisms that play a role in syngas biomethanation are acetogens, syntrophic acetate-oxidizing bacteria (SAOB), and methanogens (Paniagua et al., 2022). An overview about the most important biochemical reactions carried out by the different microbial groups is presented in Table 1. Hydrogenotrophic methanogens are also able to produce CH_4 from H_2 and CO_2, which are the same substrates that are utilized by homoacetogenic bacteria to produce acetate, resulting in a competitive relationship for H_2. A subgroup of hydrogenotrophic methanogens can directly convert CO to CH_4, while carboxydotrophic acetogens can convert it into acetate (Paniagua et al., 2022). Under thermophilic conditions, CO is more commonly converted into CO_2 by carboxydotrophic hydrogenogens via biological water-gas shift reaction (Sipma et al., 2003). However, the indirect route of CO conversion through acetate as an intermediate is usually more

* Corresponding author at: Department of Energy and Technology, SLU, Box 7032, 750 07, Uppsala, Sweden.
E-mail address: florian.gabler@slu.se (F. Gabler).

https://doi.org/10.1016/j.biteb.2025.102353
Received 18 July 2025; Received in revised form 30 September 2025; Accepted 6 October 2025
Available online 16 October 2025

Table 1
Biochemical reactions within syngas biomethanation mediated by different microbial groups.

Microbial group	Biochemical reaction	ΔG^0 [kJ/mol]
Hydrogenotrophic methanogens	$CO_2 + 4H_2 \rightarrow CH_4 + 2H_2O$	−136
Homoacetogens	$2CO_2 + 4H_2 \rightarrow CH_3COOH + 2H_2O$	−105
Acetoclastic methanogens	$CH_3COOH \rightarrow CH_4 + CO_2$	−31
Syntrophic acetate-oxidizing bacteria	$CH_3COOH + 2H_2O \rightarrow 4H_2 + 2CO_2$	+95
Carboxydotrophic methanogens	$4CO + 2H_2O \rightarrow CH_4 + 3CO_2$	−212
Carboxydotrophic acetogens	$4CO + 2H_2O \rightarrow CH_3COOH + 2CO_2$	−176
Carboxydotrophic hydrogenogens	$CO + H_2O \rightarrow CO_2 + H_2$	−20

predominant because of its preferable thermodynamics compared to direct conversion by carboxydotrophic hydrogenogens (Sancho Navarro et al., 2016).

Furthermore, syngas biomethanation is reported to show higher CH_4 productivity and greater CO tolerance at higher temperature (55–70 °C), combined with enhanced syntrophic acetate oxidation, leading to higher CH_4 yields as well as increased process stability (Andreides et al., 2022).

In general, CH_4 productivity is limited by temperature-dependent poor liquid-gas mass transfer and the slow kinetics of methanogens (Grimalt-Alemany et al., 2017). For the biomethanation of either syngas (H_2, CO_2, and CO) or only H_2 and CO_2, the trickle-bed reactor (TBR) is a feasible reactor to circumvent mass transfer restrictions (Paniagua et al., 2022). TBRs are gastight columns filled with microbe-covered carrier material, over which the liquid is trickled to supply nutrients to the microbial community. The carriers enhance the gas-liquid phase boundary interaction by offering the biofilm to develop on a large specific area relative to the reactor volume. Studies on biomethanation in TBR have illustrated the importance of various parameters, such as the choice of inoculum, temperature change, or the addition of external H_2, as reviewed in Feickert Fenske et al. (2023b). Moreover, to reach long-term process stability, it is essential that the nutrient supply contains sufficient nutrient concentrations to allow microbial activity and growth in TBRs. Substitutes for defined nutrient media, e.g., digestates, are increasingly utilized in recent studies (Aryal et al., 2021; Kamravamanesh et al., 2023; Ali et al., 2024; Goonesekera et al., 2024).

The hydraulic retention time (HRT) is usually used to describe the average time that the nutrient media liquid phase remains in the bioreactor before being discharged. A properly maintained HRT contributes to a stable pH, buffering capacity, as well as sufficient nutrient supply, which is the basis for effective syngas biomethanation (Kamravamanesh et al., 2023). Furthermore, the HRT of the nutrient liquid in the TBR is of importance for assessing economic feasibility as handling large volumes of nutrient media is associated with high operational costs. For TBR syngas biomethanation using digestate as a nutrient medium, HRTs between 5 and 31.5 d are documented (Andreides et al., 2022; Cheng et al., 2022; Ali et al., 2024; Goonesekera et al., 2024; Gabler et al., 2025) but have so far not been systematically investigated for TBR syngas biomethanation. Lowering nutrient feeding can influence the biological syngas conversion and CH_4 productivity and, thus, the techno-economic characteristics of the process. Finding a well-balanced supply of nutrient media is therefore essential for an efficient operation of syngas biomethanation. Closely connected to the HRT is the nutrient medium supply rate (NMSR), which takes the liquid reservoir volume of the TBR setup into consideration, allowing comparability among different TBR biomethanation studies.

The liquid recirculation regime relates to different approaches, which include frequency, duration, and the liquid volume flow rate, and does not only provide essential nutrients to the biofilm and removes inhibitory metabolites but also creates a liquid barrier for efficient gas-liquid mass transfer on the carrier (Sieborg et al., 2021). Studies about TBR syngas biomethanation were performed both with continuous recirculation (Asimakopoulos et al., 2021; Andreides et al., 2022; Ali et al., 2024; Goonesekera et al., 2024) and semi-continuous, i.e., intermittent recirculation (Aryal et al., 2021; Cheng et al., 2022; Bilgiç et al., 2025; Gabler et al., 2025). However, the intensive liquid recirculation is reported to negatively affect MER and H_2 conversion rates in TBR biomethanation of H_2 and CO_2 (Ashraf et al., 2021; Sieborg et al., 2021). A decreasing recirculation is suspected to allow higher gas loads to the TBR, resulting in higher methane productivity (Burkhardt et al., 2015). However, to date, there are only two studies that have systematically assessed this research question. Ashraf et al. (2021) were testing different supply methods, i.e., flushing, flooding, and continuous recirculation within a 0.5 L TBR for the biomethanation of H_2 and CO_2. It was concluded that applying a large flow of liquid disrupted the gas-liquid mass transfer. In line, Sieborg et al. (2021) assessed the influence of different recirculation regimes for biomethanation of H_2 and CO in mesophilic fed-batch operated 1.5 L TBRs, observing a significant enhancement of H_2 consumption rate when recirculation was applied once per week instead of once per day. For the biomethanation of syngas, this parameter has not been evaluated, and the liquid recirculation has been operated in continuous mode in most studies (Asimakopoulos et al., 2020; Andreides et al., 2022; Goonesekera et al., 2024). It can be hypothesized that insufficient recirculation can impair CO and H_2 conversion due to localized inhibition of the prevailing microbial groups.

The objective of this study was to assess the influence of the NMSR and the liquid recirculation regime concerning the H_2 and CO conversion and the CH_4 production of syngas biomethanation in a thermophilic TBR using diluted manure-based digestate as the sole nutrient medium. To our knowledge, this study presents the first systematic assessment of the recirculation regime for syngas biomethanation using a TBR, assessing the recirculation frequency in combination with the recirculation duration. An additional aim of the study was to examine microbial community development with an emphasis on possible variations based on the applied changes in process parameters.

2. Materials and methods

2.1. TBR setup and nutrient media

The reactor setup used in this study is described in detail in a previous article (Gabler et al., 2025) and presented in Fig. S1, Supplementary Material (SM). Briefly, the TBR was a stainless-steel column with a packed bed volume of 5 L and a liquid volume of 1 L, and was operated at a temperature of 56 ± 1 °C. The TBR used in the present study had been continuously operated with digestate as the sole nutrient source in a previous study for 382 days, mainly maintaining an HRT of 7.5 d. For biofilm growth, high-density polyethylene carrier material AnoxKaldnes K1 500 (10 mm diameter, surface area 500 m^2/m^3, density 1.2 g/m^3) was used. The utilized syngas was an artificial mixture supplied by Air Liquide (Paris, France) with 40 % H_2, 30 % CO, 20 % CO_2, and 10 % N_2 to mimic an industrial syngas mixture according to the GobiGas project, utilizing forestry biomass as gasification substrate (Larsson et al., 2019). The syngas load was controlled by a mass flow regulator (MFR, Aalborg DPC17; Orangeburg, US) and was continuously added through a port between the liquid reservoir and the packed bed (Fig. S1; SM) to meet the liquid coming from the top, thus operating in a counter-current manner. No significant overpressure was applied to the TBR. The product gas was collected above the packed bed at the top of the reactor. Its volume was measured using a drum meter (TG 0.5; Ritter, Germany) after it passed through a condensed water trap. It then passed another condensed trap and entered the gas storage. Using an ETG MCA 100 Syn Biogas Multigas Analyzer (ETG Risorse e Tecnologia s.r.l., Chivasso, Italy), the composition of the produced gas was analyzed for CH_4, CO_2, CO, O_2, and H_2 in batches of around 3 L from the gas storage, resulting in semi-continuous measurements every 40 to 50 min.

The digestate used as a nutrient medium was collected from a

mesophilic biogas reactor (SLU, Lövsta, Uppsala, Sweden), which primarily operates with manure from pigs and cows. Batches of approximately 60 L were collected at the beginning of the study (day 382) and on day 574 for subsequent storage at 2 °C. Before application to the reactor, the digestate was filtered through a mesh column (4/2/1 mm), diluted with 50 % tap water to reduce the risk of clogging in the reactor, and subsequently stored at 6–8 °C before being pumped into the reactor. Diluted digestate was pumped into the liquid reservoir using peristaltic pumps (WMC, 200 Series, Southwick, UK), depending on operational conditions within the corresponding periods (Fig. 1). Table 2 shows the initial characterization of the diluted digestate used as the nutrient medium. To maintain a constant liquid volume in the TBR, the process liquid was manually sampled every 3–4 days from the liquid reservoir (Fig. S1, SM).

2.2. Key performance indicators

The average inflow-based hydraulic retention time (HRT) of the nutrient media was calculated based on the addition of nutrient medium V_M (L/d) to the reactor and the total liquid volume V_L in the reactor (1 L), as follows:

$$HRT = \frac{V_L}{V_M} \quad (1)$$

To allow comparability of the nutrient addition strategies among the literature, the Nutrient Medium Supply Rate (NMSR) [mL/(L_{pbv}·d)] was calculated by dividing the addition rate of fresh nutrient medium (mL/d) by the total packed bed volume (V_{pbv}) of the TBR (Eq. 2).

$$NMSR = \frac{V_M}{V_{pbv}} \Big/ 1000 \quad (2)$$

To analyze reactor performance concerning CH_4 production, the Methane Evolution Rate (MER) was calculated as shown in Eq. 3. Here, F_{out} (NL/(L_{pbv}·d)) is defined as the total normalized product gas flow rate (1013.15 mbar, 273.15 K), and c_{CH4} is the CH_4 composition in the product gas.

$$MER = F_{out} * c_{CH4} \quad (3)$$

To follow the conversion of H_2 and CO, the conversion rate (%) of each component was calculated according to Eq. 4, where F_i *in* is the normalized flow rate of the specific gas compartment in the inlet gas (NL/(L_{pbv}·d)) and F_i *out* is the normalized flowrate of it in the product gas at the outlet of the TBR.

$$conversion\ rate = \frac{F_i\ in - F_i\ out}{F_i\ in} * 100 \quad (4)$$

Table 2
Initial characteristics of (diluted) digestate used as nutrient medium.

Parameter	Unit	Diluted digestate
pH	–	8.5
Alkalinity	mg $CaCO_3$/L	7264
Volatile Fatty Acids	g/L	0.07
Ammonium	mg/L	850
Sulphate	mg/L	282
Phosphate	mg/L	70
Sodium*	mg/L	206
Potassium*	mg/L	1510
Calcium*	mg/L	146
Magnesium*	mg/L	51
Iron*	mg/L	12
Cobalt*	µg/L	15
Copper*	µg/L	1180
Molybdenum*	µg/L	63
Nickel*	µg/L	94
Zinc*	µg/L	3060

* Analysis of Na, K, Ca, Mg, Fe, Co, Cu, Mo, Ni, and Zn was externally conducted by the accredited ALS Scandinavia AB according to SS-EN ISO 17294-2:2016 and SS-EN ISO 11885:2009 on day 525 (with an error margin of 10–15 %).

The inflow-based Gas Retention Time (GRT) was defined as the average time for the gas to stay in the packed bed volume without conversion of the gases according to Eq. 5, where V_{pbv} is the active packed bed reactor volume (mL), and F_{in} is the total normalized inflowing gas load (mL/h).

$$GRT = \frac{V_{pbv}}{F_{in}} \quad (5)$$

2.3. Process operation

The present study follows a previous study where diluted manure-based digestate was utilized in the same TBR setup at an NMSR of 27 mL/(L_{pbv}·d), resulting in MERs of up to 4.5 L/(L_{pbv}·d) and high H_2 and CO conversion rates above 95 %, dominated by *Methanothermobacter* in both TBR liquid and carrier biofilm (Gabler et al., 2025).

The major operational guideline of this study was to maintain similar high H_2 and CO conversion rates (>95 %) throughout the experiment. The adjustments of process parameters, such as syngas loads or nutrient supply, were based on the development of the conversion rates, accompanied by changes in MER.

The effect of the nutrient medium supply rate (NMSR) was evaluated during the first 182 days of the study (from day 382 to day 564, considering the entire reactor operation time). The NMSR was adjusted

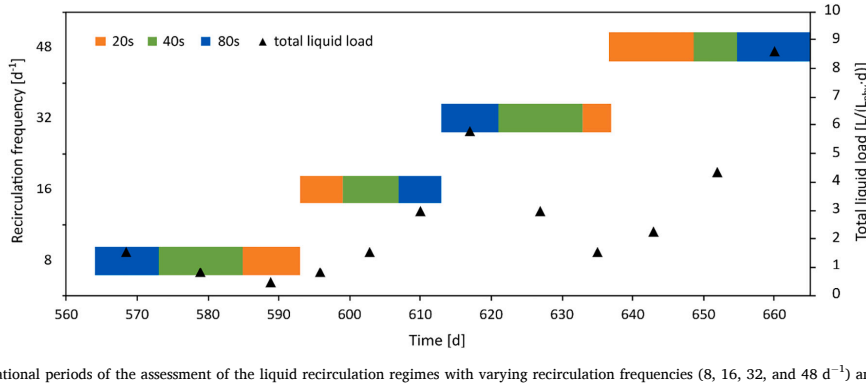

Fig. 1. Operational periods of the assessment of the liquid recirculation regimes with varying recirculation frequencies (8, 16, 32, and 48 d^{-1}) and recirculation duration (80s, 40s, and 20s) resulting in different total liquid loads (0.3–8.5 L/(L_{pbv}·d) between day 564 and 665.

as described in Table 3 and the liquid recirculation regime was kept constant (20 s recirculation duration at a frequency of 144 d^{-1}, total average flow of 40 L/h, nutrient liquid load of 6.4 $L/(L_{pbv}\cdot d)$). The liquid recirculation regime was investigated between day 564 and day 665, by periodically increasing the recirculation frequency [d^{-1}], i.e., the number of trickling occasions, combined with varying recirculation duration (20s, 40s, and 80s) according to Fig. 1. The applied total liquid loads ranged between 0.4 and 8.5 $L/(L_{pbv}\cdot d)$. The NMSR was kept constant at 14 $mL/(L_{pbv}\cdot d)$, resulting in a corresponding HRT of 14.5 d.

2.4. Sampling and chemical analysis

The removed process liquid from the liquid reservoir was used for chemical and microbial analyses. Carriers from the TBRs were sampled on two occasions, on day 564 and day 665 from the valves at the top, middle and bottom of the reactor (Fig. S1, SM) while flushing with N_2 (5 mL/min). Removed carriers were replaced by clean ones.

Analysis of alkalinity, pH, macronutrient concentrations (NH_4^+, SO_4^{2-}, PO_4^{-3}) in the liquid phase, and hydrogen sulfide (H_2S) in the product gas were performed as in a previous study (Gabler et al., 2025). Volatile fatty acids (VFA) were analyzed by high-performance liquid chromatography, Shimadzu 2050 Series, equipped with an ion exclusion column (Rezex ROA - Organic Acid H+, 300 × 7.80 mm, Phenomenex) and detected by a RID detector. The mobile phase used was 5 mM H_2SO_4 with a flow rate of 0.6 mL/min. Samples (700 µL) were mixed with 70 µL of H_2SO_4 (5 M), centrifuged (14.000 RCF, 15 min), and filtered through a 0.2 µm syringe filter into an HPLC glass vial. Micronutrients (Na, K, Ca, Mg) and trace elements (Fe, Co, Cu, Mo, Ni, Zn) were analyzed externally by the accredited ALS Scandinavia AB using ICP-AES and ICP-SMFS.

2.5. Microbial sequencing and analysis

The DNA extraction was completed on 2 mL of liquid sample using FastDNA Spin Kit for Soil (MP Biomedicals, Illkirch-Graffenstaden, France) following the manufacturer's instructions. Modifications were made in step 7 (10 min centrifugation at 14000 RCF) and step 9 (10 min of matrix settling). In addition, an additional cleaning step between steps 11 and 12 was applied to remove PCR-inhibiting components, as suggested by the manufacturer, with the procedure for humic acid removal for soil samples (MP Biomedicals, LLC). Additional steps were taken for carrier samples as described in Gabler et al. (2025). The carrier samples were extracted in quadruplicate to collect enough material from the biofilm on the carriers. Sequencing libraries were prepared and generated by Novogene Europe, Munich, Germany, using Illumina MiSeq targeting 16 s rRNA as described previously (Westerholm et al., 2018). The paired-end reads were filtered based on quality and trimmed reads to 250 bp. Downstream processing of the reads was completed using Division Amplicon Denoising Algorithm2 (DADA2, v. 1.32.0) in RStudio running R v.4.4.1 as previously described in Westerholm et al. (2018), truncating forward and reverse reads at positions 180 and 200, respectively. The sequences for the quadruplet carrier samples were merged for downstream analysis. The SILVA reference database v. 138 was used for microbial classification. Phyloseq v1.48.0 was used to organize the sequence data. Weighted principal coordinate analysis (PCoA) was calculated using the UniFrac method based on the neighbor-joining phylogenetic tree generated with DECIPHER (v3.0.0) and phangorn (v.2.12.1) (GTR model). To determine the correlation of process performance with each principal coordinate axis, parameter vectors (H_2 conversion, CO conversion, and syngas load) were fit to the PCoA ordination using the "envfit" function from vegan (v. 2.6.6.1). For the archaeal and bacterial PCoA plots, two outliers (day 606 and 627) were removed due to operational and monitoring malfunction. ASV species similarity was determined using the Basic Local Alignment Search Tool (BLAST) algorithm provided by the National Center for Biotechnology Information (NCBI) was used. Raw sequence data have been deposited in the NCBI.

Table 3
Applied nutrient medium supply rates and corresponding hydraulic retention times between days 382 and 564.

Duration	Nutrient medium supply rate	Hydraulic retention time
[d]	[$mL/(L_{pbv}\cdot d)$]	[d]
382–410	22	8.9
410–441	19	10.5
441–472	14	14
472–522	11	18
522–564	14	14.5

3. Results

The results in this section are divided into three parts: the effect of the nutrient medium supply rate (NMSR) at different HRTs, the effect of the liquid recirculation regime, and the microbial community development.

As a result of the major operational guideline to maintain high H_2 and CO conversion rates, no periods of VFA accumulation (< 0.3 g/L) were observed during the entire operation of 283 days (Fig. S2d and S3d, SM). The potential contribution of CH_4 in the diluted digestate used as a nutrient medium was negligible. In the present study, both the TBR setup and the nutrient medium were identical to a previous study (Gabler et al., 2025), where the maximum daily CH_4 production from the digestate, based on the highest supply rate (NMSR 27 $mL/(L_{pbv}\cdot d)$) and residual methane potential (20 ml/g VS), would only result in ca. 2 mL CH_4/d when the daily syngas-derived CH_4 production was up to 22 L.

3.1. Nutrient medium supply rate

The nutrient medium supply rate (NMSR) was decreased stepwise as presented in Table 3, starting with 22 $mL/(L_{pbv}\cdot d)$ on day 382, reaching the lowest assessed NMSR (11 $mL/(L_{pbv}\cdot d)$; HRT 18.9 d) on day 472. From the start until day 494, the syngas load was kept constant at a range of 24–25 $L/(L_{pbv}\cdot d)$ corresponding to GRT 1 h, maintaining full conversion of H_2 and CO (Fig. 2b). Due to the temporary malfunction of the drum meter that was used to measure the volume of the product gas, the methane evolution rate (MER) achieved were assessed based on the observed conversion rates of H_2 and CO and the applied syngas load (Fig. 2a). The resulting calculated MER in this period was approximately 4.3 $L/(L_{pbv}\cdot d)$. During the NMSR periods 19, 14, and 11 $mL/(L_{pbv}\cdot d)$ (HRT 8.9, 10.5, and 14 d), H_2 and CO conversion rates were very high (>99 %). Throughout the study, the pH in the process liquid remained stable between 7.5 and 8, with a temporary increase to 8.3 during the standby period. It returned to normal levels without pH control after syngas application was continued. During the whole operation, alkalinity remained sufficient, ranging from 4000 to 5500 mg $CaCO_3$/L (Fig. S2c and S3c, SM).

Between operation days 494 and 503 (at NMSR 11 $mL/(L_{pbv}\cdot d)$, the operation was set to a standby mode for instrument maintenance and repair. The TBR received a low inflow of pure nitrogen (no syngas was supplied) and the temperature and NMSR were kept constant. This 9-day-long standby period subsequently affected H_2 and CO conversion rates and CH_4 productivity. After a stepwise increase of the syngas loads to the previous level of 24 $L/(L_{pbv}\cdot d)$ (GRT 1 h) on day 516, the conversion for H_2 and CO reached 98 % and 97 %, respectively. To continue recovering conversion rates of H_2 and CO to previous levels above 99 %, the syngas load was decreased to ca. 22 $L/(L_{pbv}\cdot d)$, corresponding to GRT 1.1 h, from 517 onwards. However, the H_2 and CO conversion rates did not reach the previous levels, even with this reduced syngas load compared to the previous periods before day 494. Based on the hypothesis that lower H_2 and CO conversion rates and CH_4 productivity

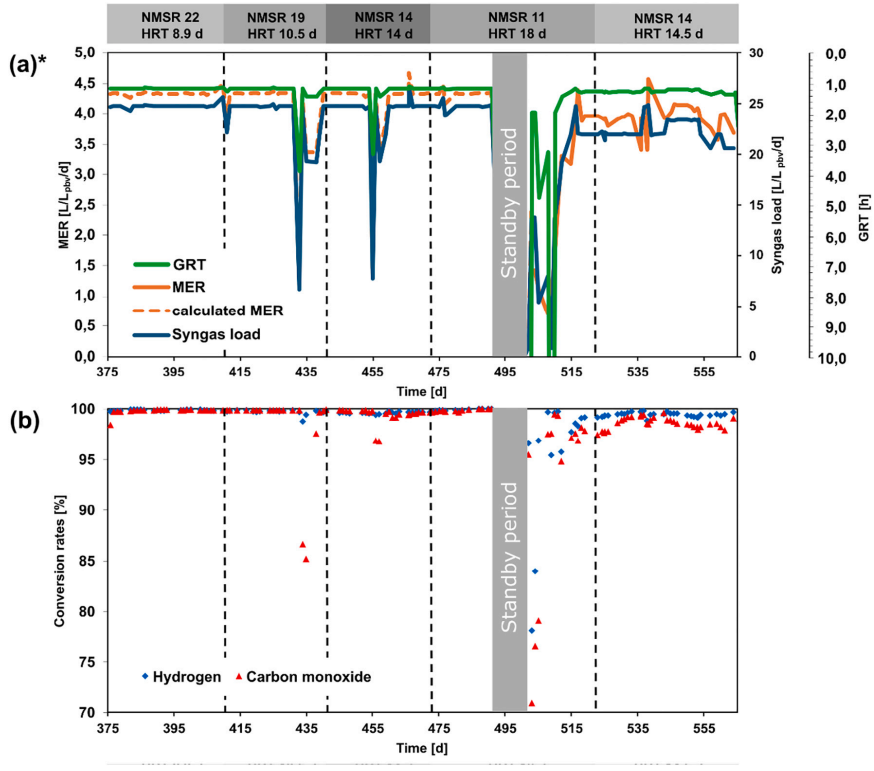

Fig. 2. Evaluation of the nutrient media supply rate (NMSR) between day 382 and 564: (a) Development of syngas load and (calculated) Methane Evolution Rate (MER)*, (b) H_2 and CO conversion rates. Data between day 0 and 381 is presented in a previous article (Gabler et al., 2025). *Up to day 500, the volumetric measurements of the product gas were not working correctly; therefore, the MER was calculated based on syngas inflow and achieved syngas conversion rates. Two major declines in the applied syngas load on days 433 and 455 were due to mechanical problems with the pressure control unit at the top of the syngas cylinder.

were related to the NMSR of 11 mL/(L_{pbv}·d), which was low in comparison to other similar studies under thermophilic conditions (Andreides et al., 2022; Ali et al., 2024; Goonesekera et al., 2024; Gabler et al., 2025), and as no obvious shortages of macronutrients in the TBR liquid were observed, the NMSR was increased back to 14 mL/(L_{pbv}·d). This resulted in a decreased average HRT of 14.5 d, which was kept until the end of the experiment. By increasing the NMSR, H_2 and CO conversion rates slowly improved to levels above 99 % between days 525 and 535. To further maximize MERs and maintain high conversion rates, the syngas load was increased from 21.9 to 23.3 L/(L_{pbv}·d) on day 543. However, this resulted in slowly decreasing conversion rates for H_2 (99 %) and CO (98 %).

3.2. Recirculation regime

After carrier sampling on day 564, the liquid recirculation sub-trial started on day 564 by reducing the recirculation frequency from 144 d^{-1} to 8 d^{-1} accompanied by a 4-fold increase of the recirculation duration from 20 s to 80 s (Fig. 1). The syngas flow subsequentially started in a reduced manner at 10 L/(L_{pbv}·d) (GRT 1.8 h) and was stepwise increased to 19 L/(L_{pbv}·d) (GRT 1.3 h) on day 572 resulting in a maximum MER of ca. 3.4 L/(L_{pbv}·d) (Fig. 3a). During this period until day 573, decreasing CO conversion rates were observed (98 to 96 %). At a recirculation duration of 40 s in the next period (until day 584), the conversion rates remained stable at 99 % and > 96 % for H_2 and CO, respectively. However, when reducing the duration to 20 s with a frequency of 8 d^{-1}, a significant drop in the CO conversion rates to 90 % was observed, which might be rather associated with a rapid syngas load increase from 14 to 19 L/(L_{pbv}·d) between day 586 and 588 than with the change of the recirculation regime. At syngas loads of 19 L/(L_{pbv}·d) (GRT 1.2–1.3 h), the CO conversion rates did not reach the previously observed high levels and levelled off at around 93 %. This trend continued during the next period with a 20 s recirculation duration and an increased recirculation frequency of 16 d^{-1} (days 593 to 599). However, CO conversion improved from day 605 onwards when a recirculation duration of 40 s at a frequency of 16 d^{-1} was applied, reaching H_2 and CO conversion rates of >96 %. These rates remained stable after a further increase of the recirculation duration to 80 s (day 608). After day 613, when the recirculation frequency was increased to 32 d^{-1}, conversion rates for H_2 were > 99 % and for CO were 97–98 %. Between days 630 and 665, at a frequency of 48 d^{-1} (regardless of the recirculation duration), the conversion rates were constant in the range of 99 % for H_2 and 96 % for CO. As for the NMSR sub-trial, no VFA accumulation was observed due to the applied major guideline to maintain high H_2 and CO conversion rates (Fig. S3d, SM). Moreover, the nutrient status reflected in Fig. S3a and b (SM) did not indicate any limitation in this part of the study.

To further evaluate the influence of liquid recirculation, the

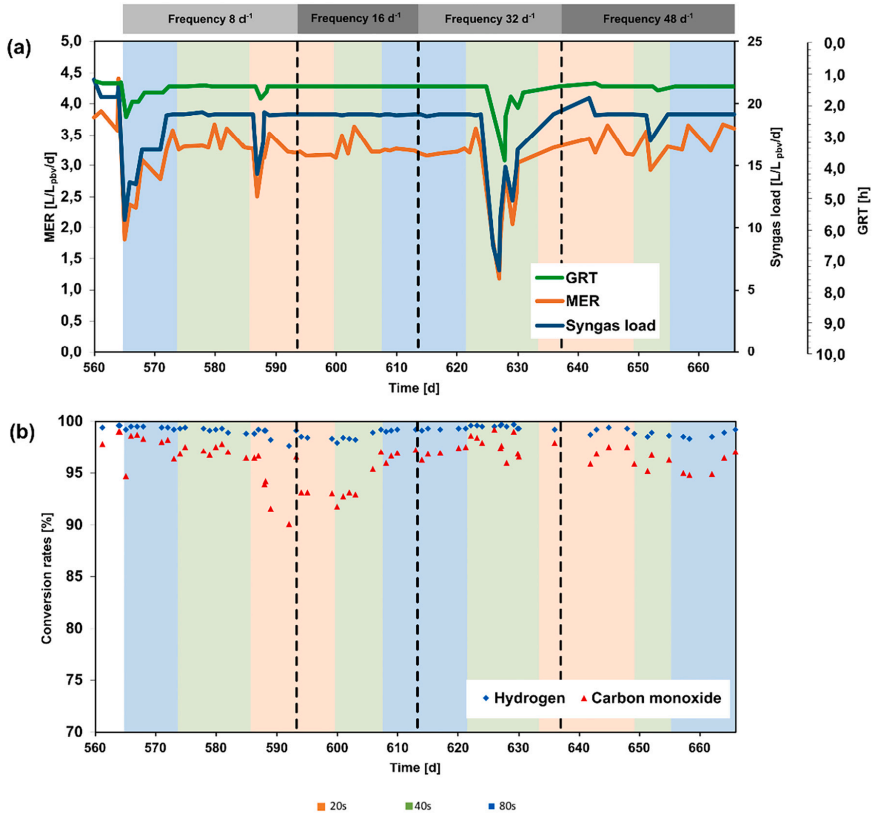

Fig. 3. Liquid recirculation assessment under different trickling frequencies and trickling durations according to Fig. 2 between day 564 and 665: (a) Development of syngas load and Methane Evolution Rate (MER), (b) H_2 and CO conversion rates.

concentrations of H_2 and CO in the product gas were observed at a higher resolution (24 h) during selected operation days (573, 579, and 590), under a recirculation frequency of 8 d^{-1} (Fig. 4). The variation in CO concentration in the product gas showed 8 peaks within 24 h, a pattern that clearly corresponded to the recirculation frequency (Fig. 4). Each trickling occasion resulted in an increase in CO concentration in the product gas from ca. 1.2 % to 1.6 %. The recirculation duration, however, did not have any influence on the overall CO conversion (Fig. 4). The concentration of H_2 was around 0.4 % and was not affected by the recirculation occasions or recirculation durations, except for the long duration (80 s) where the 8 peaks-pattern observed for CO was also detected for H_2, although the difference between peaks and valleys were lower for H_2 (ca. 0.1 %) compared to CO conversion (ca. 0.4 %).

3.3. Microbial community development

PCoAs were performed to identify correlations between microbial community and TBR performance parameters during the different operational period of both sub-trials. One PCoA illustrates that the microbial community differed between the nutrient medium and the TBR (liquid phase and carrier biofilm) (Fig. S4, SM). Looking at the taxonomic affiliation, the overall microbial community showed only small changes during the changes of NSMRs and liquid recirculation regime, both in the TBR liquid and on the carriers (Figs. S5-S8, SM). In another PCoA, Fig. 5 shows some separation of both the archaeal (Fig. 5a) and the bacterial (Fig. 5b) communities in the liquid and on the carriers during the different operational periods, but no strong positive correlation was found to syngas load or to the H_2 or CO conversion rates. These results demonstrate the robustness of the microbial community in the process for operational changes and the low impact of the complex nutrient source. Considering the most abundant microbes (>1 % in relative abundance (RA)), 28 amplicon sequence variances (ASVs) in the NMSR period and 27 ASVs in the liquid recirculation regime period represent approximately 90 % of the community. A more detailed presentation of ASVs showing presence persisting through the entirety of each experimental phase is shown below.

3.3.1. Archaea

The archaeal community consisted primarily of an ASV belonging to the genus Methanothermobacter. This ASV was the dominating methanogen in the liquid phase throughout both sub-trials, representing 33–51 % of the total community and > 75 % of the archaea (Figs. S5 and S7, SM). NCBI analysis of the ASV assigned the closest relative as *Methanothermobacter thermautotrophicus*. The same ASV also dominated on the carriers, during the NMSR trial and in similar RA as in the liquid (day 564) and recirculation regime (day 665, 33–40 % RA), with very

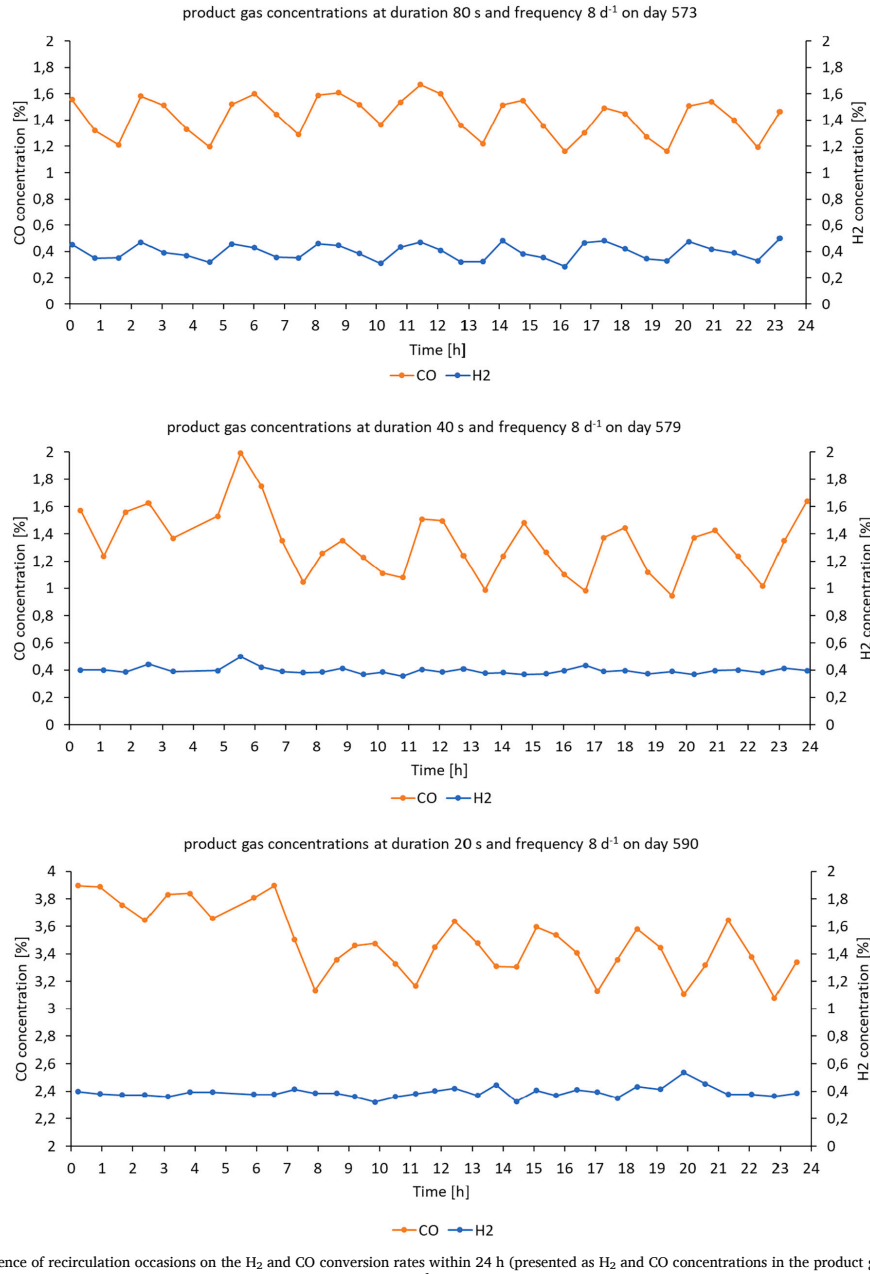

Fig. 4. Influence of recirculation occasions on the H_2 and CO conversion rates within 24 h (presented as H_2 and CO concentrations in the product gas) at different recirculation durations (80s, 40s, and 20s) at a recirculation frequency of $8d^{-1}$.

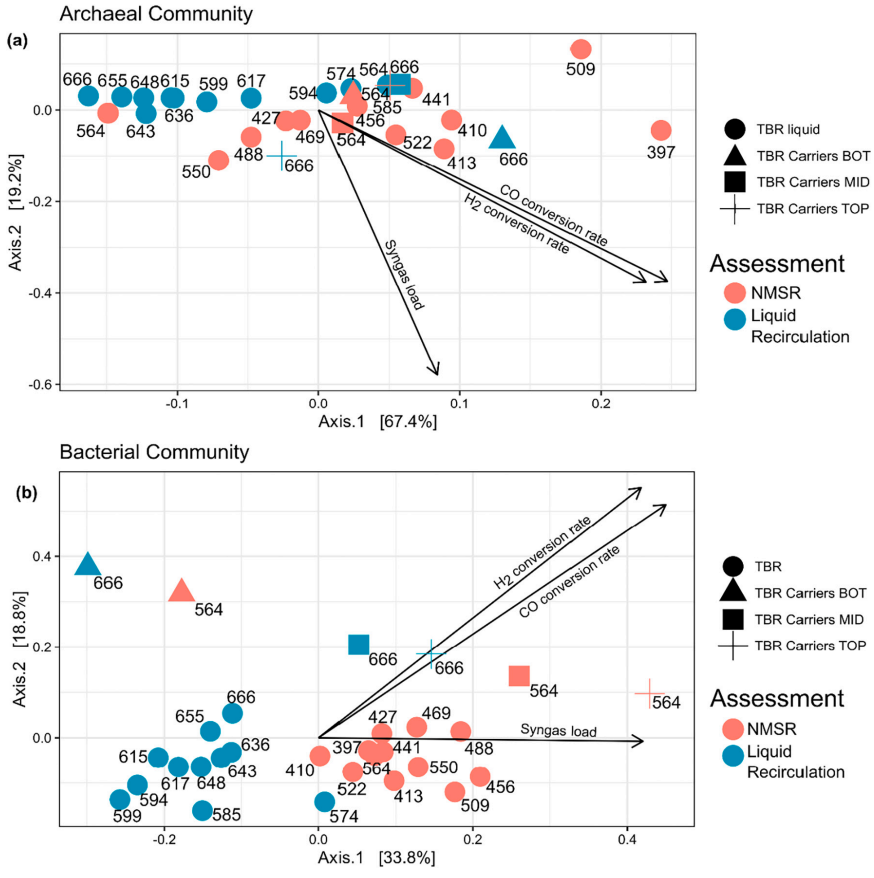

Fig. 5. Principal coordinate analysis (PCoA) plots of (a) the archaeal community and (b) the bacterial community in the TBR liquid and on the carriers using UniFrac. Indicators of process performance associated with changes in microbial community structure are plotted as vectors, where the direction and length indicate the contribution of the variable to the principial coordinates. The numbers indicate the day of operation in both conducted sub-trials (NMSR and Liquid Recirculation).

small differences between top or bottom of the TBR (Figs. S5 and S7, SM). Additional methanogens, both hydrogenotrophic, acetoclastic, and methylotrophic methanogens, were detected at very low RA (Figs. S5 and S7, SM). Of the low-abundant methanogens, one was identified at slightly higher RA, both in the liquid phase (mainly during the NMSR sub-trial) and on the carriers. This ASV was identified as *Methanobacterium formicicum* (Table 4). In addition, Methanosarcina, closely related to *Methanosarcina thermophila* (100 % similarity), showed a comparably higher RA on the top carriers during the NMSR sub-trial (Figs. S5 and S7, SM, Table 4). In the PCoA plot presented in Fig. 5a, the archaeal community clusters close to the center along principal coordinate 1 (67 % variance). Samples from the NMSR sub-trial show a broader spread compared to the liquid recirculation sub-trial. The vectors indicated that the CO and H_2 conversion rates are more associated with the positive direction of principal coordinate 1, while syngas load is more associated with principal component 2 (19 % variance).

3.3.2. *Bacteria*

The bacterial community composition in the TBR liquid did not show any major differences throughout the experimental period including both sub-trials (Figs. S6 and S8, SM). ASVs, present throughout both sub-trials, were represented by Aggregatilineales, D8A-2, Desulfitobacteriaceae, DTU014, Haloplasma, Hydrothermae, MBA03, Symbiobacterium, Syntrophaceticus, and W5 (Figs. S6 and S8, SM). Caldicoprobacter was present in the NMSR sub-trial but decreased in RA below 1 % after day 564 (during the liquid recirculation sub-trial) (Figs. S6 and S8, SM). A similar trend was seen for *Tepidanerobacter*. In contrast, Acetomicrobium and Coprothermobacter increased in abundance after 456 and 594 days, respectively. Tepidimicrobium was also more prevalent after day 574 (Fig. S8, SM). In the PCoA plot presented in Fig. 5b, the bacterial community shows a clearer separation between NMSR and liquid recirculation sub-trial than the archaeal community (Fig. 5a), with liquid recirculation samples clustering to the negative side of principal coordinate 1 and NMSR samples positioned more toward the positive side aligning strongly with syngas load and conversion rates vectors. Analysis of the bacterial community on the carrier at different positions of the TBR indicated some differences, such as Syntrophaceticus and Tepidanaerobacter being more abundant at the bottom, and DTU14, Acetomicrobium, and Hydrothermae showing higher RA at the top (Figs. S6 and S8, SM). In addition, Thermoactogenium, not present in the

Table 4
ASV taxonomic assignments and their closest relatives determined by NCBI BLAST.

ASV taxonomic assignment	NCBI BLAST analysis	Similarity (%)
Archaea		
Methanothermobacter	*Methanothermobacter thermautotrophicus*	100
Methanobacterium	*Methanobacterium formicicum*	100
Methanosarcina	*Methanosarcina thermophila*	100
Bacteria		
Acetomicrobium	*Acetomicrobium mobile*	98
Aggregatilineales	Bacterium YC-LK-LKJ3	88
Caldicoprobacter	*Caldicoprobacter* sp. Acc8	93
Coprothermobacter	*Coprothermobacter proteolyticus*	100
D8A-2	'*Candidatus* Syntrophonatronum acetioxidans'	91
Desulfitobacteriaceae	*Desulfosporosinus* sp. FE18	96
Desulfitibacter	*Calderihabitans maritimus strain KKC1*	92
DTU014	*Koleobacter methoxysyntrophicus*	88
Haloplasma	Bacterium ADC-6-1	100
Hydrothermae	*Thermotogaless p.* SRI-15	96
MBA03	Bacterium *ADC-6-6*	100
Symbiobacterium	*Symbiobacterium thermophilum*	100
Syntrophaceticus	*Syntrophaceticus schinkii*	94
Tepidimicrobium	*Tepidimicrobium ferriphilum*	93
Thermacetogenium	*Thermacetogenium phaeum*	99
W5	'*Candidatus* Cloacamonas acidaminovorans'	89

liquid, appeared only on the carriers at the bottom. This difference between the TBR levels (top, middle and bottom) can be observed in Fig. 5b, where the separation along the first principal component (34 % variance) indicates the difference in the carrier biofilm bacterial community for day 564 (NMSR-trial) and day 666 (liquid recirculation trial), respectively. However, the bacterial community in the TBR liquid on the corresponding days only shows minor differences with the carriers along the second principal component (19 % variance).

4. Discussion

4.1. The effect of nutrient medium supply rate on syngas biomethanation

Recent studies have demonstrated that digestates can serve as viable substitutes for defined nutrient media in syngas biomethanation (Andreides et al., 2022; Cheng et al., 2022; Ali et al., 2024; Goonesekera et al., 2024). However, digestates differ significantly in nutrient composition due to variations in origin and treatment, which complicates direct comparison between studies and limits the generalization of results beyond the specific digestate used. Still, digestate from a well-functioning biogas process would indicate that nutrients for microbial activity and growth are present in the sufficient concentrations. The definition of nutrient media addition varies among the literature (either as HRT or as addition rate (mL/d), making it difficult to compare the process performances concerning the nutrient medium supply. Therefore, the present study introduced the new parameter presented as Nutrient Medium Supply Rate (NMSR; mL/(L_{pbv}·d)), which combines the TBR setup (volume of packed bed and volume of liquid in the TBR) with the nutrient medium addition rate (mL/d) and relates them to the total packed bed volume (L_{pbv}).

The present study was performed with NMSRs below the average values reported in the literature (mentioned below), none of which observed nutrient limitations. NMSRs in the literature for continuous TBR syngas biomethanation using digestate as nutrient medium were recalculated based on liquid reservoir volume and HRT and range from 6 to 200 mL/(L_{pbv}·d), with corresponding HRTs of 5–31.5 days (Andreides et al., 2022; Cheng et al., 2022; Ali et al., 2024; Goonesekera et al., 2024; Gabler et al., 2025). In the present study, NMSRs were between 11 and 22 mL/(L_{pbv}·d) (HRT 9–18 d), with conversion rates of H_2 and CO exceeding 99 %, at an NMSR of 14 mL/(L_{pbv}·d) and an HRT of 14 days. During the assessment of different operation temperatures using a 1 L TBR, Andreides et al. (2022) set the NMSR to 200 mL/(L_{pbv}·d) (HRT 5 d), the highest reported value for continuous TBR syngas biomethanation studies. They achieved H_2 and CO conversion rates similar to those observed in our study but with comparably lower MERs of 1.5 and 2.1 L/(L_{pbv}·d) under mesophilic and thermophilic conditions, respectively. Similarly to the present study, they did not observe limitations in macronutrient concentrations, as no decrease in syngas conversion rates occurred. The syngas load was maintained at 13.5 L/(L_{pbv}·d) throughout their study, and it was assumed that the maximum consumption capacity of the biofilm had not been reached; therefore, the nutrient level was sufficient compared to the demand (Andreides et al., 2022). In line with Andreides et al. (2022), another study for TBR syngas biomethanation reported significantly higher MERs under thermophilic conditions (4.6 L/(L_{pbv}·d)) compared to mesophilic conditions (1.9 L/(L_{pbv}·d)), operating a NMSR of 153 mL/(L_{pbv}·d) (HRT 8 d) with a defined nutrient medium (Asimakopoulos et al., 2020). The reported MERs are slightly above those of the present study.

In another study by Ali et al. (2024), where the utilization of CO was assessed as a sole carbon source in a 0.7 L TBR, a NMSR of 41 mL/(L_{pbv}·d) (HRT 31.5 d) was applied, achieving optimal performance at a GRT of 1 h with an 88 % CO conversion rate. Furthermore, in a study by Goonesekera et al. (2024), an NMSR of 50 mL/(L_{pbv}·d) (HRT 20 d) was used for a thermophilic 1 L TBR, where process limitations related to syngas composition and mass-transfer conditions were examined. At this NMSR and similar GRT of 1 h compared to the present study, H_2 and CO conversion rates ranged approximately between 80–90 % and 40–80 %, respectively, depending on the applied liquid recirculation rate. The addition of trace elements and an increased liquid recirculation rate led to a 59 % increase in CH_4 productivity and full syngas conversion at a GRT of 1 h (Goonesekera et al., 2024). High syngas loads of 27–28 L/(L_{pbv}·d) (GRT 0.9 h) with high H_2 and CO conversion rates (>99 %) were achieved using an NMSR of 27 mL/(L_{pbv}·d) (HRT 7.5 d) in a thermophilic 5 L TBR (Gabler et al., 2025). Cheng et al. (2022) observed decreased H_2 and CO conversion rates and the corresponding MERs when the NMSR was stepwise decreased from 29 mL/(L_{pbv}·d) to 6 mL/(L_{pbv}·d) (HRT 5–25 d) in a mesophilic 35 L TBR. Moreover, low NMSRs were identified to cause declining conversion of H_2 and CO (Cheng et al., 2022), which is in line with our results observing reduced conversion rates at an NMSR of 11 mL/(L_{pbv}·d) under thermophilic conditions. Most efficient syngas biomethanation was observed at a minimum NMSR of 14 mL/(L_{pbv}·d) for the conditions within the present study.

The fast recovery after the standby period from day 494 to 503 illustrates the robustness of TBR biomethanation systems. The microbial community could remain without gaseous substrate over a long period, in line with the results of previous studies on biomethanation of H_2 and CO_2 (Jønson et al., 2022; Feickert Fenske et al., 2023a). Jønson et al. (2022) were regaining the initial TBR performance within 6–12 h after standby periods between 0.5 and 3 days. Moreover, Feickert Fenske et al. (2023a) observed a fast recovery of a biomethanation process of H_2 and CO_2, continuously operated in an 800 L pilot-scale TBR, testing standby periods of 14 and 49 days, obtaining CH_4 productivity to recover by >96 % within 24 h. The results of the present study suggest that restarting after a standby period should be characterized by comparatively low syngas loads of ca. 20 % of the maximum previously applied syngas loads, followed by stepwise increases of syngas loads considering the observed conversion rates of H_2 and CO.

The syngas biomethanation performance in the last period (days 522–564), characterized by a NMSR of 14 mL/(L_{pbv}·d) (HRT of 14.5 d), was lower compared to the periods before the standby period (Fig. 2). Given that the concentration of macronutrients measured in the TBR liquid phase was sufficient, a potential shortage of N, P or S can be excluded. This observation is in line with findings from a previous study, which utilized the same digestate (Gabler et al., 2025). Goonesekera et al. (2024) observed a positive effect on syngas biomethanation due to

trace element supplementation. It might be possible that the consecutive decrease of NMSR from 22 to 11 mL/(L_{pbv}·d) before the standby period resulted in the lack of certain trace elements. However, this can only be assumed because the concentrations of, e.g., Fe, Ni, and Co in the liquid phase were not systematically followed. Another possible reason for the reduced reactor performance after day 520 could be the accumulation of solids and sediments in both the reactor liquid and the packed bed. During the periods with lower NMSR, the liquid phase remained longer in the TBR compared to periods of higher nutrient media addition, and less volume, including solids and sediments, was discharged. This could also have resulted in partial clogging within the packed bed, hindering the syngas from reaching all zones of biofilm on the carriers and, thus, leading to a less active reactor volume and lower total gas-liquid mass transfer area.

4.2. The influence of liquid recirculation regimes on syngas biomethanation

Balancing the liquid recirculation related to nutrient supply and gas-liquid mass transfer limitations is a key parameter for efficient TBR syngas biomethanation. Lowering the liquid recirculation rate might be associated with potential clogging in TBRs. However, the volatile suspended solids in the TBR liquid are considered to be very low, as reported by Asimakopoulos et al. (2019) (< 0.6 g/L), in comparison to other reactor designs such as CSTR (Figueras et al., 2021) (11 g/L). Our observations during carrier sampling did not indicate any clogging for the TBR setup used. Still, reduced liquid recirculation can improve gas-liquid mass transfer, as the liquid thickness on the biofilm is lower (Burkhardt et al., 2015). Similar findings were reported by Sieborg et al. (2021), observing increased H_2 conversion rates at reduced liquid recirculation in TBR biomethanation of H_2 and CO_2. Among different studies in the literature for syngas biomethanation, the liquid recirculation regimes have been operated both continuously and intermittently (Aryal et al., 2021; Andreides et al., 2022; Ali et al., 2024; Goonesekera et al., 2024; Gabler et al., 2025).

The reduced liquid recirculation, i.e., the lower recirculation frequencies compared to the NMSR sub-trial, resulted in reduced syngas biomethanation performance with lower syngas loads of 19 L/(L_{pbv}·d) (with a corresponding GRT of 1.3 h) and lower MERs of 3.4 L/(L_{pbv}·d). More specifically, the biological conversion of CO was more affected, whereas the H_2 conversion was more resilient, with conversion rates ranging between 98 and 99 % (Fig. 3). This is consistent with several other studies and highlights that the gas-liquid mass transfer of CO is the major bottleneck for syngas biomethanation due to low CO solubility compared to H_2 (Asimakopoulos et al., 2021; Paniagua et al., 2022). Underlining this, it has been shown that every single recirculation occasion can have an inhibitory influence on the biological conversion of CO (Fig. 4), whereas the H_2 conversion is not as affected, which can be explained by a higher solubility of H_2 compared to CO and by the reduced transfer of gaseous substrate into the microbial cells when the liquid covers the biofilm (Sieborg et al., 2021). Similar findings were reported by Jensen et al. (2021) who observed significant declines in H_2 conversion rate (99 to 79 %) and CH_4 concentration in the product gas (94 to 67 %) after intermittent recirculation of the liquid phase during biomethanation of H_2 and CO_2 in a mesophilic 8.3 L TBR. In another study for the biomethanation of H_2 and CO_2 in a 0.5 L TBR using pasteurized cow manure as nutrient media, Ashraf et al. (2021) found that a 20-fold increase in the nutrient liquid flow rate during continuous recirculation resulted in reduced H_2 conversion rate (−9 %) and CH_4 productivity (−13.5 %). Here, the authors suspected a change in hydrodynamics, leading to a higher gas-liquid boundary inhibiting the gas from reaching the active biofilm to convert H_2 and CO_2 into CH_4. In opposite, Goonesekera et al. (2024) observed and improved mass transfer and increased conversion rates of (+10 %) and CO (+40 %) due to increased liquid recirculation rate from 20 to 280 mL/min. However, the examined liquid recirculation duration in the present study did not seem to affect the H_2 and CO conversion rates, which is reasonable as the average recirculation flow rate of the pump (40 L/h) was constant, likely resulting in a comparable liquid-biofilm boundary section among the different recirculation durations of 20, 40, and 80 s.

An important aspect to consider regarding recirculation regimes in TBR biomethanation is the liquid hold-up capacity of the carrier material. Jensen et al. (2021) compared plastic, cellulosic, and clay-based carriers concerning their liquid hold-up capacity for TBR biomethanation of H_2 and CO_2. Clay-based carriers are characterized by a high porosity and a similar specific area (550 to 1020 m^2/m^3), compared to the more commonly used plastic equivalents (300–950 m^2/m^3), and can hold the liquid to a significantly higher percentage after 30 min (7–14 vol% compared to 1–3 vol% for the plastic and cellulose-based carriers). Based on that, Jensen et al. (2021) selected crushed clay as carrier material for subsequent biogas upgrading trials in a mesophilic 8.3 L TBR while recirculating the liquid phase once per day. Interestingly, the H_2 conversion rate decreased below 70 % after the daily liquid recirculation and did not fully recover within 210 min afterwards. A similar behavior of long recovery time, but for CO conversion only, was found within the present study (Fig. 4). However, the disruptive influence of each recirculation occasion on the H_2 and CO conversion rates was not as pronounced as mentioned by Jensen et al. (2021) (Fig. 4). In the present study, the TBR was filled with a high-density polyethylene carrier (AnoxKaldness K1 500) that has a specific surface area of 500 m^2/m^3, which is within the range of plastic carriers (320–950 m^2/m^3) used in other TBR syngas biomethanation studies (Aryal et al., 2021; Asimakopoulos et al., 2021; Andreides et al., 2022; Cheng et al., 2022; Goonesekera et al., 2024). Plastic carriers have a significantly lower liquid hold-up capacity and, to maintain effective syngas biomethanation, those TBRs utilizing such material need more regular liquid recirculation compared to TBRs with clay-based carriers. Continuous recirculation is not necessary; however, the recirculation regime should be based on the TBR settings, such as the liquid hold-up capacity of the carriers, the applied syngas loads, and the utilized nutrient medium. Thus, for a sufficient nutrient supply to the biofilm, a low recirculation duration of 20 s combined with higher recirculation frequencies (> 48 d^{-1}) can be assumed as a well-balanced condition for our setup.

4.3. Microbial community development

While the process performance experienced some fluctuations, the microbial community did not show any major changes in both sub-trials concerning NMSR and liquid recirculation regime, with only small differences, even during the standby period and the subsequent decreases in the syngas loads (Figs. 4 and S5-S8, SM).

In line with several other studies on thermophilic biomethanation with syngas or H_2 and CO_2, the dominating methanogenic genus was *Methanothermobacter* (Porte et al., 2019; Ali et al., 2024; Gabler et al., 2025). This genus can grow with either CO or CO_2 as the sole carbon source and utilize formate and H_2 and CO_2 as the sole energy source at thermophilic temperatures (Diender et al., 2016). In addition, mainly during the NMSR sub-trial, *Methanobacterium* was present at comparably higher abundance and identified to belong to *M. formicicum*. Even though this methanogen is a mesophilic species, it has also been found in thermophilic biomethanation (Porte et al., 2019). *M. formicicum* can utilize H_2/CO_2 and formate as a carbon and energy source (Battumur et al., 2016). Interestingly, during the recirculation regime period, the same ASV for *Methanobacterium* dropped to below 1 % RA, suggesting a negative effect on this methanogen by decreasing the liquid recirculation frequency. In contrast to *Methanothermobacter,* members within *Methanobacterium* have not been previously shown to utilize CO, and thus the decrease of this ASV was likely not linked to the observed reduction in CO conversion. The presence of this methanogen mainly during the NMSR sub-trial might explain the separation of the archaeal community in addition to the correlation with CO and H_2 conversion

rates, as seen in Fig. 5a. The *Methanosarcina* ASV observed at higher RA on the top carrier during the NMSR sub-trial was closely identified as *M. thermophila*, an acetate-utilizing species that also may slowly grow on H_2 and CO_2 (Zinder et al., 1985). Members in the genus *Methanosarcina* have been previously recovered in both mesophilic and thermophilic syngas biomethanation processes (Aryal et al., 2021; Goonesekera et al., 2024), several at higher RA on the carriers as compared to liquid, as seen in the present study.

During both phases of the experiment, several fermenting bacteria likely producing acetate and other organic acids were identified. Hydrothermae was abundant in both phases of the experiment. This ASV was closely identified with *Thermotogales* sp. SRI-15, belonging to the order Thermotogales, is known to include thermophilic fermenting members that produce acetate and H_2/CO_2 (Reysenbach et al., 2001). The type species of Haloplasma (*H. contractile*) is fermentative and produces lactate. *Tepidimicrobium* ASV most likely represented another acetate producer (Niu et al., 2009), sharing 93 % similarity with *T. ferriphilum*. Members of the *Caldicoprobacter* genus are fermenters that can produce lactate, acetate, ethanol, and H_2/CO_2 (Yokoyama et al., 2010). *Acetomicrobium*, more abundant during the liquid recirculation sub-trial, was confirmed by NCBI BLAST to be *A. mobile*, which is a sugar and organic acid fermenter producing acetate and H_2/CO_2 (Menes and Muxi, 2002). *Coprothermobacter*, showing the same pattern, is a proteolytic fermenter producing acetate and H_2/CO_2 as main products, and its growth has been shown to be enhanced when combined with *M. thermautorophicus* (Sasaki et al., 2011). *Coprothermobacter* has been previously described as part of the core bacterial group in thermophilic biomethanation systems (Chen et al., 2021; Sieborg et al., 2025). These fermenting bacteria were likely feeding on organic components available in the digestate nutrient medium and/or on decaying biomass (Sieborg et al., 2025). The increase of *Acetomicrobium* and *Coprothermobacter* ASVs coincided with the transition to the liquid recirculation sub-trial, which could link the RA increase with the reduced liquid recirculation frequency.

Furthermore, *Acetomicrobium* and *Coprothermobacter* were found with comparably higher RA on the carriers in the top and middle sections of the reactor, closest to the liquid inflow. Another potential acetate producer may belong to the ASV that is assigned as W5, which has been suggested to be a syntrophic propionate degrader producing acetate and H_2 as end products (Dyksma and Gallert, 2019). Interestingly, no known acetogens seem to be present, which mirrors findings in other studies on thermophilic biomethanation processes (Ali et al., 2024; Sieborg et al., 2025). Due to thermodynamic advantages and higher substrate affinity, methanogens can thrive at lower dissolved H_2 concentrations, giving them an advantage over acetogens (Wegener Kofoed et al., 2021). However, under some conditions, like low temperatures, elevated H_2 levels, acetogens become more competitive (Liu et al., 2016; Fu et al., 2019; Voelklein et al., 2019). In line with this, acetogens have been found during continuously operated TBR syngas biomethanation under mesophilic conditions (Cheng et al., 2022). Notably, even though acetate most likely was produced, acetoclastic methanogens (*Methanosarcina* and *Methanothrix*) were observed only in low RA throughout the NMSR sub-trial. *Methanosarchina* has some members that, in addition to acetate, can also use H_2/CO_2 and CO (Rother et al., 2007; Luo et al., 2013). Thus, it cannot with certainty be said that this species was using acetate. *Methanothrix*, on the other hand, can only use acetate. However, more abundant were several known and potential acetate-oxidizing bacteria, indicating their importance for acetate consumption. Potential acetate consumers were represented by *Syntrophaceticus*, *Thermacetogenium*, *Tepidanaerobacter, DTU014*, and *MBA03*. The ASV belonging to known genera were assigned by NCBI BLAST closely to *S. schinkii*, *T. phaeum,* and *T. syntrophicus*. *S. schinkii* is a known SAOB that has previously been detected in thermophilic biogas processes and described to play a key role in syngas conversion while partnering with *Methanothermobacter* (Singh et al., 2023; Ali et al., 2024). *Tepidanaerobacter* is known to have members that are SAOBs, but *T. syntrophicus* is described as a syntrophic alcohol- and lactate-degrading bacterium (Sekiguchi et al., 2006; Westerholm et al., 2011). *T. phaeum* is known to convert acetate in syntrophy with hydrogenotrophic methanogens but can also take on the role of an acetogen by producing acetate by converting H_2 and CO_2 (Hattori et al., 2005), why it is not possible to determine the true role of *T. phaeum*. Notably, several of these known SAOBs were found on the carriers in the bottom fraction of the reactor, where the inlet of syngas is located with a high partial pressure of H_2. However, SAOBs typically only thrive at very low H_2 partial pressure, i.e., $<10^{-4}$ atm at 35 °C (Lee and Zinder, 1988). The relatively higher abundance of these bacteria on the bottom carriers indicates biofilm formation on the carriers could change the microbial kinetics and provide efficient gas-liquid mass transfer to potentially ensure efficient methanogenic H_2 removal to maintain favorable conditions for SAOBs (Stewart, 2003). However, additional investigations of microbial kinetics are required to provide in-depth explanations of the high presence of SAOBs near the gas inlet. The ASVs belonging to *DTU014* and *MBA03* have also been previously proposed to be potential SAOBs (Kamravamanesh et al., 2023), and additionally, the D8A-2 ASV could represent another acetate oxidizer as the NCBI BLAST analysis identified with the closest known relative to be '*Candidatus Syntrophonatronum acetioxidans*', which has been characterized to oxidize acetate in the presence of sulfate-reducing bacteria (SRB) (Sorokin et al., 2014). SRB use the same substrates as methanogens, and some can also use CO as an electron donor (Parshina et al., 2005). In the presence of sulfate, these bacteria are strong competitors with methanogens, and their activity results in H_2S (Dar et al., 2008). The concentration of sulfate in the nutrient medium was between 160 and 320 mg/L throughout the first part of the study until day 564, which was accompanied by H_2S levels of mainly 10–60 ppm in the product gas (Fig. S2b, SM), suggesting some activity of sulfate-reducing bacteria. SRBs could have been represented by two ASVs, one belonging to Desulfitobacteriaceae, according to NCBI blast, most closely related to genus *Desulfosorinus* (Pester et al., 2012), and one belonging to *Desulfitibacter* (Nielsen et al., 2006), present both in the liquid and on the carriers consistently throughout the study.

5. Conclusions

Nutrient medium supply rate (NMSR) and liquid recirculation regimes were assessed for continuous biomethanation of syngas (40 % H_2, 30 % CO, 20 % CO_2, 10 % N_2) in a thermophilic 5 L TBR, using polyethylene carrier material and diluted digestate for nutrient supply. Over time, the reduced nutrient supply rate resulted in a slow decline of H_2 and CO conversion rates, especially of CO. At a minimum NMSR of 14 mL/(L_{pbv}·d), high H_2 and CO conversion rates (>99 %) were achieved with a corresponding maximum methane evolution rate (MER) of 4.3 L/(L_{pbv}·d) at a gas retention time of 1 h. Intermittent liquid recirculation for efficient syngas biomethanation was studied, applying different frequencies and durations. At reduced recirculation frequencies, the biological syngas conversion deteriorated, leading to a maximum MER of 3.4 L/(L_{pbv}·d), whereas the recirculation duration per se did not influence the syngas biomethanation performance.

The microbial community profile in the TBR showed similar structures throughout the different operational phases, with only small differences, and the community was also similar between the carrier and liquid. Thus, the observed differences in process performance were likely caused by differences in activity and not community structure or methanogenic abundance. The syngas converting community was mainly composed of the hydrogenotrophic methanogen *Methanothermobacter*, with the ability to consume both H_2/CO_2 and CO, and different syntrophic acetate-oxidizing bacteria, such as *Syntrophaceticus* and *Thermacetogenium*. In addition, different heterotrophic fermentative bacteria were present, likely to feed on organic carbon in the nutrient medium or cell debris.

CRediT authorship contribution statement

Florian Gabler: Writing – original draft, Visualization, Formal analysis, Data curation, Conceptualization. **George Cheng:** Writing – review & editing, Visualization, Formal analysis, Data curation. **Leticia Pizzul:** Writing – review & editing, Visualization, Supervision, Funding acquisition, Conceptualization. **Anna Schnürer:** Writing – review & editing, Supervision, Funding acquisition, Conceptualization. **Åke Nordberg:** Writing – review & editing, Supervision, Funding acquisition, Conceptualization.

Declaration of competing interest

The authors declare that they have no known competing financial interests or personal relationships that could have appeared to influence the work reported in this paper.

Acknowledgments

This project was funded by the Swedish Energy Agency [149656-1] and Formas (2018-01341). The authors acknowledge Vasiliki Tsamadou for assistance with DNA extraction.

Appendix A. Supplementary data

Supplementary data to this article can be found online at https://doi.org/10.1016/j.biteb.2025.102353.

Data availability

The sequence data generated and analyzed from this study are made available in the NCBI repository in BioProject PRJNA1276488.

References

Ali, R., Samadi, H., Yde, L., Ashraf, M.T., 2024. Carbon monoxide conversion by anaerobic microbiome in a thermophilic trickle bed reactor. Biochem. Eng. J. 212. https://doi.org/10.1016/j.bej.2024.109492.

Andreides, D., Stransky, D., Bartackova, J., Pokorna, D., Zabranska, J., 2022. Syngas biomethanation in countercurrent flow trickle-bed reactor operated under different temperature conditions. Renew. Energy 199, 1329–1335. https://doi.org/10.1016/j.renene.2022.09.072.

Aryal, N., Odde, M., Petersen, C.B., Ottosen, L.D.M., Kofoed, M.V.W., 2021. Methane production from syngas using a trickle-bed reactor setup. Bioresour. Technol. 333. https://doi.org/10.1016/j.biortech.2021.125183. ARTN 125183.

Ashraf, M.T., Yde, L., Triolo, J.M., Wenzel, H., 2021. Optimizing the dosing and trickling of nutrient media for thermophilic biomethanation in a biotrickling filter. Biochem. Eng. J. 176. https://doi.org/10.1016/j.bej.2021.108220.

Asimakopoulos, K., Gavala, H.N., Skiadas, I.V., 2019. Biomethanation of syngas by enriched mixed anaerobic consortia in trickle bed reactors. Waste Biomass Valoriz. 11 (2), 495–512. https://doi.org/10.1007/s12649-019-00649-2.

Asimakopoulos, K., Łężyk, M., Grimalt-Alemany, A., Melas, A., Wen, Z., Gavala, H.N., Skiadas, I.V., 2020. Temperature effects on syngas biomethanation performed in a trickle bed reactor. Chem. Eng. J. 393. https://doi.org/10.1016/j.cej.2020.124739.

Asimakopoulos, K., Kaufmann-Elfang, M., Lundholm-Høffner, C., Rasmussen, N.B.K., Grimalt-Alemany, A., Gavala, H.N., Skiadas, I.V., 2021. Scale up study of a thermophilic trickle bed reactor performing syngas biomethanation. Appl. Energy 290. https://doi.org/10.1016/j.apenergy.2021.116771.

Battumur, U., Yoon, Y.-M., Kim, C.-H., 2016. Isolation and characterization of a new Methanobacterium formicicum KOR-1 from an anaerobic digester using pig slurry. Asian Australas. J. Anim. Sci. 29 (4), 586–593. https://doi.org/10.5713/ajas.15.0507.

Bilgiç, B., Andersen, T.O., Abera, G.B., Sposób, M., Feng, L., Horn, S.J., 2025. Syngas biomethanation using trickle bed reactor, impact of external hydrogen addition at high loading rate. Bioresour. Technol. Rep. https://doi.org/10.1016/j.biteb.2025.102197.

Burkhardt, M., Koschack, T., Busch, G., 2015. Biocatalytic methanation of hydrogen and carbon dioxide in an anaerobic three-phase system. Bioresour. Technol. 178, 330–333. https://doi.org/10.1016/j.biortech.2014.08.023.

Chen, L., Du, S., Xie, L., 2021. Effects of pH on ex-situ biomethanation with hydrogenotrophic methanogens under thermophilic and extreme-thermophilic conditions. J. Biosci. Bioeng. 131 (2), 168–175. https://doi.org/10.1016/j.jbiosc.2020.09.018.

Cheng, G., Gabler, F., Pizzul, L., Olsson, H., Nordberg, A., Schnurer, A., 2022. Microbial community development during syngas methanation in a trickle bed reactor with various nutrient sources. Appl. Microbiol. Biotechnol. 106 (13–16), 5317–5333. https://doi.org/10.1007/s00253-022-12035-5.

Dar, S.A., Kleerebezem, R., Stams, A.J., Kuenen, J.G., Muyzer, G., 2008. Competition and coexistence of sulfate-reducing bacteria, acetogens and methanogens in a lab-scale anaerobic bioreactor as affected by changing substrate to sulfate ratio. Appl. Microbiol. Biotechnol. 78 (6), 1045–1055. https://doi.org/10.1007/s00253-008-1391-8.

Diender, M., Pereira, R., Wessels, H.J., Stams, A.J., Sousa, D.Z., 2016. Proteomic analysis of the hydrogen and carbon monoxide metabolism of *Methanothermobacter marburgensis*. Front. Microbiol. 7, 1049. https://doi.org/10.3389/fmicb.2016.01049.

Dyksma, S., Gallert, C., 2019. Candidatus Syntrophosphaera thermopropionivorans: a novel player in syntrophic propionate oxidation during anaerobic digestion. Environ. Microbiol. Rep. 11 (4), 558–570. https://doi.org/10.1111/1758-2229.12759.

Feickert Fenske, C., Kirzeder, F., Strubing, D., Koch, K., 2023a. Biogas upgrading in a pilot-scale trickle bed reactor - long-term biological methanation under real application conditions. Bioresour. Technol. 376, 128868. https://doi.org/10.1016/j.biortech.2023.128868.

Feickert Fenske, C., Strubing, D., Koch, K., 2023b. Biological methanation in trickle bed reactors - a critical review. Bioresour. Technol. 385, 129383. https://doi.org/10.1016/j.biortech.2023.129383.

Figueras, J., Benbelkacem, H., Dumas, C., Buffiere, P., 2021. Biomethanation of syngas by enriched mixed anaerobic consortium in pressurized agitated column. Bioresour. Technol. 338, 125548. https://doi.org/10.1016/j.biortech.2021.125548.

Fu, B., Jin, X., Conrad, R., Liu, H., Liu, H., 2019. Competition between chemolithotrophic acetogenesis and hydrogenotrophic methanogenesis for exogenous H2/CO2 in anaerobically digested sludge: impact of temperature. Front. Microbiol. 10, 2418. https://doi.org/10.3389/fmicb.2019.02418.

Gabler, F., Cheng, G., Pizzul, L., Schnürer, A., Nordberg, Å., 2025. Comparative evaluation of digestate and reject water as nutrient media for syngas biomethanation in thermophilic trickle-bed reactors. Bioresour. Technol. 435. https://doi.org/10.1016/j.biortech.2025.132893.

Goonesekera, E.M., Grimalt-Alemany, A., Thanasoula, E., Yousif, H.F., Krarup, S.L., Valerin, M.C., Angelidaki, I., 2024. Biofilm mass transfer and thermodynamic constraints shape biofilm in trickle bed reactor syngas biomethanation. Chem. Eng. J. 500. https://doi.org/10.1016/j.cej.2024.156629.

Grimalt-Alemany, A., Skiadas, I.V., Gavala, H.N., 2017. Syngas biomethanation: state-of-the-art review and perspectives. Biofuels Bioprod. Biorefin. 12 (1), 139–158. https://doi.org/10.1002/bbb.1826.

Hattori, S., Galushko, A.S., Kamagata, Y., Schink, B., 2005. Operation of the CO dehydrogenase/acetyl coenzyme a pathway in both acetate oxidation and acetate formation by the syntrophically acetate-oxidizing bacterium Thermacetogenium phaeum. J. Bacteriol. 187 (10), 3471–3476. https://doi.org/10.1128/JB.187.10.3471-3476.2005.

Jensen, M.B., Poulsen, S., Jensen, B., Feilberg, A., Kofoed, M.V.W., 2021. Selecting carrier material for efficient biomethanation of industrial biogas-CO2 in a trickle-bed reactor. J CO_2 Util 51, 101611. https://doi.org/10.1016/j.jcou.2021.101611.

Jønson, B.D., Tsapekos, P., Tahir Ashraf, M., Jeppesen, M., Ejbye Schmidt, J., Bastidas-Oyanedel, J.R., 2022. Pilot-scale study of biomethanation in biological trickle bed reactors converting impure CO(2) from a full-scale biogas plant. Bioresour. Technol. 365, 128160. https://doi.org/10.1016/j.biortech.2022.128160.

Kamravamanesh, D., Rinta Kanto, J.M., Ali-Loytty, H., Myllärinen, A., Saalasti, M., Rintala, J., Kokko, M., 2023. Ex-situ biological hydrogen methanation in trickle bed reactors: Integration into biogas production facilities. Chem. Eng. Sci. 269. https://doi.org/10.1016/j.ces.2023.118498.

Larsson, A., Gunnarsson, I., tengberg, F., 2019. The GoBiGas Project - Demonstration of the Production of Biomethane from Biomas Via Gasification. AB, G.E.

Lee, M.J., Zinder, S.H., 1988. Hydrogen partial pressures in a thermophilic acetate-oxidizing methanogenic coculture. Appl. Environ. Microbiol. 54 (6), 1457–1461. https://doi.org/10.1128/aem.54.6.1457-1461.1988.

Liu, R., Hao, X., Wei, J., 2016. Function of homoacetogenesis on the heterotrophic methane production with exogenous H2/CO2 involved. Chem. Eng. J. 284, 1196–1203. https://doi.org/10.1016/j.cej.2015.09.081.

Luo, G., Wang, W., Angelidaki, I., 2013. Anaerobic digestion for simultaneous sewage sludge treatment and CO biomethanation: process performance and microbial ecology. Environ. Sci. Technol. 47 (18), 10685–10693. https://doi.org/10.1021/es401018d.

Menes, R.J., Muxi, L., 2002. *Anaerobaculum mobile* sp. nov., a novel anaerobic, moderately thermophilic, peptidefermenting bacterium that uses crotonate as an electron acceptor, and emended description of the genus *Anaerobaculum*. Int. J. Syst. Evol. Microbiol. 52, 157–164. https://doi.org/10.1099/00207713-52-1-157.

Neto, A.S., Wainaina, S., Chandolias, K., Piatek, P., Taherzadeh, M.J., 2025. Exploring the potential of syngas fermentation for recovery of high-value resources: a comprehensive review. Curr. Pollut. Rep. 11 (1), 7. https://doi.org/10.1007/s40726-024-00337-3.

Nielsen, M.B., Kjeldsen, K.U., Ingvorsen, K., 2006. *Desulfitibacter alkalitolerans* gen. nov., sp. nov., an anaerobic, alkalitolerant, sulfite-reducing bacterium isolated from a district heating plant. Int. J. Syst. Evol. Microbiol. 56 (Pt 12), 2831–2836. https://doi.org/10.1099/ijs.0.64356-0.

Niu, L., Song, L., Liu, X., Dong, X., 2009. *Tepidimicrobium xylanilyticum* sp. nov., an anaerobic xylanolytic bacterium, and emended description of the genus *Tepidimicrobium*. Int. J. Syst. Evol. Microbiol. 59 (Pt 11), 2698–2701. https://doi.org/10.1099/ijs.0.005124-0.

Paniagua, S., Lebrero, R., Munoz, R., 2022. Syngas biomethanation: current state and future perspectives. Bioresour. Technol. 358, 127436. https://doi.org/10.1016/j.biortech.2022.127436.

Parshina, S.N., Kijlstra, S., Henstra, A.M., Sipma, J., Plugge, C.M., Stams, A.J., 2005. Carbon monoxide conversion by thermophilic sulfate-reducing bacteria in pure culture and in co-culture with Carboxydothermus hydrogenoformans. Appl. Microbiol. Biotechnol. 68 (3), 390–396. https://doi.org/10.1007/s00253-004-1878-x.

Pester, M., Brambilla, E., Alazard, D., Rattei, T., Weinmaier, T., Han, J., Lucas, S., Lapidus, A., Cheng, J.F., Goodwin, L., Pitluck, S., Peters, L., Ovchinnikova, G., Teshima, H., Detter, J.C., Han, C.S., Tapia, R., Land, M.L., Hauser, L., Kyrpides, N.C., Ivanova, N.N., Pagani, I., Huntmann, M., Wei, C.L., Davenport, K.W., Daligault, H., Chain, P.S., Chen, A., Mavromatis, K., Markowitz, V., Szeto, E., Mikhailova, N., Pati, A., Wagner, M., Woyke, T., Ollivier, B., Klenk, H.P., Spring, S., Loy, A., 2012. Complete genome sequences of *Desulfosporosinus orientis* DSM765T, *Desulfosporosinus youngiae* DSM17734T, *Desulfosporosinus meridiei* DSM13257T, and *Desulfosporosinus acidiphilus* DSM22704T. J. Bacteriol. 194 (22), 6300–6301. https://doi.org/10.1128/JB.01392-12.

Porte, H., Kougias, P.G., Alfaro, N., Treu, L., Campanaro, S., Angelidaki, I., 2019. Process performance and microbial community structure in thermophilic trickling biofilter reactors for biogas upgrading. Sci. Total Environ. 655, 529–538. https://doi.org/10.1016/j.scitotenv.2018.11.289.

Ren, J., Liu, Y.-L., Zhao, X.-Y., Cao, J.-P., 2020. Methanation of syngas from biomass gasification: an overview. Int. J. Hydrog. Energy 45 (7), 4223–4243. https://doi.org/10.1016/j.ijhydene.2019.12.023.

Reysenbach, A.-L., Huber, R., Stetter, K.O., Davey, M.E., MacGregor, B.J., Stahl, D.A., 2001. Phylum BII. Thermotogae phy. nov. In: Boone, D.R., Castenholz, R.W., Garrity, G.M. (Eds.), Bergey's Manual® of Systematic Bacteriology: Volume One : The Archaea and the Deeply Branching and Phototrophic Bacteria. Springer New York, New York, NY, pp. 369–387. https://doi.org/10.1007/978-0-387-21609-6_19.

Rother, M., Oelgeschlager, E., Metcalf, W.M., 2007. Genetic and proteomic analyses of CO utilization by *Methanosarcina acetivorans*. Arch. Microbiol. 188 (5), 463–472. https://doi.org/10.1007/s00203-007-0266-1.

Sancho Navarro, S., Cimpoia, R., Bruant, G., Guiot, S.R., 2016. Biomethanation of syngas using anaerobic sludge: shift in the catabolic routes with the CO partial pressure increase. Front. Microbiol. 7, 1188. https://doi.org/10.3389/fmicb.2016.01188.

Sasaki, K., Morita, M., Sasaki, D., Nagaoka, J., Matsumoto, N., Ohmura, N., Shinozaki, H., 2011. Syntrophic degradation of proteinaceous materials by the thermophilic strains Coprothermobacter proteolyticus and Methanothermobacter thermautotrophicus. J. Biosci. Bioeng. 112 (5), 469–472. https://doi.org/10.1016/j.jbiosc.2011.07.003.

Sekiguchi, Y., Imachi, H., Susilorukmi, A., Muramatsu, M., Ohashi, A., Harada, H., Hanada, S., Kamagata, Y., 2006. Tepidanaerobacter syntrophicus gen. nov., sp. nov., an anaerobic, moderately thermophilic, syntrophic alcohol- and lactate-degrading bacterium isolated from thermophilic digested sludges. Int. J. Syst. Evol. Microbiol. 56 (Pt 7), 1621–1629. https://doi.org/10.1099/ijs.0.64112-0.

Sieborg, M.U., Jensen, M.B., Jensen, B., Kofoed, M.V.W., 2021. Effect of minimizing carrier irrigation on H2 conversion in trickle bed reactors during ex situ biomethanation. Bioresour. Technol. Rep. 16. https://doi.org/10.1016/j.biteb.2021.100876.

Sieborg, M.U., Engelbrecht, N., Singh, A., Schnürer, A., Mørck Ottosen, L.D., Wegener Kofoed, M.V., 2025. Unraveling the effects of temperature on mass transfer and microbiology in thermophilic and extreme thermophilic trickle bed biomethanation reactors. Chem. Eng. J. https://doi.org/10.1016/j.cej.2025.161179.

Singh, A., Schnurer, A., Dolfing, J., Westerholm, M., 2023. Syntrophic entanglements for propionate and acetate oxidation under thermophilic and high-ammonia conditions. ISME J. 17 (11), 1966–1978. https://doi.org/10.1038/s41396-023-01504-y.

Sipma, J., Lens, P.N.L., Stams, A.J.M., Lettinga, G., 2003. Carbon monoxide conversion by anaerobic bioreactor sludges. FEMS Microbiol. Ecol. 44 (2), 271–277. https://doi.org/10.1016/S0168-6496(03)00033-3.

Sorokin, D.Y., Abbas, B., Tourova, T.P., Bumazhkin, B.K., Kolganova, T.V., Muyzer, G., 2014. Sulfate-dependent acetate oxidation under extremely natron-alkaline conditions by syntrophic associations from hypersaline soda lakes. Microbiology (Reading) 160 (Pt 4), 723–732. https://doi.org/10.1099/mic.0.075093-0.

Stewart, P.S., 2003. Diffusion in biofilms. J. Bacteriol. 185 (5), 1485–1491. https://doi.org/10.1128/jb.185.5.1485-1491.2003.

Voelklein, M.A., Rusmanis, D., Murphy, J.D., 2019. Biological methanation: strategies for in-situ and ex-situ upgrading in anaerobic digestion. Appl. Energy 235, 1061–1071. https://doi.org/10.1016/j.apenergy.2018.11.006.

Wegener Kofoed, M.V., Jensen, M.B., Mørck Ottosen, L.D., 2021. Biological upgrading of biogas through CO2 conversion to CH4. In: Emerging Technologies and Biological Systems for Biogas Upgrading, pp. 321–362. https://doi.org/10.1016/b978-0-12-822808-1.00012-x.

Westerholm, M., Roos, S., Schnurer, A., 2011. Tepidanaerobacter acetatoxydans sp. nov., an anaerobic, syntrophic acetate-oxidizing bacterium isolated from two ammonium-enriched mesophilic methanogenic processes. Syst. Appl. Microbiol. 34 (4), 260–266. https://doi.org/10.1016/j.syapm.2010.11.018.

Westerholm, M., Isaksson, S., Karlsson Lindsjö, O., Schnürer, A., 2018. Microbial community adaptability to altered temperature conditions determines the potential for process optimisation in biogas production. Appl. Energy 226, 838–848. https://doi.org/10.1016/j.apenergy.2018.06.045.

Yokoyama, H., Wagner, I.D., Wiegel, J., 2010. Caldicoprobacter oshimai gen. nov., sp. nov., an anaerobic, xylanolytic, extremely thermophilic bacterium isolated from sheep faeces, and proposal of Caldicoprobacteraceae fam. nov. Int. J. Syst. Evol. Microbiol. 60 (Pt 1), 67–71. https://doi.org/10.1099/ijs.0.011379-0.

Zinder, S.H., Sowers, K.R., Ferry, J.G., 1985. *Methanosarcina thermophila* sp. nov., a thermophilic, acetotrophic, methane-producing bacterium free. Int. J. Syst. Bacteriol. 35 (4), 522–523. https://doi.org/10.1099/00207713-35-4-522.

Acta Universitatis Agriculturae Sueciae

Doctoral Thesis No. 2025:87

Harnessing the power of microbes, this research demonstrates the potential of trickle-bed reactors to efficiently transform syngas into renewable methane. By optimizing nutrient supply, liquid recirculation, and gas composition, long-term stable methane production was achieved, reaching promising conversion rates and methane concentrations. This work not only highlights the resilience of microbial communities under challenging conditions but also paves the way for integrating biomass-derived syngas into renewable energy systems, offering a promising step toward a greener, low-carbon future.

Florian Gabler received his B.Eng. degree in Environmental Technology from the University of Applied Sciences of Jena, Germany, and holds a M.Sc. degree in Environmental Engineering from the Bauhaus-University of Weimar, Germany.

Acta Universitatis Agriculturae Sueciae presents doctoral theses from the Swedish University of Agricultural Sciences (SLU).

SLU generates knowledge for the sustainable use of biological natural resources. Research, education, extension, as well as environmental monitoring and assessment are used to achieve this goal.

ISSN 1652-6880
ISBN (print version) 978-91-8124-071-9
ISBN (electronic version) 978-91-8124-117-4